BERICHTE
aus dem Fachbereich Geowissenschaften
der Universität Bremen

No. 278

Bohrmann, G., V. Blinova, K. Dehning, D. Evtushenko, C. Friese, A. Hiruta,
D. Hüttich, M. Ivanov, S. Klapp, J. Körber, G. Komakhidze, E. Kopiske, K. Lange,
H.A. Mai, T. Malakhova, Y. Marcon, G. Meinecke, T. Pape, V. Ratmeyer,
R. Rehage, J. Renken, C. Reuter, M. Reuter, M. Römer, H. Sahling,
E. Sakvarelidze, P. Wintersteller, M. Zarrouk

REPORT AND PRELIMINARY RESULTS OF RV MARIA S. MERIAN CRUISE MSM 15/2, ISTANBUL (TURKEY) – PIRAEUS (GREECE), 10 MAY - 2 JUNE 2010. ORIGIN AND STRUCTURE OF METHANE, GAS HYDRATES AND FLUID FLOWS IN THE BLACK SEA .

Berichte, Fachbereich Geowissenschaften, Universität Bremen, No. 278, 130 pages,
Bremen 2011

ISSN 0931-0800

The "Berichte aus dem Fachbereich Geowissenschaften" are produced at irregular intervals by the Department of Geosciences, Bremen University.

They serve for the publication of experimental works, Ph.D.-theses and scientific contributions made by members of the department.

Reports can be ordered from:

Monika Bachur

DFG-Forschungszentrum MARUM

Universität Bremen

Postfach 330 440

D 28334 BREMEN

Phone: (49) 421 218-65516

Fax: (49) 421 218-65515

e-mail: MBachur@uni-bremen.de

Citation:

Bohrmann, G. and cruise participants

Report and preliminary results of RV MARIA S. MERIAN Cruise MSM 15/2, Istanbul (Turkey) – Piraeus (Greece), 10 May - 2 June 2010. Origin and structure of methane, gas hydrates and fluid flows in the Black Sea. Berichte, Fachbereich Geowissenschaften, Universität Bremen, No. 278, 130 pages. Bremen, 2011.

ISSN 0931-0800

R/V MARIA S. MERIAN
Cruise Report MSM15/2

Origin and structure of methane, gas hydrates and fluid flows in the Black Sea

MSM15, Leg 2a and b
Istanbul - Piraeus
10 May – 02 June 2010

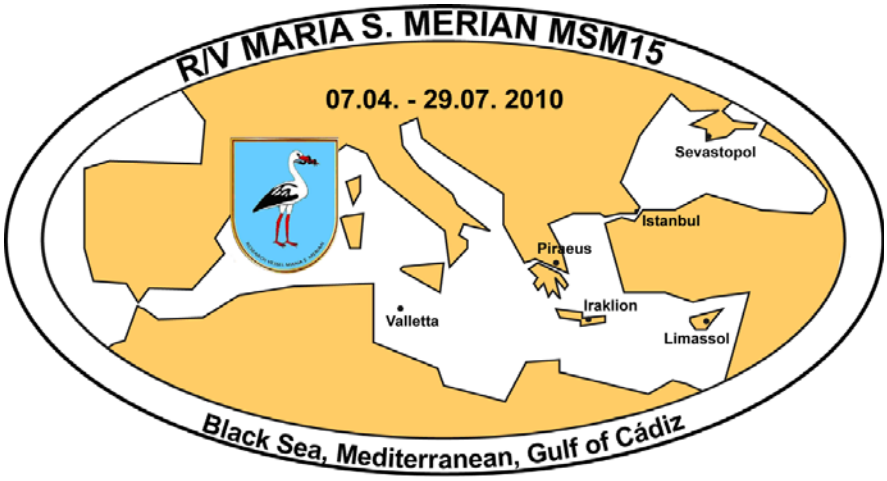

Cruise sponsored by: Deutsche Forschungsgemeinschaft (DFG)
Bundesministerium für Bildung und Forschung (BMBF)

Edited by
Gerhard Bohrmann and Greta Ohling
with contributions of cruise participants

The cruise was performed by
MARUM Center for Marine Environmental Sciences

Universität Bremen

marum

R/V MARIA S. MERIAN Cruise Report MSM15/2

Table of Contents

PREFACE

The investigation of natural gas emission sites and gas hydrates within sediment deposits was the scientific mission. This expedition was based on former results of earlier cruises and on the experiences of our cooperating partners in Russia and Ukraine. Methane emission sites from the seabed are well known from sediments in the Black Sea, and we intended to define the emission rates of the methane using different methods. Methane emissions in the water column are connected to the presence of near-surface gas hydrate deposits. The quantification and the dynamics of gas hydrates are important for geoscientists because methane as a greenhouse gas reaching the atmosphere can also be relevant for climate change. From sediments of the Black Sea the first gas hydrates ever had been recovered.

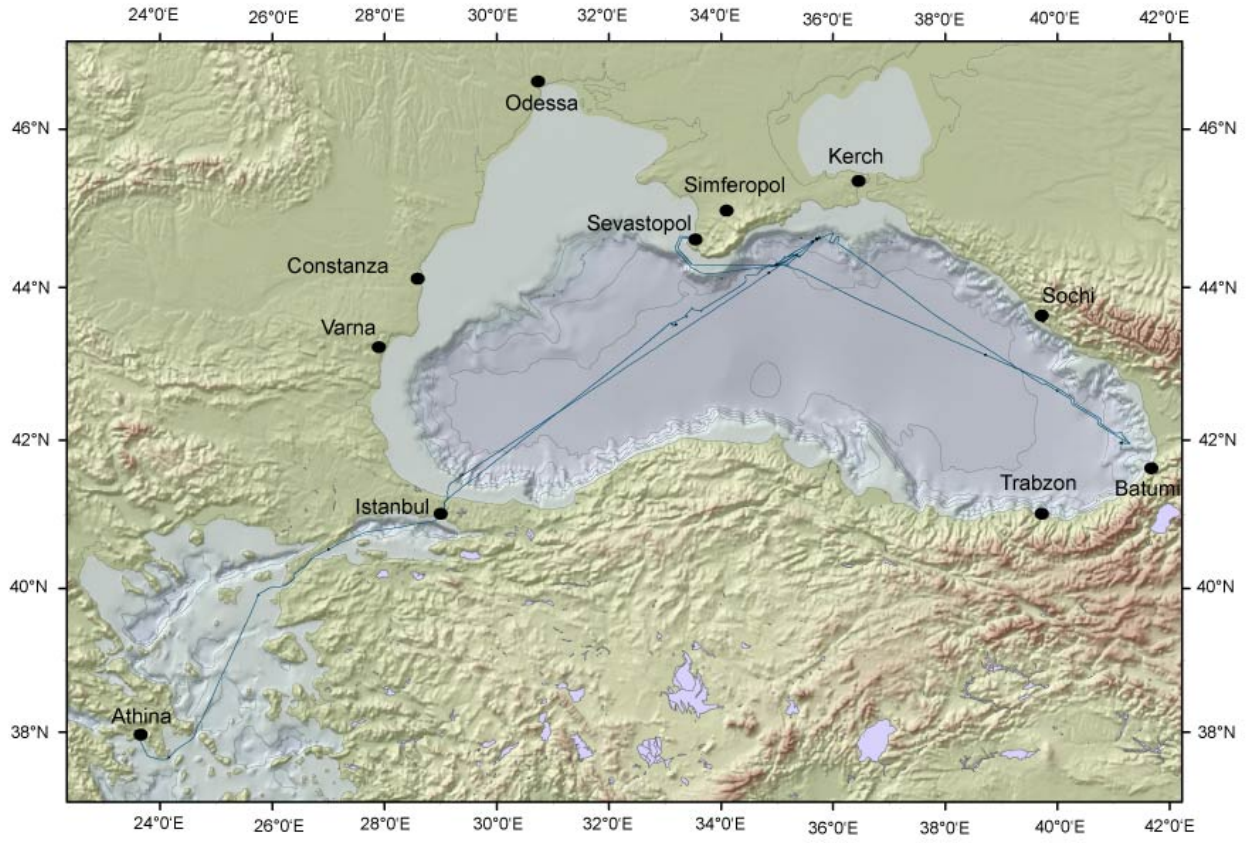

Fig. 1: Cruise track of R/V MARIA S. MERIAN Cruise MSM15/2 from Istanbul to Athina.

During this second leg of cruise 15 the autonomous underwater vehicle AUV SEAL 5000 and the remotely operating vehicle ROV QUEST 4000 as well as our autoclave piston corer were planned to deploy and were installed on board.

Major objective was methane and methane hydrate in the Black Sea, the better understanding of its origin, the structure of gas hydrate and the fluid flows between sediment and water column. The emphasis of the investigations is focussed on the presence and the dynamics of gas hydrate in the seabed and within upper 50 m of sedimentary column, from where the methane could reach very fast the seabed, therewith also the water column and possibly also the atmosphere. Another focus was the quantification of gas emissions at selected locations.

Fig. 2: Research vessel MARIA S. MERIAN in the harbour of Istanbul (left). AUV SEAL 5000 recovered from its first dive during the cruise (right).

Fig. 3: Welcome poster at Nachimow Quai in Sevastopol (left). Press conference onboard R/V MARIA S. MERIAN (right).

Fig. 4: Ambassador Dr. Hans-Jürgen Heimsoeth and the mayor of the city of Sevastopol introduced by ROV project leader Volker Ratmeyer to the pilot work within the ROV helmstand container (left). Opening of the Ukraine-German workshop "Germany – Competent partner in marine research" at the O.A. Kovalevski Institute (IBSS) in Sevastopol (right).

The cruise with R/V MARIA S. MERIAN was planned in preparation of a MeBo drilling cruise which is planned for 2011.

In the frame of this research cruise mainly two topics have been in the focus. One aim of the expedition was to record micro-bathymetry by using the AUV SEAL 5000, in order to come to a

better understanding of the dynamics in formation and decomposition of gas hydrates in the shallow sediments. Furthermore the high-resolution maps together with other geophysical and geological background information shall help to determine the drilling locations for MeBo in 2011. A further aim of the cruise was to quantify the gas emissions by means of optic and acoustic methods with the ROV QUEST. The estimation of the gaseous methane flows on the one hand helps to understand the biogeochemical processes in the water column. On the other hand the estimation helps to achieve an integrated view on how much methane is dissolved or absorbed, how much is converted and how much methane escapes. As the MeBo cruise exclusively concentrates on the quantification of methane in the sediments, the aims of this research cruise are of basic importance.

Personel aboard R/V MARIA S. MERIAN

Table 1: Scientific crew.

Name	Working group	Affiliation	Participation
Gerhard Bohrmann	Chief scientist	GeoB	Leg 2a & b
Klaus Dehning	DAPC, cores	MARUM	Leg 2a & b
Carmen Friese	ROV works	GeoB	Leg 2a & b
Akihiro Hiruta	GIS mapping	MARUM	Leg 2a
Daniel Hüttich	ROV	MARUM	Leg 2a &b
Stephan A. Klapp	Sediments	GeoB	Leg 2a
Jan-Hendrik Körber	PARASOUND	MARUM	Leg 2a & b
Eberhard Kopiske	AUV	MARUM	Leg 2a & b
Kerstin Lange	Public relations	MARUM	Leg 2b
Hoang Anh Mai	ROV	MARUM	Leg 2a & b
Yann Marcon	GIS mapping	MARUM	Leg 2b
Gerrit Meinecke	AUV	MARUM	Leg 2a & b
Thomas Pape	Gas analyses	GeoB	Leg 2a & b
Volker Ratmeyer	ROV	MARUM	Leg 2a & b
Ralf Rehage	ROV	MARUM	Leg 2a & b
Jens Renken	AUV	MARUM	Leg 2a & b
Christian Reuter	ROV	MARUM	Leg 2a & b
Michael Reuter	ROV	MARUM	Leg 2a & b
Miriam Römer	Gas quantification	GeoB	Leg 2a & b
Heiko Sahling	ROV survey.	GeoB	Leg 2a & b
Paul Wintersteller	Maps	MARUM	Leg 2a & b
Marcel Zarrouk	ROV	MARUM	Leg 2a & b
Dmytro Yevtushenko	Observer	IBSS, Sevastopol	Leg 2a
Mikhail Ivanov	Geology	MSU, Moscow	Leg 2a
Tatiana Malakhova	Gas analyses	IBSS, Sevastopol	Leg 2a
Evgeni Sakvarelidze	Geology	TSU, Tbilise	Leg 2b
Valentina Blinova	Geochemistry	MSU, Moscow	Leg 2b
George Komakhidze	Observer	BSMC, Tbilise	Leg 2b

Participating Institutions

BSMC	National Environmental Agency_Black Sea Monitoring Center, 51, Rustaveli Str., 6010, Batumi, **Georgia**
GeoB	Fachbereich Geowissenschaften, University of Bremen, Klagenfurter Str. 28334 Bremen, **Germany**
IBSS	A. O. Kovalevsky Institute of Biology of the Southern Seas, Ukrainian Academy of Sciences, 2 Nakhimov Av., 99011 Sevastopol, **Ukraine**
MARUM	MARUM Zentrum für marine Umweltwissenschaften, University of Bremen, Leobener Str., 28334 Bremen, **Germany**
MSU	Geology and geochemistry of fuel minerals, Geological faculty Moscow State University, Leninskie Gory, 119992 Moscow, **Russia**
TSU	Faculty of Geography, Tbilisi State University, Cholokashvili Ave., Tbilisi 0126, **Georgia**

Fig. 5: Groups of scientists and technicians sailed during Legs MSM15/2a (left) and MSM15 /2b (right).

Table 2: Crew members onboard.

Name	Work onboard	Name	Work onboard
Friedhelm von Staa	Master, Leg 2a	Steffen Jescheniak	Seaman
Ralf Schmidt	Master, Leg 2b	Karsten Peters	Seaman
Björn Maas	Chief Officer	Andreas Wolff	Seaman
Holm Behnisch	Officer	Frank Schrage	Seaman
Johannes Werther	Officer	Daniel Fachbach	Seaman
Thomas Ogrodnik	Chief Engineer	Sven Kröger	Cook Mate
Manfred Boy	Engineer	Iris Seidel	Steward
Hendrik Schmidt	Electrician	Johann Ennenga	Cook
Michael Maggiulli	System Operator	Mario Schmalfeld	Engineer
Frank Riedel	Electronics	Olaf Lorenzen	Motorman
Norbert Bosselmann	Bosun	Olaf Wiechert	Locksmith
Rene Papke	Seaman	Rainer Badtke	Seaman

Shipping operator

Briese Schiffahrts GmbH & Co. KG Abt. Forschungsschifffahrt, Hafenstr. 12, 26789 Leer, **Germany**

1. Introduction and Geological Background

(G. Bohrmann)

1.1 Objectives

Methane is twenty times more effective as a greenhouse gas than CO_2, however, its concentration within the atmosphere is much smaller. In contrast, methane generated by microbial decay and thermogenic breakdown of organic matter seems to be a large pool in geological reservoirs. Numerous features such as shallow gas accumulations, pockmarks, seeps, and mud volcanoes are present in a wide variety of oceanographic and geological environments (Judd, 2003). Release and uptake of methane by such sources may provide positive and negative feedback to global warming and/or cooling and are therefore focal points of current research (Kvenvolden, 1998).

Studying methane emission sites will elucidate how stable these reservoirs are and how the pathways to the atmosphere are working. Because of their high methane density, gas hydrates are of special interest, when they occur close to the seafloor. Previous investigations have shown that hydrates generate extremely high and variable fluxes of methane to the overlying water column due to their exposed position close to the sediment/water interface. Not only do they influence their immediate environment, but they may also contribute substantially to the transfer of methane to the atmosphere.

Shallow gas hydrates, potentially associated with free gas, are known from sediments in several areas and are of specific interest in the Black Sea where a large number of active methane emission sites exist. New investigations on mud volcanoes have shown that even deep at the stability field in 2,000 m depth hydrates are very close to their stability limit and may serve as emission sites (Bohrmann et al., 2003). Most of the few studies dealing with this phenomenon were made without using appropriate pressurized sampling techniques and are therefore of limited value. Because of the sensitivity of gas hydrate stability and the connection of methane to environmental change, pressurized autoclave sampling technology and investigations as well as experiments under *in situ* conditions are essential for constraining the potential of environmental hazards from methane in sediments. The technical application of the autoclave tools was performed to better understand the dynamics of gas and gas hydrates within the Black Sea (Abegg et al. 2008; Pape et al. 2010).

The focus of the program is to investigate near-surface methane and methane hydrates in the Black Sea in order to understand their origin, structure, and behavior as well as their interaction with the sedimentary and oceanic environment. This is critical for evaluating and quantifying their importance in the global carbon cycle. Research activities are concentrated on the Black Sea for various reasons. It is the largest anoxic basin with much higher methane concentrations than in any other marginal sea. Sediments of 10-19 km thickness reveal a large potential reservoir for methane generation, and hundreds of methane emission sites are known from water column investigations performed by our Russian and Ukrainian colleagues. In addition, fluid venting, active mud volcanoes, pockmarks and gas-bearing sediments have been discovered and reported in the literature (Ivanov et al., 1998; Bouriak and Akhmezjanov, 1998). It was in the Black Sea and Caspian Sea that samples of gas hydrates were first recovered from marine sediments (Yefremova and Zhizchenko, 1974). Based on the stability field of methane hydrate, areas deeper than 750 m water depth are of particular interest (Pape

et al. 2008, 2010).

R/V MARIA S. MERIAN Cruise MSM15/2 followed several other research cruises (Fig. 6) to the Black Sea conducted over the course of the last couple of years and it was the last cruise within the BMBF initiatives OMEGA and METRO (Bohrmann & Schenck 2002; Sahling et al. 2004; Akhmezjanov et al. 2007; Bohrmann and Pape 2007). Using different techniques of seafloor mapping (multibeam bathymetry, deep-towed sidescan sonar, and video observation), the aim of the project was to identify and map various facies and environments that are related to near-surface gas hydrates and methane seeps off the coast of Georgia, Ukraine, and Turkey. Besides the need for quantification of the total amount of methane bound in gas hydrates, it is important to determine the portion of gas hydrates and free gas that are reactive. Hydrates occur in the subseafloor from several tens of meters below the sediment surface down to the base of the methane hydrate stability field, which is reached around 500 m sediment depth in the deep Black Sea area (Bohrmann et al.; 2003). Gas released from the seafloor or hydrate outcrops are known from a few locations, where they may interact with the ocean or even reach the atmosphere in the form of gas bubbles. The determination of the extent of these 'reactive' locations and understanding their formation is crucial in assessing the potential impact of gas hydrates and their dissociation on the isotopic chemistry of the ocean and on climate.

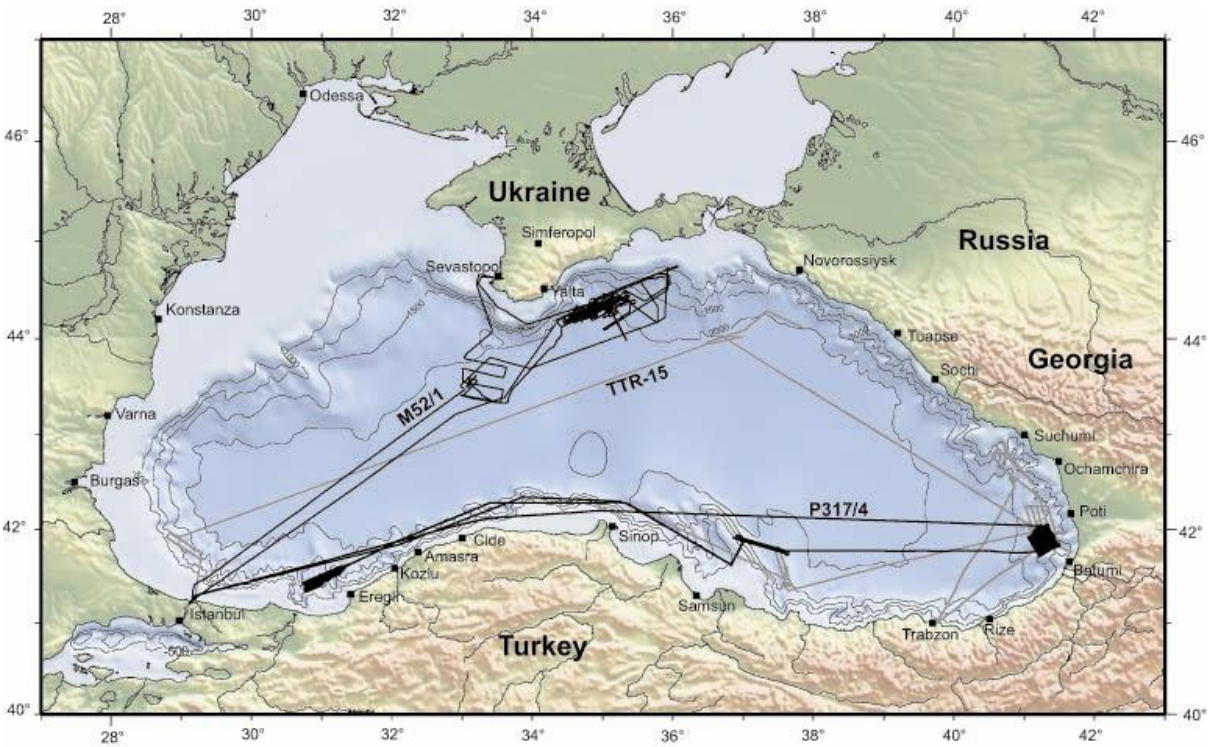

Fig. 6: Black Sea map with track lines of former gas hydrate cruises R/V METEOR M52/1, R/V POSEIDON Cruise P317/4 and R/V PROFESSOR LOGATCHEV Cruise TTR-15.

Previously, mud volcanoes in the central part of the Black Sea and the Sorokin Trough were investigated during R/V METEOR cruise M52/1 (MARGASCH I, January 2002). In addition, other seeps, like gas and oil seeps in various geological settings, were investigated in the Gurian Trough area (Sahling et al., 2004, Klaucke et al., 2005; Akhmetzhanov et al., 2007). During the last cruises we used pressurized sampling techniques and remotely operated

vehicles (ROVs). Since gas hydrates react rapidly to changes in pressure and temperature, pressurized autoclave sampling technology, and investigations and experiments under *in situ* conditions are essential. Beside the Ocean Drilling Program, the technical development of these capabilities were first shown by the former projects, and the applications of the autoclave technology greatly improved the understanding of gas hydrate dynamics (Abegg et al., 2008).

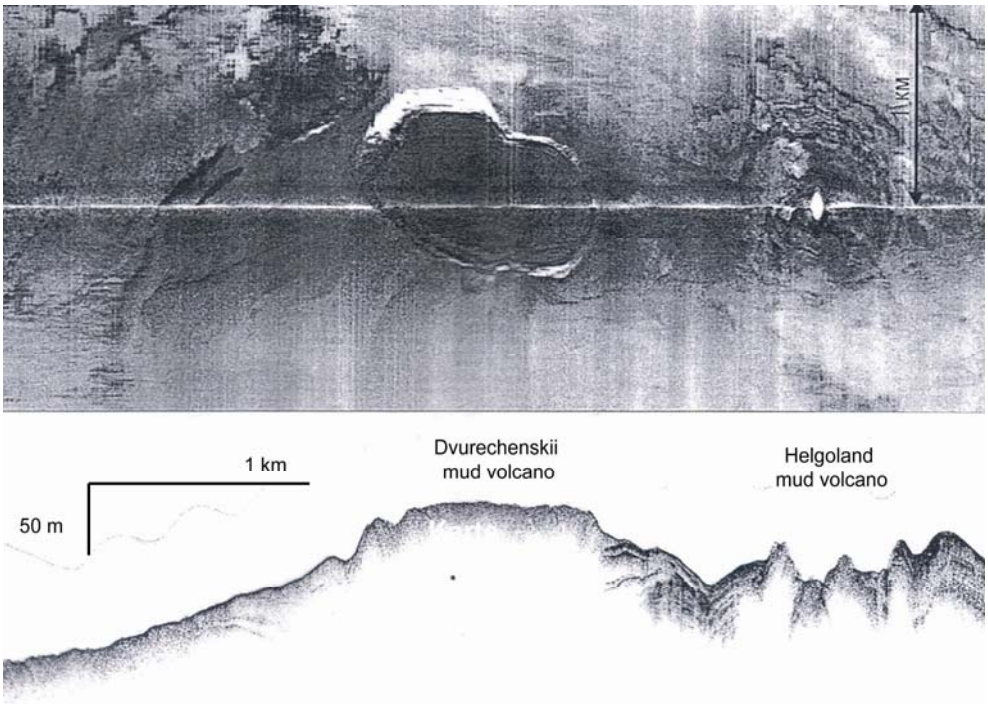

Fig. 7: Side-scan sonar image of the Dvurechenskii mud volcano obtained TTR-6 cruise by the deep towed MAK-1 during (from Woodside et al. 1997). The mud volcano close to the east was named Helgoland mud volcano during the cruise MSM 15/2 investigation.

Because the Black Sea water is anoxic at ~ 100 m below sea level, seep sites below that water depth show no colonization by chemosynthetic clams or tube worms because of the lack of oxygen, which these organisms need for their symbiotic metabolism with bacteria. Other seep manifestations that help to identify active venting are bacterial mats and carbonate buildups (Fig. 6, right), which form at seep sites because of increased rates of anaerobic methane oxidation (Michaelis et al., 2002). During the last few years, gas bubble emanating from the seafloor were increasingly observed predominately in shallow water areas like the GHOSTABS-field in the Dneper paleo-delta (Artemov et al., 2007). Free-gas releasing seeps were typically identified by hydroacoustic plumes in the water column that show strong backscatter signals with flare-like shapes detected by single-beam echosounders. The flares are often rooted at the seafloor where the gas seeps from the sediment deposits (Artemov et al., 2007).

During this second leg of MARIA S. MERIAN Cruise 15, the autonomous underwater vehicle AUV SEAL 5000 and the remotely operating vehicle ROV QUEST 4000 as well as our autoclave piston corer was deployed on mud volcanoes (Fig. 7) and other seep sides The cruise with R/V MARIA S. MERIAN was conducted in preparation of a MeBo drilling cruise which is now scheduled for 2011 (February 26 – April 2) onboard of R/V METEOR.

1.2 Black Sea Overview

The Black Sea is located north of Turkey and south of Ukraine and Russia. To the West it is bordered by Romania and Bulgaria and to the East by Georgia. It is a marginal ocean with a water depth of 2-2.2 km. The Black Sea is surrounded by Cenozoic mountain belts like the Great Caucasus, the Pontides, and the Balkanides (Fig. 8; Robinson, 1997). Two deep basins, the western and eastern Black Sea basins, are underlain by oceanic or thinned continental crust with a sediment cover of 10-19 km thickness (Tugolesov et al., 1985).

The area changed to a compressional regime during the Eocene, and the tectonic evolution of the basin is characterized by a subsidence history that resulted in the separation of the two basins (Nikishin et al., 2003). Modern stress field observations from structural data, earthquake foci, stress field measurements onshore in the Crimean and Caucasus regions, and GPS data show that the Black Sea region is still in a dominantly compressional environment (Reilinger et al., 1997; Nikishin et al., 2003). The general source of compression is the collision between the Arabian, Anatolian, and the Eurasian plates (Fig. 8).

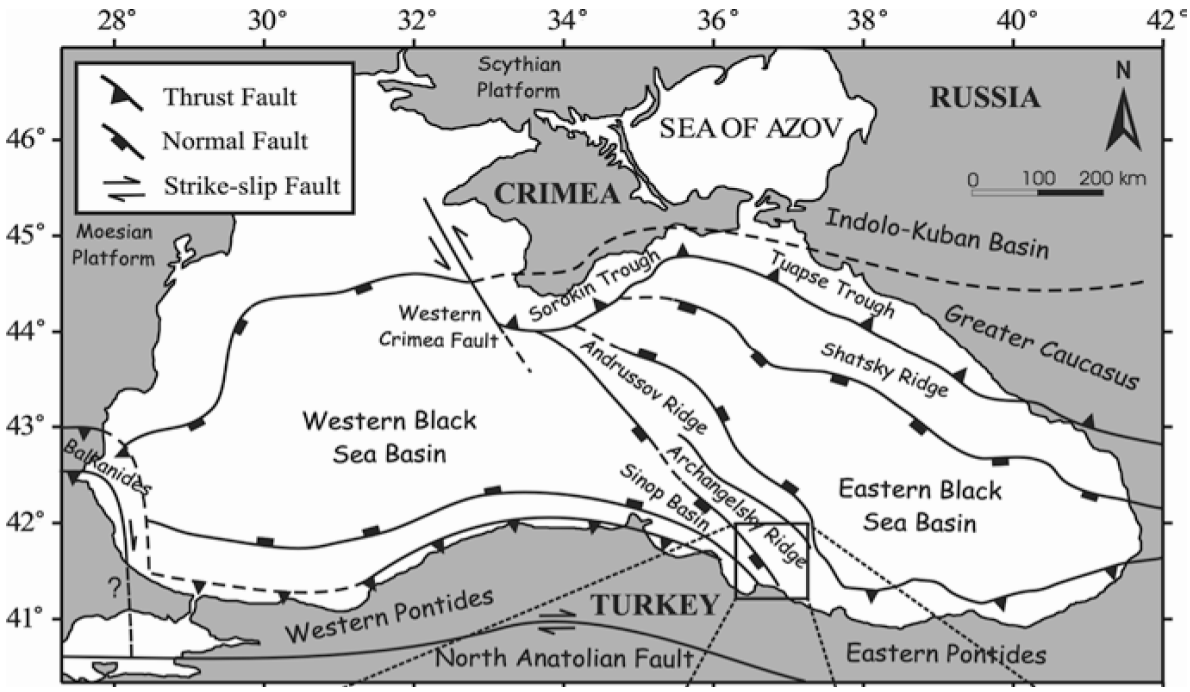

Fig. 8: Simplified tectonic map showing the major tectonic elements of the Black Sea (from Çifçi et al., 2003).

The basins are separated by the Andrusov Ridge which is formed from continental crust and overlain by only 5-6 km of sediment. The origin of the Black Sea is interpreted as a back-arc basin evolved during late cretaceous times (Nikishin et al., 2003). The Sorokin Trough is a foredeep basin of the Crimean Mountains belonging to the eastern basin of the Black Sea. It forms a large depression, which is 150 km in length and 50 km in width, southeast of the Crimean Peninsula (Tugolesov et al., 1985). A large number of its mud volcanoes evolved from diapiric zones in a compressional regime between the Cretaceous to Eocene blocks of the Tetyaev Rise and the Shatskiy Ridge (Tugolesov et al., 1985). The sediments extruded in the mud volcanoes are clay-rich deposits from the Maikopian Formation that forms an

Oligocene-Lower Miocene sequence of 4-5 km in thickness. The Maikopian Formation is overlain by at least 2-3 km thick Pliocene to Quaternary sediments. A second foredeep basin specially filled with thick Maikopian sediments forms the Tuapse Trough which strikes parallel to the northeast coast of the Black Sea. Similar to the Sorokin Trough, the basin was compressed between the Shatsky Ridge and the Greater Caucasus (Nikishin et al., 2003). Sediments from the Caucasus fold belt are overthrusting deposits of the Tuapse basin to the west.

1.3 Natural Oil Seepage in the Eastern Black Sea Revealed by Satellite Imagery

That the Black Sea bears major resources of higher hydrocarbons is known for many years (e.g. Robinson et al., 1996 and references therein). Seepage of oil at the seafloor of the Eastern Black Sea was noted already during preceding research cruises, i.e. M72/3 in 2007 and TTR15 in 2005. At two sites in the Georgian waters of the Black Sea seep structures were discovered, where gas is emanating at the seafloor and gravity coring revealed the presence of oil in the shallow sediments. Thin oil films were noticed on the sea surface at the sampling sites during these cruises.

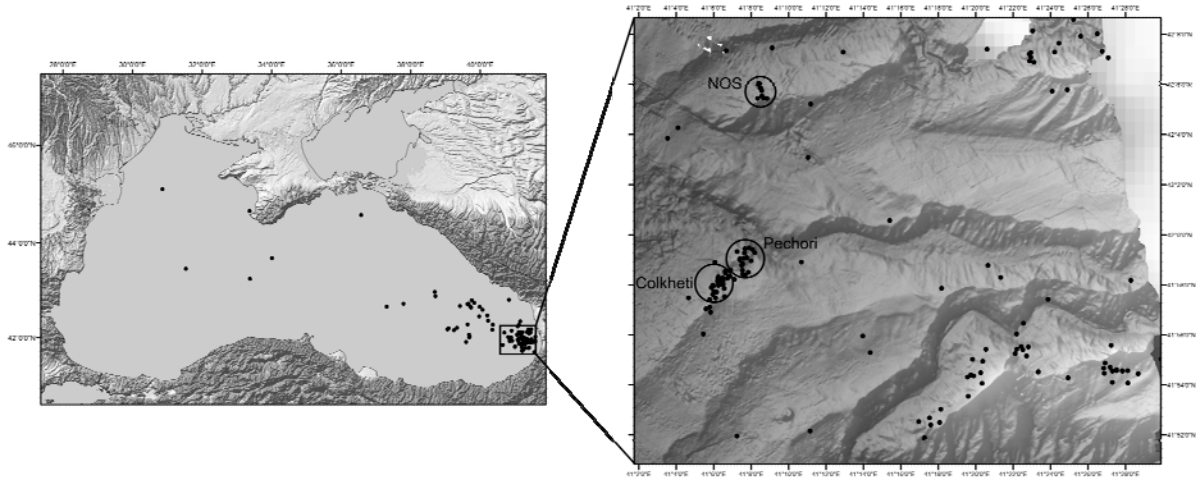

Fig. 9: Dots indicating potential origins of oil slicks (OSOs); zoom in the Georgian parts of the Black Sea where highest densities of OSOs were identified. Circles show sites for which seepage was confirmed.

In preparation of the MSM15/2 cruise satellite images were analysed to investigate if oil on the sea surface can be assigned to natural seepage which forms characteristic large scale oil slicks on the sea surface (e.g. MacDonald et al., 1993). Advanced Synthetic Aperature Radar (ASAR) images acquired by the ENVISAT satellite and provided by the *European Space Agency* (ESA) have been used to detect potential sites of natural oil seepage in Ukrainian and Georgian parts of the Black Sea. The ASAR sensor is an active radar sensor that emits microwaves and captures the radiation scattered back by the earth or sea surface. The smoother the surface is, the less energy is reflected towards the sensor, following Bragg's law. Smooth areas will thus look darker on the processed satellite image than rougher surfaces.

Surfactants which might be biogenic films or oil, dampen small capillary waves of the sea surface and create a surface which is less rough than the adjacent sea. These small differences in wave patterns can be captured by the ASAR sensor (e.g. Topouzelis, 2008 and references therein). A critical factor in the oil slick detection on ASAR images is the wind speed which prevailed during image acquisition. Low wind speeds will cause a uniform weak backscatter signal of the entire sea, whereas too high wind speeds eliminate the smoothing effect of surfactants. Generally, a wind speed range between 2 and 10 m/s is considered to be suitable for identifing oil slicks with an optimum being in the range from 3 to 5.8 m/s (Wahl et al., 1994, Garcia-Pineda et al., 2008). Taking into account this narrow range of optimal wind speeds, the number of suitable images available for oil slick detection in the Ukrainian and Georgian parts of the Black Sea is limited.

About 120 ASAR images were manually analysed to find out whether natural oil seepage that reaches the sea surface occurs in the northern and eastern Black Sea or not. All images were ASAR Image Mode Precision Images with a resolution of approximately 30m. This fine resolution allows even surface films of small extent to be identified. All images were converted from ESAs native N1 to geoTiff format and loaded to a geo database for further analyses in a geographic information system (GIS). Areas showing elongated, curved surface slicks were manually identified on the images and their origins marked in an image specific point shape file. After investigation of all images the resulting point shape files were overlain and dense cluster of potential oil slick origins (OSOs) identified as location where natural oil seepage is likely to occur (Fig. 9).

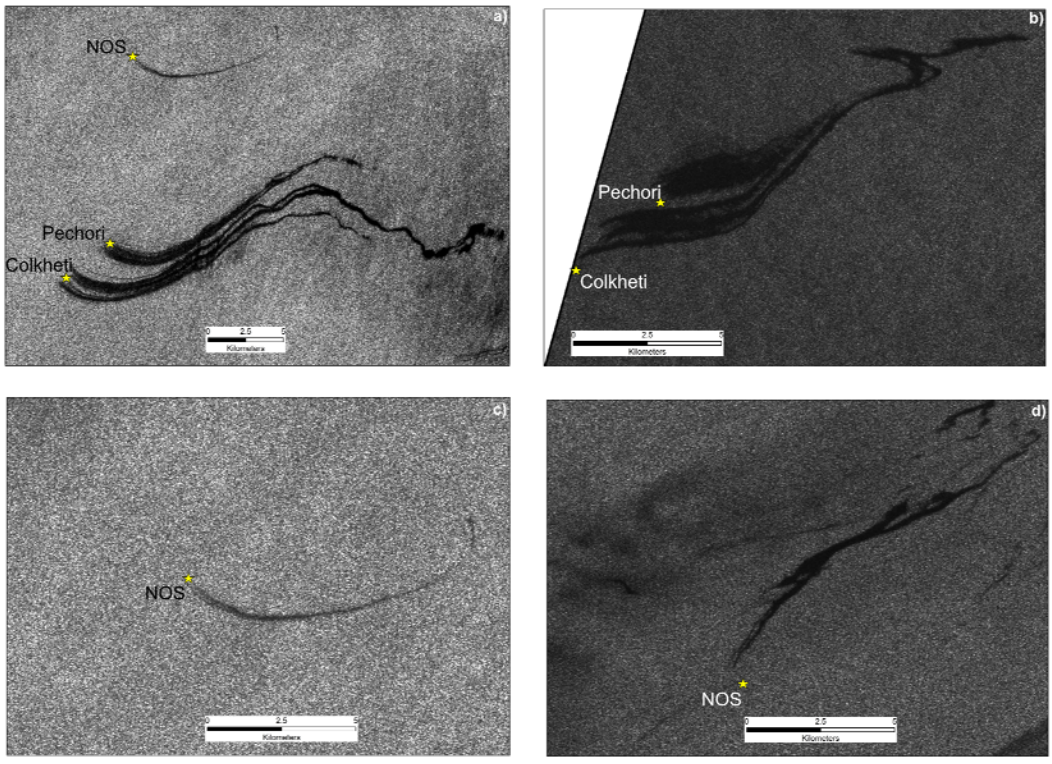

Fig. 10: Sub-scenes of ESA ASAR IMP images showing surface slicks originating from natural oil seepage. Images were acquired on: a) & c) 15 Sep. 2003, b) 07 Feb. 2007, d) 14 May 2009. All images provided by *European Space Agency*.

Upon preliminary analysis of all images, clear evidence for natural oil seepage was found only in Georgian waters of the Black Sea. Within the Ukrainian Exclusive Economic Zone many oil slick like features could be identified. However, no site showing persistence oil slicks could be pinpointed from the available images, suggesting that the identified slicks originated from biogenic films or man made oil pollution. In contrast to this, in Georgian waters seven sites were identified where natural oil seepage seem to occur at least since 2003, which is the year satellite images are available from. The most prominent sites, showing oil slicks up to 20 km long, are located at the Colkheti Seep and Pechori Mound (Fig. 10a & b). The second most active site *New Oil Seep* (NOS) is located about 8 nm north of Colkheti Seep and Pechori Mound (Fig. 10c & d). During transit from Ukrainian waters to the Batumi seep on May 24, this site was crossed by one line, and the PARASOUND system revealed a clear acoustic anomaly (‘flare’) in the water column, rising approximately 300 m above the seafloor confirming active seepage.

On May 26, oily bubbles were seen to surface above the Colkheti seep, spreading out on the sea surface, forming silver to red-brownish shining films. Since the sea was extremely calm during the day, it was possible to see a large oil slick towards the north. Additionally, it was possible to see a surface roughness anomaly in the ships own ice radar at the location where the oil slick was located.

It was not possible to investigate other sites for which the satellite image analyses suggested natural oil seepage, but the striking similarities of the slick patterns between these sites and the ones for which seepage of oil was confirmed make the occurrence of natural oil seeps very likely.

2. Cruise Narrative

(G. Bohrmann)

On 10 May 2010, R/V MARIA S. MERIAN started from the port of Haydapasar (Istanbul), at 8:42 local time, heading for the Black Sea. Investigations of natural gas emission sites and gas hydrates within sediment deposits were the scientific mission. This expedition was based on former results of earlier cruises and on the experiences of our cooperating partners in Russia, Georgia and Ukraine. Methane emission sites from the seabed are well known from sediments in the Black Sea, and we intended to define the emission rates of the methane using different methods. Methane emissions in the water column are connected to the presence of near-surface gas hydrate deposits. The quantification and the dynamics of gas hydrates are very important for geoscientists because methane as a greenhouse gas reaching the atmosphere can also be relevant for climate change. From sediments of the Black Sea the first gas hydrates ever had been recovered.

Before leaving the harbour of Istanbul, R/V MARIA S. MERIAN stayed for two days in the port for exchange of the scientific crews and equipment between its first and second leg of cruise no. 15. During the second leg, the autonomous underwater vehicle AUV SEAL 5000 and the remotely operating vehicle ROV QUEST 4000 as well as our autoclave piston corer were planned to deploy and were installed on board. In total 7 containers were transported from Germany to Istanbul and unloaded on board containing our entire scientific equipment.

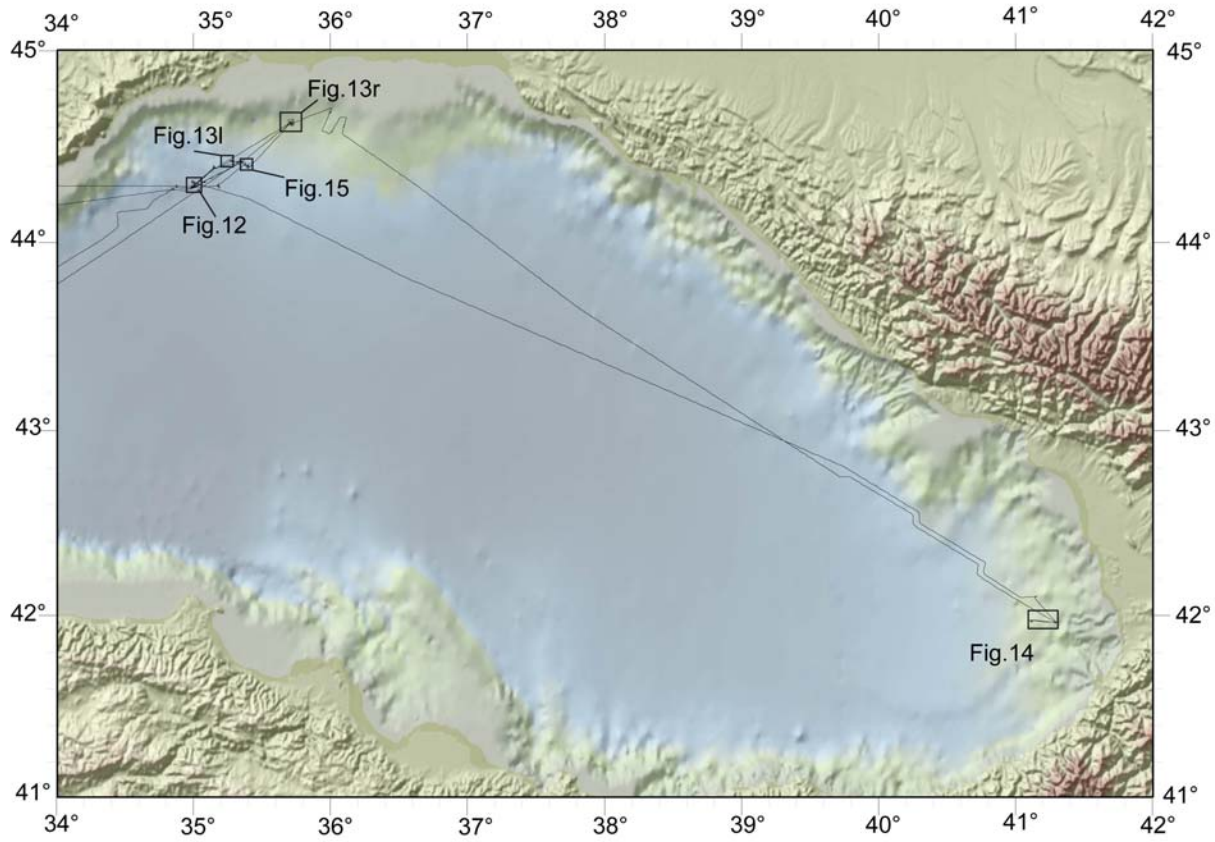

Fig. 11: Cruise track of R/V MARIA S. MERIAN Cruise MSM15/2 in the eastern part of the Black Sea. Boxes are showing the areas of detailed maps (see Figures 12-15).

On 9 May the scientists from Germany, Japan, Russia and Ukraine embarked and used the Sunday for the necessary deck works together with the ship's crew and also to install the laboratories. After leaving its berth in the port, R/V M. S. MERIAN soon passed on Monday the Bosporus and reached the Black Sea already after just one hour. Many colleagues enjoyed the passage with sunny weather and a magnificent view on the scenery at the rising landscape left and right. The pilot left the vessel at 10:05 and we could steam forward into the Black Sea towards the Crimean Peninsula.

After a 12-hour transit through Turkish territory we reached the Ukrainian border where our research could start. First profile measurements on the water's acoustic velocity were started for calibration of some acoustic systems. At the same time we started the recording of PARASOUND and multibeam echosounder data in the area of the central province of mud volcanoes. By means of PARASOUND we verified the activities of some mud volcanoes, searching for gas emissions indicated by acoustic anomalies. In the western Sorokin Trough for the first time ever we found signs of gas emissions on the Dvurechenskii mud volcano (DSV) as well as above some other mud volcanoes in its neighbourhood. In 2007 the DSV showed no gas seepage during all for 4 weeks. A temperature chain had been anchored then in the mud of DSV in order to document possible eruptions of the mud volcano by temperature measurements. The ROV QUEST dive on Thursday, 13 May, thus showed that the temperature anchoring had disappeared and that the seafloor in this area is characterised by fresh mud flow.

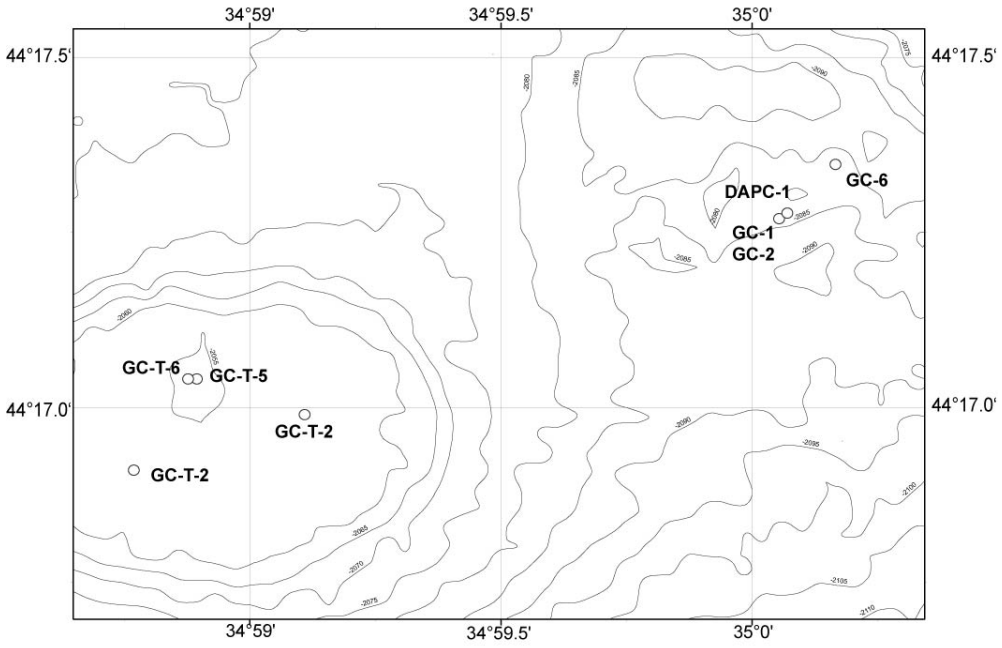

Fig. 12: Sampling stations on Dvurechenskii and Helgoland mud volcano (for location of the area see Figure 11).

In the meantime probably a heavy volcanic mud eruption has plunged our mooring station to the deep mud. Contrary to the situation three years ago now free gas escapes in small quantities at several places which we interpreted as a last sign of a mud volcano eruption dying away. Further work concentrated mainly on a prominent gas emission in 900 m water depth on the slope south of the Kerch Peninsula. There we could create for the first time a complete micro-bathymetric map during a 24-hour measurement with the AUV SEAL 5000

disclosing completely new possibilities of processing and interpretation of gas seeps. We are very happy about this and also about the two successful ROV dives with a detailed inspection of gas emissions in the Kerch Flare area. Due to this scientific success we are quite confident with this first week of the expedition.

On Monday 17 May, two AUV mapping dives on the Dvurechenskii mud volcano were accomplished during daytime which took time until the evening hours. Subsequently we did a ROV dive on a flare emission at a possible fault zone which had been newly detected by PARASOUND. Tuesday was characterised by recording profiles as well as sampling with the autoclave piston corer and the gravity corer. During the ROV dive in the evening we could retrieve the temperature mooring which we earlier thought had been lost on DSV. The successful recovery of the temperature logger will allow us to analyse the data of the temperature logger about the volcanic activities during the past three years. The AUV measurements done before had enabled us to determine the exact coordinates of the temperature mooring.

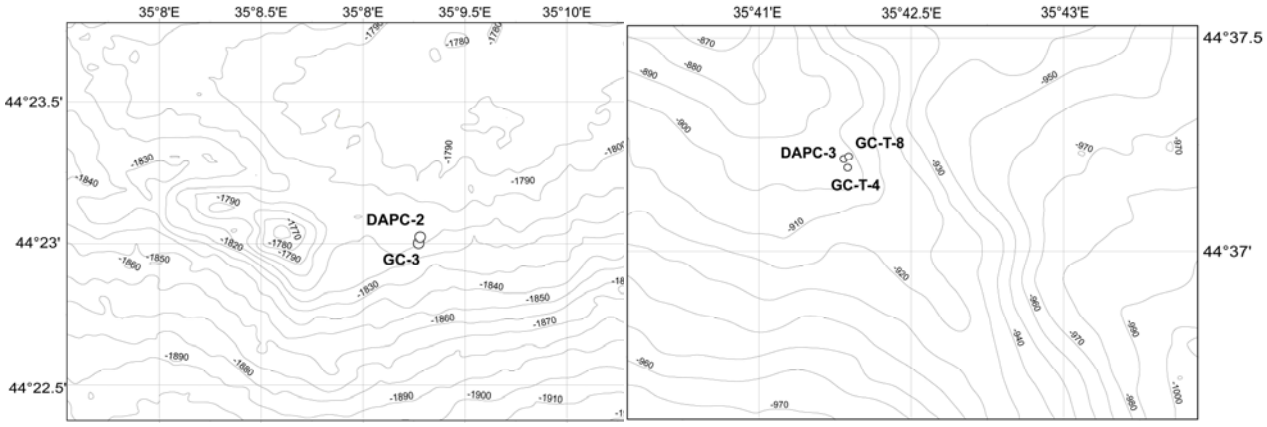

Fig. 13: Sampling at Odessa mud volcano (left) and at Kerch Flare (right); for location of the areas see Figure 11.

On Thursday 20 May, R/V MARIA S. MERIAN punctually passed the port entrance of Sevastopol and berthed on its scheduled place at Nachimow Quay. This quay is situated in the city center and just three walking minutes from the aquarium and the cooperating O.A. Kovalevski Institute (IBSS). The visit of MARIA S. MERIAN in Ukraine was the start of the "German week at the Crimean Peninsula" which had been accomplished by the German Embassy in Kiev. The event started at 11:00 with a press conference accomplished by the German Ambassador Hans-Jürgen Heimsoeth as well as representatives from the German Ministry of Education and Science (BMBF) and from the Ukrainian Academy of Sciences, under attendance of more than 35 journalists and press representatives. In the afternoon we guided several groups of visitors across the vessel, and their enthusiasm made us very happy.

For the evening the Captain and the Chief Scientist had invited 120 guests and representatives of public life, including 13 Ambassadors from different EU countries for a festive reception on board the vessel. The BMBF had also taken the opportunity of MARIA S. MERIAN's visit to invite for the workshop "Germany – Competent Partners in Marine Research" on 21 May. For this event also representatives of the most important German

marine research institutions had arrived. Scientists and crew members passed the day in Sevastopol under bright sunshine and could explore the city and its surroundings.

On 22 May R/V MARIA S. MERIAN left Sevastopol and arrived already in the afternoon at the working area of the western Sorokin Trough. The last AUV map we had compiled on the „nameless mud volcano“ was the basis for our subsequent ROV dive which during the night became one of our highlights. Contrary to the flat Dvurechenskii mud volcano (Fig. 12) the “nameless mud volcano” is characterised by its detailed morphology. A ring elevation is followed to the inside by a ring depression bordering the central active area of about 150 m in diameter. This central area is characterised by a small scale morphology, too, which we could understand to the smallest detail due to the high resolution ability of our Bremen AUV SEAL 5000. Thus the biggest surprise was found in the mud volcano’s center where considerable quantities of free gas bubbled into the water column. There were a big mud pond and several smaller mud pools to be found which were filled with very liquid mud, and where the methane emissions bubbled into the water in a very spectacular manner. As per our knowledge such spectacle has never been documented on a mud volcano in the depth of 2000 m.

Highly motivated by these deep sea scenes we continued the sampling program, and our fifth ROV dive ended very successfully early in the next morning. A gravity core sampling was accomplished in the outer central area of the volcano and a further gravity corer fitted with temperature loggers was discharged more than 50 m deep into the seafloor of the centre. The existing temperature of 30°C shows the high activity of the mud volcano. Furthermore the Whitsunday was characterised by the transit to Georgia and gave opportunity to everybody for maintenance of our labs and devices as well as for personal matters.

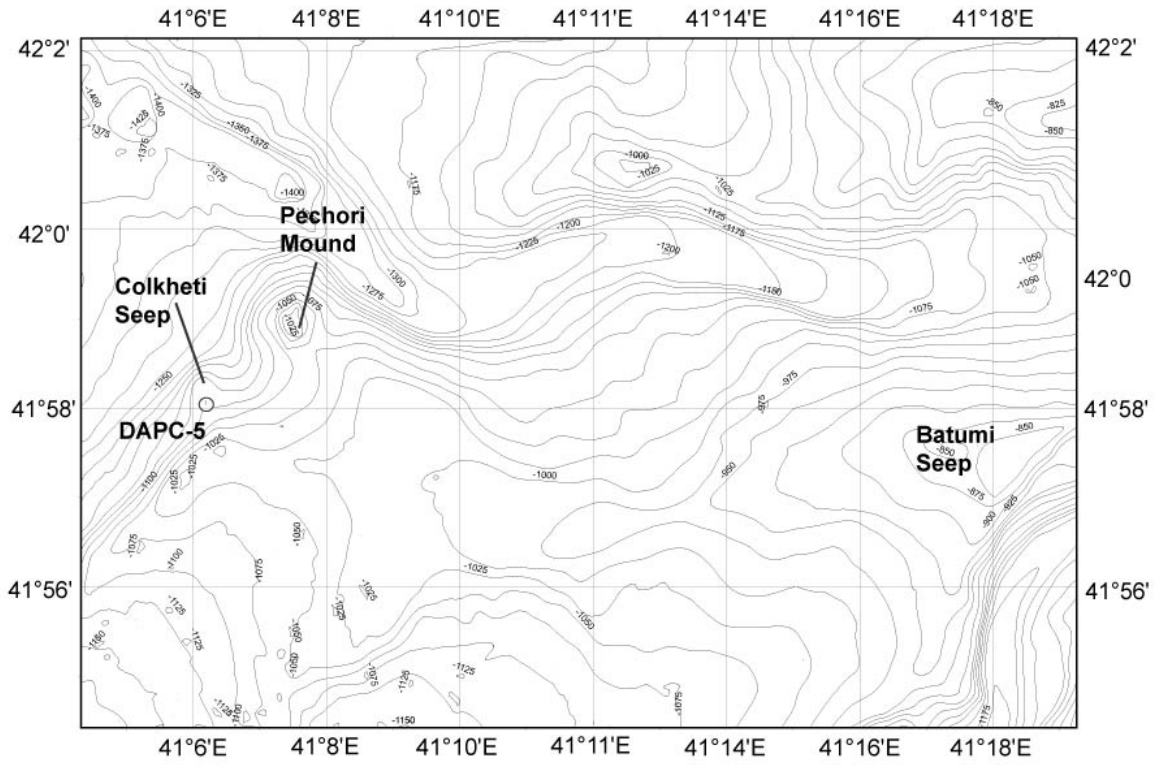

Fig. 14: Working area on Kobuleti Ridge showing the main seep sites and the sampling station at Colkheti Seep (for location of the area see Figure 11).

After a 24-hour transit from the first research area at Ukraine through the Russian sector arriving in the Georgian territory, on our way to the Batumi seep area, we approached a location whose position was known to us due to SAR slick analyses. There had been observed an oil slick on the water surface in several image series for a longer time which is fed by a source at the sea bottom (see Chapter 1.3). Actually we found a broad acoustic anomaly in the water column which indicates a gas emission site at the seafloor. Later during the expedition we wanted to verify the hypothesis that oil and gas escape together from the seafloor. First of all we now had to accomplish a dive at the Batumi seep area (Fig. 14). There, in an area of about one km², occur about 25 gas bubble streams in 10 distinguishable clusters. This is the area in the Black Sea with the strongest gas emission within the gas hydrate stability zone, and we have been prepared for an intense diving program here and at two oil seeps close by. During the first dive we analysed three of the known Batumi clusters, and a sonar module (called ASSMO) which would register the gas bubble streams for several days was left at cluster 3. After this first successful dive we accomplished an AUV mapping dive at the Colkheti oil seep which is about 12 km away. While AUV SEAL mapped its programmed track at the ground we could take first oil samples from the water surface in a rubber boat. In the late afternoon we were called by the German Embassy in Tbilisi advising us to stop our work. Although we had obtained the official research permission from Georgian authorities we were ordered to cease our work. The reason was that there were still some open questions on our research. As the following day was a Georgian holiday and we could already see the end of our cruise we decided to leave Georgia and to use the remaining time in Ukraine.

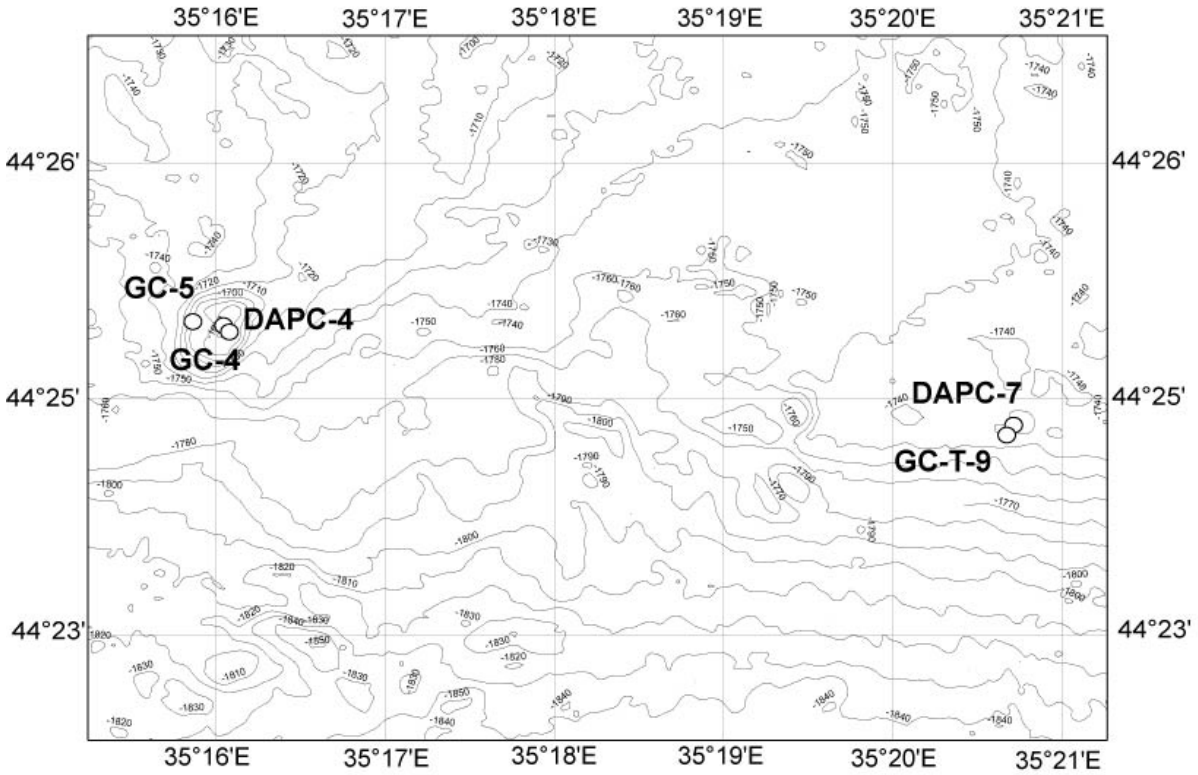

Fig. 15: Sampling sites on Tbilisi mud volcano (left) and the new flare site (right); for location of the area see Figure 11.

After a short dive to recover the ASSMO we steamed back to the eastern Sorokin Trough in Ukraine where the remaining four days would be used for detailed verification of three gas seeps. Those were the Kerch flare, the Helgoland mud volcano and a gas escape in 1700 m water depth connected to a fault. We produced detailed micro-bathymetric maps of all the three locations with the AUV SEAL 5000 giving us high-definition orientation for the accomplished ROV dives, so that our sampling and measuring program was efficient and under complete consideration of the geological structures (Figs. 13 and 14). The escaping gas could be successfully sampled at all the emission places so that we have information about their chemical composition and at the same time obtain important information about the sources. The fluxes of numerous bubble streams could successfully be defined, so that considering the exact seafloor mapping we could cover the regional extension of each seep. Due to this we will be able to present a quantification of gas emissions from the deep gas seeps of the Sorokin Trough soon after the analysis of the expedition, so that the scientific goal of the expedition has been reached. We are very glad about this because the technical challenge of this expedition was very high, and we are well aware that technical problems could heavily diminish the success of an expedition.

After the station program was finished RV MARIA S. MERIAN steamed to the entrance of the Bosporus. On Monday, 31 May we passed the Bosporus, Marmara Sea and Dardanelles towards the Mediterranean Sea where we berthed in the harbour of Elefsina (Greece) on Wednesday 2 May. We thank both captains, Friedhelm von Staa and Ralf Schmidt, and also their crew for the outstanding support of our scientific work on board the research vessel. At the same time we thank both teams of ROV and AUV, without their achievements we would not have reached our scientific goals. The ship time of MARIA S. MERIAN was provided by the Deutsche Forschungsgemeinschaft within the core program METEOR/MERIAN. We thank also all helpers of the “Leitstelle” in Hamburg, the shipping operator “Briese Schifffahrts GmbH” and the German embassies in Kiev and Tbilisi.

3. Multibeam Swathmapping

(P. Wintersteller, M. Roemer, H. Sahling)

The shipside mounted *KONGSBERG* EM120 multibeam echo sounder (MBES) has been used during MSM15/2 to survey the areas of interest (AOI) as well as transit lines to fill gaps in the ongoing bathymetric mapping of the whole Black Sea. Below listed the specification of the EM120 echo sounder on MS MERIAN:

Main operating frequency	12 kHz (varies from 11.25 to 12.60 kHz for sector coding)
Beams:	191/Ping
Apex angle:	2x2 °
Beam distance:	Angle constant or distance constant
Coverage:	up to 150° (recommended <130°)
Depth range:	20...11000 m
Depth resolution:	10...40 cm, due to other limits 0.2 to 0.3% of the water depth.
Pulse duration:	2 ms, 5 ms, 15 ms

3.1 Sound Velocity Profiles (SVP)

Four SVP's and several AUV-CTD profiles have been taken during the cruise. A shipside SvPlus 3453 probe was used to acquire the SVP's down to its max 2000 m water depth. The variability of sound velocity in surface waters mainly depends on the changes of water temperature. This can be seen within a very short period of some days during our cruise (Fig. 16). The area of Dvurechenskii mud volcano (DMV) has been visited twice, on12 and 17 of May. The temperature difference is about 3°C where else this makes a 10 m/s difference in sound velocity that visibly affect the MBES results.

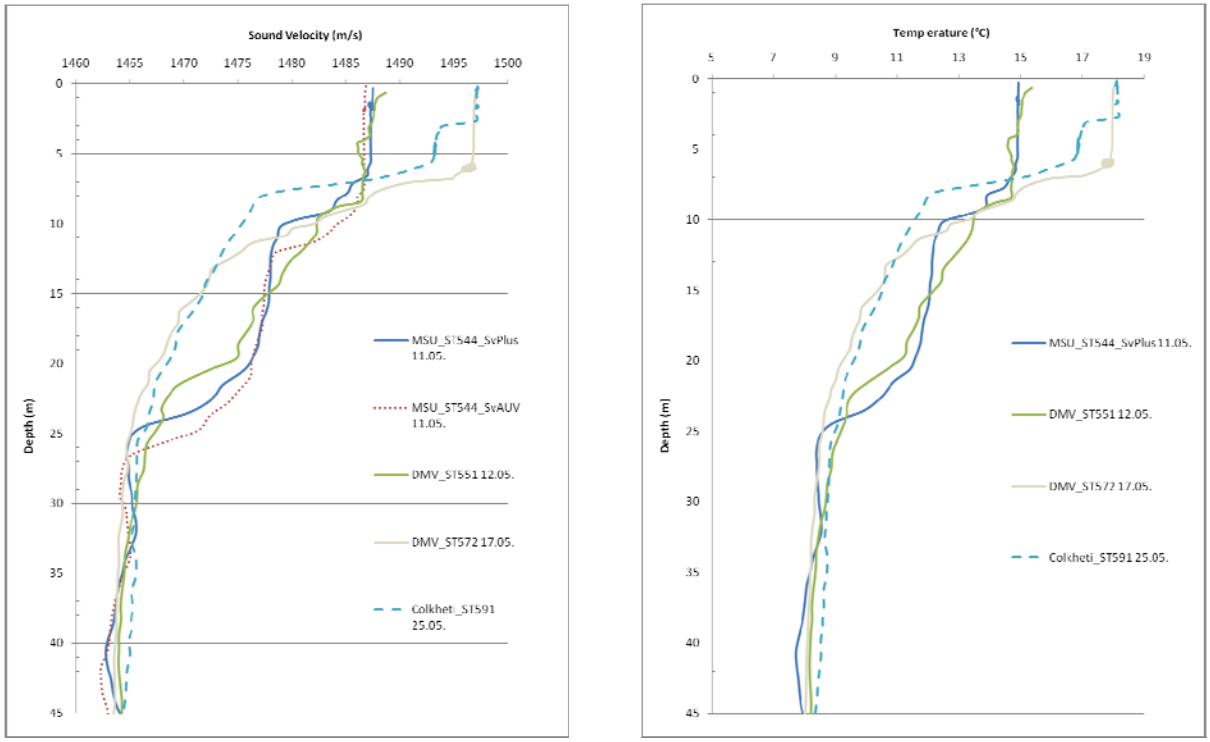

Fig. 16: SVPs by SvPlus compared with one AUV-CTD (left). Temperature taken with SvPlus (right).

Our measurements clearly fit to the climatic surface sea temperature fields based on hydrographical measurements (Simonov and Altmann, 1991) and satellite data (Ginzburg et al., 2004). Also one can assume an exchange of water masses between 8 and 25 m water depth looking at the two lines of DMV.

As soon as an SVP has been taken it was applied to the Kongsberg's acquisition software *SIS* in order to collect corrected data. Especially the multibeam data recorded during transits need sound velocity correction during final post processing since the applied SVP's do not match the conditions by distance to the place recorded.

3.2 EM120 Survey Settings

Since most of the AOI were already covered with former surveys this cruises aims were more detailed high resolution bathymetry with AUV and sub bottom surveys but only partly combined with shipside MBES. Wherever possible we tried to close some gaps in present bathymetric grids. Fig. 17a shows an overview of all the survey lines done with EM120 during this cruise. A quick onboard post processing has been carried out with NEPTUNE for backscatter and bathymetric maps. The final post processing is realised with CARIS HIPS&SIPS. The survey speed was varying between 2 and 6 knots but up to 12 knots during transits. The angular coverage for the swath was usually set to 110° or 120°.

The offsets and lever arms, given to the EM120 processing unit (PU), are stored in the so called "Installation Parameters" of *SIS*. These vessel unique values are very important for proper acquisition and post processing. All the given offsets refer to the vessels "Centre of Gravity", a given reference point. Since a SEAPATH GPS sensor is used, there are no offsets given for navigation at the installation parameters of the echo sounders. This offsets have been set inside the SEAPATH which combines GPS and motion reference unit (MRU) data and reference itself to the vessels reference point.

3.3 EM120 Results

Although the vessel mounted EM120 is just 2x2° in beamwidth grid resolutions of 15-30 m, show very detailed structures like dunes and tiny pockmarks especially in the Sorokin area (Fig. 17c). For a final post processing some data still need sound velocity correction.

All maps were made with ArcGIS v. 9.3, displayed in Mercator Projection with datum WGS84. For the overview map (Fig. 17a) the GEBCO dataset of 2003 is underlying.

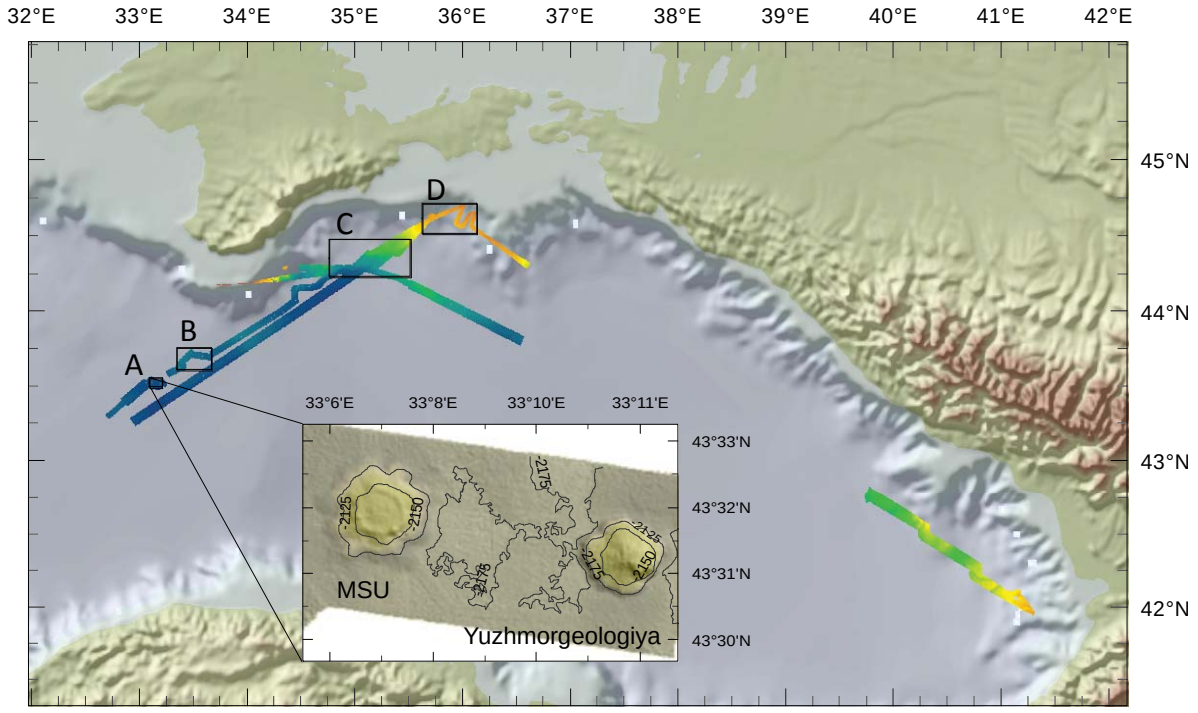

Fig. 17a: Overview of all lines collected during MSM15/2. The zoomed region (A) shows the two mud volcanos MSU (left) and Yuzhmorgeologiya (right).

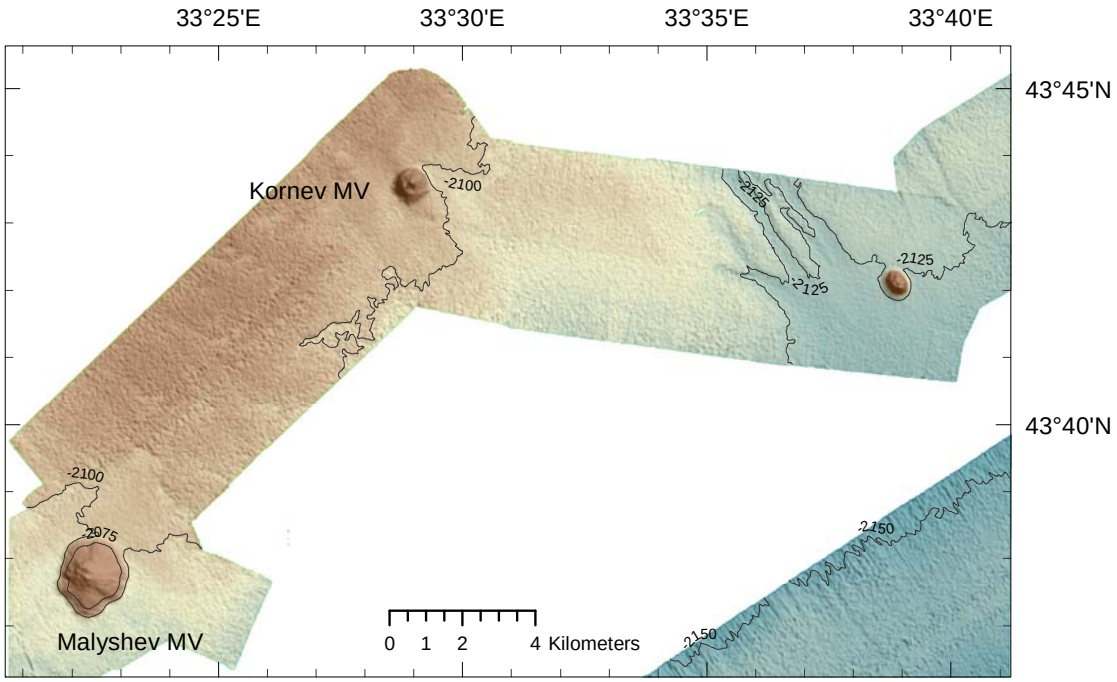

Fig. 17b: The mud volcanoes in the western part of the Black Sea have been visited before seeps in the Sorokon trough were studied.

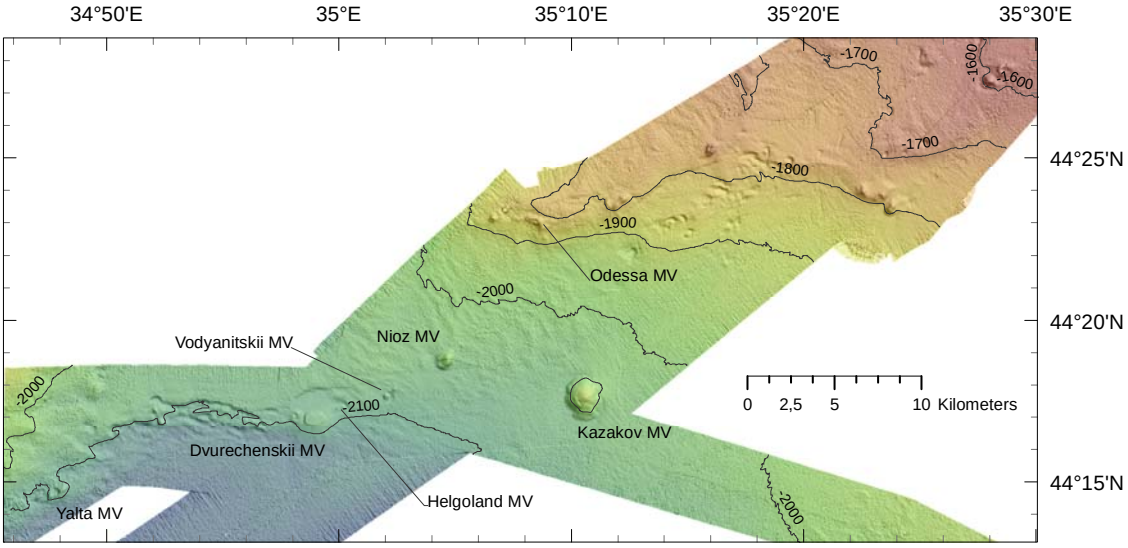

Fig. 17c: Area C shows the central part of Sorokin trough.

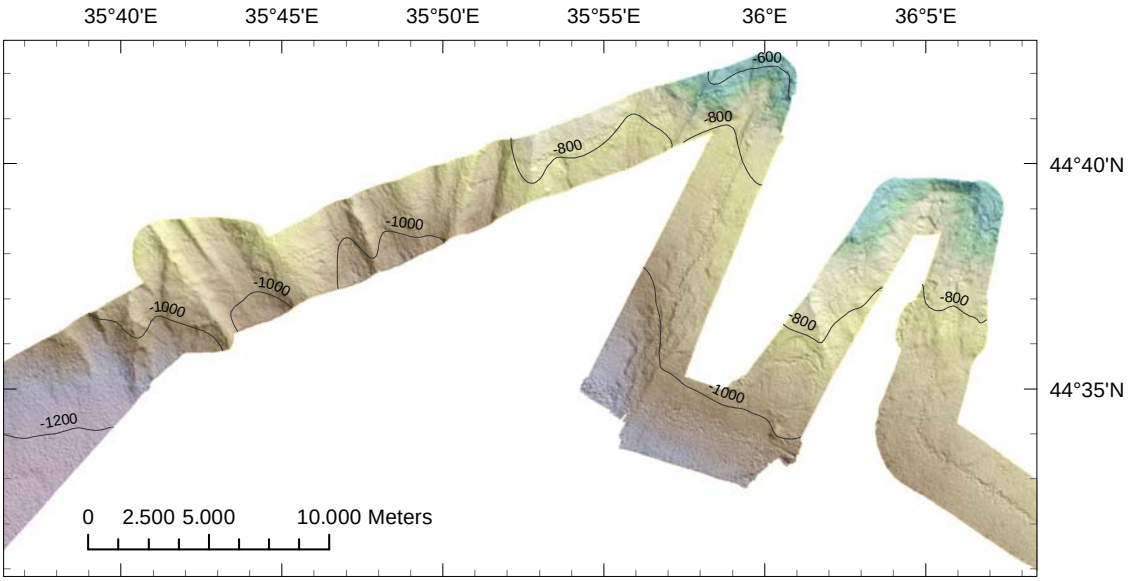

Fig. 17d: Area D is covering Kerch flare and the western part of the Kerch deep sea fan.

3.4 EM1002 Calibration

Due to the water depths at locations of AOI the vessel mounted EM1002, a shallow and mid-water MBES, was not used. Also, the moon pool, the EM1002 usually is situated, has been used for other acoustic instruments needed for AUV and ROV dives. During our transit to Piraeus the chief scientist has been asked to spend almost 6 hours calibrating the vessel side EM1002 echo sounder. Therefore Mr. Terje Moe, senior engineer from *KONGSBERG* came

aboard MS MERIAN in Istanbul, on Monday 31 of May 2010. We attended the calibration works since it is of expedient interest to us and other scientist working with MBES.

- The location for calibration must have flat ocean bottom at less than 100 m water depth. The test was performed with 2 cross lines perpendicular directions. This was done 3 times and 2 different sound velocity profiles were used, to verify the stability of the sound velocity. Recommended calibration method is 1 "long" line, with min 3 perpendicular cross lines.
- Important notice to further users: Parameter for "Outer Beam Angle Offset" was changed from 0.5 to 0.0. in SIS. Located under "Installation Parameters, System Parameters". This setting should not be changed.

The major problem of the EM1002 was a wrong calibration file that affected the outer beams.

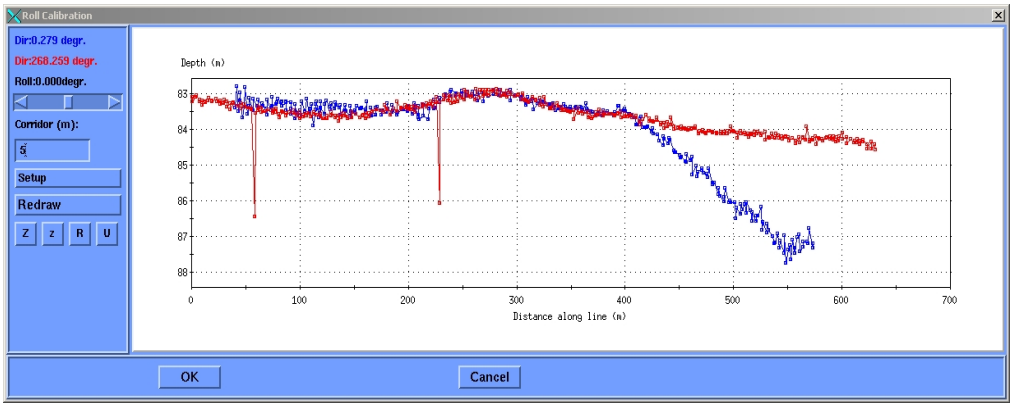

Above: Outer beam check with calib.txt, empty.

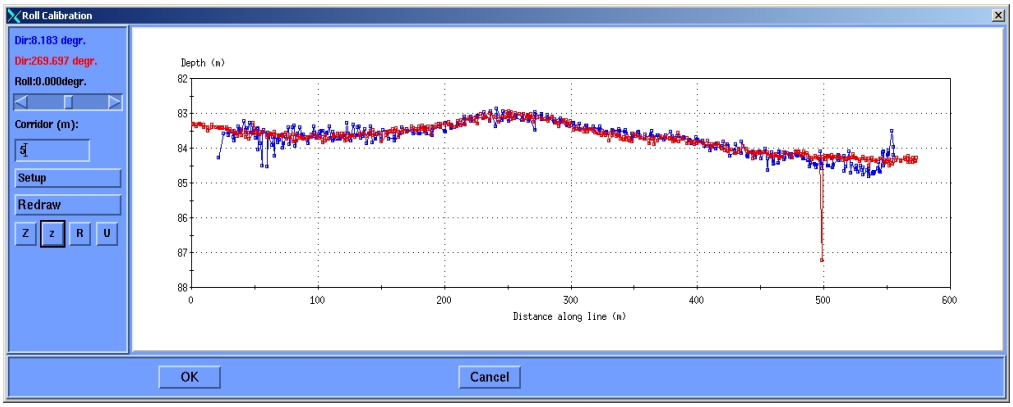

Above: Outer beam check with final calib.txt.

Fig 18: Below screenshots of all 111 beams related to the centre beam, during the baseline /cross line testing.

4. Subbottom Profiling and Plume Imaging

(M. Römer, P. Wintersteller, H. Sahling, M. Ivanov)

Integrated hydroacoustic systems were used to detect and localize gas emissions at the sea floor and characterize the shallow subbottom sediment structures in the working areas studied during this MERIAN Cruise MSM15/2.

4.1 Analytical Methods

In order to image bubbles rising up from the sea floor we used the echosound system PARASOUND, which works with the parametric effect of two primary released frequencies. Due to the two frequencies it is not only possible to use the resulting signal of 4 kHz (SLF) to image the subbottom structures but also to use the 19 kHz signal (PHF) for plume imaging in the water column. For this purpose the following hydrocontrol settings of the PARASOUND have been chosen:

Basic settings:
Transmission sequence: Single pulse
Transmission source level: Manual – Max TX Voltage; 160.00 V (maximum, 140.00 if system works not stable)
Pulse characteristics: Pulse length: manual; Manual pulse length: 0.500 ms; No. of periods: 2
Pulse type: Continuous wave Pulse Shape: Rectangular
Frequencies: Desired PHF: 19.3 kHz; Desired SLF or PLF: 4.00 kHz

Advanced settings:
Transmission beam width: standard (8*16 Elements)
Reception shading (for PHF+SHF and SLF+PLF):Mode: Shading table;
Shading table: No shading
Receiver band width: PHF+SHF: Mode: manual
PHF: output sample rate: 12.2 kHz Band width: 33%
SHF: output sample rate: 6.1 kHz Band width: 66%
SLF+PLF: Mode: manual Output sample rate: 6.1 kHz Band width: 66%
Receiver amplification:
PHF: Mode: Automatic; Gain shift: 30.00 dB SLF: Automatic
Sonar target settings:
Correlation: yes Targets in the water column: no
S/N Ratio: 20.00 dB for 1 m below transducer
Automatic transmission termination: OFF Stave data recordings: no

Sounder environment:
System depth source: Controlled by PHF Blanking output: no
C-Mean: Source: Manual Manual: 1500 m/s
C-keel: Source: Manual Manual: 1500 m/s
Desired bottom penetration: 150 m
Mode: Variable min/max depth limit (min. depth: 600 m, max. depth: 3000 m)

Operation:
Trigger: autonomous operation Data recording: all: full profile

The settings to choose in PARASTORE for PHF and SLF echograph imaging are highly dependent on water depth, water and weather conditions and have not been fixed. Generally the filtering in the PHF window have been used to image gas emissions in the water column: Low pass: on, Iteration: 2, High cut: 1.The amplitude scale is also important for this purpose: Clip: between 300 and 700 mV, no Threshold, negative Flanks Suppression or Gain. For SLF subbottom imaging no filtering has been used. Amplitude scale with a clip between 1000 and 3000 mV, no Threshold and Negative Flanks Suppression, but sometimes a Gain: Bottom TVC of 0.1 to 0.25 was chosen to get a deeper bottom penetration.

There have been error messages when for the storage of the PHF a window scale over 1000 m was chosen, so the window scale has been set always to 1000 m and not for the whole water column have been stored in the case the water depth was deeper than 1000 m. For storage mode the option “with phase and carrier” has been selected.

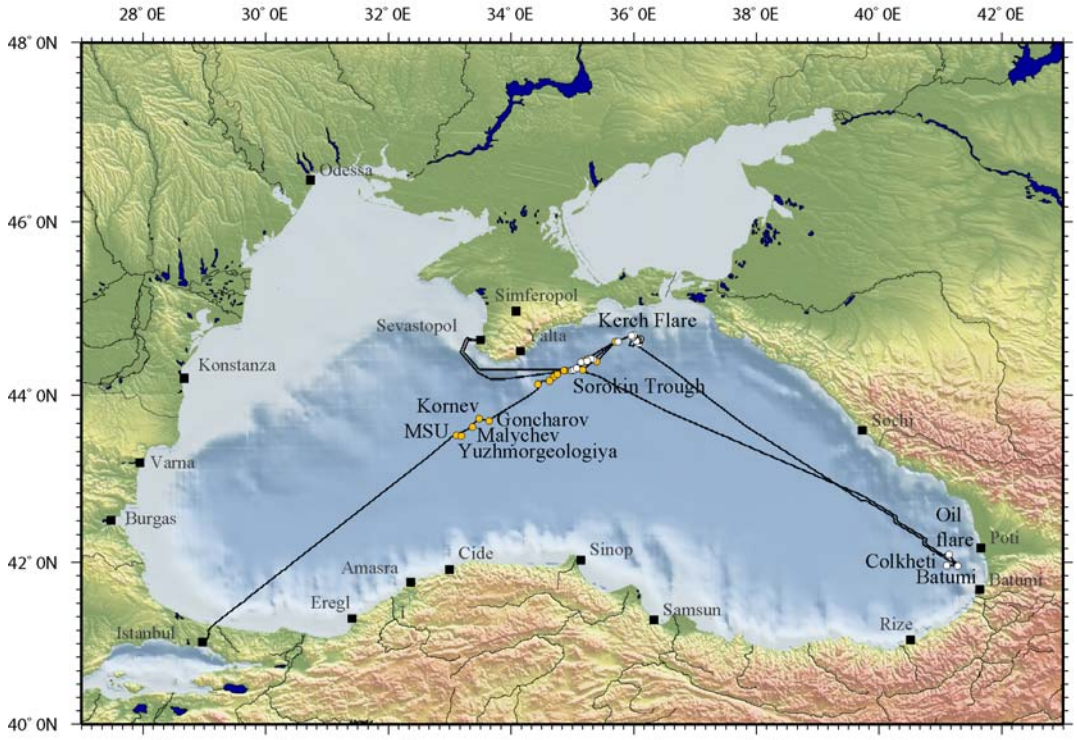

Fig. 19: Bathymetric map of the Black Sea with the ship track of MSM15/2. Passed seafloor structures are marked by points, whereas those with hydroacoustic anomalies recorded by PARASOUND echograph are white coloured and the inactive ones during observation time are illustrated by yellow points.

4.2 Results

During the 22 days of data recording and 15 PARASOUND-surveys 25 prominent morphologic structures have been crossed in order to detect gas emission sites. At twelve of them we could confirm active gas seepage as PHF images show obvious anomalies in the water column above these sites (flares). Table 3 list all of the crossed seafloor structures and their activity observed during this cruise.

Within the Black Sea we investigated four different working areas with known gas emission activities. The following map shows an overview of the track line and passed structures (points) of this cruise. Yellow points mark inactive sites; white points are active structures with flare observations.

4.2.1 Central Mud Volcanoes (MSU, Yuzhmorgeologiya, Malychev, Kornev, Goncharov)

All five mud volcanoes in this area have been crossed several times but no flare activity has been observed. Only the subbottom echograph has shown some interesting internal structures of MSU, which we interpreted as different mud flow layers illustrating the evolution of this structure.

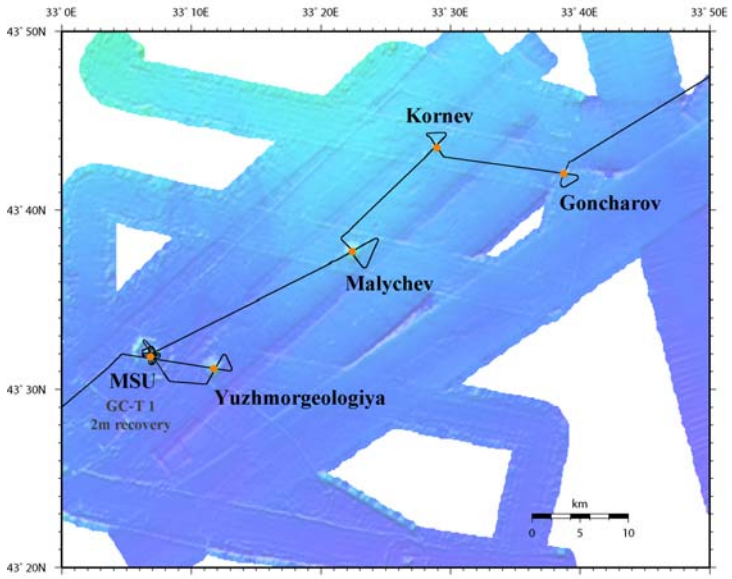

Fig. 20: Detailed map of the central area. Five mud volcanoes have been crossed in order to search for activity with PARASOUND echosounder but no gas flare has been observed at these structures.

In this working area lots of mud volcanoes are located in a relatively small area. Most of these mud volcanoes have been active during this cruise with exception of Kazokov and Istanbul MV. We also found a "New Flare Site" (NFS), which is not correlated to a mud volcano but to a fault zone known before due to side scan sonar images taken on an earlier cruise to this area. Several prominent sea floor structures described by Michelle Wagner (Wagner-Friedrichs, 2007) have been passed to prove their activity. Only at M12 we found gas emission during this cruise. The medium intense flare was observed 600 m high into the water column.

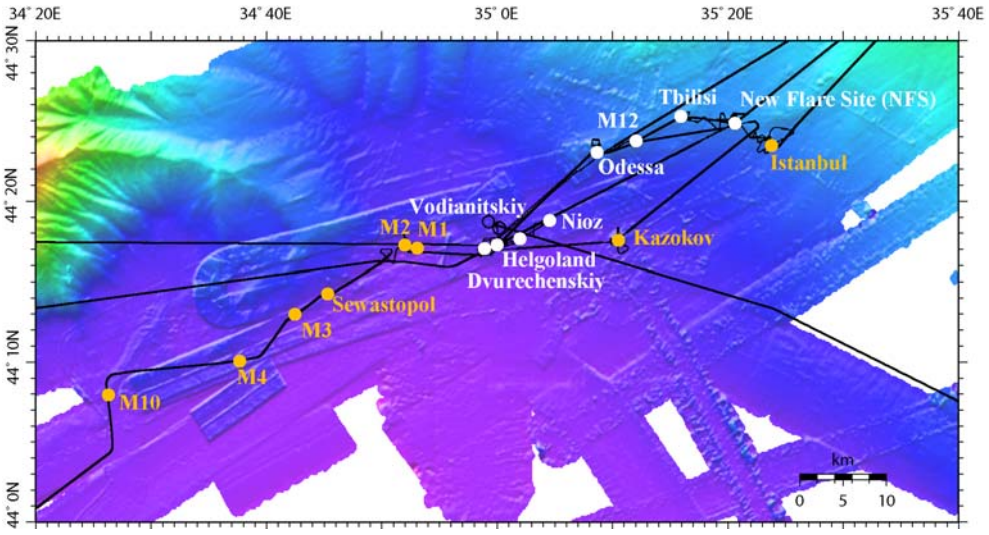

Fig. 21: Overview map of the Sorokin Trough. The black line is the ships track of MSM15/2 and points mark the seafloor structures crossed during the cruise. At the white coloured sites were flares observed.

4.2.2 Dvurechenskiy MV, Helgoland MV, Vodianitskyi MV and Nioz MV

All four mud volcanoes have been surveyed during this cruise in detail and all have shown active gas emissions. They have been investigated also in former cruises and are known to be instable in activity.

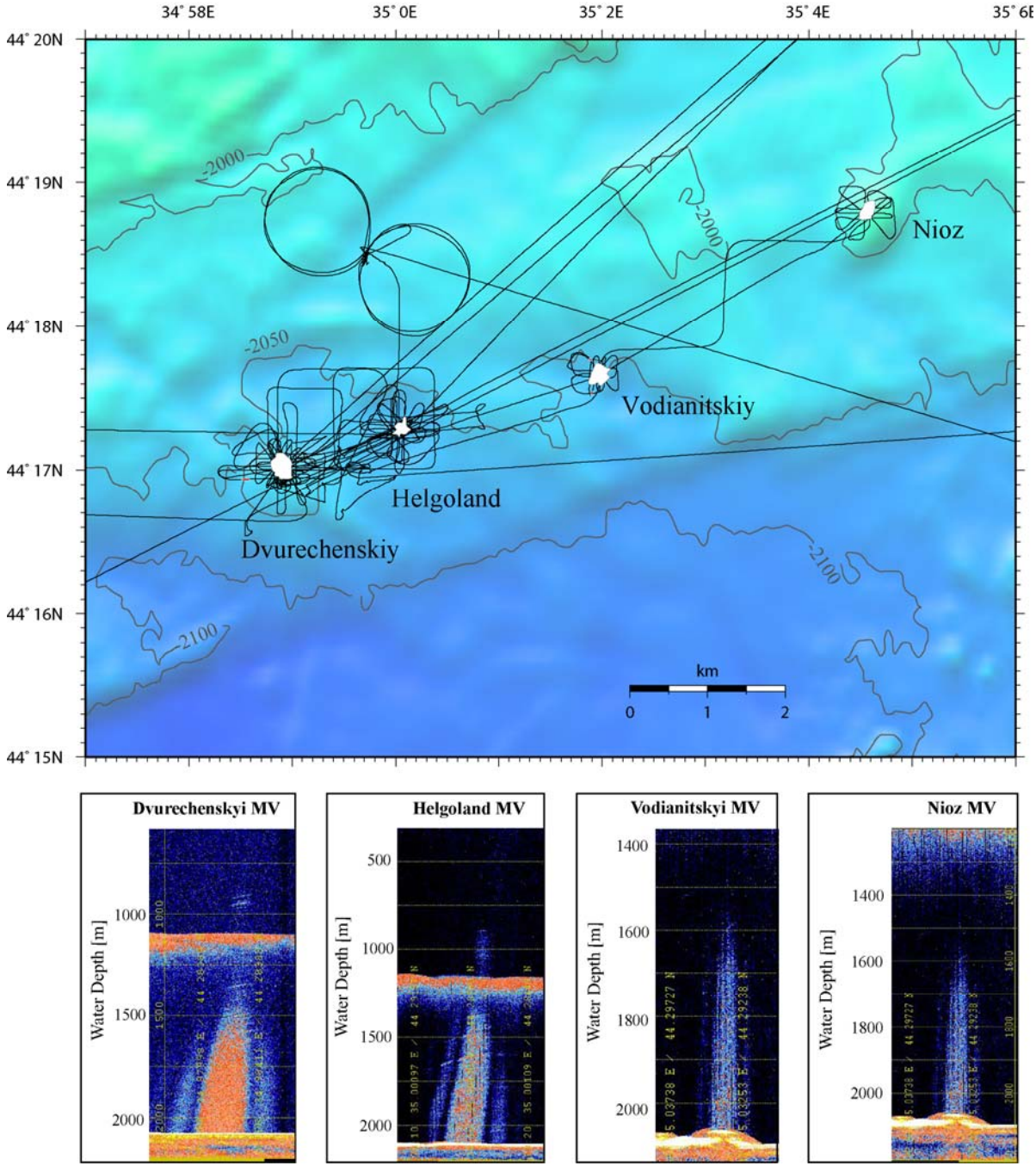

Fig. 22: a. Detailed map of the four mud volcanoes in the Sorokin Trough which have been intensively surveyed. The highlighted white patches illustrate the area where flares have been recorded during the PARASOUND surveys. **b.** Each echogram shows the flare of the four mud volcanoes. The images of the flares often show sidelobes, as clearly visible in these examples. This are artefacts and do not indicate several emission sites.

4.2.3 Odessa MV and M12

M12 was crossed during transit and not investigated in more detail but at least we could prove that there is an active seepage related to this morphologic structure. Odessa MV has been surveyed several times due to preparation for a possible dive site. We observed at least two flare sites at this uncommonly formed mud volcano structure and it seems to change the active sites within several days. During the first survey the most intense flare was in the southwestern part of the mud volcano whereas the survey at the end of the cruise we observed the centre of activity northeast wards where only a weak anomaly has been observed before.

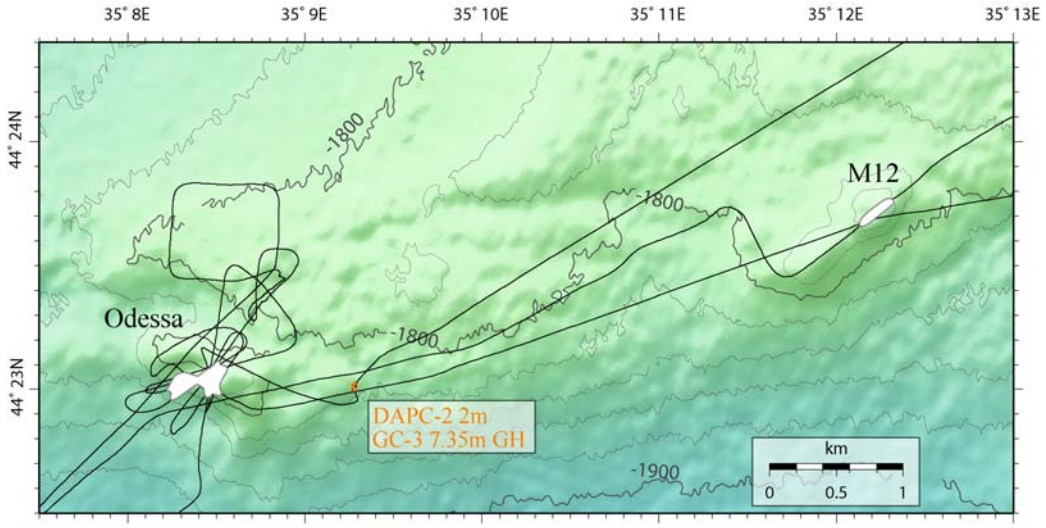

Fig. 23: Bathymetric map of Odessa MV and M12. Both were actively degassing during the cruise proven by anomalies recorded during PARASOUND surveys.

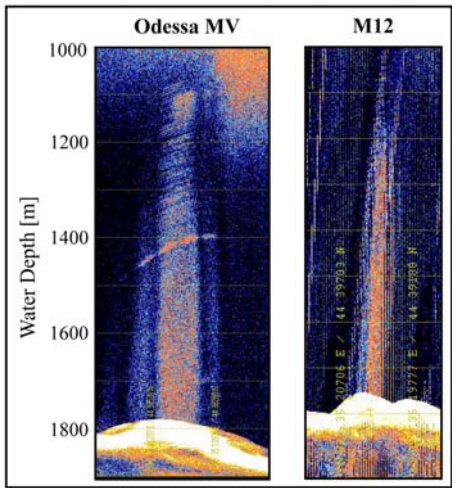

Fig. 24: The echograms show the flares observed at Odessa MV and M12. The flare at Odessa MV is up to 900 m high, at M12 up to 600 m into the water column.

4.2.4 Kazokov MV

A short survey has been performed at this huge mud volcano. Kazokov MV is the greatest and highest mud volcano in the area. No gas emission is known, but in former expeditions coring proved gas hydrate abundance in shallow sediment depths. We crossed the peak of the mound several times without any evidence of gas emissions but due to the great extend we cannot state that we mapped the entire structure without gaps.

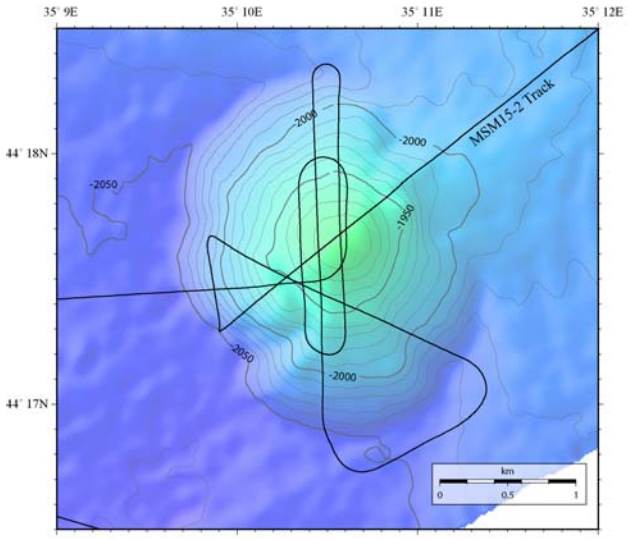

Fig. 25: The bathymetric map of Kazokov MV. The line shows the short survey crossing several times the mud volcano structure.

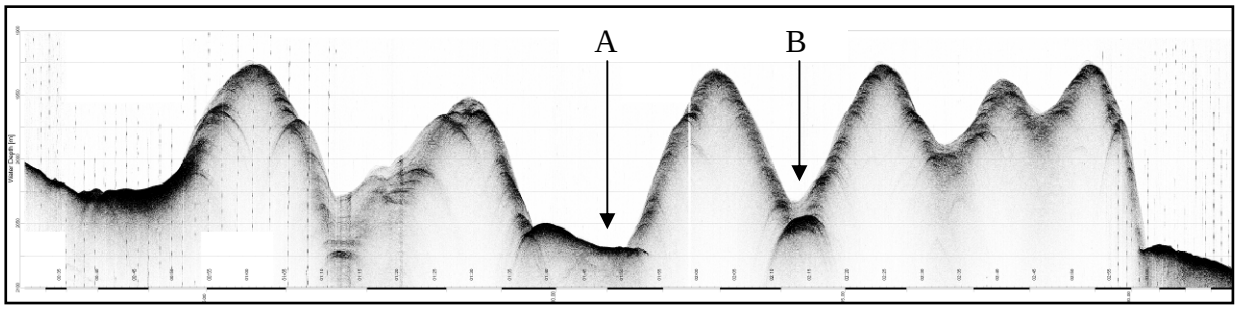

Fig. 26: The SLF record of the survey crossing Kazokov MV. A and B mark start and end point of S-N profile indicated in Fig. 25.

4.2.5 Tbilisi MV, Istanbul MV and "New Flare Site" (NFS)

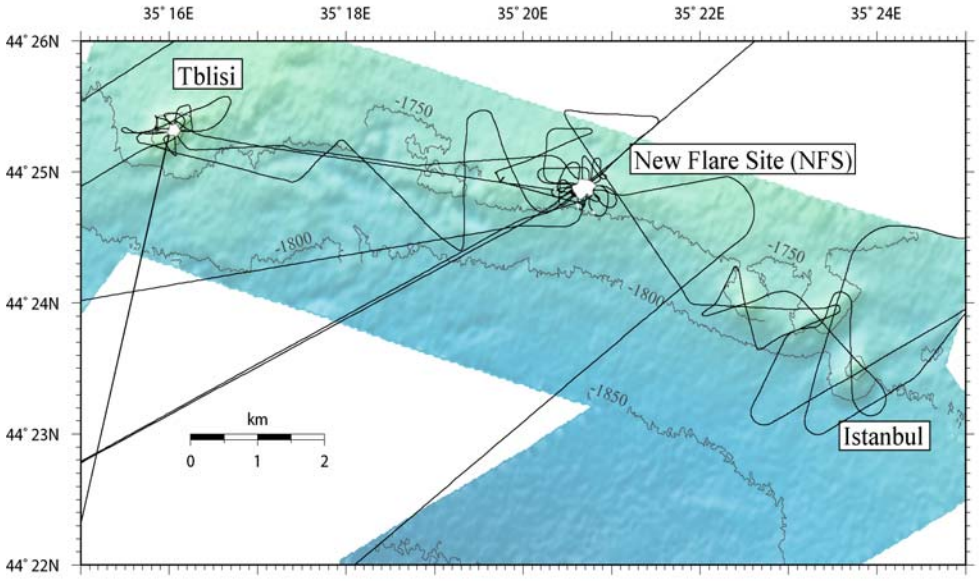

Fig. 27: Track lines crossing several structures that probably are actively degassing in the area of Istanbul MV and Tbilisi MV. Istanbul MV did not show any anomaly during the cruise, but a new site (NFS) has been found with a strong flare in the PARASOUND records and intensely surveyed.

Istanbul MV did not show any gas flare in the PARASOUND recordings but at Tbilisi MV we could detect and locate an over 500 m high flare right at the peak of the mound. Bathymetric maps show a crater like structure east of the mound but the flare is clearly related to the centre of the mud volcano and not to this crater. By accident we found a new emission site by crossing some pronounced backscatter anomalies visible on a sidescan sonar map acquired during a former TTR cruise. The intense and more than 1000 m high flare is obviously connected to a fault trending W to E and is probably a result of several emissions located along this fault zone.

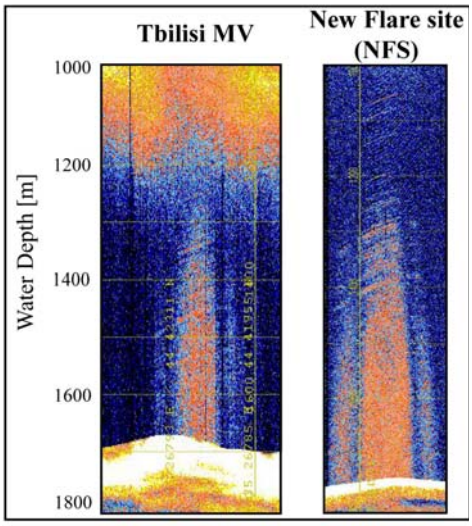

Fig. 28: The echograms of Tbilisi MV and NFS show intense gas emissions up to 500 and 1000 m into the water column, respectively.

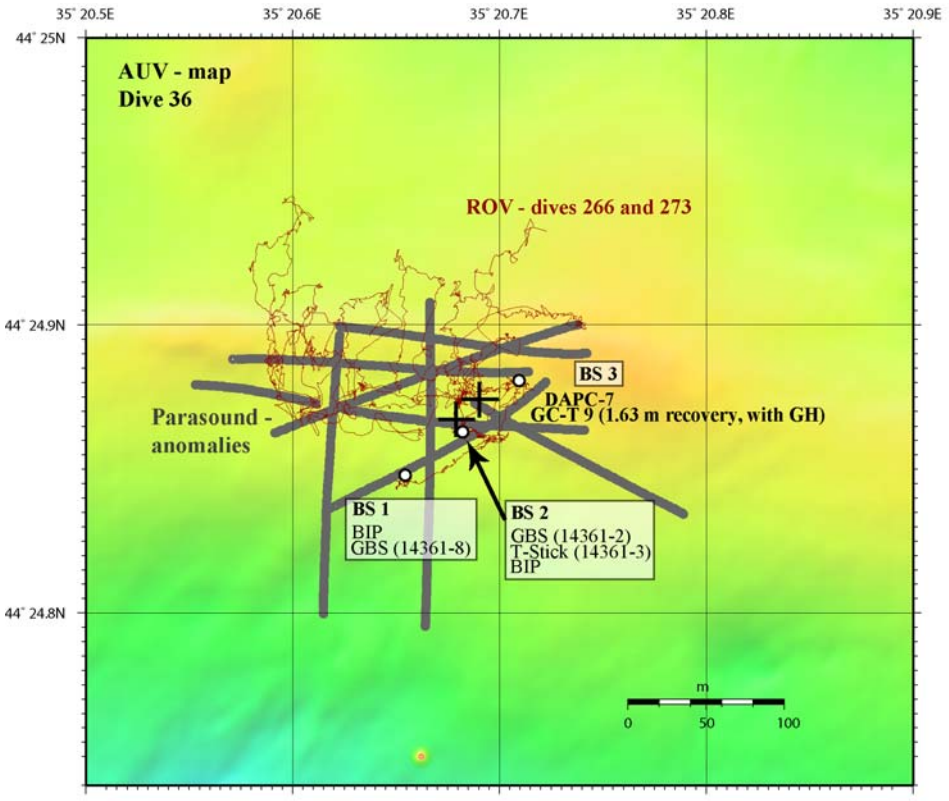

Fig. 29: Bathymetric map conducted with AUV (Dive 36) of the NFS. The red line shows the ROV-divetracks, grey lines indicate the locations where anomalies in the water column have been recorded during PARASOUND surveys. The three white points are the positions where bubble streams have been found at the seafloor during ROV dives 266 and 273.

4.2.6 Kerch Area (Kerch Flare and Kerch Fan)

Kerch flare has been surveyed several times to locate and detect the gas flares as exact as possible for ROV-dive preparation. A survey along the Kerch Fan in water depths between 600 and 900 m resulted in, beside the known shallow water flare sites, two new flares in water depth within the Gas Hydrate Stability Zone (GHSZ). Although this occurrence prove that Kerch flare is not the only emission site within the GHSZ in this area, both new sites show very weak intensities and rising heights less then 200 m.

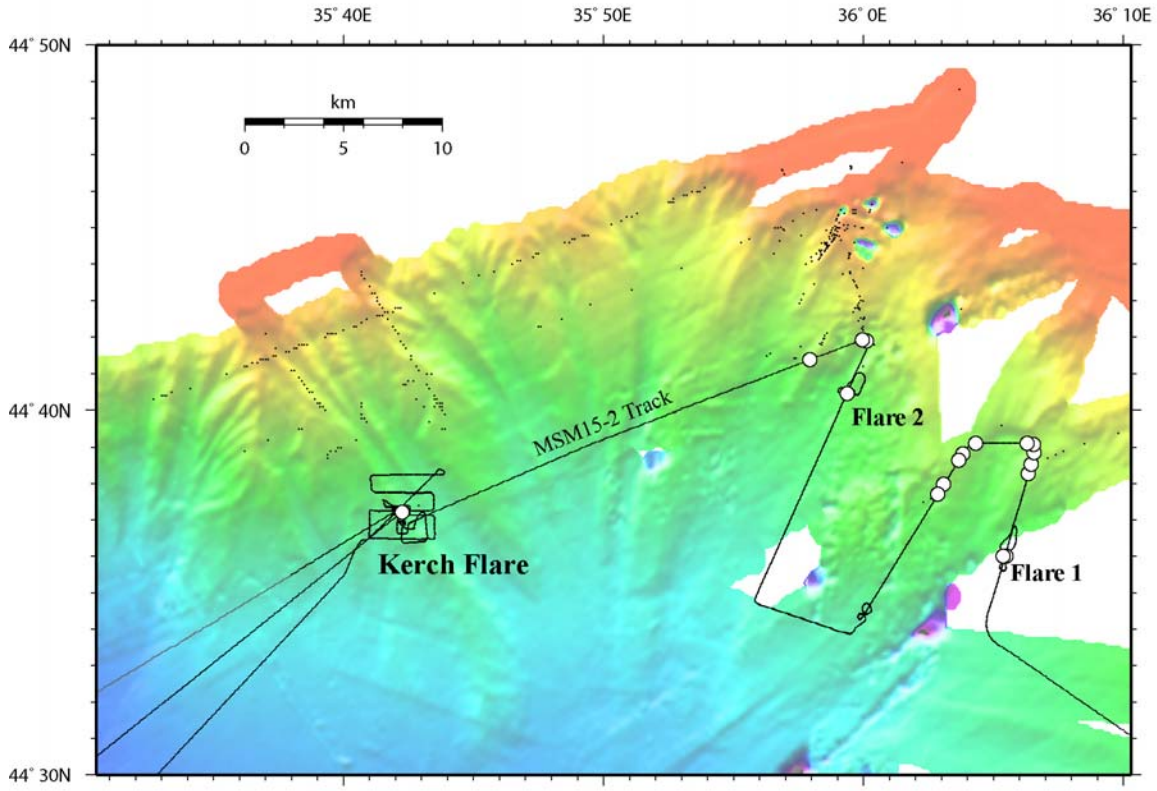

Fig. 30: Bathymetric map of the Kerch area. The black line shows the ship track and red points indicate the flares recorded during the PARASOUND surveys.

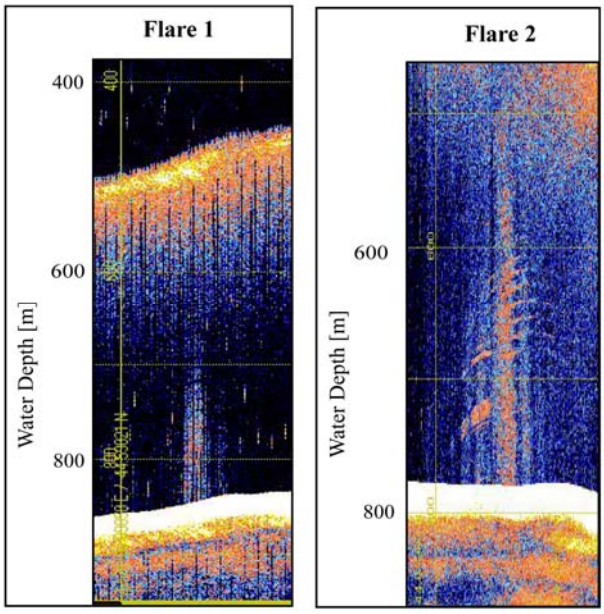

Fig. 31: The two echograms show the flares observed during the PARASOUND survey conducted in the Kerch area which indicate gas emissions within the GHSZ.

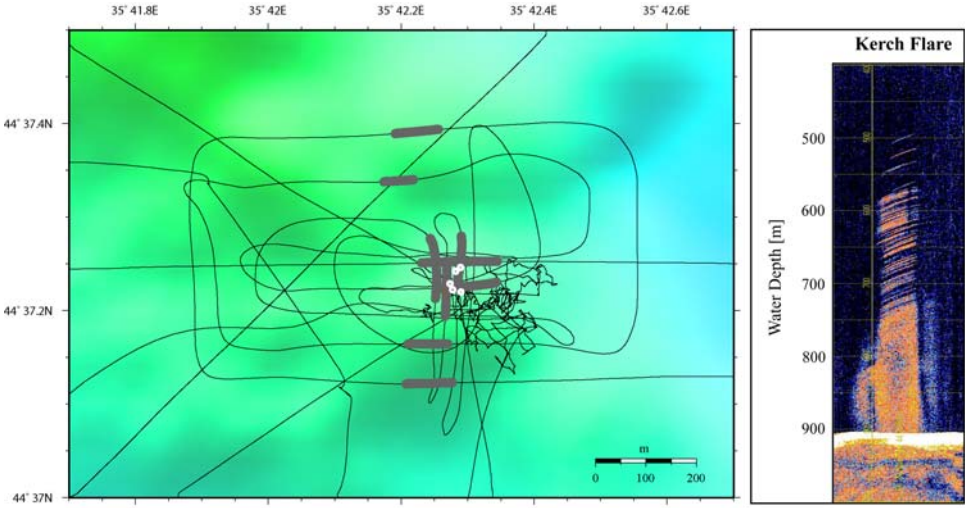

Fig. 32: Detailed map of the Kerch flare. The black line is the ship track indicating the detailed survey conducted at this site in order to detect gas flares. The bold yellow line marks the locations where anomalies have been observed during this survey. The echogram shows an example of a flare recorded at this site.

4.2.7 Georgia (Oil Flare, Batumi, Colkheti)

In order to fill the gap in the bathymetry and due to oil slick observations in SAT images we passed a ridge without any evidence for bubble emission so far. Fortunately, a pronounced and more than 300 m high flare was found. We crossed it two times but could not spend more time for detailed investigations. At the Batumi seep area we had no detailed survey but used the PARASOUND during dive operations when the ship was located over the seep area without moving. In these recordings very strong gas emissions were observed that rose at least up to 100 m below sea floor. The noise of fish and particles in the echograph in the upper 100 – 150 m in the water column makes it impossible to state if the bubbles reach the sea surface.

Also due to lack of time at Colkheti there has not been any survey for flare search but during DAPC deployment the PARASOUND was recording and a strong flare of up to 1100 m height was observed.

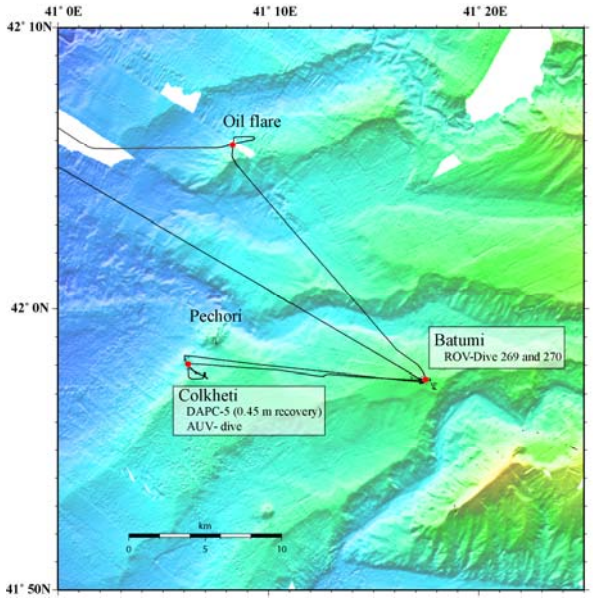

Fig. 33: Bathymetric overview map of the working area offshore Georgia. The ship track (black line) shows that the area at Batumi and at Colkheti have been shortly investigated during MSM15/2. A new flare, called here “Oil flare”, has been found on the way to Batumi.

Table 3: Passed structures and their activity observed during MSM15/2.

Mud volcano/structure	Flares	Intensity of acoustic sig.	Date	Lat N	Long E	Flare height (max)
MSU	no		11/05/2010	43°31.832	33°06.848	
Yuzhmorgeologiya	no		11/05/2010	43°31.173	33°11.742	
Malychev	no		11/05/2010	43°37.692	33°22.437	
Kornev	no		11/05/2010	43°43.485	33°28.962	
Goncharov	no		11/05/2010	43°42.039	33°38.750	
Dvurechenskiy	1	strong	12/05/2010	44°17.030	34°58.936	1250 m
Helgoland	1	strong	11/05/2010	44°17.281	35°00.015	1300 m
Vodianitskiy	1	medium	13/05/2010	44°17.668	35°01.974	800 m
Nioz	1	weak	14/05/2010	44°18.791	35°04.556	700 m
Odessa	2	medium	14/05/2010	44°23.020	35°08.657	900 m
Kerch Flare	1	strong	14/05/2010	44°37.214	35°42.276	480 m
Istanbul	no		16/05/2010	44°23.457	35°23.799	
New Flare Site (NFS)	>1	strong	16/05/2010	44°24.859	35°20.646	1000 m
Tbilisi	1	medium	16/05/2010	44°25.264	35°15.954	> 500 m
Kazokov	no		17/05/2010	44°17.542	35°10.507	
M12	1	medium	18/05/2010	44°23.750	34°12.067	600 m
M1	no		11/05/2010	44°17.067	34°53.100	
M2	no		11/05/2010	44°17.250	34°52.033	
M3	no		11/05/2010	44°12.983	34°42.483	
M4	no		11/05/2010	44°10.067	34°37.683	
M10	no		11/05/2010	44°07.933	34°26.300	
Sevastopol	no		11/05/2010	44°14.233	34°45.317	
Batumi	1	very strong	25/05/2010	41°57.469	41°17.407	> 700 m
Colkheti	1	strong	25/05/2010	41°57.753	41°06.541	1100 m
Oil flare	1	strong	25/05/2010	42°05.882	41°08.380	300 m

5. Posidonia 6000 Acoustic Positioning System

(P. Wintersteller)

IXSEA's Posidonia 6000 is an ULTRA SHORT BASE LINE (USBL) acoustic positioning system used aboard MARIA S. MERIAN (MSM) for deep sea ROV/AUV vehicle tracking as well as positioning moorings (MO), gravity cores (GC) and (TV-) multi cores (TV/MUC).

The system is based on a bi-directional exchange of acoustic signals between one or several acoustic transponders and a fixed acoustic array, mounted in one of MSM's moon pools. Fig. 34 shows the current installation on M.S.Merian.

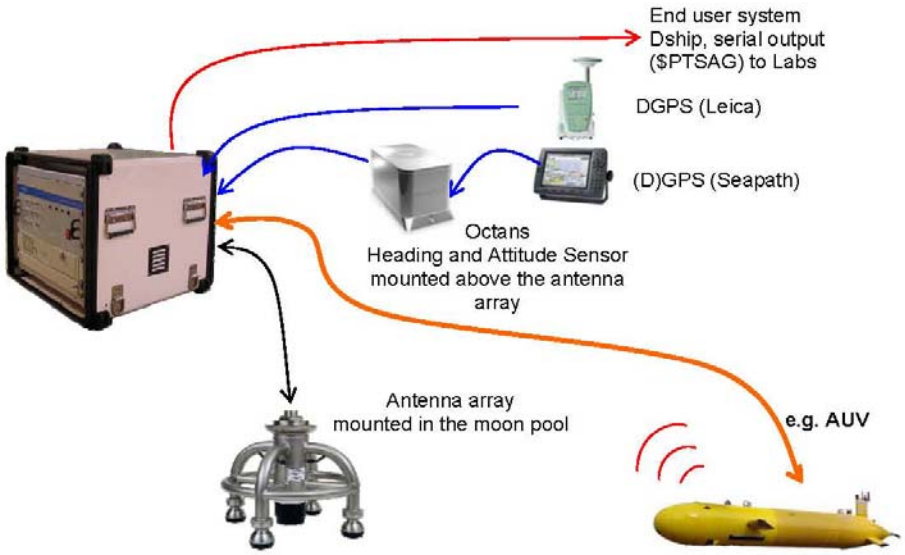

Fig. 34: Installation on MSM (Images partly from IXSEA's presentation of Posidonia 6000).

5.1 Specifications

According to the manual of Posidonia 6000 the following specifications are given:

Parameters	**Value**
Vehicle depth	50 m to 6000 m
Positioning accuracy on X,Y,Z	0.3% of the range at 1 sigma
Measurement repeatability	+/- 3 m

The system is designed to operate optimally in the following conditions:

Parameters	**Value**
Sea state	≤ 5
Maximum ship speed	Operational: 3 knots Transit: 12 knots
NIS ship noise	≤ 60 dB ref. 1µPa/√Hz
Coverage area	conical sector of +/- 30° below the ship
Storage temperature	-20°C to +70°C
Operating temperature	-5°C to +35°C
MRU sensor accuracy	σ roll: ≤ 0.15° σ pitch: ≤ 0.15° σ heading: ≤ 0.15°

Given accuracy for the Octans MRU:

Parameters	**Value**
Heading	0.1 deg secant latitude
Roll & Pitch	0.1 deg
GPS	GPS is used but not processed => absolute accuracy of POSIDONIA is affected by GPS noise and possible dropouts

5.2 Configuration and Calibration

The Octans motion reference unit in a wet pot, situated directly above the antenna array, has been calibrated in Sep. 2006. No changes where made. Also the given configuration file has been kept.

A calibration of the system has been done during MSM13/3. Find below the settings we used until 23 Mai. Due to mechanical malfunction of the starboard-side moon pools lifter we were forced to use the portside moon pool from this day on. Therefore a new calibration was necessary. For the hole duration of the cruise MSM15/2, the Posidonia GPS information was based on the output of the onboard SEAPATH-System.

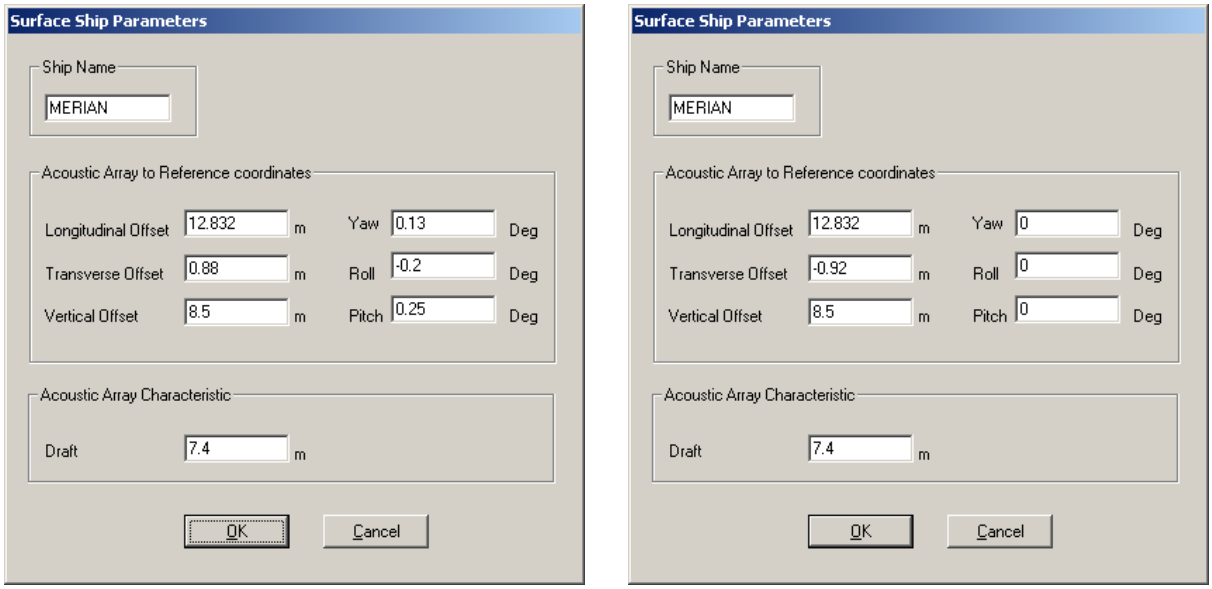

Fig. 35: Settings used until 23 May (left), settings during calibration (right).

5.2.1 Posidonia Calibration (23 May)

For the calibration a mooring with a releaser is needed. Once deployed in about 2000 m water depth the ships track should form an eight above the mooring with a circle diameter of min. 1400 m. For the calibration all parameters in terms of Yaw/Roll/Pitch needs to be set to zero (see above Fig. 35).

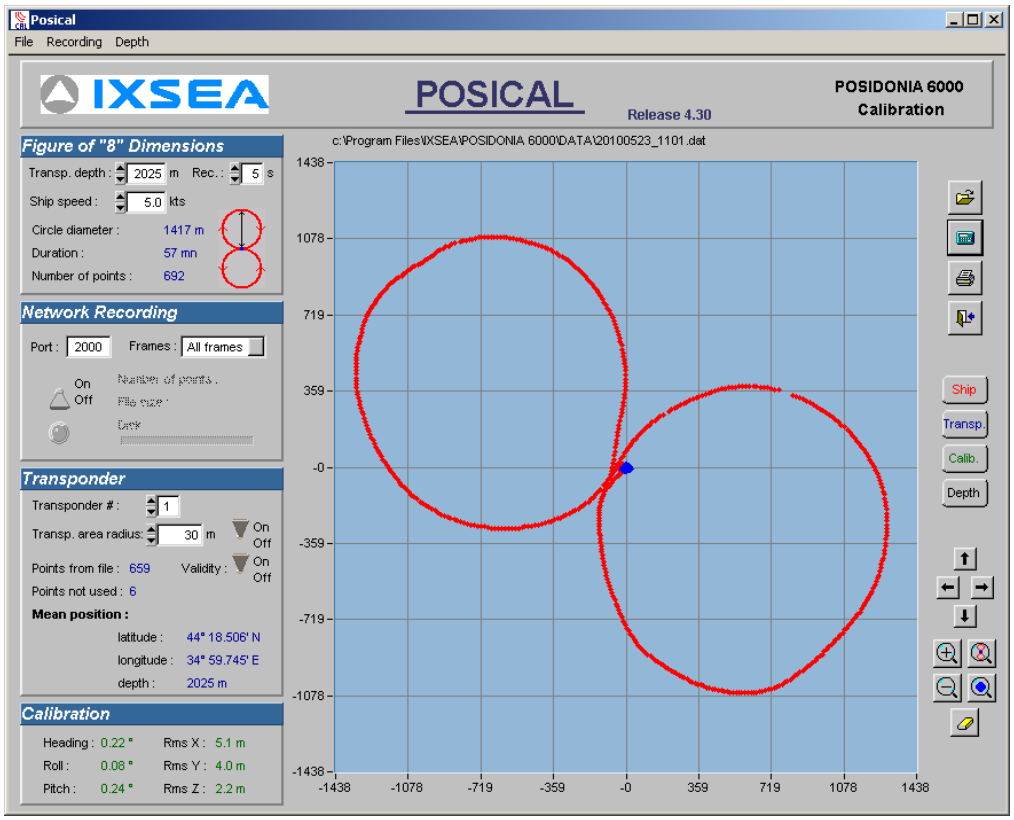

Fig. 36: The calibration track is being recorded through Posidonias acquisition software *ABYSS* and can be replayed afterwards in software called "*POSICAL*" (ABYSS-POSICAL screenshot right after calibration.)

Using the calibration results, shown in the lower text, we did a second circle to approve the result. The values for Roll/Pitch and Heading should be towards zero.

Calibration:

Heading:	-0.00	Rms X:	4.8 m
Roll:	0.01	Rms Y:	4.3 m
Pitch:	0.09	Rms Z:	2.3 m

5.3 Operational Mode

Four transponders were used during MSM15/2 cruise. Transponder #1, a ship owned releaser-type #482, was mainly used on the wire for GC and TV/MUC. Transponder #2 and #3 where used and owned by the MARUM-ROV QUEST4000, where else #4 is the AUV-mounted transponder. The transponder numbers #1 to #4 belong to an internal list of *ABYSS*. It is important to mention that only the transponders #1 to #3 are recorded inside the shipside database DSHIP. The reason simply is that there is no place holder for more transponders created inside the database. Thus the ROV transponder #3 has been replaced in the ABYSS list by the AUV transponder temporarily. The settings in terms of frequency and blanking time can be seen in the following figures.

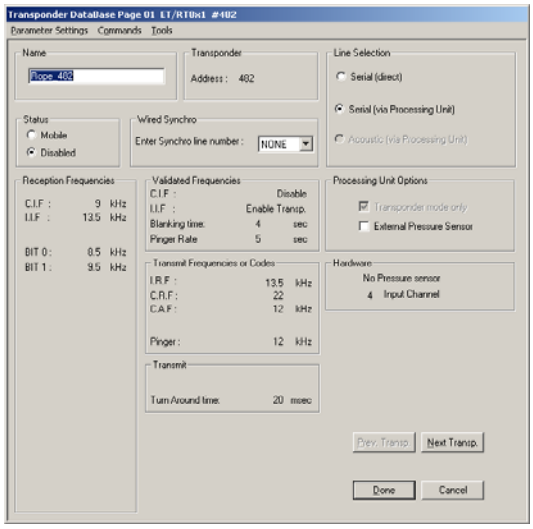

Acoustic release

Fig. 37: Screenshot of Transponder # 1, used on the wire for GC and TV/MUC.

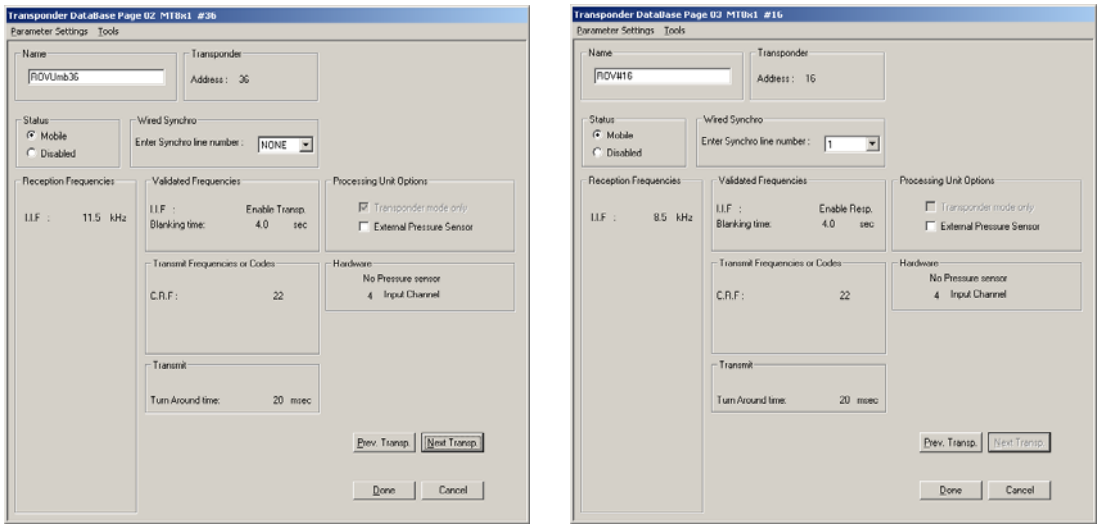

Fig. 38: Screenshots of Transponder # 2 (ROV Rope), left, Transponder # 3 (ROV), right.

Based on the experiences during post processing it is recommended to use filtering during acquisition. There are different filters depending on the equipment and their behavior. “Lissage” and “Rejection” where applied for the most ROV- as well as AUV-dives.

6. TV-Sled Investigations

(H. Sahling, M. Römer)

During the MS MERIAN Cruise 15/2 the TV-sled was used only once in the area of Kerch flare (Station 596). The objective of this deployment was to systematically look for evidence of gas bubble emission using the horizontally looking sonar Imaginex Model 881A (max. water depth 1000 m). The sonar was mounted about 30 m above the frame of the sled allowing scanning the surrounding without significant disturbance by the frame of the sled itself (Fig. 39). Towing at 30 m above the bottom and applying a range of 50 m during the scans were adequate settings in order to detect gas bubble emissions.

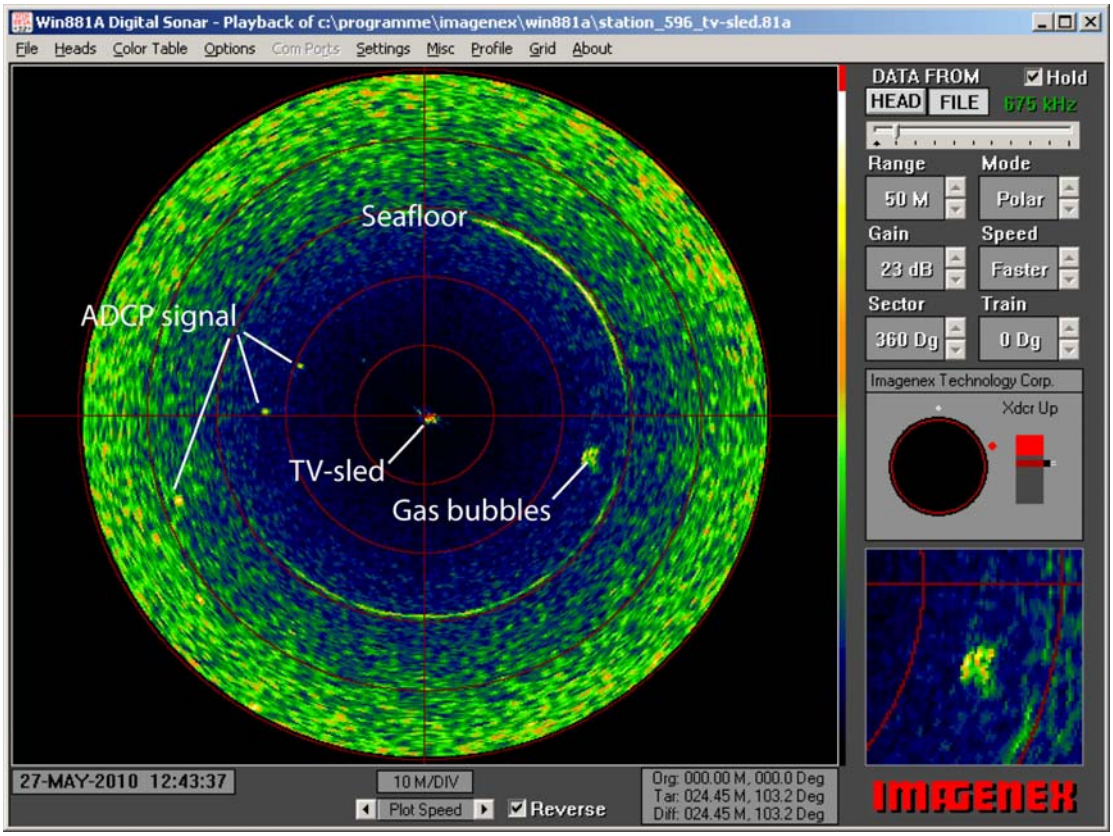

Fig. 39: Screenshot of the horizontally looking sonar mounted on the TV-sled.

After finding the evidence for bubble emission the sled was lowered to the seafloor in order to observe it by the two video cameras (black and white, colour). Two Xenon lights provided the necessary light, and the Posidonia transponder mounted on the wire 20 m above the bottom provided accurate positions. The video signal was recorded digitally and, in addition, the colour video recorded by a conventional video recorder. With this set-up, the bubble emission site was found and ship directed to the exact spot within about an hour. Five bubble streams of different intensities could be observed. During the second part of the deployment the ship systematically towed the sled along three N to S transects but apart from the location found at the beginning, no additional evidence for bubble emission were found.

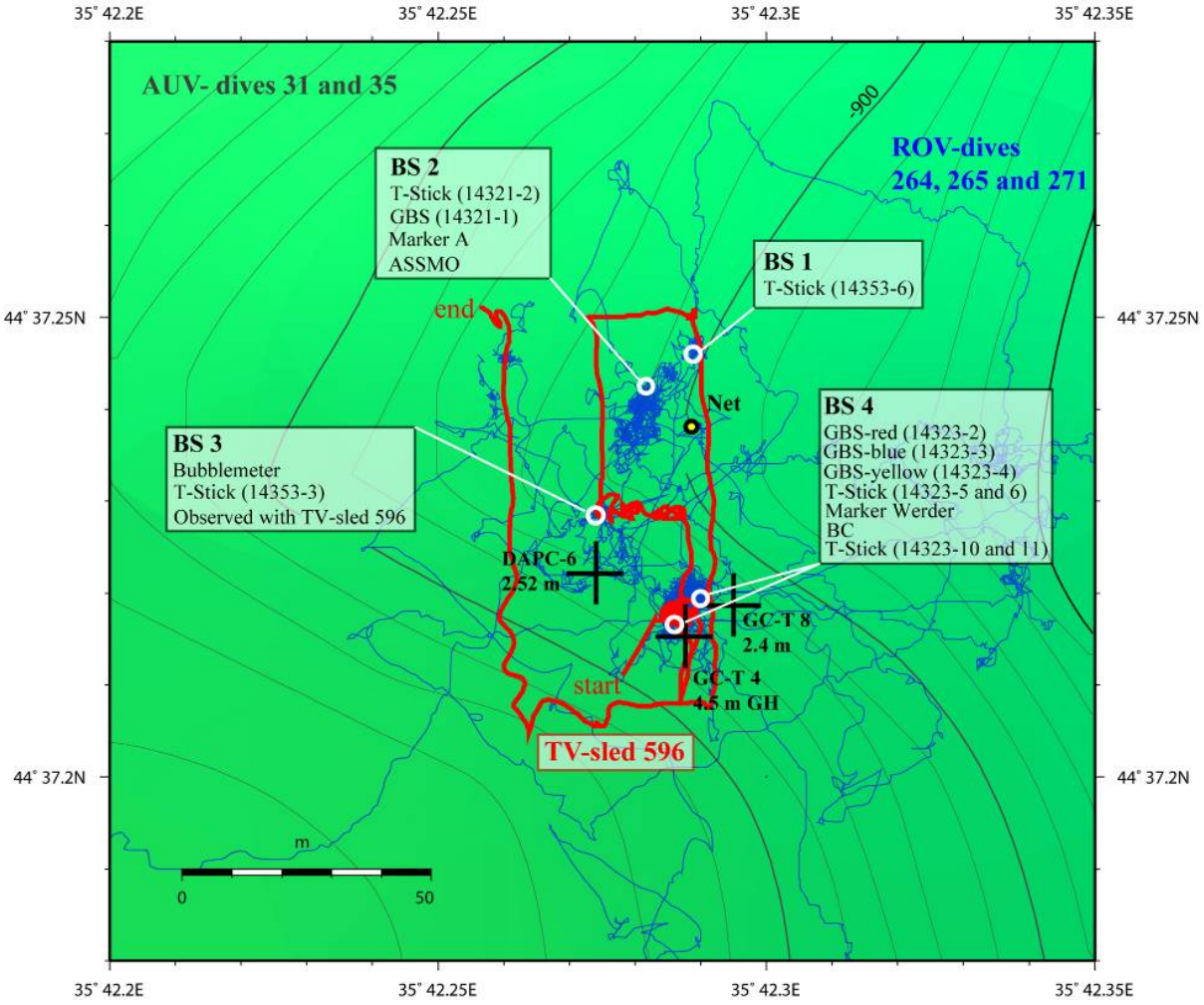

Fig. 40: Map of the surveyed area in the centre of Kerch flare. The red line shows the track of the TV-sled. Only bubble site 3 (BS 3) was active and observed during the survey.

7. Station Work with the Autonomous Underwater Vehicle (AUV) SEAL 5000

(G. Meinecke, E. Kopiske, J. Renken, P. Wintersteller)

In the year 2006 the MARUM ordered a deep diving autonomous underwater vehicle (AUV), designed as a modular sensor carrier platform for autonomous underwater applications. The AUV was built in Canada by the company International Submarine Engineering (I.S.E.). In June 2007 the AUV "SEAL" was delivered to MARUM and tested afterwards on the French vessel N/O SUROIT (June 2007) and the German R/V POSEIDON (November 2007) in the Mediterranean Sea as extended Factory Acceptance test.

7.1 SEAL Vehicle – Basics

The AUV Seal is No. 5 of the Explorer-AUV series from the company I.S.E. Two other very similar AUVs are operated by IFREMER (La Seine sur Mer), one by University New Foundland and one by Memorial University Mississippi. The SEAL AUV is the largest one and has the highest depth range of 5000 m.

The AUV is nearly 5.75 m long, with 0.73 m diameter and a weight of 1.35 tons. The AUV consists of a modular atmospheric pressure hull, designed from 2 hull segments and a front and aft dome. Inside the pressure hull, the vehicle control computer (VCC), the payload control computer (PCC), 8 lithium batteries and spare room for additional "dry" payload electronics are located. Actually, the inertial navigation system PHINS and the RESON multibeam-processor are located as dry payload here. The tail and the front section, built on GRP-material, are flooded wet bays. In the tail section the motor, beacons for USBL, RF-radio, flash light, IRIDIUM antenna, DGPS antenna and the pressure-sensor are located. In the front section the Seabird SBE 49 CTD, the Sercel MATS 200 acoustic modem, the DVL (300kHz), KONGSBERG pencil beam (675kHz), the RESON MBES 7125B (400kHz) and the BENTHOS dual frequency (100/400kHz) side scan sonar are located. The SEAL AUV has a capacity of approx. 15 kwh main energy and additional capabilities for 4.0 – 6.0 kwh more main energy without design change.

For security aspects, several hard- and software mechanisms are installed on the AUV to minimize the risk for malfunction, damage and total loss. More basic features are dealing with fault response tables, up to a emergency drop weight, either released by user or completely independent by AUV itself.

MARUM put special emphasis on open architecture in hard- and software design in order to be as much as possible modular and flexible with the vehicle after delivery. Therefore the VCC is based to large extend on industrial electronic components and compact-PCI industrial boards and only very rare proprietary hardware boards. The software is completely built QNX 4.25 – a licensed UNIX derivate, to large extend open for user modifications. The payload PC is built on comparable hardware components, but running with Windows and/or Linux on demand.

On the support vessel, the counterpart to the VCC is located on the surface control computer (SCC). It is designed as an Intel based standard PC, also running with same QNX and a Graphic User Interface (GUI) to control and command the SEAL AUV. Direct communication with the AUV is established by Ethernet-LAN, either by hardwired 100 mb LAN cable plugged to AUV on deck, or by Ethernet-RF-LAN modem once vehicle is on

water. The typical range of RF-communication is around 1 – 2 km distance to vehicle. Within this range the user has all options to operate the AUV in Pilot-Mode, e.g. to manoeuvre the AUV on water or change settings. Once the AUV is under water, all communication links were shut down automatically and the AUV has to be in Mission-Mode, means it is working based on specific user-defined mission.

Despite being in mission-mode it is necessary to communicate with the AUV when it is under water, for instance asking for actual position, depth and status. To achieve this, onboard the support vessel an acoustic underwater modem with dunking transducer has to be installed (Sercel MATS modem) communicating with the counterpart on the AUV, on request. Due to limited acoustic bandwidth only rare data sets are available.

7.2 Mission Mode

The AUV as dedicated autonomous vehicle has to be pre-defined operated under water. As mentioned, only at sea surface a manoeuvring by the pilot is possible - once it dives, it will loose communication and therefore must be in a mission-mode. Initialized correctly, fault prevention mechanisms should prevent the AUV for damage/loss in that case.

Simplified, an AUV mission is a set of targets, clearly defined by its longitude, latitude, and a given depth/altitude the vehicle should reach/keep by a given speed of AUV in a distinct time. The AUV needs to be in a definite 3-dimensional underwater space to know exactly its own position over mission time in order to actively navigate on this. To achieve this basic scenario, the AUV is working at sea surface with best position update possible, e.g. DGPS position. Once it dives, it takes the actual position as starting point of navigation, looks for its own heading and the actual speed and calculating its ongoing position change based on the last actual position, e.g. method known as dead reckoning. To achieve highest precision in navigation, a combination of motion reference unit (MRU) and Inertial Navigation System (INS) is installed on the SEAL AUV – the PHINS inertial unit from IXSEA Company. Briefly, the MRU is “feeling” the acceleration of the vehicle in all 3 axis (x,y,z). The INS is built on 3 fibre-optic gyro’s (x,y,z) and gives a very precise/stable heading, pitch and roll information, based on rotation-changes compared to the axis. Even on long duration missions, the position calculating by the AUV should be very accurate based on that technique.

7.3 Mission Planning

In principle and very briefly, it would be accepted by the vehicles VCC to receive a simple list of waypoints as targets for the actual mission, in a specific syntax. In order to arrange it more efficient and convenient a graphical planning tool is used for this mission planning. The MIMOSA mission planning tool is a software package, developed by IFREMER, specially designed to operate underwater vehicles (AUVs, ROVs). The main goal of this software is to plan the current mission, observe to AUV once it is underwater and to visualize gathered data from several data sources and vehicles.

MIMOSA is mainly built on 2 software sources, e.g. an ArcView 9.1 based Graphical Information System (GIS) and a professional Navigation Charting Software offered by Chersoft UK.

In order to plan a mission the user has to work on geo-referenced charts with a given

projection (MERCATOR), either GIS maps, raster charts or S-57 commercial electronic navigational charts (ENCs). These basic chart sets could easily be enlarged with user specified GIS projects, enhanced with already gathered data, e.g. multibeam data, points of interest. Once installed in MIMOSA, one can create AUV missions by drawing the specific mission by mouse or using implemented sets of tools (MIMOSA planning mode). Missions created in that way are completely editable, movable to other geographical locations and exportable to other formats. In order to be interpretable by the SEAL AUV, the created mission will be translated in the I.S.E. specific syntax; a set of targets, waypoints, depth information and timer will be created and written into an export path. From here the mission file can be uploaded via the SCC (support vessel) into the VCC (AUVs control PC); the AUV has its mission and is capable to dive based on mission plan.

7.4 Mission Observing/Tracking

The MIMOSA planning tool is also used to monitor the vehicle at sea surface, more interesting under water (MIMOSA observation mode). The MIMOSA software is client based, means one dedicated server is used for planning, while the others are in slave/client mode, picking up actual missions. Therefore, position data strings from the AUV are being sent to local network and fed into the MIMOSA software to display actual vehicle position, e.g. DGPS signal once it is on sea surface. During dive the AUV can be tracked automatically via ultra short baseline systems (USBL), e.g. IXSEA GAPS or POSIDONIA, using the onboard AUV installed USBL transponder beacon (deliver position where the vehicle “actually is”).

In addition to this independent position source vehicles own position (deliver where the vehicle “thinks” it is) can be displayed also. This position is based on transmitted data strings from MATS underwater acoustic modem, only coming from AUV on user request.

To summarize, usually you have displayed in tracking mode:

- position of support vessel
- either DGPS of AUV during surface track, or
    - USBL position (GAPS or POSIDONIA)
    - and MATS position (underwater acoustic on request)

7.5 Operational Aspects

The SEAL AUV was used at least 5 times on field cruises so far (2 times for technical trials). Thus, several different vessels have been in operation and on each vessel the handling of the AUV is quite a bit different. In principle, the A-frame seems to be the best position to launch and recovery the AUV, because the tendency to hit ships wall is minimized compared to sideward operation, based on experiences.

On R/V MARIA S. MERIAN the launch and recovery was planned with crane No. 5 at starboard side of vessel, because the gear boom was used by gravity corer and the A-frame was blocked by ROV QUEST operations. The same operation was performed before on R/V MARIA S. MERIAN cruise M13/4.

In principle the AUV can be operated out of the lab, based on simple PC console racks. On MSM 15/2 cruise, the AUV operations were run out of a 20” operation/workshop van, located on the main deck. The consoles, fileserver and printer are installed in the container,

workbench, tools and spares also.

Prior to launch of AUV, the PHINS onboard the AUV needs to be calibrated. Therefore, the PHINS needs to be reset and the vessel has to be standing still for at least 5 minutes. After that initial phase, the vessel needs to run a rectangular course of 3 minutes times 3 knots each line. At the end of that time span and course, the PHINS is in so-called “normal mode”, that means it has its highest position quality.

7.6 AUV Deployments during MSM 15/2

Prior to AUV missions, it was necessary to adjust the AUV to ambient salinity conditions at Black Sea. Therefore, the first operation was a trim or balancing test with the AUV at station no. 545. The AUV was deployed free floating at sea surface and ballasted with additional trim weights from zodiac personnel. Unfortunately, the sea state was to rough for a good balancing.

Afterwards, all missions are planned with the RESON multibeam as standard payload. Therefore, the AUV was set into altitude mode, means the AUV steers 40 m above seafloor. In order to have a good overlap of datelines, the spacing in between the transect lines was set to 60 m as standard. Based on experiences so far, the data quality is pretty fine with that setup.

Dvurechenskii Mud Volcano - AUV Dive 29 (GeoB 14306) at May 12

A mission was planned at Dvurechenskii Mud Volcano. At 7:56, after the initial test mission the AUV was set to mission mode, but failed. The AUV didn’t start the mission, because it couldn’t dive down. This reaction has been seen before and is related to bad trimming. Instead recovery of vehicle, some additional weights have been mounted on outer surface of AUV via the zodiac. Finally, after some tries, the vehicle started the mission and went down.

In 1611 m depth a pitch fault occurs and the AUV ascended to surface. First checks have shown no real faults on the vehicle and the dive was repeated. Again, in 1460 m a pitch fault occurred and the vehicle came up to surface. It was clear, that the trimming was not good enough, especially with weights mounted on outer AUV surface. Finally, the AUV dive was stopped and postponed. The trimming of the AUV was modified again.

Dvurechenskii Mud Volcano - AUV Dive 30 (GeoB 14316) at May 14

The already planned mission at Dvurechenskii Mud Volcano should be repeated. At 7:47 the AUV was sent to mission. In 202 m water depth a groundfault occurred and the vehicle stopped its mission. Due to the groundfault, the AUV had to be recovered, because it could not be fixed on water. A plane was changed and connector maintained; both could have been the reason for the groundfault.

Kerch Flare - AUV Dive 31 (GeoB 14322) at May 15

A mission was planned at Kerch flare site. At 9:19 the AUV was sent to mission. The AUV descended well and started multibeam mission without a problem. After half of the mission a mission time out error occurred for unknown reasons. This means the vehicle could not reach the next waypoint in a given time. An initial jump to the next waypoint failed and the AUV ascended at 13:34 to surface. The mission was modified and the AUV was send down at 14:24 on the second half of Kerch mission again. Finally, at 17:46 the mission was completed and

the AUV ascended to surface.

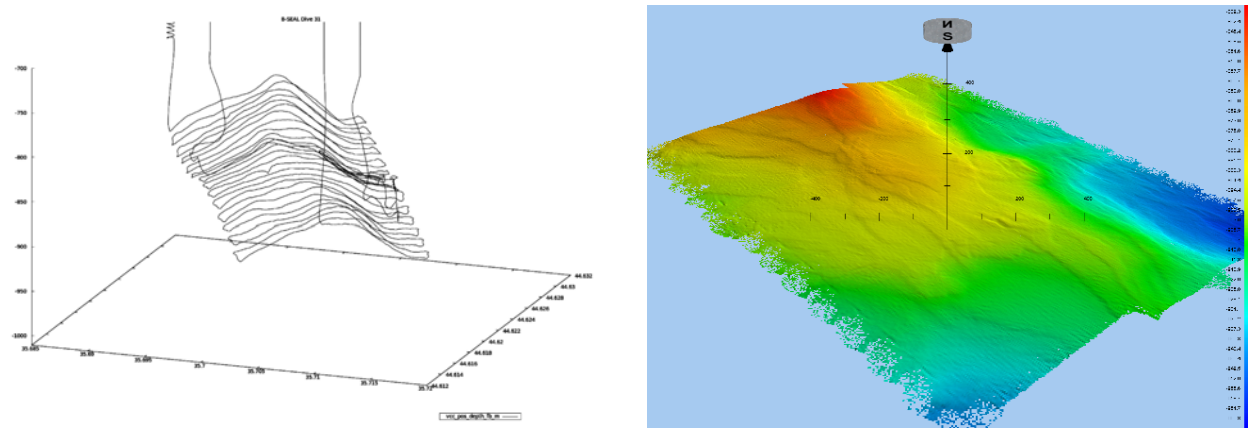

Fig. 41: Dive 31: Path of AUV under water as 3D plot of depth over time vs. position (left). Raw grid of Kerch1 MBES AUV mission (right).

Dvurechenskii Mud Volcano - AUV Dive 32 (GeoB 14328) at May 17

A mission was planned at Dvurechenskii Mud Volcano. At 7:40, after the initial test mission the AUV was set to mission mode and performed well without any problem. At 16:42 the mission was completed and the AUV ascended to surface.

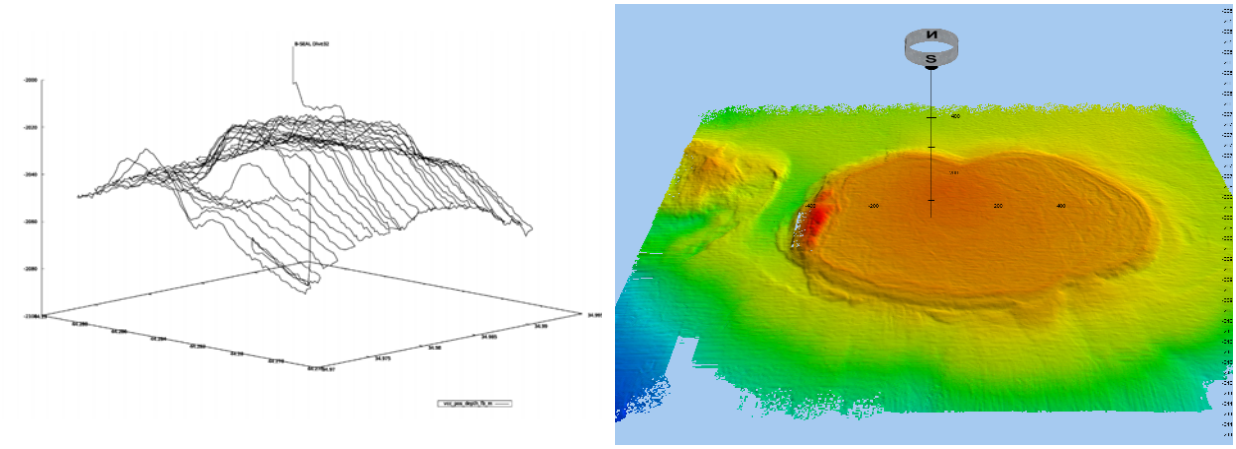

Fig. 42: Dive 32: Path of AUV under water as 3D plot of depth over time vs. position (left). Raw grid of Dvurechenskii MBES AUV mission (right).

New Seep Site - AUV Dive 33 (GeoB 14338) at May 19

A mission was planned at New Seep Site. At 9:03 the AUV was set to mission. The mission was performed without any problems until the mission ended on 16:58. The AUV ascended to surface again and the mission was completed successfully.

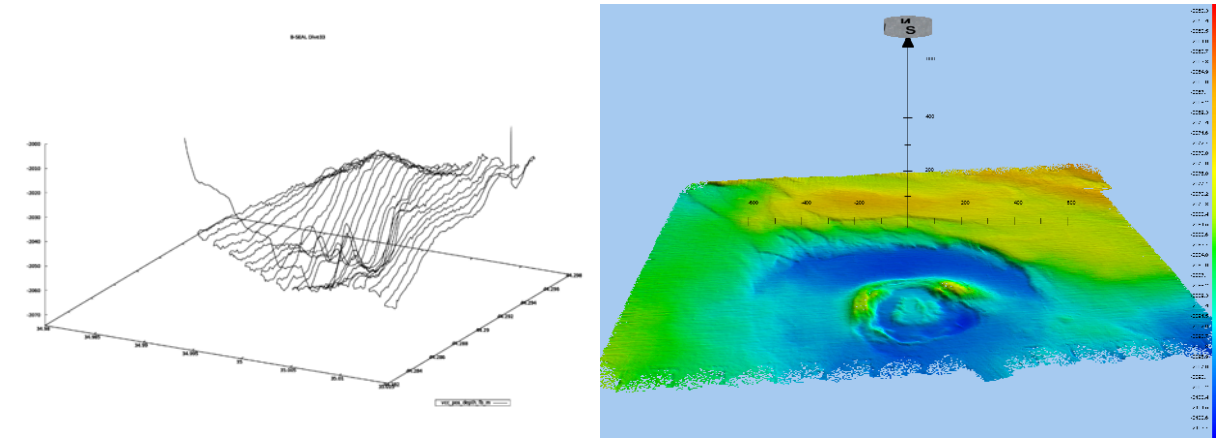

Fig. 43: Dive 33: Path of AUV under water as 3D plot of depth over time vs. position (left). Raw grid of New SS MBES AUV mission (right).

Colkheti Seep - AUV Dive 34 (GeoB 14346) at May 25

A mission was planned at Colkheti Seep Site. The mission was more complicated, because the target area offered a more complex and steep structured topography. The mission was separated in 4 parts, in order to maximize the chance to map the initial parts of area. The steepest areas should be mapped at the end of mission. The mission was started at 9:35. The AUV mapped all mayor parts of Colkheti, but dropped out of mission at 16:38 in the steepest terrain, with a low altitude alarm and the AUV went back to surface.

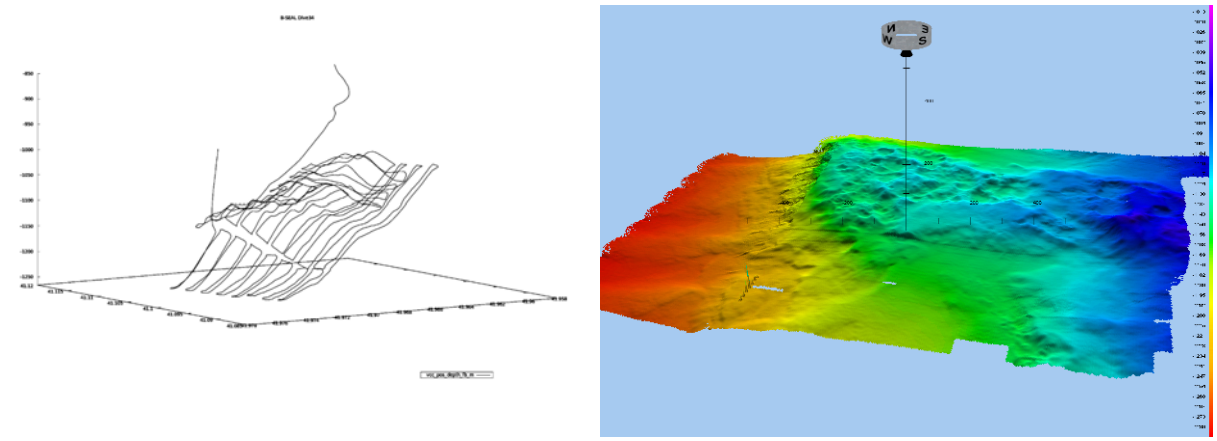

Fig. 44: Dive 34: Path of AUV under water as 3D plot of depth over time vs. position (left). Raw grid of Colkheti Seep MBES AUV mission (right).

Kerch Flare Site - AUV Dive 35 (GeoB 14350) at May 27

A mission was planned at Kerch flare site, focussed on exact flare positions. The first time the RESON multibeam and the BENTHOS sidescan sonar were used in parallel. The AUV was sent to mission on 7:43 and the AUV performed the mission without any problems until mission end at 12:00.

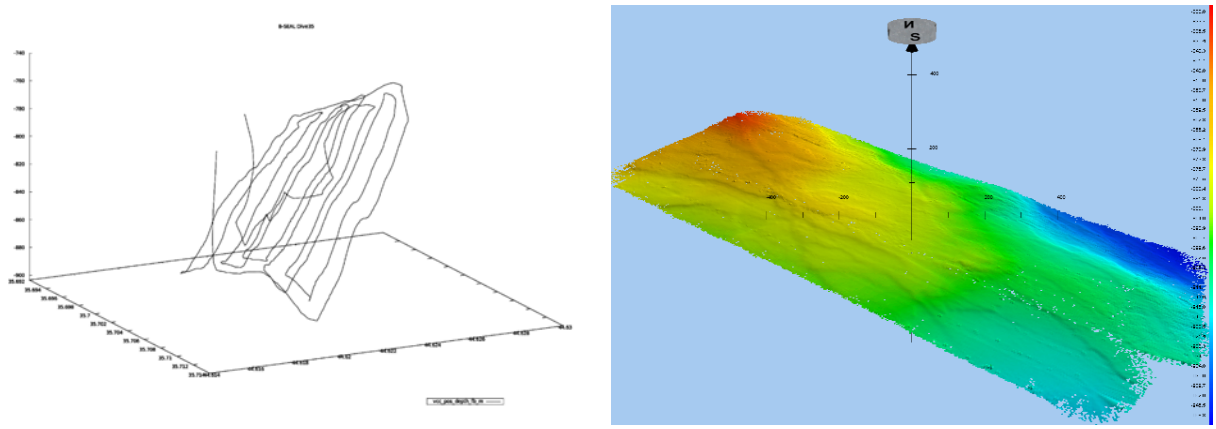

Fig. 45: Dive 35: Path of AUV under water as 3D plot of depth over time vs. position (left). Raw grid of Kerch 2 Flare MBES/SSS AUV mission (right).

Helgoland Seep Site - AUV Dive 36 (GeoB 14355) at May 28

A mission was planned at Helgoland seep site. The AUV was sent to mission at 8:54 and worked without any problems until mission end at 18:11.

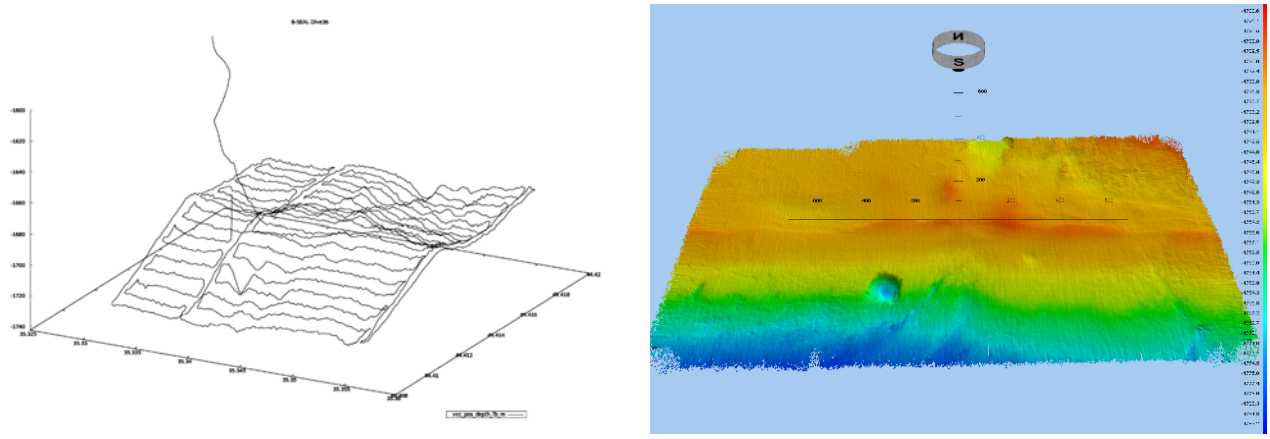

Fig. 46: Dive 36: Path of AUV under water as 3D plot of depth over time vs. position (left). Raw grid of Helgoland MBES AUV mission (right).

Odessa Mud Volcano - AUV Dive 37 (GeoB 14357) at May 29

A mission was planned at Odessa Mud Volcano. The vehicle was sent on mission at 9:03. Immediately after mission mode the AUV appeared at surface again. Several tries to let the AUV dive malfunctioned, due to pitch angle faults in uppermost water column. This fault was connected with 3 resets of main AUV computer. Finally, for technical and for safety reasons the AUV mission was cancelled and the AUV was recovered.

7.7 Results

The AUV operations started with trimming problems on the vehicle, which have been seen before on other cruises as well. As experience, it clearly shows how sensible the AUV even for slight miss-arrangements in weight and balance actually is. Especially a water column situation like Black Sea, with less saline water in upper 100 m and more saline water below

that is not as easy for an autonomous vehicle as for a ROV. After solving theses balancing problems, station work with AUV runs perfectly. The new installed battery stack works absolutely fine, even long missions up to 50 km worked well and without any technical problems. Unfortunately, the last AUV mission failed without any visible reason. Some troubleshooting was done afterwards on board, but not with striking results in fault solving.

The RESON multibeam worked fine as well. Nevertheless, despite calibration lines (roll, pitch, yaw) it is clear that additional fine tuning in data and AUV handling is necessary to enhance the overall quality of bathymetry data. It is assumed by the AUV operator that synchronisation problems finally causing some “ripple features” in the MBES data – which needs to be proven in lab.

The first operation with the BENTHOS SIS 1624 clearly shows the interference from all sounding devices onboard the AUV. It was clear before operation, for this reason only the 100 kHz operation frequency for sidescan was used. Nevertheless, all sounding systems (DVL, RESON, KONGSBERG Single beam and BENTHOS) have to be synchronized, which is not an easy task. Further testing is necessary on this field of operation.

8. Remotely Operated Vehicle (ROV)

8.1 Technical Performance of the Remotely Operated Vehicle (ROV) QUEST

(V. Ratmeyer, D. Huettich, H. Anh Mai, M. Reuter, C. Reuter, R. Rehage, M. Zarrouk)

The deepwater ROV (remotely operated vehicle) QUEST 4000 m used during MSM15/2 aboard RV MERIAN is installed and operated at MARUM, Center for Marine Environmental Sciences at the University of Bremen, Germany. The ROV QUEST is based on a commercially available 4000 m rated deepwater robotic vehicle designed and built by Schilling Robotics, Davis, USA. Since installation at MARUM in May 2003, it was designed as a truly mobile system specially adapted to the requirements of scientific work aboard marine research vessels for worldwide operation. Today, QUEST has a total record of 273 dives during 24 expeditions, including this cruise.

During MSM15/2 QUEST performed a total of 11 dives to depths between 830 and 2068 m. QUEST was operated by a team of 7 pilots/technicians on a 12 hour basis. Overall, a resulting mean bottom time of 7.1 hrs was achieved, ranging from 0.75 to 10.25 hours bottom time per deployment. A total of 78.5 hrs bottom time (105.5 hrs total dive time) was achieved during the entire cruise (see Table 4). Detailed data for the individual dives are listed within the dedicated scientific chapters of this report. The crew was prepared to cope regular intermediate dive and maintenance operations on a daily basis, with a mean diving schedule during the night. A turn-over time of 10 hrs could be regularly maintained during the entire cruise.

Dive operations included gas and sediment sampling, in-situ measurements, different instrument deployments and a heavy load recovery at depth. The vehicle performed well and without major technical issues during the entire cruise. Also, a new developed cable management procedure allowed diving without termination or damage during all dives. This was a great success after several cruises with severe cable issues before MSM15/2.

Close cooperation between ROV team and ship's crew on deck and bridge allowed a smooth and professional handling during all deployment and recovery situations. During diving, this cooperation allowed precise positioning and navigation of both ship and ROV, which was essential for accurate sampling and intervention work such as sampling, instrument deployment and cable management with an additional umbilical beacon at depth. The ROV team is very grateful for this kind of steady support from the entire ship's crew during the cruise.

QUEST System description

The total QUEST system weighs about 45 tons (including the vehicle, control van, workshop van, electric winch, 5000-m umbilical, and transportation vans) and can be transported in four standard ISO 20-foot vans. A MacArtney Cormac electric driven storage winch is used to manage up to 5000 m of 17.6 mm NSW umbilical cable.

QUEST internal equipment and online tooling

The space inside the QUEST 5 tool skid frame allows installation of mission-specific marine science tools and sensors. The initial vehicle setup includes two manipulators (7-function and

5-function), 7 color video cameras, a digital still camera (insite SCORPIO, 3.3 Mega-Pixel), a light suite (with various high-intensity discharge lights, HMI lights, lasers, and low-power dimmable incandescent lights), a Sea&Sun online CTD, a tool skid with draw-boxes, and an acoustic beacon finder. Total lighting power is almost 3 kW, total additional auxiliary power capacity is 8 kW. In addition, the permanently installed Kongsberg 675kHz Type 1071 forward looking Scanning Sonar head provided acoustic information of bottom morphology and was used for detection of gas emissions. However, the sonar lost its internal heading some times, but could be interpreted correctly after short time.

Video Setup, HDTV and vertical imaging

Continuous PAL video footage was continuously recorded on two MiniDV tapes with two color-zoom cameras (insite PEGASUS or DSPL Seacam 6500). In order to gain a fast overview of the dive without the need of watching hours of video, video is frame-grabbed and digitized at 5sec intervals, covering both PAL and HD video material.

For extremely detailed video close up filming, a near-bottom mounted broadcast quality (>1000 TVL) 3CCD HDTV 14 x zoom video camera was used (insite Zeus). Spatial resolution of this camera is 2.2 Mega-Pixel at 59.94 Hz interlaced. Recording was performed on demand onto tapes in broadcast-standard digital Sony HDCAM format, using uncompressed 1.5 Gbit HD-SDI transmission over a dedicated fibre-optic connection. Image display takes place on an HD 46” TFT display screen inside the control van, providing excellent close-up view and covering the full dynamic range of the camera. Distribution of the cameras HDTV video signal was performed through dedicated cabling into the science lab, allowing real-time display on a 26” HD TFT screen at full resolution.

As a standard still image camera, an Insite Scorpio Digital Still camera was used, providing 3.3. Mega-Pixel spatial image resolution and highly corrected underwater optics.

For the task of video mosaicking and vertical downward viewing, a broadcast quality downward looking camera with dedicated corrected underwater optics – Insite ATLAS - was installed for the second time in this functionality on the tool skid in conjunction with one high power HID wide angle flood light. Orientation of light and camera was adjusted in order to gain a large angle between optical axes. Thus, reduced backscatter allowed clear imagery from up to 7 meters above seafloor. A new digital still camera with 14 Mpix resolution was installed aside the ATLAS, providing regular high resolution vertical seafloor photography.

During MSM15/2, the following scientific equipment was handled with QUEST:
- ROV based tools, installed on vehicle:
- ROV interchangeable draw-box baskets
- Sea and Sun CTD real-time probe with turbidity sensor
- Autonomous temperature loggers on frame and T-lance
- Hand-Nets
- acoustic Beacon markers
- Simple site markers
- Hydraulic cable cutter
- Simple “Freddy” knife for manipulator operations
- Sonar tripod

- Optical Bubblemeter
- Gas Samplers
- Heavy load recovery gear, lowered on 2nd ships wire

Table 4: Divelog summary ROV QUEST MSM15/2 (UTC time).

No.	Dive No.	Date	Site		Depth (m)	Time Launch	Time Start bottom	Time End bottom	Time Recovery	Bottom Time	Total Dive Time	Bottom hours	Total Dive hours
1	263	13.05.2010	GeoB14314	DMV	2040	09:20	11:10	17:30	18:56	06:20	09:36	**6,33**	**9,60**
2	264	14.05.2010	GeoB14321	Kerch	908	16:41	17:31	02:25	03:15	08:54	10:34	**8,90**	**10,57**
3	265	15.05.2010	GeoB14323	Kerch	908	18:14	19:05	05:20	06:10	10:15	11:56	**10,25**	**11,93**
4	266	17.05.2010	GeoB14330	New Flare	1698	17:53	19:19	03:01	04:22	07:42	10:29	**7,70**	**10,48**
5	267	18.05.2010	GeoB14337	DMV	2058	17:33	19:16	03:40	03:15	04:39	09:42	**4,65**	**9,70**
6	268	22.05.2010	GeoB14339	Helgo land	2066	16:42	18:04	03:40	05:01	09:36	12:19	**9,60**	**12,32**
7	269	24.05.2010	GeoB14344	Batumi	834	17:00	17:53	02:20	03:11	08:27	10:11	**8,45**	**10,18**
8	270	25.05.2010	GeoB14348	Batumi	834	18:56	19:35	20:20	21:08	00:45	02:12	**0,75**	**2,20**
9	271	27.05.2010	GeoB14353	Kerch	896	15:22	16:10	01:22	02:04	09:12	10:42	**9,20**	**10,70**
10	272	28.05.2010	GeoB14356	Helgo land	2068	19:17	20:35	03:25	04:43	06:50	09:26	**6,83**	**9,43**
11	273	29.05.2010	GeoB14361	New Flare	1737	17:00	18:15	00:07	01:24	05:52	08:24	**5,87**	**8,40**
				Max. Dive depth (m):	**2068**				Mean bottom time per dive (hrs):	**7,14**	Total hours:	**78,53**	**105,52**

8.2 Dive Observations and Protocols

(H. Sahling)

A total of eleven dives were performed during cruise MSM 15/2 (Table 4). Generally, the performance of the ROV was excellent and all of the major objectives were achieved. Only the forward-looking sonar mounted on the ROV had technical problems with serious disadvantages for the scientific program. Although just maintained by the company, there have been serious problems with determining the direction in which the sonar is actually looking. So there was a mismatch between the actual direction the sonar beam was oriented and the heading that was displayed on the screen. It took several dives to become aware of the problem and to find acceptable solutions for this problem.

The main objective at Dvurechenski Mud Volcano (DMV) in the Sorokin Trough was to recover the data logger of the long-term temperature mooring deployed during Meteor 72/2 in 2007. During Dive 263 this mooring could not be located at the seafloor. The remaining dive time was used to search for gas bubble emissions that were found to be transient. The exact location of the mooring was determined by sidescan data of the multibeam conducted during

an AUV deployment at DMV. This survey showed that the mooring is now located about 80 m south of the original deployment station. With this information, it was possible to find the mooring during Dive 267 and to recover not only the logger but also the mooring itself.

Kerch Flare is characterised by a prominent flare within the gas hydrate stability zone that has been repeatedly detected by hydroacoustic techniques during many visits by Ukrainian and German research vessels. Three dives (264, 265, and 271) were conducted and could confirm the vigorous emission of bubbles at one site. In addition, several minor emission sites were documented. Again, the emission was found to be transient. The attempt to quantify the emission using a bubblemeter consisting of a strong backlight illumination and a high-speed camera failed due to technical problems (dive 271).

In the eastern part of the Sorokin Trough a prominent flare was found at a fault system between Tbilisi and Istanbul Mud Volcano. This site was termed New Flare Site (NFS) and studied during the two Dives 266 and 273. The first dive was unsuccessful due to severe problems with the forward-looking sonar. During the second dive at NFS the emission sites were found but appeared to be not very active during the visits.

At Batumi Seep in Georgian waters, only the two Dives 269 and 270 were conducted. The initial dive was used to deploy the autonomous scanning sonar module (ASSMO) with the objective to observe bubble emission for a ten day period with sonar at the seafloor. However, as we were not allowed to continue the work in the area, the tool was recovered during the second dive and no additional samples were taken.

8.2.1 Dive 263 (MSM Station 558, GeoB 14314)

Area:	Dvurechenskii Mud Volcano	
Responsible scientist:	Heiko Sahling	
Date:	Thursday 13 May 2010	
Start at Bottom (UTC):	11:10	
End at Bottom (UTC):	17:30	
Bottom time:	06:20	
Start at Bottom:	44°16.972’N	34°58.910’E
Water depth:	2040 m	

Scientist planned schedule:

2.0 h ca. 11:10 – 12:00	Heiko Sahling	Gerhard Bohrmann
2.0 h ca. 12:00 – 14:00	Heiko Sahling	Miriam Römer
2.0 h ca. 14:00 – 16:00	Thomas Pape	Miriam Römer
2.0 h ca. 16:00 – 18:00	Gerhard Bohrmann	Akihiro Hiruta

Points of interest:

M72 Station 307	44°17.027’N	34°58.892’E
M72 T-mooring	44°16.972’N	34°58.910’E
Dive 263 bubble emission	44°17.031’N	34°58.883’E

Key results:
No T-String mooring found.
Gas emission is transient and was not quantified, gas was not sampled.

Technical description:
The general performance of the ROV was ok, but due to computer problems DVL navigation and sonar was temporarily several times not available and demanded time-consuming restart of the computer. Time information of sonar bitmaps equivocal. No Alamer protocol at the beginning of dive. No images associated to the protocol.

Samples and measurements:
Sonar recording (screenshot bitmaps, continued recording), T-stick measurement in freshly looking mud deposits. No photo taken.

Table 5: Instruments and tools deployed during ROV Dive 263.

GeoB	Instrument	Time	Position	Depth	Comment
14314-1	T-Stick	15:44:35	44°17.0299'N 34°58.8791'E	2040.0 m	in bubble site

Dive description:
The main objective of Dive 263 was the recovery of the data logger of the T-string mooring deployed during Cruise M72/2 by Tom Feseker in 2007 (M72 T-mooring; Fig. 47). We searched in the area of the deployment for about 2.5 hours using the ROV sonar as well as by visually inspecting the seafloor. However, there was no sign of the mooring. The sediment surface in the area was generally structured and changed on small scales. For example, in some parts elongated ridges of about 0.5 m height structured the seafloor and are probably related to mudflows. At other locations the seafloor was rather smooth.

The second part of the dive was used to find gas emissions employing the sonar mounted on the ROV in the area with the most pronounced sediment temperature anomalies (M72 Station 307). The procedure was generally to rise with the ROV up to 30 m above the ground to scan the water and to look for acoustic anomalies related to gas bubbles. Several sonar scans showed clear evidence for gas emissions but their backscatter was rather weak and very localized (Fig. 48). In addition, the sonar recordings indicated the transient nature of the emissions seen by the coming and going of the anomalies in the sonar display. On the other hand, several emissions occurred on each sonar scan showing that the transient bubble release is a characteristic of the most active part of the mud volcano. Seafloor observations could confirm the sporadic release of a few individual bubbles or some trains of bubbles being released from the seafloor for a couple of seconds (Dive 263 bubble emission). As a result, neither sampling nor quantification of bubbles was performed.

Very soft mud with turbidity in depressions of morphological structures was interpreted as considerable fresh mud flows. The T-stick was deployed in the extremely soft and unconsolidated sediments. After releasing the T-stick it easily moved within the mud and felt to the side. The dragging of the T-stick out of the sediments induced the release of bubbles and up to 2-3 cm sized gas hydrate chips.

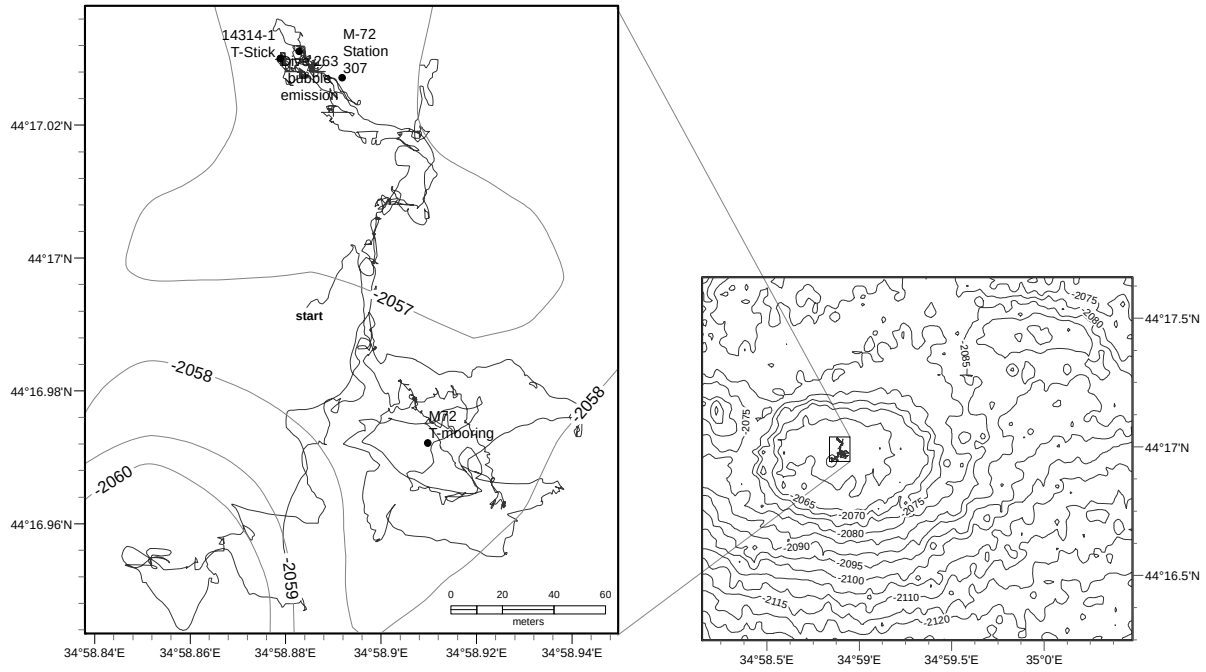

Fig. 47: Track of ROV QUEST Dive 263 at Dvurechenskii mud volcano.

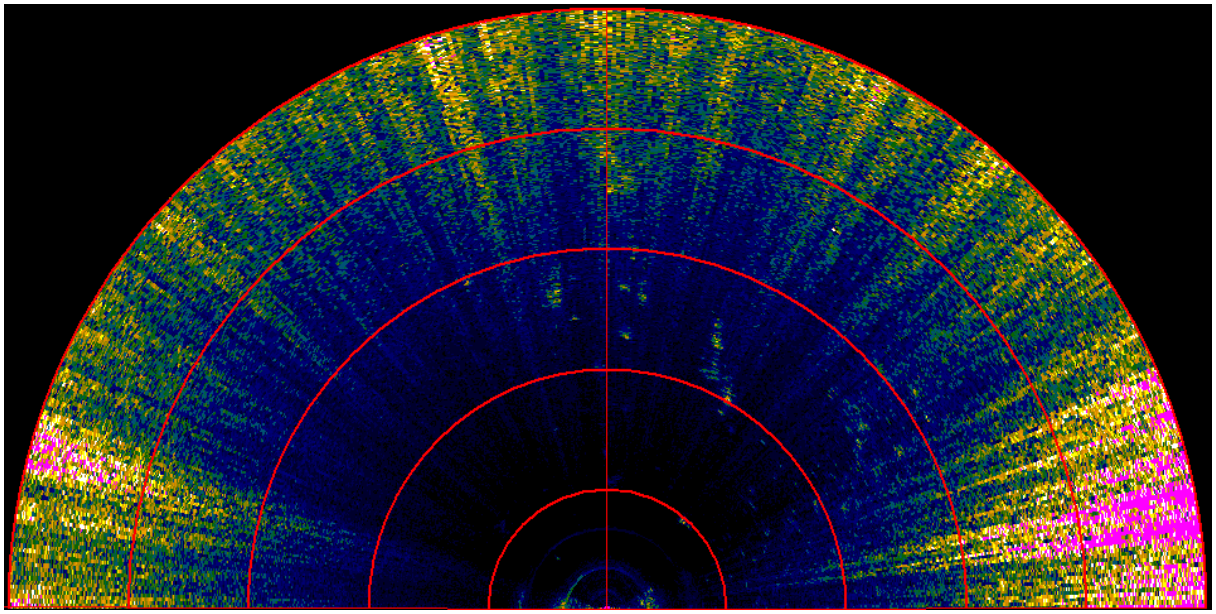

Fig. 48: Screenshot of the forward-looking sonar Kongsberg DT MS1000 showing gas emissions as distinct anomalies about 12 to 18 m ahead of ROV QUEST (UTC 143406, File Dive 263.163406). The vehicle height was about 26 m, the red circles are placed 6 m apart per division resulting in a total range of 30 m. Sonar settings: Panel Gain 195, Pulse length 34µs, Sector scan, Advanced settings: TVG-mode: 30log, TVG-limit 94.

8.2.2 Dive 264 (MSM Station 565, GeoB 14321)

Area:	Kerch Flare
Responsible scientist:	Miriam Römer
Date:	Friday 14 May 2010
Start at Bottom (UTC):	17:31

End at Bottom (UTC): 02:25
Bottom time: 08:54
Start at Bottom: 44°37.2'N 35°42.2'E
Water depth: 908 m

Scientist planned schedule:

2.0 h ca. 21:00 – 23:00	Akihiro Hiruta	Gerhard Bohrmann
2.0 h ca. 23:00 – 01:00	Heiko Sahling	Michael Ivanov
2.0 h ca. 01:00 – 03:00	Tatyana Malakhova	Miriam Römer
2.0 h ca. 03:00 – 05:00	Dimitry Evtushenko	Miriam Römer

Points of interest:

Flare AUV 1	44°37.266'N	35°42.273'E
Flare AUV 2	44°37.231'N	35°42.342'E
Flare AUV 3	44°37.178'N	35°42.281'E
Flare AUV 4	44°37.225'N	35°42.242'E
Emission Site 1	44°37.222'N	35°42.277'E
Emission Site 2	44°37.240'N	35°42.283'E

Key results:
Two gas emission sites have been found. Marker A set at the site that has been documented and sampled and where a temperature measurement has been conducted.

Technical description:
No problems with the ROV.
Storage difficulties with the digital video recording due to wrong storage pathways in Adelie Video. Sonar with increasing noise frequency made good mapping impossible and we tried to solve the problem caused about one hour time.

Samples and measurements:
Sonar recordings (screenshots and continued recording), T-stick measurement in a bubble stream, laserpoints for scaling the seep area, GBS sample taken.

Table 6: Instruments and tools deployed during ROV Dive 264.

GeoB	Instrument	Time	Position	Depth	Comment
14321-1	GBS	20:52	44°37.2412'N 35°42.2840'E	883.9 m	with T-logger at Emission Site 2
14321-2	T-Stick	21:17	44°37.2396'N 35°42.2828'E	884.1 m	in bubble site at Emission Site 2
14321-3	Marker A	21:21	44°37.2394'N 35°42.2811'E	884.1 m	deployment of Marker with the letter A at the sampled bubble site at Emission Site 2

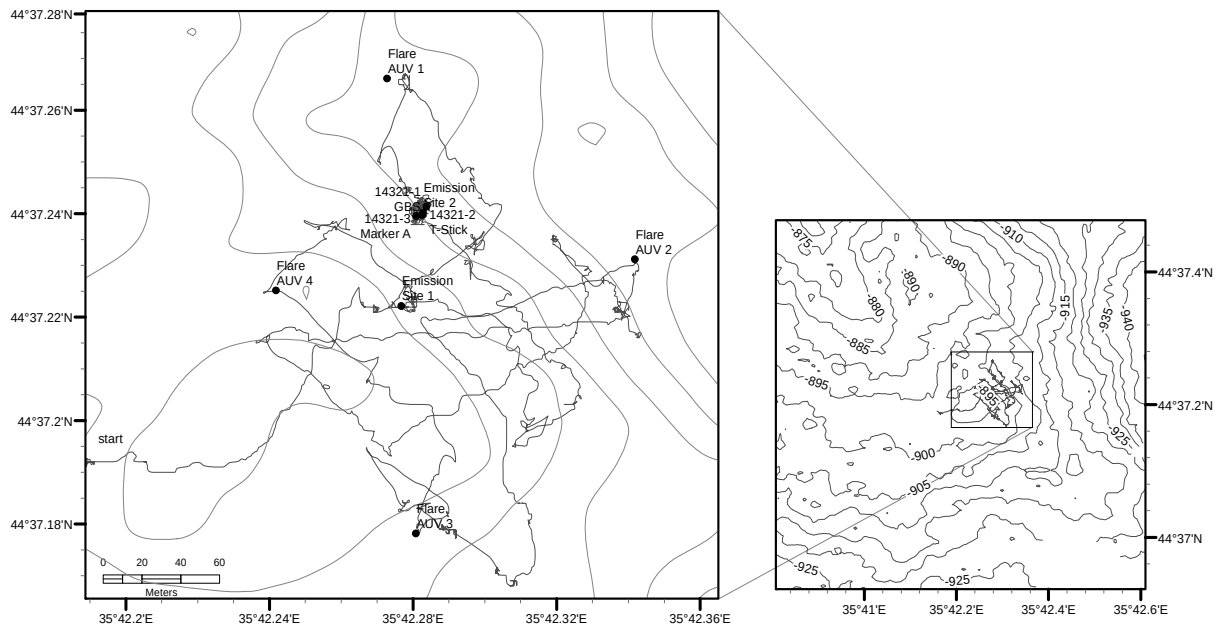

Fig. 49: Track of ROV QUEST Dive 264 at Kerch flare.

Dive description:

During a detailed PARASOUND survey before the dive we observed strong flares at this site. With these recordings a central and most active area could be determined. The main objective of this dive was to map this central area with sonar recordings and to find the emission sites – in the sonar and at the sea floor. For sonar mapping the ROV surveyed 30 m above sea floor. The first emission (Emission Site 1) has been observed in the SW of the mapped area and proven at the sea floor (see Fig. 49). The seep area is only some meters in diameter and clearly visible by darker sediment colour with numerous small holes, probable built by gas bubble ebullition. Several small gas streams could be documented. Due to a somehow weak bubble flow we decided to continue to search for more intensive emission sites for sampling. A second site has been found near the northern edge of the area with sonar and also at the sea floor (Emission Site 2). The sea floor looks very similar to what has been observed at the other site before, darker sediment and numerous bubble holes in an area of a few meters. But bubble streams are more intense, so we decided to document and sample these emissions. Marker A has been set on the side of the documented bubble stream. To get an idea of the extension of the site the laserpoints mounted on the ROV have been used (distance of the two points is 20 cm) and the whole sampling time has been recorded with the HD-camera. The GBS–red (GeoB 14321-1) has been conducted to sample the gas. Only part of the gas formed gas hydrates during accumulation in the funnel. Finally we measured the temperature gradient with the T-Stick. Due to the penetration of the stick in the sediment, bubbles and also pieces of gas hydrate escaped from the sea floor into the water column, indicating that gas hydrates exist in the upper few cm of the sediment (Fig. 50).

After finishing the documentation ROV continued mapping the area with sonar, but due to technical problems we have not been able to find other emission site in the entire area.

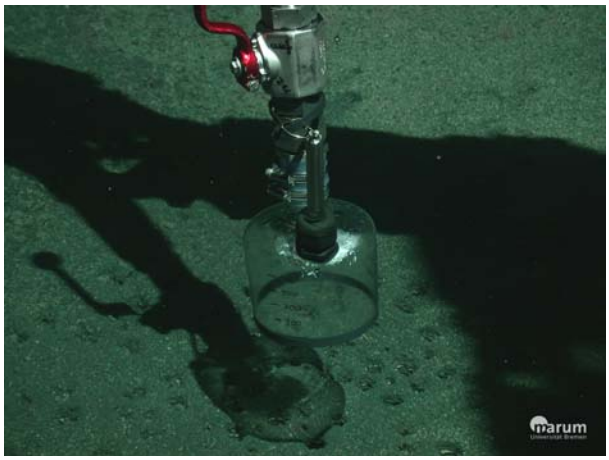

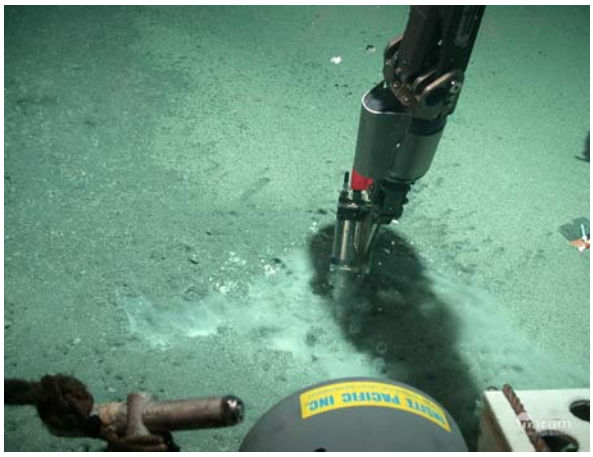

Fig. 50: Images taken by the Scorpio still camera. The seafloor is smooth and perforated by holes, gas emits through some holes and is collected by GBS (left DSCN1956). Bubbles as well as white flakes (possibly gas hydrates) rise when the sediment is disturbed by the T-stick (right DSCN2008).

8.2.3 Dive 265 (MSM Station 567, GeoB 14323)

Area:	Kerch Flare	
Responsible scientist:	Miriam Römer	
Date:	Saturday 15 May 2010	
Start at Bottom (UTC):	19:05	
End at Bottom (UTC):	05:20	
Bottom time:	10:15	
Start at Bottom:	44°37.2’ N	35°42.2’E
Water depth:	908 m	

Scientist planned schedule:

2.0 h ca. 21:00 – 23:00	Heiko Sahling	Stephan Klapp
2.0 h ca. 23:00 – 01:00	Miriam Römer	Thomas Pape
2.0 h ca. 01:00 – 03:00	Miriam Römer	Jan-Hendrik Körber
2.0 h ca. 03:00 – 05:00	Gerhard Bohrmann	Carmen Friese

Points of interest:

Emission Site 1	44°37.222’N	35°42.277’E
Emission Site 2	44°37.240’N	35°42.283’E
Emission Site 3	44°37.221’N	35°42.288’E

Key results:

ASSMO has been deployed at the beginning of the dive and recovered at the end. Found a new and extremely intense flare site with more than 19 bubble streams in a small area, which has been documented carefully and sampled.

Technical description:

ROV worked well and the sonar was repaired and recorded without problems.

Samples and measurements:
ASSMO recordings, Sonar screenshots and recordings, Laserpoints for scaling, Imaging plate for quantification, GBS sampling, temperature measurements, set Marker "Werder".

Table 7: Instruments and tools deployed during ROV Dive 265.

GeoB	Instrument	Time	Position	Depth	Comment
14323-1	Assmo	20:45	44°37.3409 35°42.2794	883.6	deployment close to bubble site at Marker A Emission Site 2 (Dive 264), recovery following day 05:11:00
14323-2	GBS (rot)	23:38:30	44°37.2177 35°42.2878	883.1	At Emission Site 3
14323-3	GBS (blau)	23:58	44°37.2201 35°42.2880	883.2	filled at 00:12 at Emission Site 3
12323-4	GBS (gelb)	00:26	44°37.2200 35°42.2891	882.9	filled at 00:32 at Emission Site 3
12323-5	T-Stick	00:41	44°37.2197 35°42.2882	883.0	out 00:52, in bubble site at Emission Site 3
12323-6	T-Stick	00:54	44°37.2199 35°42.2888	883.3	out 01:04, reference next to bubble site at Emission Site 3
12323-7	Marker Werder	01:21	44°37.2187 35°42.2884	883.4	at Emission Site 3
12323-8	BC	02:25	44°37.2191 35°42.2868	883.6	at 02:30 aborted at Emission Site 3
12323-9	BC	02:31	44°37.2195 35°42.2868	883.1	until 02:59 at Emission Site 3
12323-10	T-stick	02:49	44°37.2160 35°42.2856	882.4	out 02:59, close to bubble site at Emission Site 3
12323-11	T-stick	03:04	44°37.2158 35°42.2854	882.4	03:14, in bubble hole at Emission Site 3

Dive description:
As we could not finish a detailed sonar mapping of the central area of the Kerch Flare during Dive 264 due to technical problems, a second dive has been planned in this area. The first target was to deploy the autonomous scanning sonar module (ASSMO) next to the emission site we already found during Dive 264 at Marker A (Emission Site 2). Then we continued with the sonar search 30 m above the sea floor and relocated the additional seep site that has been documented the dive before (Emission Site 1) and searched for more indications of emissions in this area (Fig. 51). Only short time of searching was needed to find a very intense anomaly in the sonar that we followed to the sea floor. An area of only few meters is highly active and at least 19 individual bubble streams could be observed (Emission Site 3). The whole time at this site is documented with HD-video camera recording. The laserpointer have been used for

scaling (the two points have a distance of 20 cm). The ROV was positioned in front of three bubble streams which have been documented for the next four hours in detail (Fig. 52).

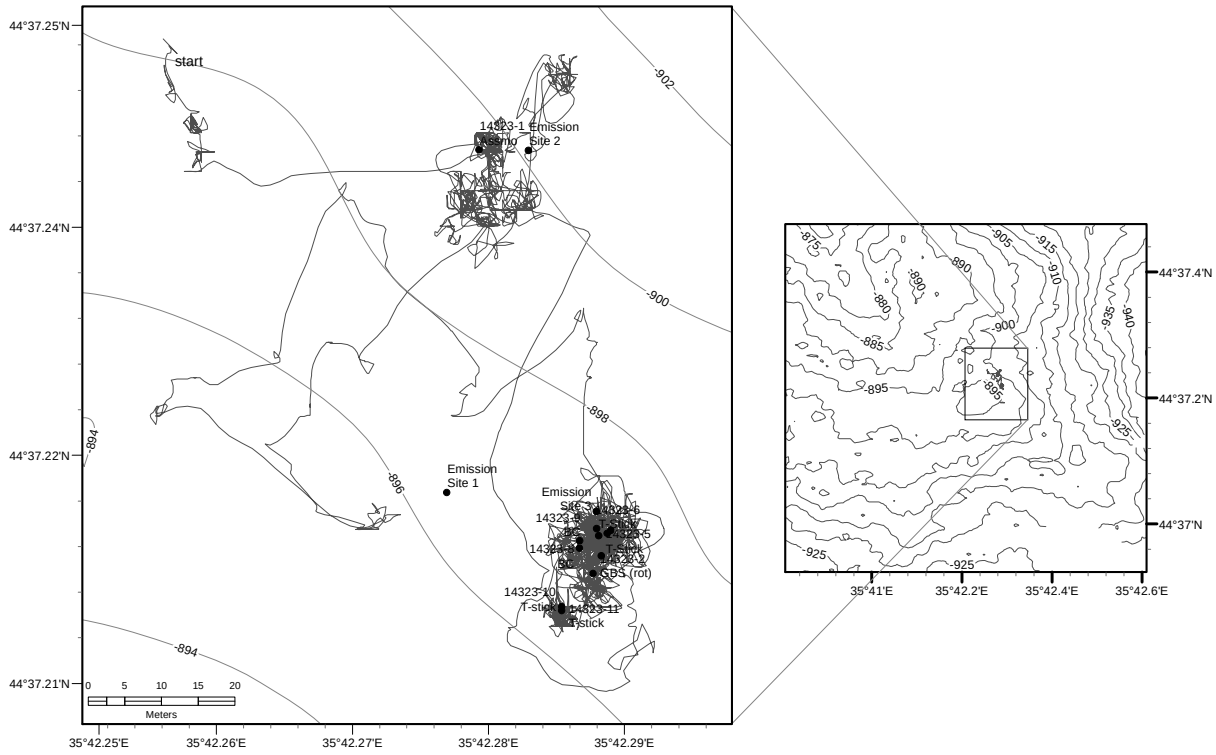

Fig. 51: Track of ROV QUEST Dive 265 at Kerch flare.

First the imaging plate was used to record the bubble streams with a black background and a scale. This allows us to quantify later the gas emissions. The plate has to be positioned just behind each bubble stream to avoid errors due to scaling inaccuracies. We tried some different setting for the shutter speed which might help to get measurements of bubble sizes more precisely. All three GBS have been filled with gas of these three bubble streams. Gas hydrates have only formed at the boundary between water and gas. The T-stick was deployed in the hole of one bubble stream and a second time as a reference approximately one meter next to this point where no bubble stream appears. The sediment is very soft but the T-stick did not fall down. At this site the Marker “Werder” has been placed. The entire seep site has been observed by moving slowly around to get a better overview. The gas bubble catcher was used to measure the bubble flux of two other bubble streams on the other side of this seep. And the T-stick has been deployed another time close to a bubble site and in a bubble hole. The last target of this dive was the recovery of the ASSMO, what has been more complicated than expected. One main problem was that the sediments were too soft such that the tool was sinking too deep when trying to fold the extendable arm away. The frame of the new constructed ASSMO was partly destroyed, but the sonar is still working.

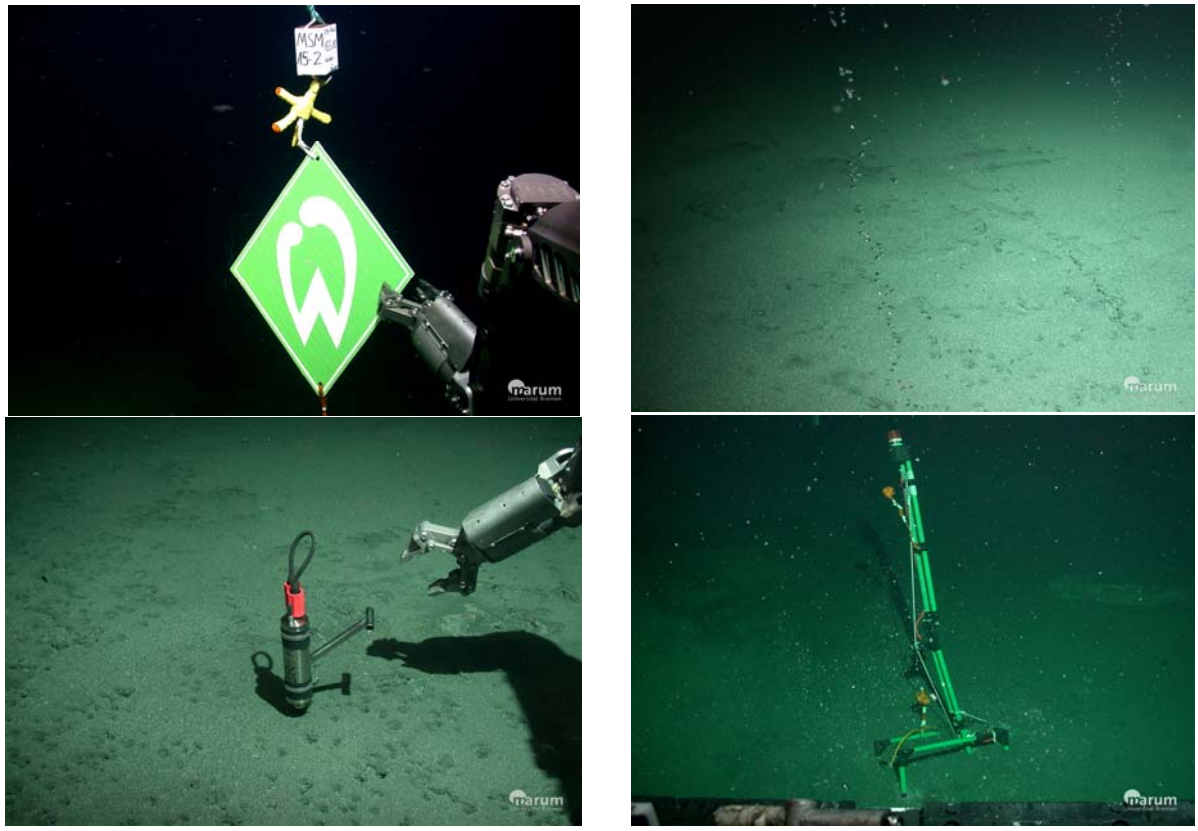

Fig. 52: Scorpio still images taken during Dive 265 at Kerch flare. Deployment of Marker W (upper left, DSCN2063), at least three bubble streams are visible on the photo, about 19 streams can be seen at this site in the sonar (upper right, DSCN2076). Deployment of T-stick at bubble site (lower left, DSCN2076). ASSMO sunken in the sediments (lower right, DSCN2112).

8.2.4 Dive 266 (MSM Station 574, GeoB 14330)

Area:	New Flare Site (NFS)	
Responsible scientist:	Heiko Sahling (originally Michael Ivanov)	
Date:	Monday 17 May 2010	
Start at Bottom (UTC):	19:19	
End at Bottom (UTC):	03:01	
Bottom Time:	07:42	
Start at Bottom:	44°24.880’N	35°20.621’E
Water depth:	1698 m	

Scientist planned schedule:

2.0 h ca. 22:00 – 24:00	Michael Ivanov	Gerhard Bohrmann
2.0 h ca. 24:00 – 02:00	Miriam Römer	Michael Ivanov
2.0 h ca. 02:00 – 04:00	Miriam Römer	Dimitriy Evtushenko
2.0 h ca. 04:00 – 06:00	Heiko Sahling	Tatyana Malakhova

Points of interest:

PARASOUND Flare 1:	44°24.88’N	35°20.008’E
PARASOUND Flare 2:	44°24.77’N	35°20.69’E

Key results:

No gas emissions found at the seafloor.

Technical description:
Sonar not working correctly. Very bad Posidonia navigation.

Samples and measurements:
No samples taken, only few minutes of HD recording.

Dive description:
The so-called New Flare Site is located at an east-west trending lineament that is probably the surface expression of a fault system. Backscatter anomalies were observed using sidescan sonar during a previous TTR-cruise. Flares were clearly detected with PARASOUND. The centers of the PARASOUND anomalies were used as target position for the ROV dive.

Nearly the entire dive time the ROV was in the water column in order to search for acoustic anomalies in the water column (Fig 53). However, no anomaly was found due to technical problems with the horizontally looking sonar mounted on the ROV. As it turned out during later dives, the sonar heading shifted. As a result, the sonar did not display the area ahead of the ROV but some non-sense data obtained in the direction to the vehicle. In addition to these problems, the navigation was very inaccurate. The Posidonia signal jumped considerably very likely due to bubble in the vicinity of the Posidonia antenna, as weather conditions decreased and the ship had to use the bow thrusters more intensively.

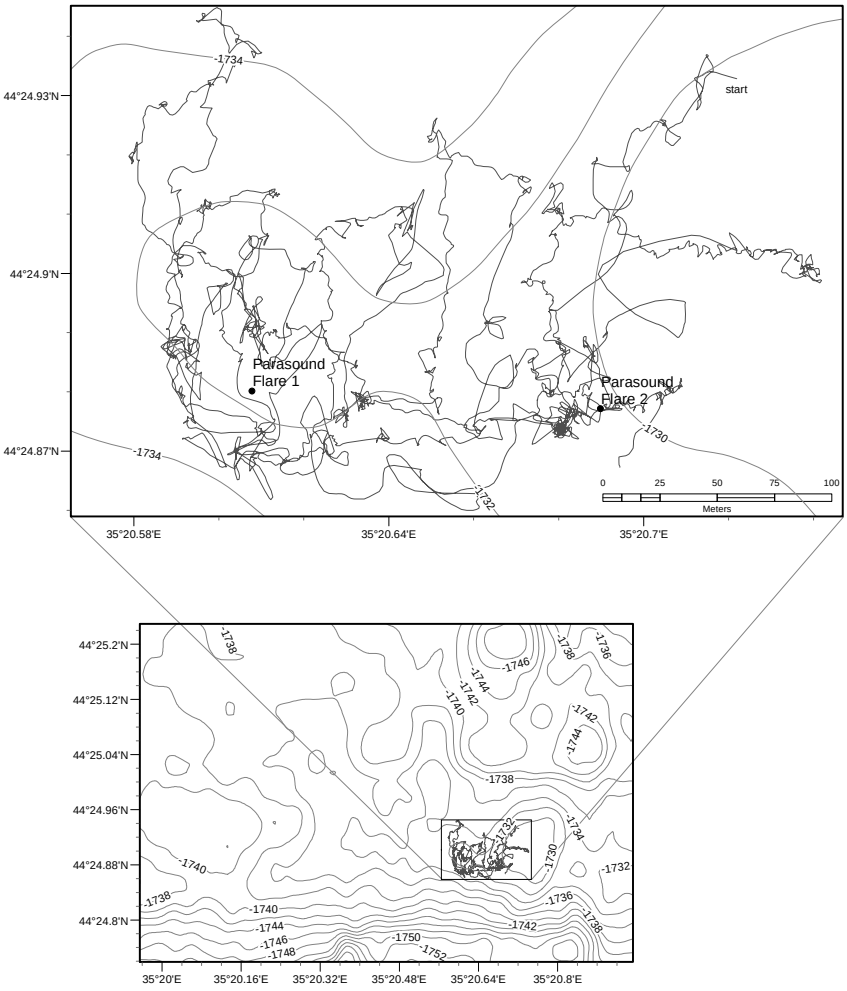

Fig. 53: Track of ROV QUEST Dive 266 at Nameless Flare Site (NFS).

8.2.5 Dive 267 (MSM Station 581, GeoB 14337)

Area:	Dvurechenskii Mud Volcano;	
Responsible scientist:	Stephan Klapp	
Date:	Tuesday 18 May 2010	
Start at Bottom (UTC):	19:16	
End at Bottom (UTC):	03:40	
Bottom time:	04:39	
Start at Bottom:	44°16.919'N	34°58.871'E
Water depth:	2058 m	

Scientist planned schedule:

2.0 h ca. 22:00 – 24:00	Stephan Klapp	Gerhard Bohrmann
2.0 h ca. 24:00 – 02:00	Stephan Klapp	Miriam Römer
2.0 h ca. 02:00 – 04:00	Thomas Pape	Miriam Römer
2.0 h ca. 04:00 – 06:00	Heiko Sahling	Akihiro Hiruta

Points of interest:

M72 Station 307	44°17.027'N	34°58.892'E
M72 T-mooring	44°16.972'N	34°58.910'E
Dive 263 bubble emission	44°17.031'N	34°58.883'E

Key results:

T-String data logger recovered.
T-String mooring recovered.
Gas emissions observed and photos taken from the sedimentary structures.

Technical description:

The general performance of the ROV was excellent. The forward-looking sonar had some problems at the beginning of the dive but the problem was fixed later. The Canon still camera was not available, no digitalized videos available, no minifilms of Zeus HD camera.

Samples and measurements:

Table 8: Instruments and tools deployed during ROV Dive 267.

GeoB	Instrument	Time	Position	Depth	Comment
14337-1	T-Mooring	20:38	44°16.9301'N 34°58.9083'E	2037.7 m	Recovery of temperature data logger from T-string mooring.

Dive description:

The T-string data logger of the mooring deployed in 2007 was re-located based on the AUV SEAL sidescan sonar data (approx. at 44°16.919'N; 34°58.871'E) recorded with the Reson swath echosounder at Dvurechenskii Mud Volcano. Located about 80 m south of the original

deployment station (Fig. 54), the mooring was prime target of Dive 267. It was found mainly using the ROV camera systems. The performance of the forward-looking sonar was not satisfying at that time, although the mooring was seen ahead of the ROV, the sonar sometimes did, sometimes did not show up on the sonar screen. The system was restarted and the settings double-checked and worked well during the rest of the dive.

After locating the data logger of the mooring, it was retrieved by simply grabbing and dragging it with the manipulator arm. It was safely stored in the drawer. After that, the mooring was retrieved by lowering a wire with a hook from the ship to the seafloor. The attachment and recovery procedure was highly professional and took about 4 hours time.

The rest of the dive time was used to search for gas emissions at the warmest part of the mud volcano just north of the center. Gas emissions were found by sonar but similar to the results obtained during Dive 263, the emissions were found to be transient. For that reason, we did not attempt to sample the gas emission but instead documented the sedimentary features related to mud flow with HD video by the Zeus video camera and the Scorpio still camera (Fig. 55). The downward looking Canon still camera was not available.

The morphology in the central part of the mud volcano was heterogeneous with small ridges and orientated lineaments on the seafloor. These are likely altered flows of mud. We tried to follow a structure in one direction but it disappeared after about 10 m. In one area the sediments were blackish in the depressions. This area might be interpreted as the centremost conduit for mud but no sampling was conducted due to time constraints.

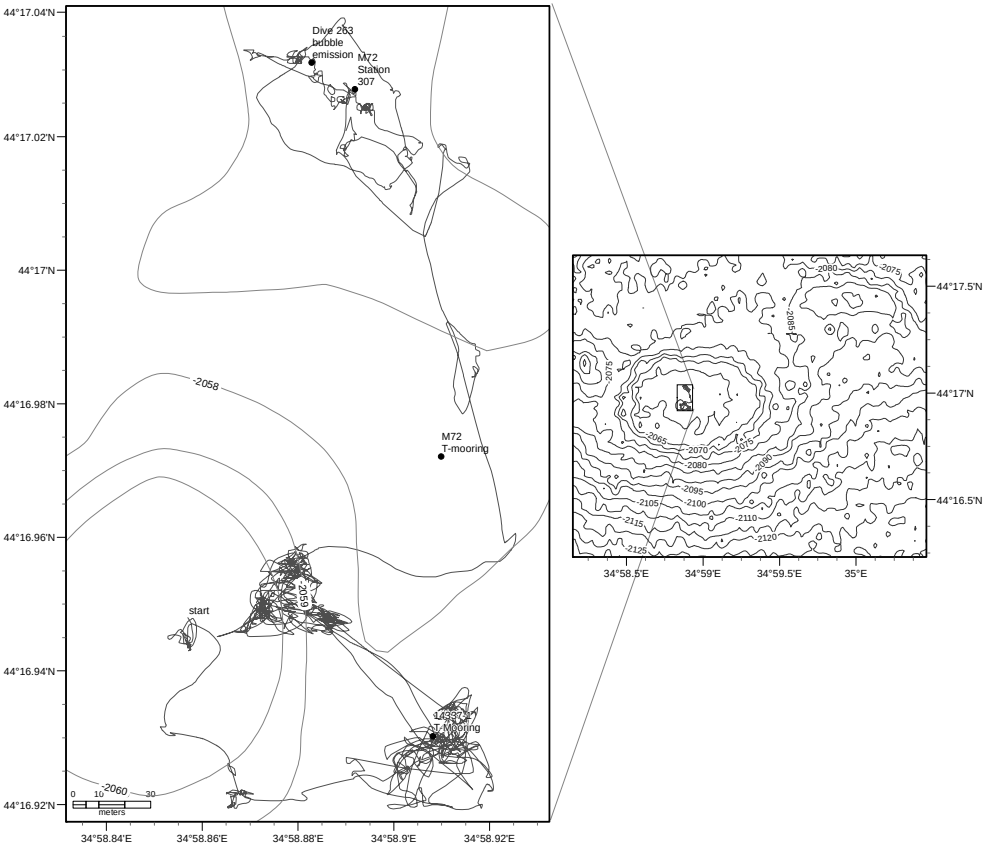

Fig. 54: Track of Dive 263 at Dvurechenskii Mud Volcano.

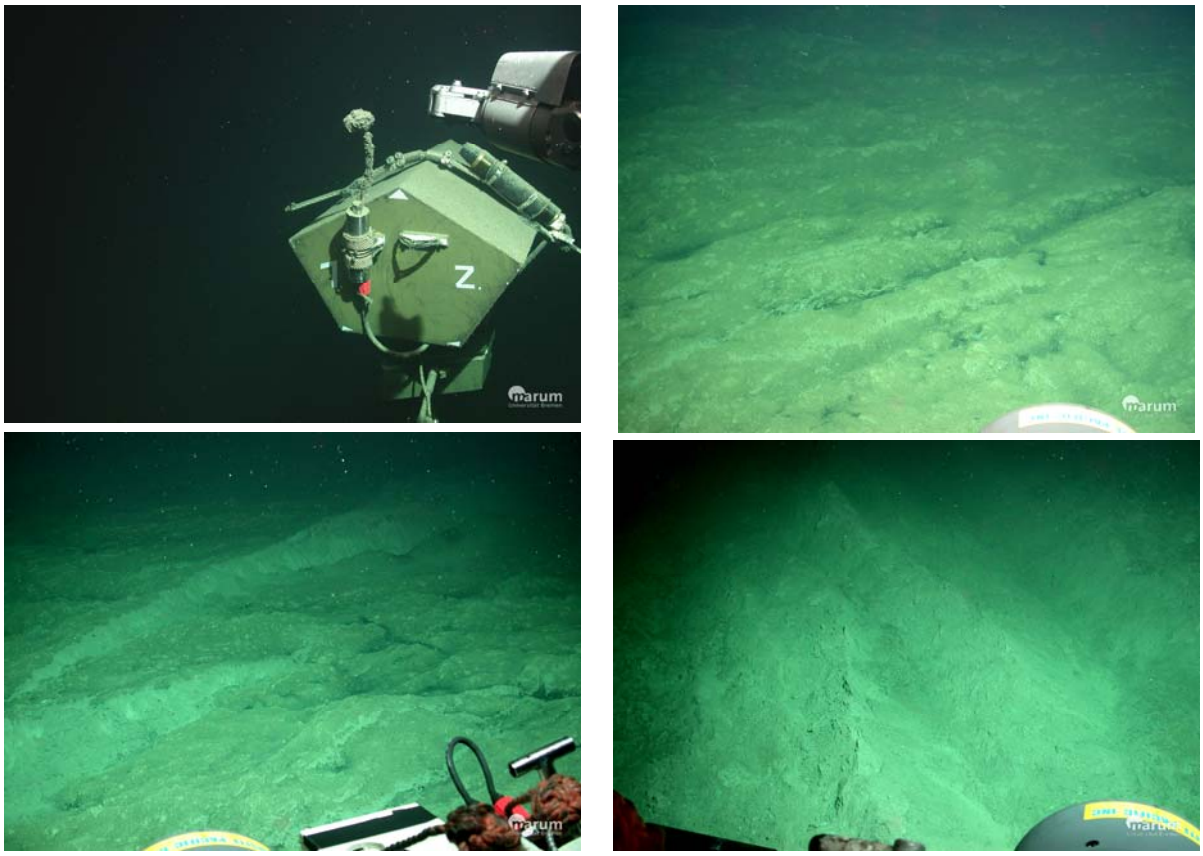

Fig. 55: Images taken during ROV Dive 267 at Dvurechenskii Mud Volcano. Recovery of the data logger of the T-mooring deployed in 2007 (upper left; DSCN2120). Seafloor fascies in the central most active area of Dvurechenskii Mud Volcano (upper right DSCN2190, lower left DSCN2232, lower right DSCN2261).

8.2.6 Dive 268 (MSM Station 583, GeoB 14339)

Area:	Helgoland Mud Volcano	
Responsible scientist:	Gerhard Bohrmann	
Date:	Saturday 22 May 2010	
Start at Bottom (UTC):	18:04	
End at Bottom (UTC):	03:40	
Bottom time:	09:36	
Start at Bottom:	44°17.30’ N	35°00.05’E
Water depth:	2066 m	

Scientist planned schedule:

2.0 h ca. 22:00 – 24:00	Jan Körber	Gerhard Bohrmann
2.0 h ca. 24:00 – 02:00	Valentina Blinova	Gerhard Bohrmann
2.0 h ca. 02:00 – 04:00	George Komakhidze	Miriam Römer
2.0 h ca. 04:00 – 06:00	Yann Marcon	Heiko Sahling

Points of interest:

Mud Pool 1	44°17.308'N; 35°00.056'E
Emission Site 1	44°17.284'N; 35°00.023'E
Emission Site 2	44°17.297'N; 35°00.047'E
Emission Site 3	44°17.299'N; 35°00.050'E

Key results:

Several emission sites found. Bubbles were emanating from a mud pool.

Technical description:

HD camera stopped around 21:24 and was not available until the end. Some problems with the forward-looking sonar at the beginning.

Samples and measurements:

Table 9: Instruments and tools deployed during ROV Dive 268.

GeoB	Instrument	Time	Position	Depth	Comment
14339-1	GBS-blue	21:38:39	44°17.3077 35°0.0560	2066.6 m	gas sampling of bubbles, emanating from mud pool – end: 21:46:09 at Mud Pool 1
14339-2	T-Stick	22:03:23	44°17.3077 35°0.0570	2066.1 m	in Mud Pool 1
14339-3	GBS-yellow	02:27:28	44°17.2992 35°0.0498	2066.4 m	gas sampling of very strong Emission Site 3 – end: 02:36:03
14339-4	T-Stick	02:53:50	44°17.2998 35°0.0512	2068.4 m	in strong bubble stream at Emission Site 3

Dive description:

Bubble emission sites have been searched for using forward-looking sonar but technical problems made it an unreliable tool. After about two hours of searching at the ground as well as in the water column an exciting mud pool (Mud Pool 1) was found. Bubbles rose through liquid mud dragging the mud into the water column from where it sedimented again (Fig. 57, upper left). Gas bubble sampler (GBS) and T-Stick measurements were conducted at the Mud Pool.

During further exploration a heavily distrupted seafloor was found through which bubbles emanated (Emission Site 1). No samples were taken. Another emissiom site was found but the activity stopped when aproaching the target with the ROV (Emission Site 2). From the sonar it was evident that the bubble stream originated from the center of a small mud flow that has spread concentrically (Fig. 57, lower left). A photomosaik using the downward looking canon still camera was conducted. At Emission Site 3 bubbles rose from several exitis. GBS and T-Stick measurments were conducted.

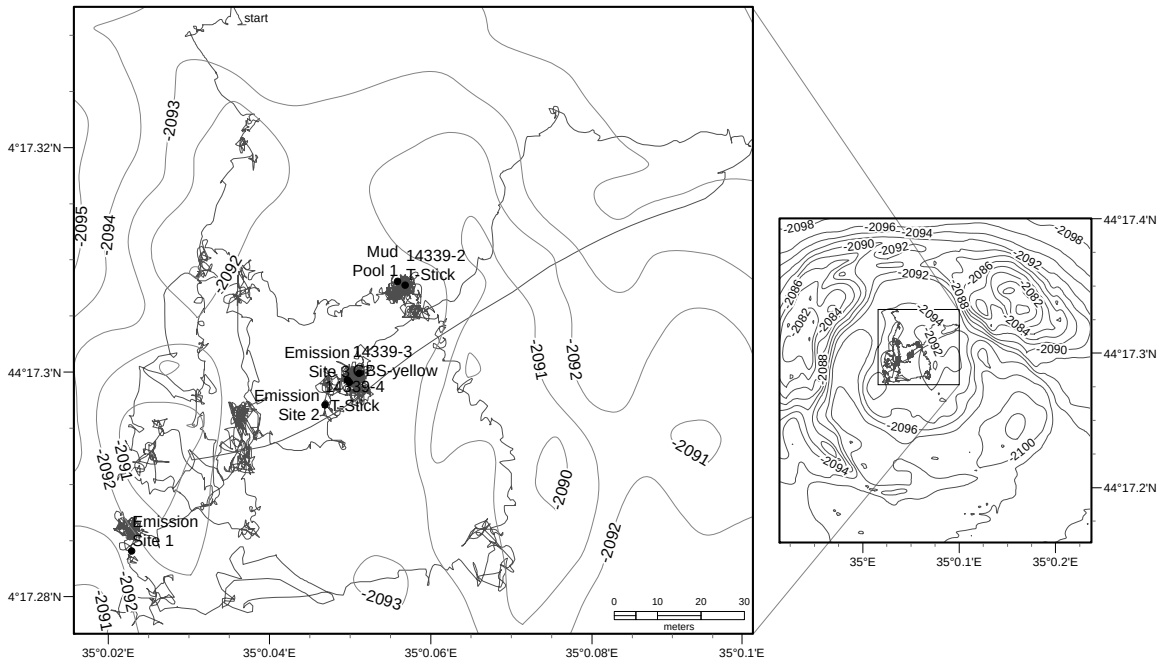

Fig. 56: Track of ROV QUEST Dive 268 at Helgoland Mud Volcano with relevant observations and sampling stations.

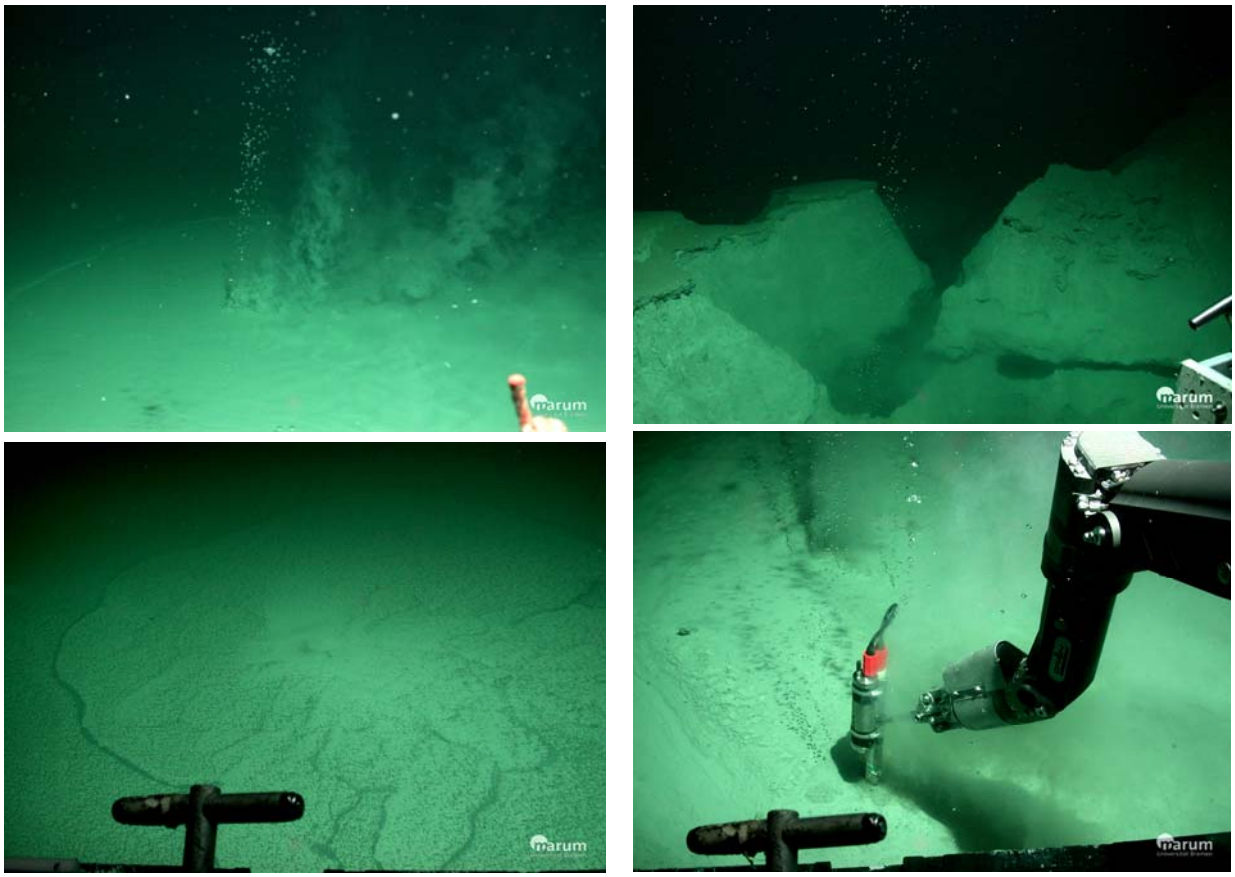

Fig. 57: Seafloor images at Helgoland Mud Volcano. Bubble emission at Mud Pool 1 (upper left). Bubble emission from between disturbed sediments at Emission Site 1 (upper right). Bubble emission stopped when the ROV approached a small mud flow at the Emission Site 2 (lower left). Samples were taken at the bubble Emission Site 2 (lower right).

8.2.7 Dive 269 (MSM Station 588, GeoB 14344)

Area:	Batumi Seep Area	
Responsible scientist:	Heiko Sahling	
Date:	Monday 24 May 2010	
Start at Bottom (UTC):	17:53	
End at Bottom (UTC):	02:20	
Bottom time:	08:27	
Start at Bottom:	41°57.445’ N	41°17.44’E
Water depth	834 m	

Scientist planned schedule:

2.0 h ca. 21 00 – 23 00	Heiko Sahling	Jan-Hendrik Körber
2.0 h ca. 23 00 – 01 00	Heiko Sahling	Thomas Pape
2.0 h ca. 01 00 – 03 00	George Komakhidze	Thomas Pape
2.0 h ca. 03 00 – 05 00	Miriam Römer	Yann Marcon

Points of interest:

41°57.5300’N	41°17.2385’E	FC 2
41°57.5290`N	41°17.2710’E	FC 3
41°57.5310’N	41°17.3420’E	FC 4
41°57.5360’N	41°17.4180’E	FC 5
41°57.5020’N	41°17.5450’E	FC 8
41°57.5420’N	41°17.5290’E	FC 7
41°57.5440’N	41°17.4720’E	FC 6
41°57.5420’N	41°17.4120’E	FC 5
41°57.4460’N	41°17.4380’E	FC 9
41°57.5300’N	41°17.2690’E	FC 3-Gusher
41°57.5430’N	41°17.3370’E	FC 4
41°57.5340’N	41°17.2660’E	FC 3
41°57.4010’N	41°17.2720’E	FC 10
41°57.3980’N	41°17.2690’E	FC 10
41°57.4440’N	41°17.4480’E	FC 9
41°57.5280’N	41°17.2710’E	Marker-1_11904-14
41°57.5440’N	41°17.4720’E	Marker-2_11907-6 (Flare Cluster 6)
41°57.5420’N	41°17.4130’E	Marker-3_11907-11 (Flare Cluster 5)

Key results:

No bubble emissions found at Flare Cluster 9 and 10. Bubble emissions at Flare Cluster 3 found (at Marker 1). Deployment of ASSMO (scanning sonar) and Gas Hydrate Experiment. Deployment of T-stick, imaging plate, and gas catcher. Sampling of chimney structure.

Technical description:
At beginning (~45 min) wrong map in DVL-Nav and problems with starting video digitalization, during the dive heading of horizontally looking sonar wrong (0° not ahead of ROV), by carefully observing bottom structures the heading was manually set to 150° the first hours, later to 108°.

Samples and measurements:

Table 10: Instruments and tools deployed during ROV Dive 269.

GeoB	Instrument	Time	Position	Depth	Comment
14342-1	ASSMO	21:11	41°57.5320 41°17.2684	835.5	close to Marker 1 Flare Cluster 3 with several bubble emissions
14342-2	GBS-yellow	21:59	41°57.5330 41°17.2719	835.2	
14342-3	BIP	22:30	41°57.5334 41°17.2728	835.3	
14342-4	Gas Hydrate Experiment I	23:30	41°57.5330 41°17.2739	835.2	
14342-5	Marker D	23:43	41°57.5330 41°17.2733	835.2	At Gas Hydrate Experiment I
14342-6	Gas Hydrate Experiment II	23:58	41°57.5334 41°17.2706	835.3	
14342-7	Gas Catcher I	00:13:55	41°57.5324 41°17.2718	835.2	To 00:28:55 filled by 3 L
14342-8	T-Stick Experiment I	00:37:30	41°57.5329 41°17.2721	835.3	To 00:48:52 only about 20 cm penetration due to hard structure in the sediment

Dive description:
The dive started with some technical problems, after coping with them, the areas where Flare Cluster 9 and 10 had been found during M 72/3 where surveyed using sonar as well as the camera systems. No active bubble emission was found. Therefore, the area at Flare Cluster 3 (Marker 1) was studied in detail and gas emissions were found. Gas was not emitting through the hole next to Marker 1, which we called “Gusher” site in 2007 but a few meters away giving an idea of the temporal and spatial variability of the system. Deployment of ASSMO next to a bubble stream (Fig. 59). This tool autonomously registers the data of a horizontally-looking sonar head. In order to place the sonar head away from the seafloor the ASSMO has to be installed, i.e. an extendable arm has to be unfolded, which worked fine.

A gas bubble sampler was taken at the gas emission site as well as the bubble imaging plate for the purpose of bubble quantification. The gas hydrate experiment I was filled with gas, closed and placed at the seafloor where Marker D was deployed, too. Gas hydrate experiment II, a Gas Bubble Catcher and the T-Stick complemented the program of this dive.

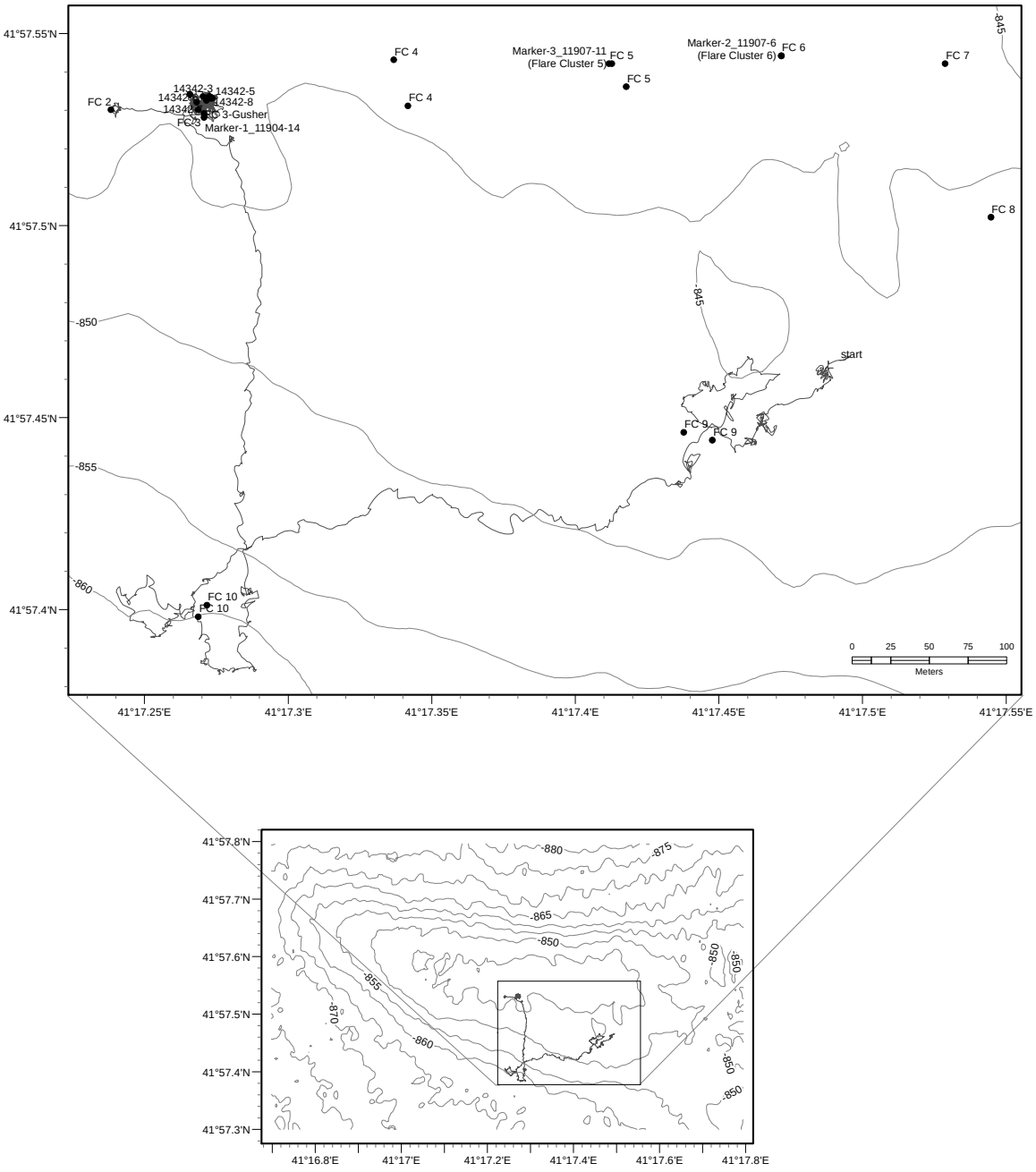

Fig. 58: Track of ROV QUEST Dive 269 at Batumi flare offshore Georgia.

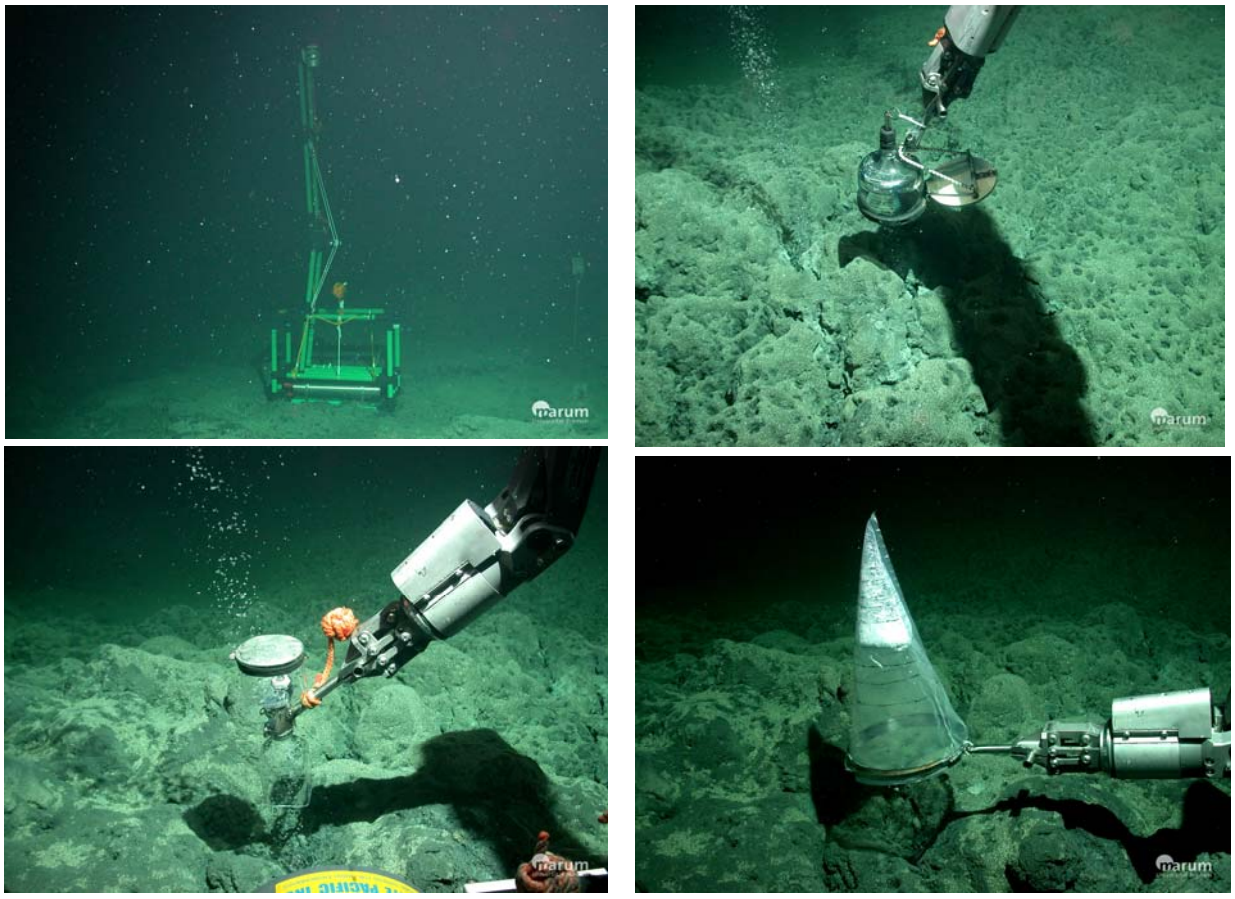

Fig. 59: Scorpio still images taken during Dive 269 at Batumi flare. ASSMO (upper left), gas hydrate experiment I (upper right), gas hydrate experiment II (lower left), and gas bubble catcher (lower right).

8.2.8 Dive 270 (MSM Station 592, GeoB 14348)

Area:	Batumi Seep Area	
Responsible scientist:	Heiko Sahling	
Date:	Tuesday 25 May 2010	
Start at Bottom (UTC):	19:35	
End at Bottom (UTC):	20:20	
Bottom time:	00:45	
Start at Bottom:	41°57.53’ N	41°17.269’E
Water depth:	834 m	

Scientist planned schedule:

2.0 h ca. 22 00 – 24 00	Heiko Sahling	Evgeni Sakvarelidze
2.0 h ca. 24 00 – 02 00	Heiko Sahling	Valentina Blinova

Points of interest:

41°57.5320’N	41°17.2680’E	ASSMO
41°57.5330’N	41°17.2740’E	Gas hydrate experiment I

Key results:
Recovery of ASSMO and gas hydrate experiments.

Technical description:
The general performance of the ROV was good.

Samples and measurements:
No samples recorded, only recovery of seafloor experiments.

Description:
As we had to leave Georgian waters, the only objective of the dive was to recover the ASSMO and the gas hydrate experiments deployed during ROV Dive 269. About 20 min after arrival at the seafloor the gas hydrate experiment was grabbed by the arm, documented by fotos (Fig. 61) and taken into the sampling box. Ten min later the ASSMO was grabbed, uninstalled and placed on the porch of the vehicle that subsequently came back to the surface.

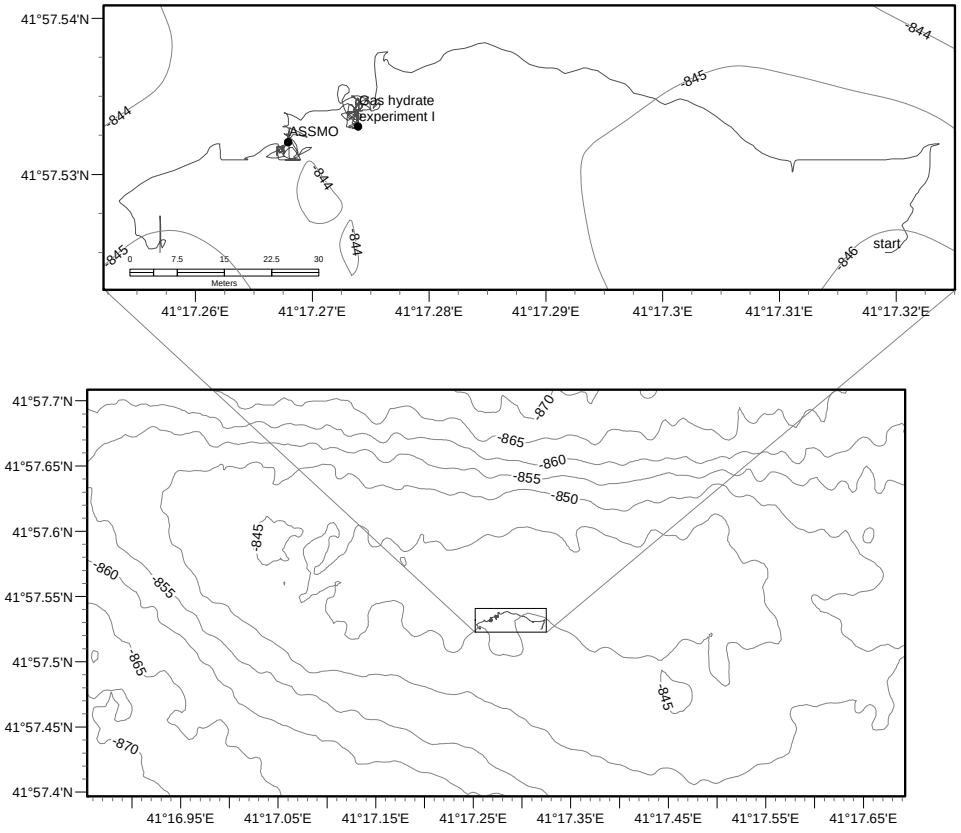

Fig. 60: Track of ROV QUEST Dive 270 at Batumi flare offshore Georgia.

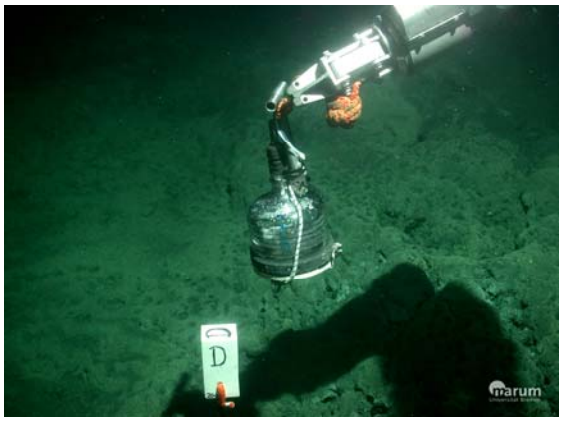

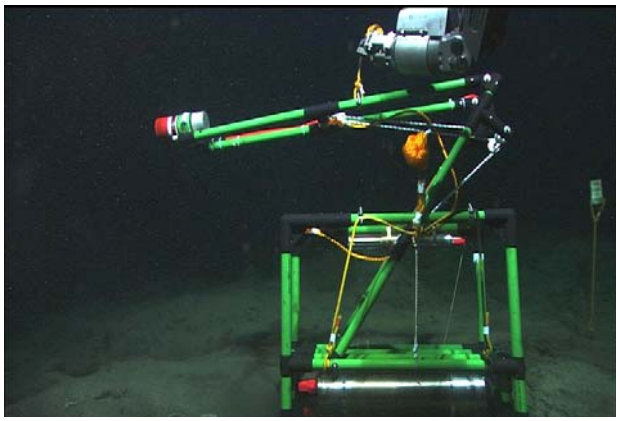

Fig. 61: Scorpio still image (left) of the gas hydrate experiment I and Zeus frame grab of ASSMO (right) taken during Dive 270 at Batumi flare offshore Georgia.

8.2.9 Dive 271 (MSM Station 597, GeoB 14353)

Area:	Kerch Flare	
Responsible scientist:	Miriam Römer	
Date:	Thursday 27 May 2010	
Start at Bottom:	16:10	
End at Bottom:	01:22	
Bottom time	09:12	
Start at Bottom:	44°37.218'N	35°42.288'E
Water depth:	896 m	

Scientist planned schedule:

2.0 h ca. 20:00 – 22:00	Heiko Sahling	Carmen Friese
2.0 h ca. 22:00 – 24:00	Miriam Römer	George Komakhidze
2.0 h ca. 24:00 – 02:00	Miriam Römer	Yann Marcon
2.0 h ca. 02:00 – 05:00	Thomas Pape	Valentina Blinova

Points of interest:

Emission Site 1	44°37.222'N	34°42.277'E
Emission Site 2	44°37.240'N	35°42.283'E
Emission Site 3	44°37.221'N	35°42.288'E

Key results:

The bubblemeter operated one time. Already known emission sites were mostly inactive. Two new but less intense emission sites could be observed.

Technical description:

Some problems with the Alamer-protocol and in the first part of the dive also some difficulties with the sonar. ROV performance in general good.

Samples and measurements:

Bubblemeter recording, Sonar recordings, T-stick measurements in two bubble streams, Laserpoints for scaling the seep area.

Table 11: Instruments and tools deployed during ROV Dive 271.

GeoB	Instrument	Time	Position	Depth	Comment
14353-1	Bubblemeter	17:01	44°37.2283 35°42.2753	881.3 m	At Emission Site 4
14353-2	T-Stick	17:51	44°37.2285 35°42.2750	882.7 m	As scale for bubble measurements at Emission Site 4
14353-3	T-Stick	18:51	44°37.2225 35°42.2789	878.7 m	In bubble hole at site 1 – hydrates rising up at Emission Site 4
14353-4	Net	20:24	44°37.2379 35°42.2894	886.3	Sediment sample, dark spot with white coloured central part
14353-5	T-Stick	21:08	44°37.2469 35°42.2900	887.3 m	As scale for bubble measurements at Emission Site 5
14353-6	T-Stick	21:14	44°37.2470 35°42.2896	886.9	In bubble hole at second site at Emission Site 5

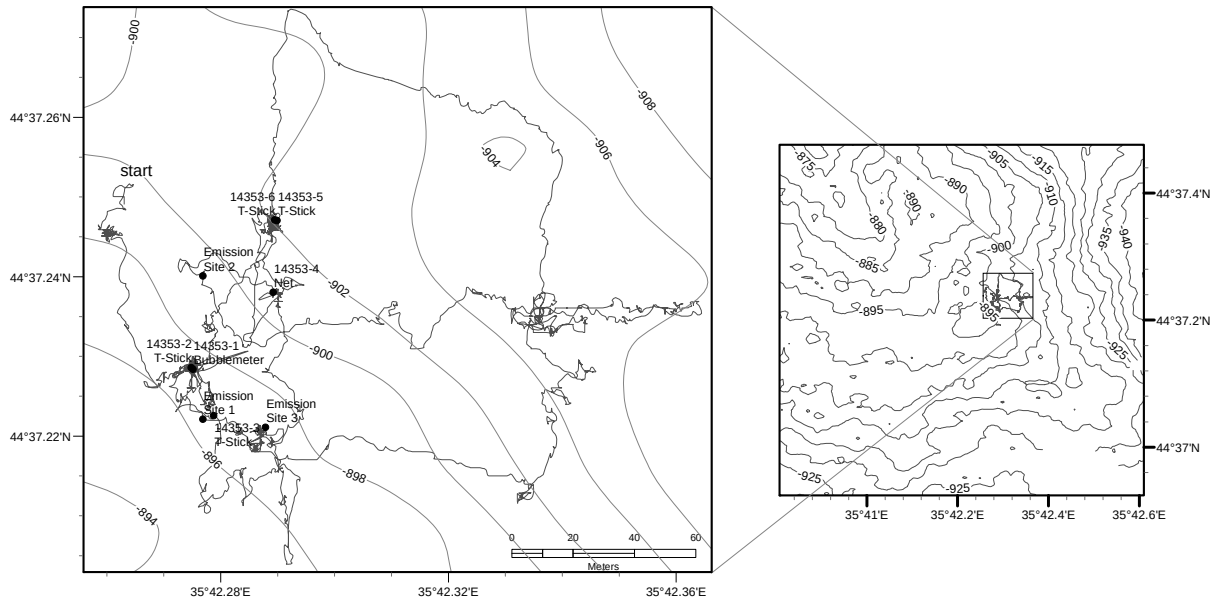

Fig. 62: Track of ROV QUEST Dive 271 at Kerch flare with relevant observations and sampling stations.

Dive description:

Shortly after arriving at the seafloor a new bubble emission site (Emission Site 4) has been found and the bubblemeter was deployed. Only one measurement for 4 seconds could be done before problems with the internal power supply did not allow any further usage of the tool (Fig. 63). Therefore, we recorded the bubble stream with the HD-camera for documentation

and bubble measurements with the T-Stick placed in the bubble stream as scale. The T-Stick has also been used for a temperature measurement in the bubble hole. By penetrating with the stick in the sediment some gas hydrates rose up, indicating that there is gas hydrate in shallow sediment depths.

The dive continued with searching for other emission sites, surveying close to the ground and using the sonar (Fig. 63). At the known emission site with the Werder Marker set during ROV dive 265 (Emission Site 3) no activity has been observed. North to this site a field of small circular structures has been found. These structures show a darker sediment colour with a central whitish part that seems to be carbonates. We took one of these patches with the net (GeoB 14353-4). But by sieving the sample on board we could not find any hard parts.

The Emission Site 2 where Marker A has been set during ROV dive 264 did not show any emission as well, but 10 m northwards a new site could be observed in the sonar and also visually at the seafloor (Emission Site 5). Three bubble streams with different intensities are located close to each other. The most intense one has been documented by using the T-Stick as scale within the bubble stream. And we performed a temperature measurement in the bubble hole. The results show that there is no significant temperature increase at this site.

Then we searched for more emission sites in the central area (Fig 64), passing all locations where we estimated gas emission sites with PARASOUND and AUV sidescan analysis. Several sites could be observed where probably gas bubbles emanate irregular, but no more active emission has been found until the end of the dive.

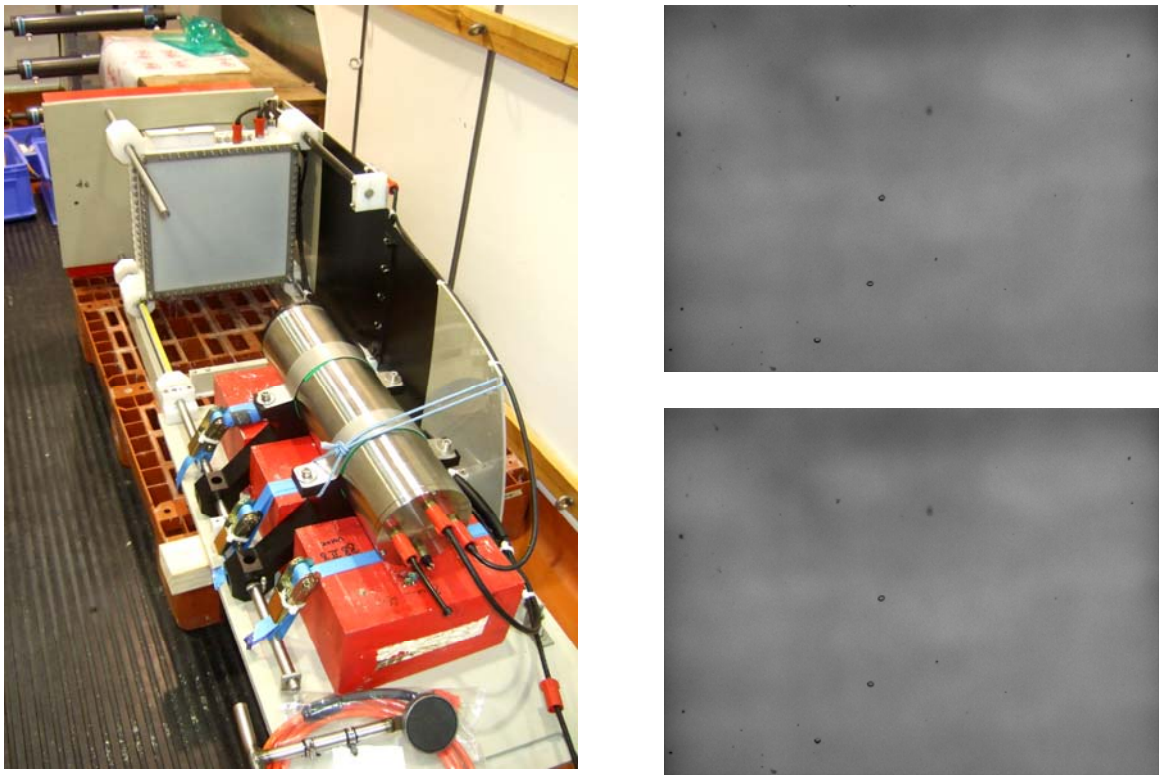

Fig. 63: The bubblemeter before integration into the ROV QUEST (left) and an example of two high-speed images taken by the bubblemeter at a gas emission site of Kerch flare. An image allows to calculate the bubble volume by automatically measure its surface assuming a rotational body. The two images shot 1/250 seconds apart allow calculating rising speeds.

Fig. 64: Scorpio still-images of the seafloor taken during ROV Dive 271. Impact hole created by DAPC or gravity corer (left, DSCN2641). Typical features observed in some areas along the track, which probably represent former gas emission sites (right, DSCN2688).

8.2.10 Dive 272 (MSM Station 600, GeoB 14356)

Area:	Helgoland Mud Volcano	
Responsible scientist:	Gerhard Bohrmann	
Date:	Friday 28 May 2010	
Start at Bottom (UTC):	20:35	
End at Bottom (UTC):	03:25	
Bottom time:	06:50	
Start at Bottom:	44°17.3’N	35°0.05’E
Water depth:	2068 m	

Scientist planned schedule:

2.0 h ca. 22:00 – 24:00	Gerhard Bohrmann	Evgeni Sakvarelidze
2.0 h ca. 24:00 – 02:00	Gerhard Bohrmann	Jan-Hendrik Körber
2.0 h ca. 02:00 – 04:00	Jan-Hendrik Körber	Yann Marcon
2.0 h ca. 04:00 – 06:00	Heiko Sahling	Kerstin Lange

Points of interest:

Mud Pool 1	44°17.308’N; 35°00.056’E
Emission Site 1	44°17.284’N; 35°00.023’E
Emission Site 2	44°17.297’N; 35°00.047’E
Emission Site 3	44°17.299’N; 35°00.050’E
Mud pool 2	44°17.312’N; 35°00.066’E
Photo Mosaik no 2	44°17.277’N; 35°00.141’E

Key results:

Finding of another Mud Pool 2. Photomosaik of a mud flow.

Technical description:

Accuracy of Posidonia positions decreased over time making orientation difficulty. The

transponder on the wire suddenly jumped and was about 1000 m higher in the water column than before. About one hour (LT 03:00 to 04:00 hour) the scientific program stopped in order to solve the problem without success. No video digitalization. Adelie frame grab of HD camera not started so there are no minifilms. Sonar still not working in a good way, as a compromise it is operated now as polar scan showing a complete 360° scan with the result of providing only slowly new data.

Samples and measurements:
HD videos of bubbles erupting through mud were taken as well as the samples listed below.

Table 12: Instruments and tools deployed during ROV Dive 272.

GeoB	Instrument	Time	Position	Depth	Comment
14356-1	GBS-yellow	21:18	44°17.3136 35°0.0658	2066.7 m	At Mud Pool 2.
14356-2	T-Stick	21:40	44°17.3113 35°0.0622	2067.3 m	At Mud Pool 2.
14356-3	Large BC	22:27	44°17.3063 35°0.0579	2067.1 m	Trying to sample liquid mud with plastic bag of large bubble catcher failed (Mud Pool 2).
14356-4	Marker C	01:05	44°17.2881 35°0.1152	2069.85 m	Marker deployed as scale for mosaic no. 1.

Dive description:
During this dive, another spectacular Mud Pool (No. 2) was found and documented (Fig. 66). Gas bubble sampler and T-stick measurements were conducted. Bubbles were also collected with the large plastic bag of the bubble catcher. Subsequent attempts of collecting the liquid mud with the bubble catcher failed due to positive buoyancy of the bag. However, a small amount was sampled.

Further exploration in the area of Helgoland Mud Volcano was hindered by problems with the Posidonia sub-positioning system. The navigation data were too inaccurate to find previously discovered seafloor features. Subsequently, the larger area outside of the center was explored. East of the center, the morphology of the seafloor was unsteady. This area was used for gaining experience with the downward looking Canon still camera for photo mosaiking (Photo mosaic no. 1). After the transects for photo mosaicking with the downward looking Canon still camera the Marker C was deployed and photographed from different heights of the ROV with the Canon still camera in order to be able to estimate the approximate field of view at different camera heights. (Zoom Factor of the Canon camera was set to the 5th interval from the left).

A visual impression with HD recording was gathered from the eastern rim of the central parts of the mud volcano when transiting towards the center. Smooth ridges several meter in

length and about 1 m high structure the seafloor at the rim before a 2-3 m step down in the morphology mark the clear limit to the relatively plain central area. The scarp-like step was steep and freshly-looking. At the central plain a nice mudflow was followed to a crater-like feature. Due to the bad Posidonia signal it is unclear if this feature has been observed before.

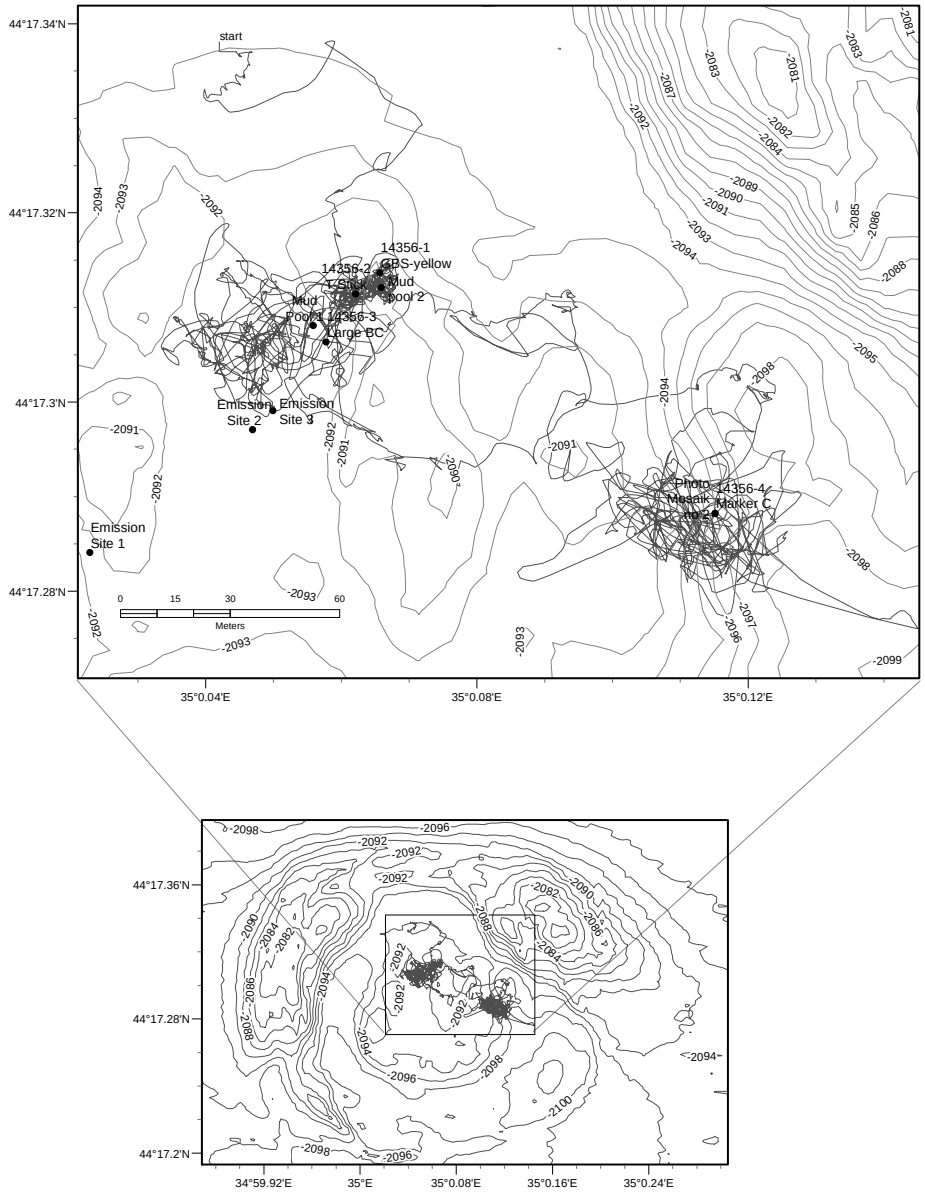

Fig. 65: Track of ROV QUEST Dive 272 at Helgoland mud volcano with relevant observations and sampling stations.

The remaining one hour dive time was used to systematically photograph the feature for mosaicking (Photo mosaic no. 2). At 4 m altitude several 20 m long parallel transects in the directions 300° and 120° with 2 m distance were conducted. The ROV heading remained the same, the altitude kept automatically, the movement was done with the function displacement at 5-8 % propulsion. The DVL navigation looked very good but it was accidentally reset during the transects causing a jump in position. The transects started approximately at the middle of the feature and covered the entire south-western part. It is unclear if the north-

western part of the feature was entirely mapped as there were still mud flows to be seen. However, they may already be connected to the adjacent mud source. During the transects rising bubbles (20 at a time) were seen in the unrecorded HD video originating from the central crater, e.g. at 02:49 UTC.

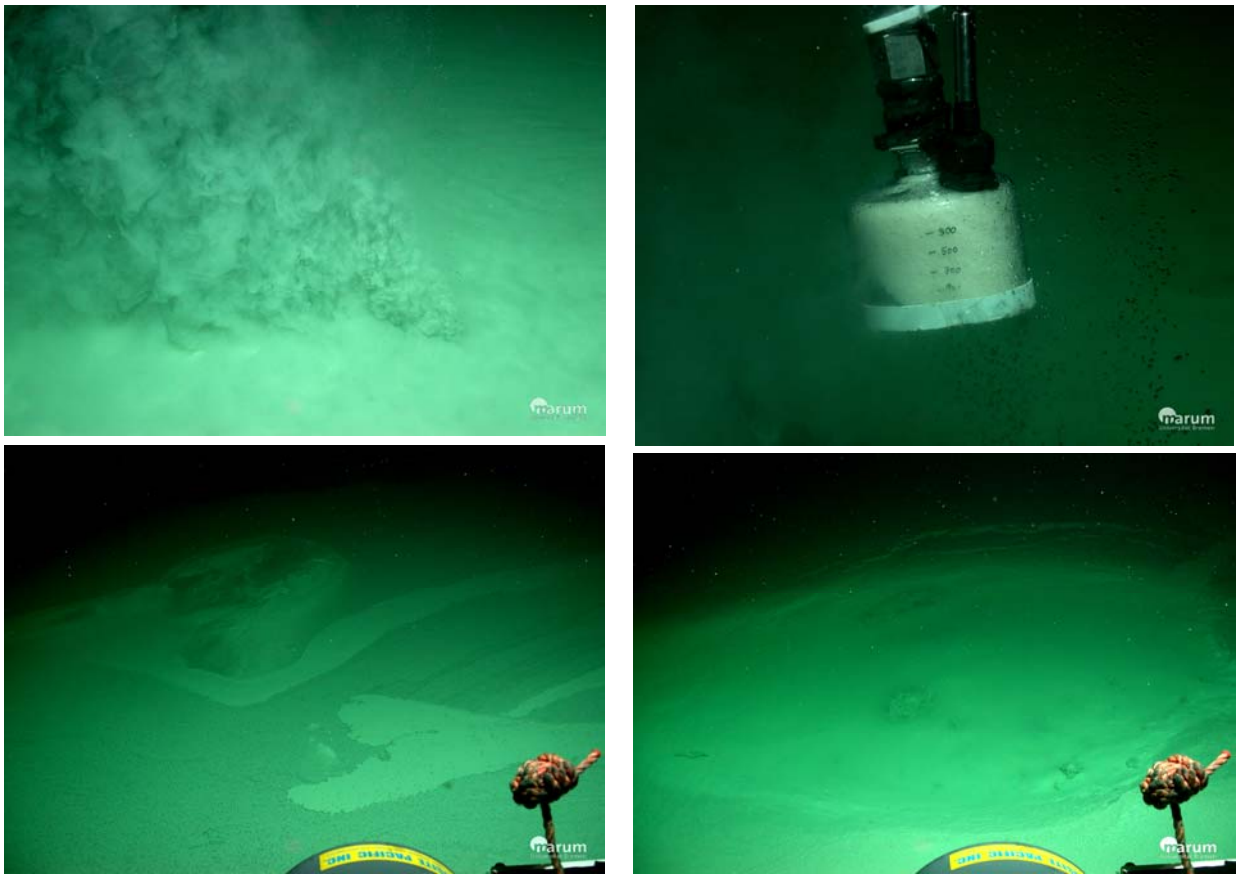

Fig. 66: Seafloor images at Helgoland mud volcano. Bubble emission at Mud Pool 2 (upper left). The collected bubbles at Mud Pool 2 are small and form gas hydrate (upper right). A photo mosaik was conducted in an area with fresh mudflows (lower left). At the end of the dive another mud pool was seen, it is unclear if this is the same seen before (lower right).

8.2.11 Dive 273 (MSM Station 605, GeoB 14361)

Area:	New Flare Site (NFS)	
Responsible scientist:	Jan-Hendrik Körber	
Date:	Saturday 29 May 2010	
Start at Bottom (UTC):	18:15	
End at Bottom (UTC):	00:07	
Bottom time:	05:52	
Start at Bottom:	44°24.874’N	35°20.685’E
Water depth:	1737 m	

Scientist planned schedule:

2.0 h ca. 20:00 – 22:00	Jan-Hendrik Körber	Thomas Pape
2.0 h ca. 22:00 – 24:00	Jan Hendrik Körber	Valentina Blinova
2.0 h ca. 24:00 – 02:00	Miriam Römer	Yann Marcon
2.0 h ca. 02:00 – 03:00	Miriam Römer	Carmen Friese

Points of interest:

Emission Site 1:	44°24.863'N	35°20.682'E
Emission Site 2:	44°24.847'N	35°20.654'E

Key results:

Gas bubble emissions were found as well as interesting seafloor features associated with gas emissions.

Technical description:

General performance of ROV good. Sonar worked well. No digitalization of videos.

Samples and measurements:

HD recording of gas emissions as well as the following samples were taken.

Table 13: Instruments and tools deployed during ROV Dive 273.

GeoB	Instrument	Time	Position	Depth	Comment
14361-1	BIP	19:01	44°24.8631 35°20.6819	1713.8 m	At Emission Site 1
14361-2	GBS-yellow	19:28	44°24.8629 35°20.6838	1713.6 m	T-logger not in the gas at Emission Site 1
14361-3	T-Stick	20:16	44°24.8620 35°20.6829	1713.9 m	At Emission Site 1
14361-4	Net	20:59	44°24.8611 35°20.6919	1713.3 m	Collect sediment, dark spot with whitish core at Marker "Volker"
14361-5	Marker "Volker"	21:11	44°24.8601 35°20.7015	1712 m	Birthday present
14361-6	Marker-St.Pauli				Near bubble site
14361-7	BIP	23:31	44°24.8471 35°20.6546	1715.2 m	Shutter speed first 500, then 250, at Emission Site 2
14361-8	GBS-black	23:48	44°24.8471 35°20.6545	1715.2 m	Only some bubbles, not filled, at Emission Site 2

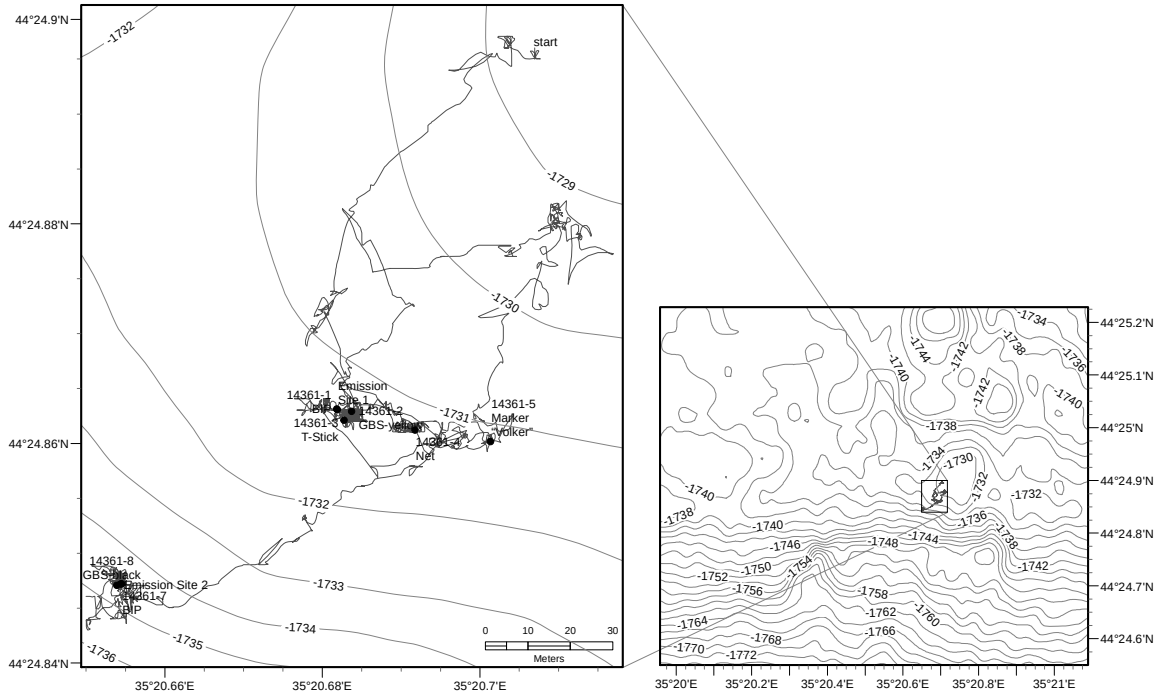

Fig. 67: Track of ROV QUEST Dive 273 at New Flare Site (NFS).

Dive description:

The main objective of the ROV Dive 273 was to investigate a site previously identified by sidescan sonar images in greater detail. Lacking a name for this new site, we call it New Flare Site (NFS). The site was crossed by a number of PARASOUND lines, which revealed active gas seepage. In advance to the ROV dive the AUV B-SEAL was deployed in order to get high resolution bathymetry data as well as to use sidescan information of the AUV to detect small gas emissions, which might not have an effect on the PARASOUND signal.

In contrast to other flare sites investigated during the MSM 15/2 cruise the New Flare Site is neither a mud volcano nor another morphological structure, which would be clearly visible on bathymetric maps with coarser resolution than the one achieved by AUV mapping. The NFS is more a fault-like structure with an elongated shape.

The positioning of the vehicle using the Posidonia underwater navigation system was good so that the ROV was landed ‘on the spot’ of the desired lowering position. After an initial bottom contact the ROV was heaved about 10 above the seafloor in order to detect gas flares with the horizontally looking sonar system mounted on the ROV (Fig. 67, tracks of dive 266 and 273). After a short while a bubble stream became visible in the sonar and was followed down to the seafloor (Emission Site 1). Reaching the seafloor small bubble holes became visible on the seafloor, aligned in a trending line on the slope of a about 1.5 m high morphological structure. Bubbles emanated only from a few holes in low frequency. Strong bottom currents made it at first difficult to stabilize the ROV on the point. Since no other bubble streams in the closer vicinity could be detected the bubble imaging plate (BIP) was deployed and the bubble stream was recorded in with the HD camera for about 10 min. After the BIP measurements were completed a gas bubble sampler with a large funnel and attached

temperature logger was used to collect a gas sample. The sampling took about 30 min but the amount of gas caught was still insufficient to cover the temperature logger entirely so that no information on the temperature was acquired. To complete the sampling procedure at this site the T-Stick was used.

When stowing away the T-Stick the pilots faced some problems with the ROVs manipulators. Already during the sampling procedure the left manipulator did not work very smoothly. After the measurement was completed the right one started uncontrolled turning. Fortunately the problems were solved and the dive continued as planned.

After the sampling was accomplished we continued eastwards in order to investigate the morphologic structure in greater detail and to start a photo documentation of the area. On the highest point of the structure an elongated depression became visible as well as a number of whitish patches surrounded by darker sediments. One such patch was sampled (Fig. 68) using the large bubble catcher. Already during the sampling procedure it became obvious that the light coloured sediments were probably not carbonates as we first thought. However the sampling revealed that the sediment in general is very fluffy and almost not compacted.

After the sediment sampling a marker was deployed and documented as a birthday gift for Volker Ratmeyer.

After the deployment of the marker we continued cruising in the water column in order to detect more bubble flares. For this purpose the ROV was elevated about 20 m above the seafloor to be able to scan the water column with the sonar. Another bubble emission site was detected by the sonar but turned out to be too small to start a sampling program. The ROV was heaved again for about 15 m above the seafloor to scan the water column for bubble streams towards the east. As no indication for gas emissions was seen, neither in the sonar nor by visual observation, the track continued towards the southwest. On the way another marker was placed on the seafloor. Marker and surrounding seafloor were documented by HD video and the HD photo camera Zeus. Approaching a potential flare site previously identified by AUV sidescan sonar, an acoustic signal appeared in the sonar, but ceased when reaching the site. Anyway a bubble emission site (Emission Site 2) was found at the seafloor and turned out to be weak but steady. Another sampling program was started including the use of the second GBS, deployment of the BIP and HD video recording for later analysis of the physical bubble properties. While the BIP was deployed different shutter speeds of the camera (500 and 250 ms) were chosen in order to find the optimal setup for the bubble imaging. While the BIP was moved back to the drawer the DSPL camera was hit by right manipulator of the ROV which resulted in a malfunction of the pan/tilt unit of the camera. Also, the scanning sonar stopped working reliable and was turned off. The sonar system seemed to get stucked and not to scan the water column entirely – a problem which was known from previous dives already.

The second GBS, equipped with a small funnel was filled successfully and the formation of gas hydrate at the water/gas interface in the funnel was nicely documented by HD video recordings. After the gas sampling was completed the scientific program at the seafloor was stopped and the ROV started to ascend to the surface.

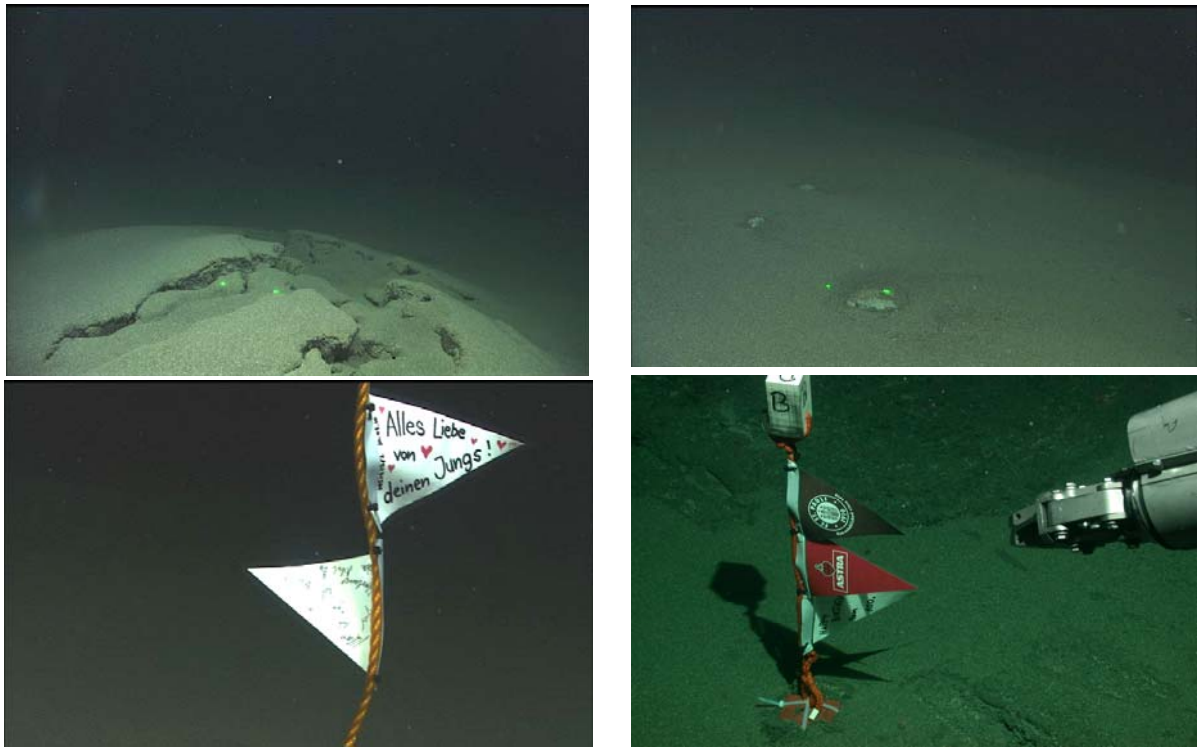

Fig. 68: Scorpio images taken during ROV Dive 273 at the Nameless Flare Site (NFS). Structured seafloor at Emission Site 1 (upper left) and the remains of former gas emission sites before sampling by net (GeoB14361-4) (upper right). Two markers were deployed in the area (lower left and lower right).

9. In Situ Sediment and Bottom Water Temperature Measurements

(H. Sahling, Y. Marcon, S. A. Klapp)

Temperature measurements in the vicinity of fluid seepage sites give detailed insight into transport processes of mud, liquids and gas. Four different processes may be distinguished: the advection of solids with fluids (mud flow), the advection of fluids through the sediments (pore-water advection), diffusion processes (chemical diffusion, conduction), or heat transported by rising gas bubbles without advection of pore water or mud. The four processes may result in different shapes of temperature versus depth profiles: linear profiles indicating conduction of heat, concave profiles signify advective processes (mud flow, fluid advection), or unsteady profiles indicating that the heat transport may not be a simple one dimensional transport process but heterogeneous in space and time (Feseker et al., 2009a; Feseker et al., 2008). The latter processes have been found to be associated with bubble emissions (Sahling et al., 2009).

Comprehensive studies of the temperature distribution have been already conducted at Dvurechenski mud volcano (DMV) (Feseker et al., 2009b). The results show that in a central part (slightly off-set to the north of the geometric center of the mud volcano) warm mud rises to the surface. The heat flux decreases concentrically from this center towards the rim of the mud volcano. Furthermore, the temperature in the central conduit was measured by temperature outriggers on a gravity corer that penetrated more than 50 m into the sediments. The measurements suggested a pivotal role of gas hydrate that act as thermostat. If present, exothermic hydrate formation and endothermic dissolution may force the temperature to a value close to 16°C, which is close to the hydrate stability limit at the given chemical composition of the gas and the high salinity of the pore fluid.

In addition to these exciting findings, a long term temperature mooring (T-mooring) was deployed in 2007 during the METEOR Cruise M 72/2. The mooring consists of a conventional gravity corer and two temperature strings mounted on the side. The 8 temperature probes per string were equally spaced over a length of 4.9 m. One logger was recovered 18 days after the deployment (at 07/03/2007 03:30 UTC). A second logger recorded temperatures of the second T-string in 15 min intervals. A major objective of this cruise was, therefore, to continue the thermal studies at Dvurechenski mud volcano and to recover the T-mooring giving insight into the temperature development of a time period of more than 3 years.

A further objective of this cruise was the study of heat anomaly associated with gas emissions. Initial studies at Vodyanitskii mud volcano indicated significant thermal gradients at the bubbling site (Sahling et al., 2009). Furthermore, experiments were conducted to study the phenomenon of in situ formation of gas hydrate at emission sites. These studies follow the observations during the METEOR Cruise M 72/3; gas bubbles were collected by an inverted funnel within the theoretical hydrate stability zone but, surprisingly, no hydrate formation was observed.

Temperature measurements were realized by autonomous memory miniature temperature logger build by the company Antares. The loggers record the temperature at preset time intervals usually every four to ten seconds. The loggers were used as outriggers on gravity corer (Fig. 69), in the funnel of Gas Bubble Sampler (GBS) deployed by ROV QUEST, or in the gas hydrate experiments. A second type of temperature logger was build by the company

RBB recording the measurements of eight temperature probes at a time. These loggers were used with the T-Stick operated by ROV QUEST as well as in the T-mooring at Dvurechenskii mud volcano. The spacing of the T-probes from the T-stick is about 0.066 m (8 sensors equally spaced over a length of 0.465 m). Intercalibration of the different temperature probes were conducted during ROV Dive 268 where the T-Stick, all Antares loggers, as well as the Sea&Sun Technology memory CTD Ser. No. 363 were deployed (caution: CTD time minus 3 hours = UTC).

The intention of the cruise report is to give an overview of the temperature measurements in the working area indicating major results. For that reason, the temperature data have not been processed but plotted as original values. Thorough temperature analyses on land warrants further processing such as cross calibration of the temperature measurement devices and modelling of the equilibrium temperatures.

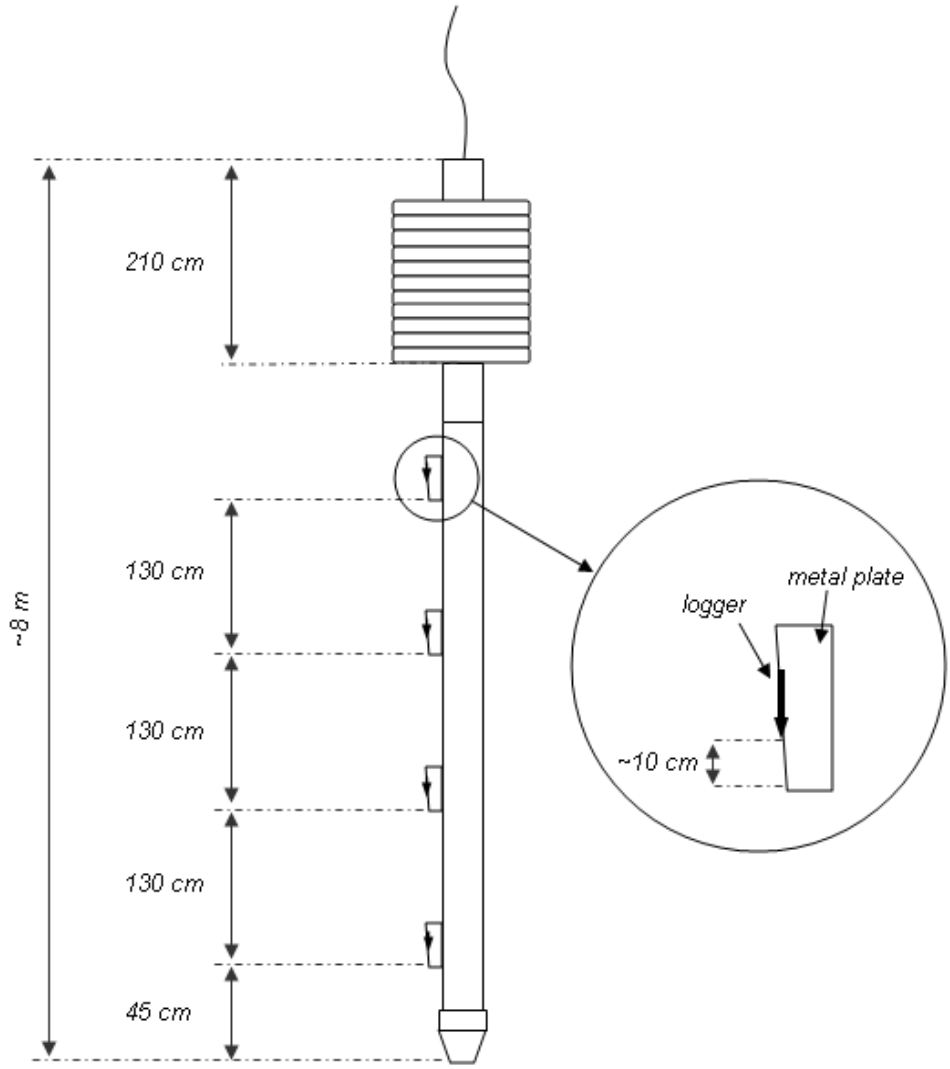

Fig. 69: Schematic drawing of the Antares T-Loggers deployed as outriggers on the gravity corer. This set-up was used from Station 568 on (GC-T-4; GeoB 14324) until the end of the cruise. Since two loggers were lost during deployment, probably due to mechanical forcing by hard rocks (e.g. carbonates). The bar protecting the loggers was fixed to the metal plate not only by screws but additionally by cable ties.

Table 14: Overview of temperature measurement conducted during Cruise MSM 15/2. Temperature measurements were conducted at MSU, Dvurechenski, and Helgoland mud volcano as well as at Kerch flare and Batumi seep.

Station	Number	GeoB	Tool	Penetration (m)	Estimated by	Equilibrium	Profile	Gradient (°C/m), max. Temp. anomaly	Comment
MSU MV									
GC-T-1	546	14302		10	Profile	yes	linear	0.0244	Logger distance 1.2 m, penetrated during hieve a second time, loss of lowermost logger
DMV									
GC-T-2	554	14310		13	Rope tension	yes	linear	0.286	Logger distance 1.2 m, lowermost logger just above core catcher
GC-T-3	555	14311		14	Rope tension	yes	linear	0.428	Logger distance 1.2 m, lowermost logger just above core catcher
GC-T-5	579	14335		34.5	Rope tension	yes	?	0.49	Further penetration prevented due to Posidonia 50 m above the tool
GC-T-6	580	14336		56.5	Rope tension	yes	?	1.12	
ROV 263	558	14314-1	T-Stick	~0.4		no	linear	4.45	Gas bubble emission site
ROV 267	581	14337-1	T-Mooring	5.9	Profile	yes	linear	1.15 to 0.78	Recovery of T-Mooring deployed in 2007
Helgoland MV									
GC-T-7	585	14341		62.5	Rope tension	yes	concave	1.16	Logger distance 1.3 m, lowermost logger about 55 cm (the logger frame is located 45 cm) above core catcher (as shown above), temperature of up to 35 °C at a depth of 60 m below seafloor
ROV 268	583	14339-1	GBS						logger 1854346, at mud pool I, ~ 0.6°C warmer than bottom water
ROV 268	583	14339-2	T-Stick	~0.4	Profile	no	concave	47	At mud pool I, asymptotic value 17.4 °C
ROV 268	583	14339-3	GBS						loggers 1854333, at strong bubble emission site, ~1.4 °C warmer than bottom water
ROV 268	583	14339-4	T-Stick	~0.4	Profile	no	concave	4.1	At strong bubble emission site without evidence for fluid mud
ROV 272	600	14356-1	GBS						1854334) and large (1854333)
ROV 272	600	14356-2	T-Stick	~0.4	Profile	no	concave	34	At mud pool II, asymptotic value 15.5°C
NFS									
GC-T-9	603	14359		<3.9	Profile	yes	linear	0.166	
ROV 273	605	14361-2	GBS						T-logger not in contact with gas phase
ROV 273	605	14361-3	T-Stick	~0.4	Profile	yes	linear	0.316	
ROV 273	605	14361-8	GBS						T-logger not in contact with gas phase
Kerch Flare									
GC-T-4	568	14324		5.2	Profile	yes	linear	0.088	Logger distance 1.3 m
GC-T-8	595	14351		3.9	Profile	yes	linear	0.132	Lowermost logger lost.
ROV 264	565	14321-1	GBS						“small GBS”, T-logger not in contact with gas phase, no temperature anomaly
ROV 264	565	14321-2	T-Stick	~0.5	Profile	yes	linear	0.234	In gas emission site at Marker A
ROV 265	567	14323-2	GBS						“small GBS”, max. temp. anomaly 0.122 °C
ROV 265	567	14323-3	GBS						“large GBS”, max. temp. anomaly 0.342 °C
ROV 265	567	14323-4	GBS						“small GBS”, max. temp. anomaly 0.126 °C
ROV 265	567	14323-5	T-Stick	~0.5	Profile	yes	linear	0.08	In bubble emission site
ROV 265	567	14323-6	T-Stick	~0.5	Profile	yes	linear	0.164	About 1 m away from bubble emission site T-stick 14323-5

ROV 265	567	14323-10	T-Stick	~0.5	Profile	yes	linear	0.132	Close to but not in bubble emission site
ROV 265	567	14323-11	T-Stick	~0.5	Profile	yes	linear	0.105	In bubble emission site near T-stick 14323-10
ROV 271	597	14353-2	T-Stick						T-stick only used as scale for HD view of bubbles in water column
ROV 271	597	14353-3	T-Stick	~0.5	Profile	no	linear	0.546	Sensor 2 not working
ROV 271	597	14353-5	T-Stick						T-stick only used as scale for HD view of bubbles in water column
ROV 271	597	14353-6	T-Stick	~0.5	Profile	yes	linear	0.0395	Sensor 2 not working
Batumi									
ROV 269	588	14344-2	GBS						T logger (1854333), large bubble sampler, max. temp. increase 0.211°C
ROV 269	588	14344-3	GH Exp. I						T logger (1854346), max temp increase ~0.2°C
ROV 269	588	14344-5	GH Exp. II						Oil Gas catcher logger (1854336), max temp increase 0.026°C
ROV 269	588	14344-7	T-Stick	~0.15	Profile	yes	linear	0.57	In bubble stream, did not penetrate well, only 2 sensors with significant temperature anomalies
ROV 269	588	14344-8	T-Stick	~0.5	Profile	yes	linear	0.17	Reference close to bubble emission site, good penetration

MSU Mud Volcano

One gravity corer was taken at MSU mud volcano in the central part of the western Black Sea (GC-T-1; GeoB14302) attempting to sample gas hydrates and to test what kind of sediments are present. During this deployment, the lowermost temperature logger was lost probably due to the occurrence of mud clasts in the sediments. The temperature profile shows background values of about 0.024 °C/m (Fig. 70).

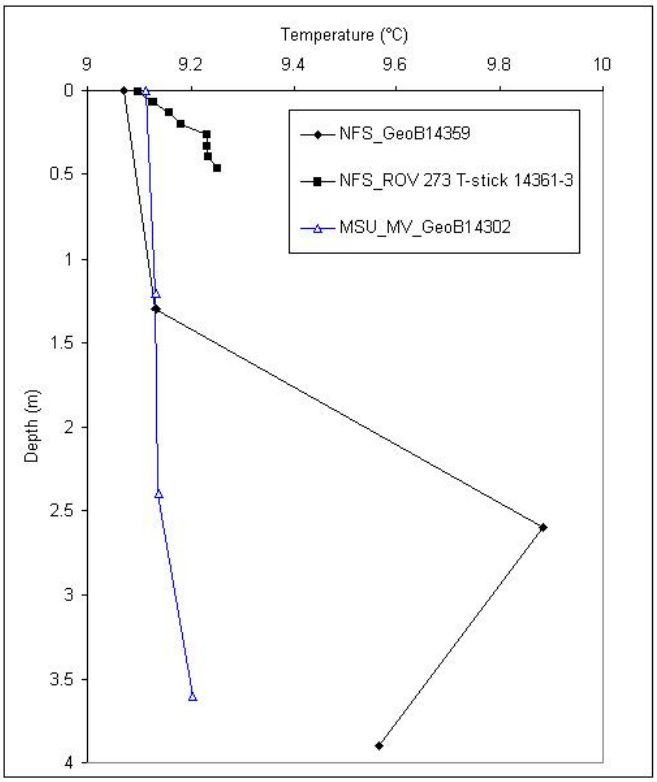

Fig. 70: Temperature versus depth profiles at MSU mud volcano and New Flare Site (NFS).

New Flare Site (NFS)

Gas emissions were found at New Flare Site, which is located at the crest of a linear ridge suggesting a fault system in the subsurface. At the gas emission, the temperature gradient increases to a value of about 0.3°C (ROV 273 T-stick 14361-3), which is significantly higher than the background value of 0.03°C that can be expected in this area. The GC-T GeoB14359 taken in the area of the gas emission (but not exactly at that site) shows a somehow erratic profile with the tendency of a temperature increase with depth higher than background values. These two measurements suggest that a thermal anomaly is associated with the gas emission at NFS.

Dvurechenski Mud Volcano

Three sets of temperature measurements were achieved at Dvurechenskii mud volcano: near surface measurements, deep-penetrating GC-T, and recovery of the T-mooring as summarized in the temperature versus depth plot (Fig. 71). The near surface measurements made by ROV (T-Stick 14314-1) as well as GC-T 2 and 3 revealed high temperature gradients ranging from 4.4 to 0.28°C/m, respectively (Tab. 14). This is in agreement with earlier findings by Feseker et al. (2010), reporting temperature gradients of up to 11°C/m at the warmest center on the plateau of the mud volcano and less steep gradients away from the center. The T-stick was deployed at a site with weak gas bubble emission. The fact that the measured temperatures (although not in equilibrium with the surrounding sediments) are lower than those at the warmest center may indicate that the central conduit is likely the main pathway for mud and pore water advection but that the bubble emission is somehow decoupled from this hot spot.

Sediments are at least at central locations at the Dvurechenskii mud volcano very fluid, allowing for deep penetration of the gravity corer into the sediments. The precise penetration depth is difficult to estimate. For example, the core recovery of GC-T 2 (GeoB 14310) was 3.4 m but the Antares logger clearly indicate penetration and frictional heat development of all loggers, accordingly, the minimum depth penetration was 4.3 m, or more. As a consequence, the penetration depth was calculated based on the rope tension and rope length as recorded in the DSHIP data base. The rope length in the moment when the rope tension is abruptly reduced due to the sediment contact of the gravity corer was zeroed at the seawater-sediment boundary. As we continued to pay out more rope, the core penetrated further into the sediments, while the rope tension was continuously relieved. When no further reduction in rope tension was observed, the rope length was taken at the deepest point that the gravity corer reached. The penetration depth was calculated based on the rope length difference between first bottom contact and deepest point. In case of GC-T 2 (GeoB 14310) this calculation based on rope tension method (Tab. 14) showed a penetration of the lowermost logger to about 13 m into the sediment. This is a realistic estimation, being corroborated by the temperature measurements: Based on the result of Feseker et al. (2010), a concave-shaped profile originating from the bottom water value of about 9.1°C to the asymptotic value of around 16°C at depth is assumed. Such a temperature profile can only be constructed when the measured gradient was at that actual depth around 13 m (Fig. 71).

The two very deep penetrating gravity corers were deployed close to the station 307 as in Feseker et al. (2010). The maximum depth was calculated based on the rope tension, though it did not work so well in case of GC-T-5 (GeoB 14335). Based on the rope length and rope

tension during the deployment time shown in Fig. 72, a maximum depth of the lowermost logger of about 34.5 m can be estimated. The corer was lowered to the deepest depth and then slowly heaved in intervals of 5 or 10 m and for each interval, the temperature probes equilibrated with the surrounding sediment temperature for 10 minutes. The comparison of logged temperature data and rope length calculation suggests that the logger must have been deeper in the sediments than 34.5 m. Based on the rope length calculation, the logger should have left the sediments towards the end of the deployment period but they obviously did not do so. Further analyses of the data are needed to solve this problem. In general, the temperature in the deep sediments is around 16.5°C with a slight increase in temperature at the most shallow depth. One logger showed a slightly higher temperature shortly after penetration. The cause for this is not clear; one explanation could be the spontaneous formation of gas hydrate, which runs exothermally and therefore evokes local heat anomalies.

The measurement was repeated during GC-T-6 (GeoB 14336), this time penetrating about 56.5 m into the sediments as revealed by the rope tension method. At that depth, the temperature increased above the value of 16.5°C up to maximum temperature of about 20°C, which is clearly outside the hydrate stability zone. Again, the logged data suggest different thermal regimes and vary up to several degrees at depths below ~30 m. Shallower than ~30 m, the temperatures of all loggers remained similar. This finding is in contrast to that of Feseker et al. (2010) who observed a temperature variability above ~30 m and explained it by the absence of gas hydrates, and recorded uniform temperatures below that depth, explained by gas hydrate acting as thermostat.

The logger of the 3-years measuring T-mooring as well as the mooring itself was recovered during ROV Dive 267 only after relocating its position using the sidescan sonar data obtained by the swath echosounder during the AUV dive at Dvurechenskii mud volcano. Surprisingly, the mooring was located about 100 m further south of the original position confined during the deployment and first logger recovery in 2007 (METEOR Cruises M72/2 and 3). Inaccuracy of the Posidonia underwater positioning system may be responsible for some of the differences in the location of the mooring but 100 m is far too much. In general, the Posidonia system worked reliably during our cruise, e.g. at Batumi seep at shallower water depth of about 860 m a marker on the seafloor placed in 2007 was found at the very same position during this cruise, with an error of less than 10 m. Therefore, we speculate that the position of the mooring 100 m further south is real and may be explained by a mud that slowly moves from the center to the outer rim. Such a movement would be accompanied by a decrease in temperature with time (and therefore distance from the center), which is actually what the data show (Fig. 74). The temperature steadily decreased over time with a gradient that decreases from 1.15 (12/03/2007 00:00) to 0.78°C/m (18/05/2010 20:00).

While the T-mooring recording generally shows a decrease in temperature over time, there is one event where there is a 0.2°C increase in temperature. This event may be explained by a movement of ~20 cm of the mooring down into the sediment.

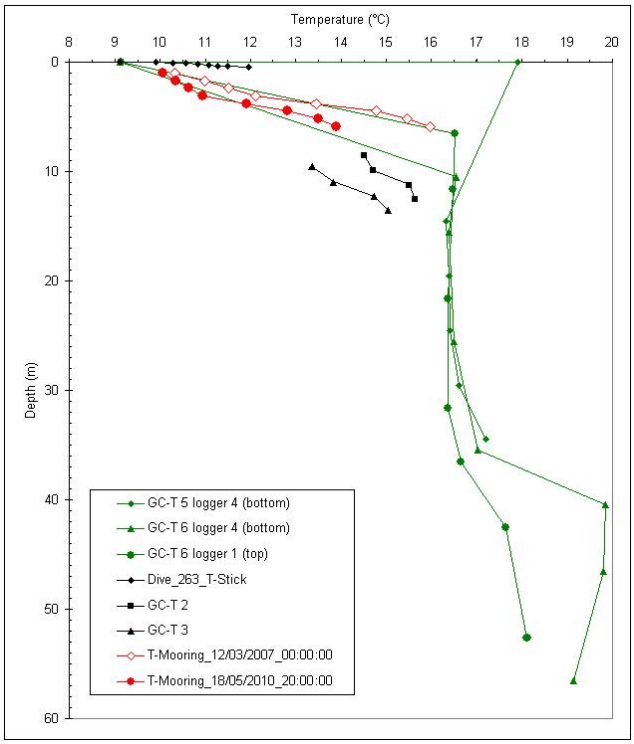

Fig. 71: Summary of temperature versus depth profiles at Dvurechenskii mud volcano.

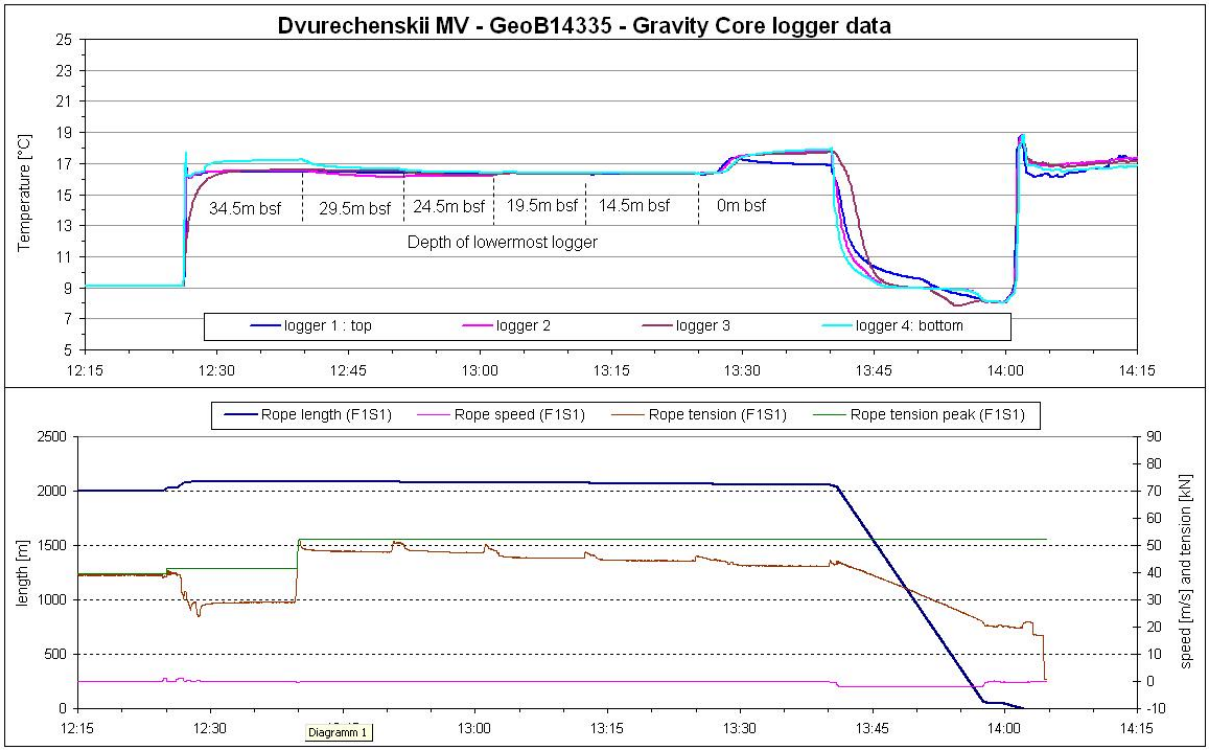

Fig. 72: The temperature (upper panel) and rope characteristic (lower panel) during the deployment time of GC-T-5 (GeoB 14335) at Dvurechenskii mud volcano (rope tension (brown), maximum rope tension (green), rope speed (pink), and rope length (blue)).

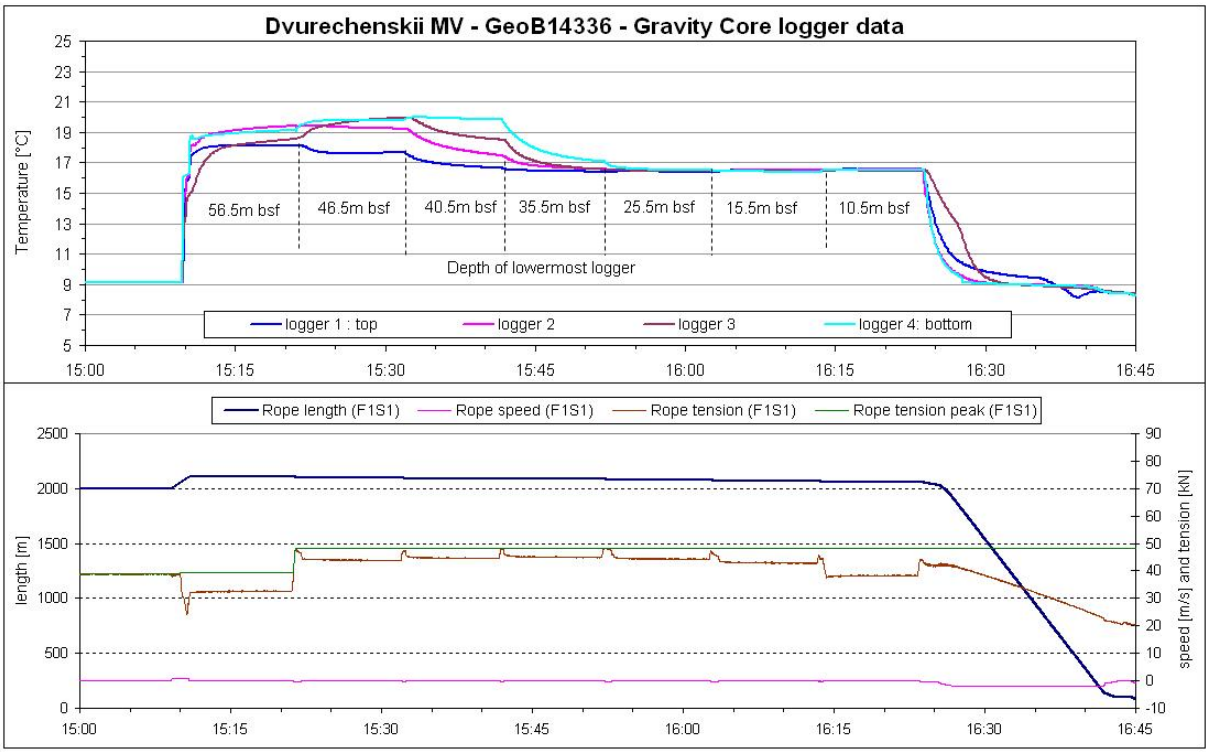

Fig. 73: The temperature (upper panel) and rope characteristic (lower panel) during the deployment time of GC-T-6 (GeoB 14336) at Dvurechenskii mud volcano (rope tension (brown), maximum rope tension (green), rope speed (pink), and rope length (blue)).

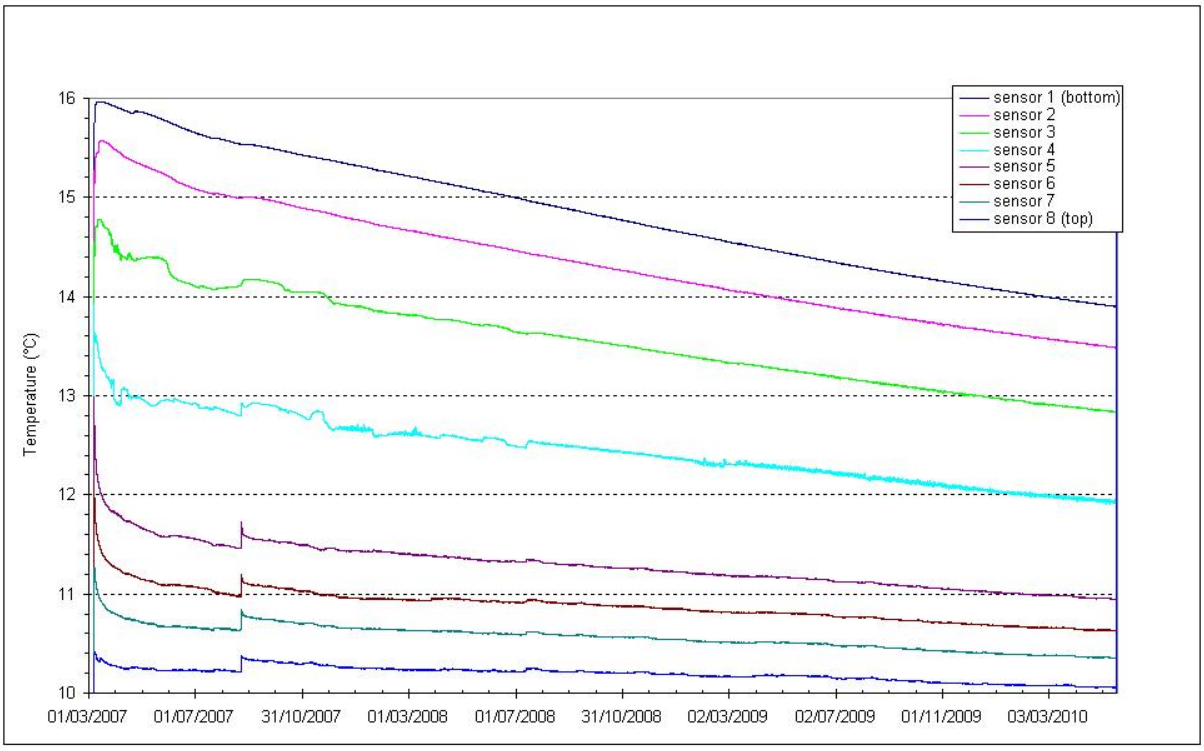

Fig. 74: The temperature data of the long-term T-mooring at Dvurechenskii mud volcano showing a near continuous decrease in all T-sensors over time. The T-mooring was deployed 7/3/2007 03:30 (UTC) and recovered 18/05/2010 20:30 UTC. The temperature was measured every 15 min. While there is a steady decline in temperature over time one event on the 22/08/2007 between ~15:15 and ~17:15 caused a rise in temperature.

Helgoland Mud Volcano

Fresh mud flows and pools with very liquid mud were found at Helgoland mud volcano (formerly described as Nameless Seep Site (Greinert et al., 2006)). Gas bubbles emit at the mud pools but also at another site without liquid mud. The temperature measurements with the T-stick at the mud pool suffer from too short time to allow the probes to equilibrate with the surrounding very warm mud (Fig. 75). Irrespective of the suspicion that the actual temperature was higher, the measured value clearly demonstrates that the temperature-depth gradient is extremely high with up to 47°C/m at mud pool I (GeoB 14339-2) (Fig. 76, Tab. 14). A further mud pool II showed slightly lower absolute temperature values (GeoB 14356-2). In contrast to the strong temperature gradients at the mud pools, a site with strong bubble emission but without evidence of fluid mud revealed a small temperature gradient.

In addition to the T-stick measurements gas was collected at the mud pools and at the gas emission site with the Gas Bubble Sampler. Temperature of the gas was measured within the funnel and shows that in general the gas has a higher temperature (Fig. 77). The increase in temperature recorded inside the GBS corresponded at the strong emission site with the temperature measured in the sediments with an increase of a bit more than 1°C. In contrast, at the mud pools, the recorded temperature anomaly inside the GBS was much less than the recorded strong temperature anomaly of the mud itself, obtained by T-stick probing. At least three main processes may account for these discrepancies: (1) the gas may originate from different depth than the mud and has, therefore, a different temperature when leaving the sediments. (2) The gas quickly loses its heat when ascending through the water. (3) The process of hydrate formation influences the temperature measurement. We assume that processes (2) and (3) may play major roles: one argument for process (2) is that for a stronger gas emission a higher temperature anomaly is measured in the gas phase because the gas cannot lose its heat quickly enough in the water. The effect of hydrate formation (process (3)) may be observed in GBS GeoB14356-1 (Fig. 77). The temperature increases by about 1°C while gas is collected in the funnel and hydrate forms from the gas and water. Hydrate formation is an exothermal process. The temperature increases a second time when the GBS was shaken by the ROV arm at around 21:26 UTC. This suggests that gas, which was kept in hydrate-coated gas bubbles got into contact with surrounding water and formed additional hydrate, increasing the temperature inside the funnel even more. The drop in temperature around 21:28 UTC corresponds to the opening of the valve and the sucking in of the gas into the pressure chamber.

The lowermost temperature logger of GC-T-7 (GeoB 14341) penetrated 62.5 m below the seafloor and measured 35.5°C in the central area of Helgoland mud volcano (Fig. 78). The temperature versus depth profile shows a clear concave shape indicative for advection processes that bring mud and fluids upwards (Fig. 76).

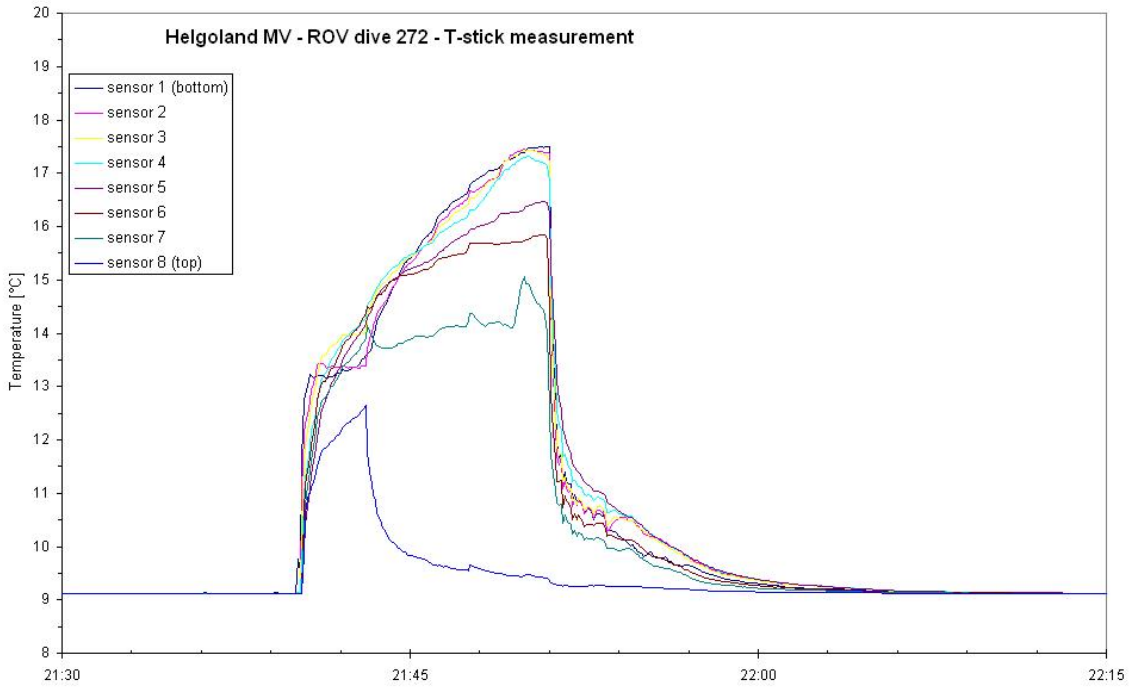

Fig. 75: Temperature versus time at Mud Pool I at Helgoland mud volcano (T-stick 14339-2).

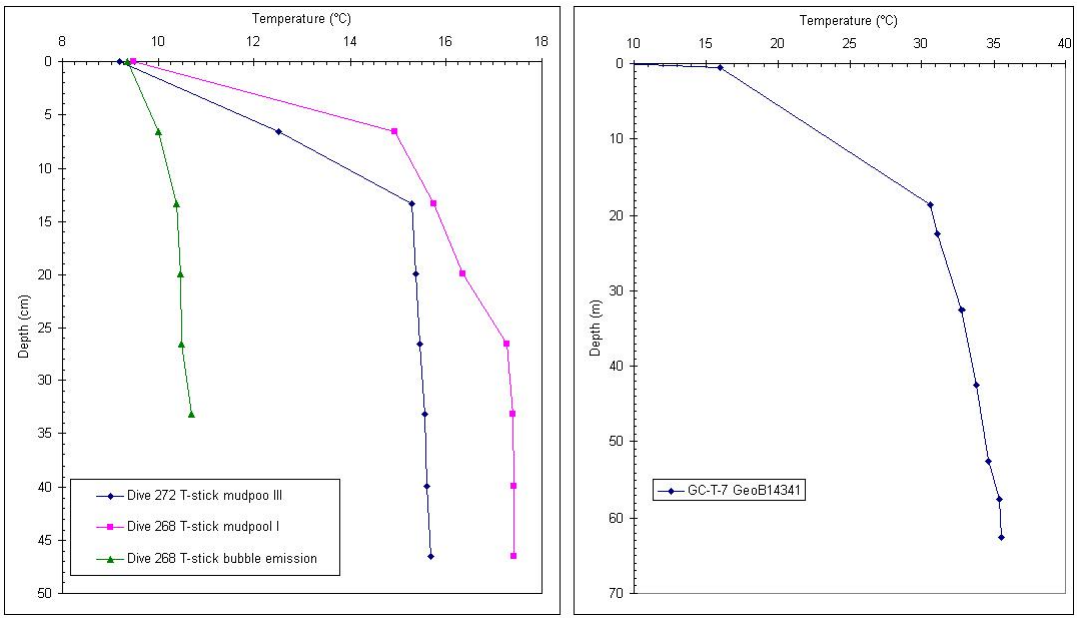

Fig. 76: Temperature-depth profiles at Helgoland mud volcano. The mud pools I and II have been sampled and showed the strongest gradient measured during the entire cruise. The gradient at the gas emission site that is not connected to a mud pool and was, in contrast, much lower.

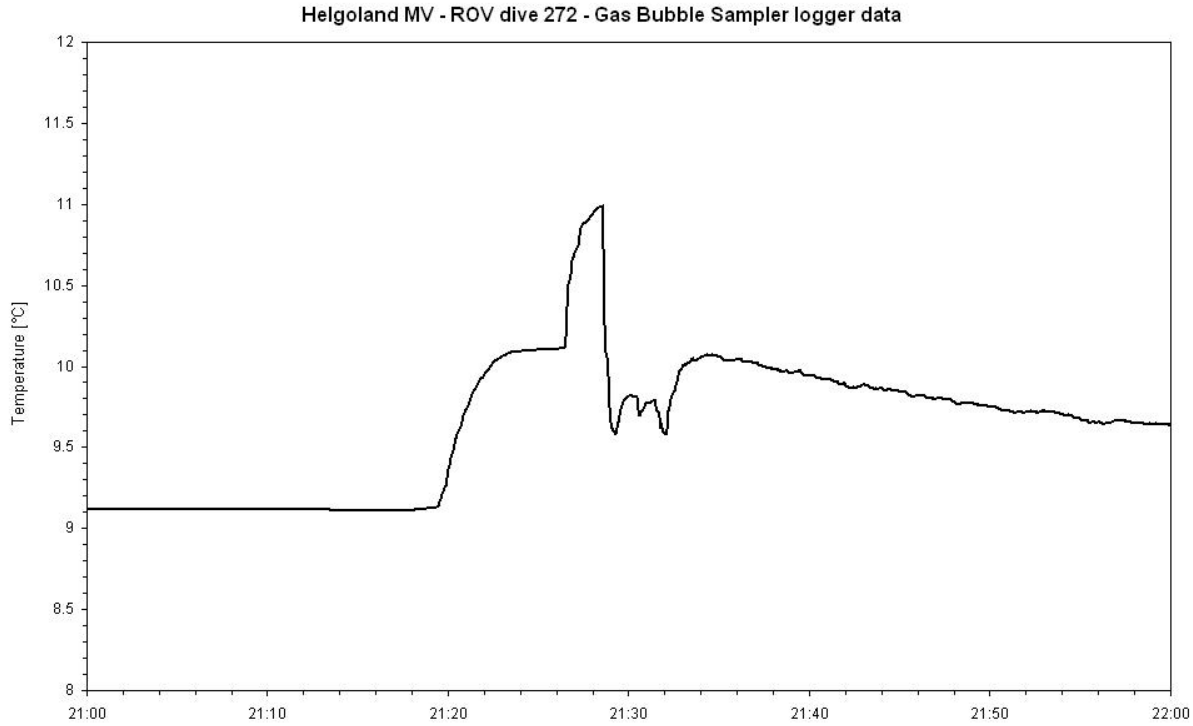

Fig. 77: Temperature versus time plot of ROV 272 GBS (GeoB 14356-1) taken above the mud pool II (T-stick GeoB 14356-2).

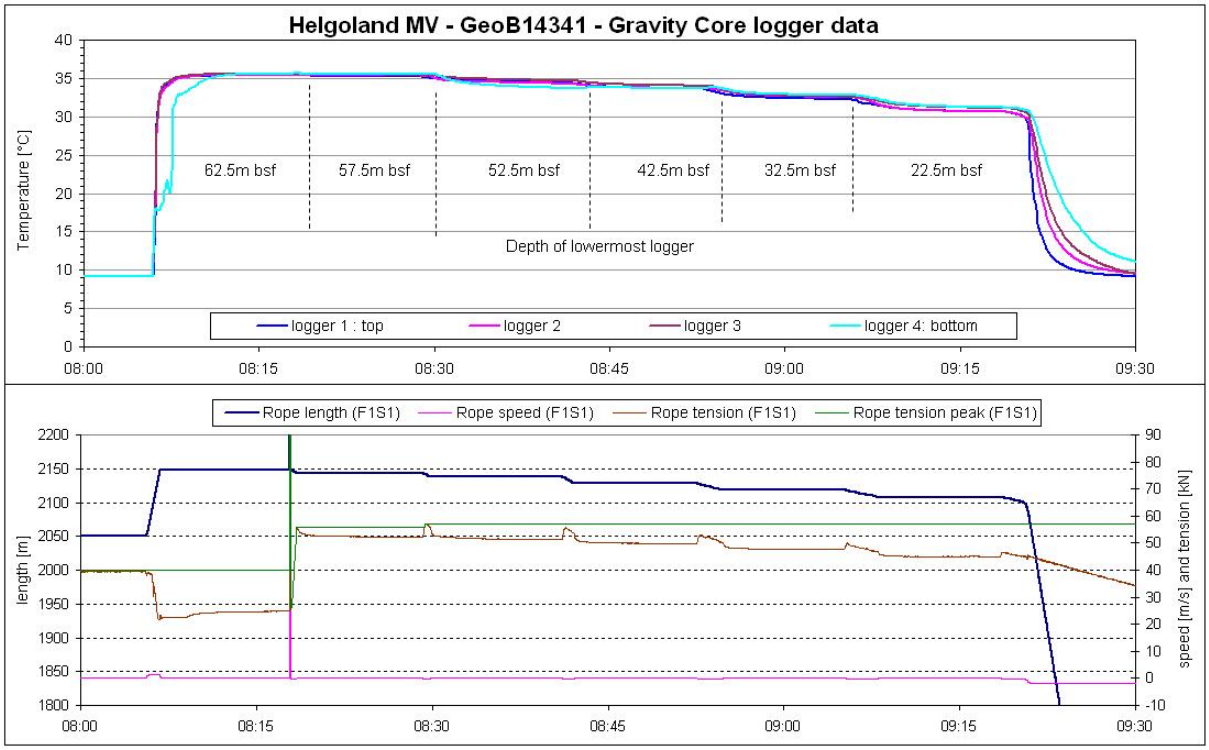

Fig. 78: Temperature and rope characteristics versus time at Helgoland mud volcano (GC-T-7, GeoB 14341) that penetrated 62.5 m in the sediment and reached temperature of up to 35.5°C.

Batumi Seep

At Batumi sSeep two T-stick measurements have been conducted, one at a bubble emission site and a second one outside. The temperature gradients were 0.57 and 0.17°C/m, respectively (Tab. 14). This indicates that the gas emissions are associated with thermal anomalies. In addition, the gas collected by the GBS and in the hydrate experiments was up to 0.2°C warmer than the bottom water (Tab. 14).

Kerch Flare

Several T-stick as well as temperature-GC measurements were conducted in the Kerch flare area (Fig. 79). The maximal temperature gradient was recorded at an active bubble emission site with 0.546°C/m (T-Stick GeoB 14353-3). The T-probes did not adequately equilibrate with the warm surroundings, thus a further analyse of the equilibration temperature is essential. The high gradient of 0.546°C/m compares well with Batumi seep (see above), an area that is dominated by bubble emission without indication of pore water advection or mud flows.

However, it is worth mentioning that at the Kerch flare in general, other T-stick measurements did not reveal such high temperature gradients, they commonly ranged between 0.04 and 0.23°C/m. An astonishing observation was made that the gradients measured at the reference stations a meter or so away from the bubble emission sites show higher gradients than those directly deployed inside the bubble emission sites (see T-stick 14323 - 5, 6, 10 and 11, Tab. 14).

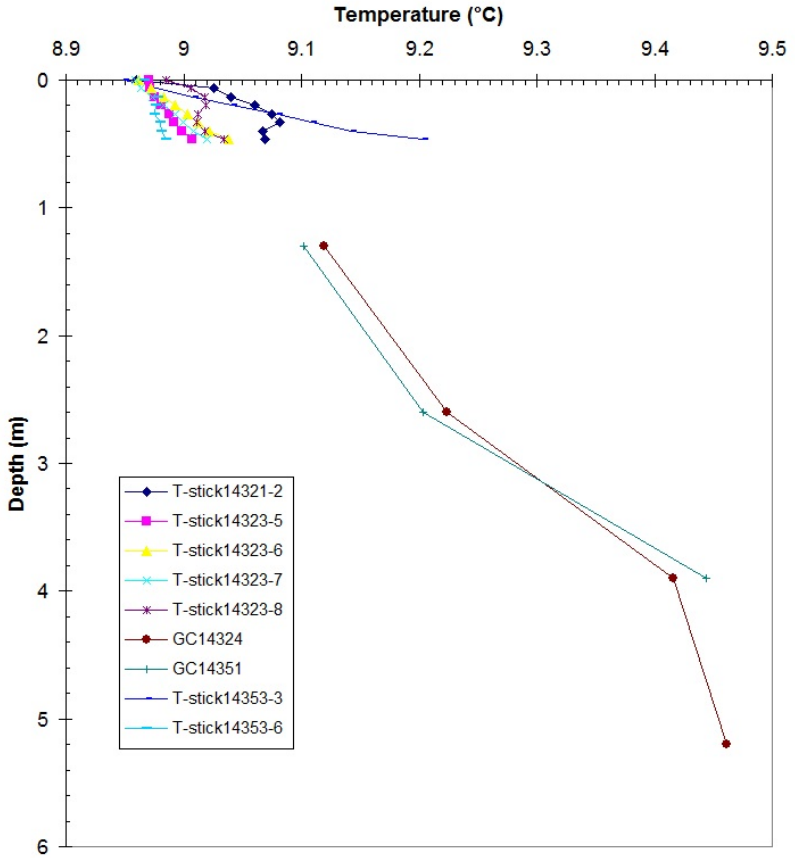

Fig. 79: Temperature versus depth profiles obtained by T-stick and T-probes outriggers at gravity corer in the area of Kerch flare.

10. Sediment Coring and Sampling

(T. Pape, V. Blinova, C. Friese, S.A. Klapp, A. Hiruta, J.-H. Körber, M.V. Ivanov, Y. Marcon, K. Dehning)

During MSM 15/2 surface sediment samples from cold seep and mud volcano environments were recovered. For the recovery of pressurized sediment cores, the Dynamic Autoclave Piston Corer I (DAPC) was deployed, while non-pressurized cores were collected with a conventional gravity corer (GC). At nine stations the GC has been equipped with temperature loggers in order to record the sediment temperature (see Chapter 9: Temperature Measurements). The sampling device was run via the deep-sea cable of the vessel. For accurate positioning, the underwater USBL navigation system POSIDONIA was mounted on the cable 50 m or 100 m above the DAPC.

10.1 Collection of Pressurized and Non-pressurized Surface Sediment

The DAPC I was used to collect gas hydrate-bearing surface sediment cores of up to 2.65 m length and 8.5 mm in diameter under in situ hydrostatic pressure for the quantification of sediment-hosted gas. Details on the technical specifications, on maintenance and handling on board, and on the degassing procedure of the DAPC can be found in the scientific literature (Heeschen et al., 2007; Abegg et al., 2008; Pape et al., 2010) and in the cruise report M72/3 (Bohrmann, Pape et al., 2007).

Table 15: Station list of sediment cores retrieved during cruise MSM 15/2.

GeoB-No.	GC/DAPC-No.	Location	Latitude [N]	Longitude [E]	Water Depth [m]	Recovery [m]	Comment
14308	DAPC-1	Helgoland MV	44:17.280	35:00.040	2.086	2.65	
14319	DAPC-2	Odessa MV	44:23.021	35:09.279	1.812	2.00	
14325	DAPC-3	Kerch Flare	44:37.218	35:42.184	880	1.73	
14333	DAPC-4	Tbilisi MV	44:25.310	35:16.075	1.679	1.80	
14345	DAPC-5	Colkheti seep	41:58.058	41:06.189	1.129	0.45	
14354	DAPC-6	Kerch Flare	44:37.222	35:42.275	895	2.52	
14360	DAPC-7	New Flare Site	44:24.874	35:20.690	1.748	1.88	
14309-1	GC-1	Helgoland MV	44:17.270	35:00.056	2.088	6.00	
14309-2	GC-2	Helgoland MV	44:17.280	35:00.040	2.087	6.00	
14318	GC-3	Odessa MV	44:23.003	35:09.275	1.813	7.35	GH
14331	GC-4	New Flare Site	44:25.302	35:16.080	1.698	2.70	
14332	GC-5	New Flare Site	44:25.328	35:15.869	1.699	5.30	GH
14340	GC-6	Helgoland MV	44:17.347	35:00.164	2.101	0.50	
14302	GC-T-1	Center MSU MV	43:32.003	33:06.830	2.100	2.00	
14310	GC-T-2	Dvurechenskii MV	44:16.990	34:59.110	2.059	3.39	GH
14311	GC-T-3	Dvurechenskii MV	44:16.910	34:58.770	2.059	5.29	GH
14324	GC-T-4	Kerch Flare	44:37.215	35:42.286	880	4.50	GH
14335	GC-T-5	Dvurechenskii MV	44:17.040	34:58.880	2.057	2.00	
14336	GC-T-6	Dvurechenskii MV	44:17.041	34:58.891	2.057	1.00	
14341	GC-T-7	Helgoland MV	44:17.311	35:00.037	2.104	6.00	
14351	GC-T-8	Kerch Flare	44:37.219	35:42.295	896	2.40	
14359	GC-T-9	New Flare Site	44:24.867	35:20.679	1.748	1.63	GH

DAPC = Dynamic Autoclave Piston Corer; GC = Gravity Corer; GC-T = Gravity Corer equipped with temperature probes; MV = Mud volcano; GH = gas hydrates present

During the seven DAPC-deployments (Table 15), the DAPC was slacked with a rope velocity of 0.5 m s^{-1} and heaved with 1.0 m s^{-1}. According to the DAPC working principle penetration of the core cutting barrel was conducted in the free fall mode. Upon completion of the controlled core degassing (see Chapter 11: Gas Analysis), the core inside a rigid PVC-liner was removed from the DAPC pressure chamber for subsequent pore water and sediment collection as well as macroscopic core descriptions (see chapter 10.4: Core descriptions).

Gravity cores were taken with a 6 m core barrel equipped with a soft plastic hose inside. The soft plastic hose enabled rapid access to gas hydrate pieces present in the sediment core. On the outside of the barrel, the GCs were furnished with temperature loggers (see chapter 9: Temperature Measurements). In the following, conventional GCs (i.e., without T-loggers) are abbreviated "GC", whereas temperature-recording GCs are abbreviated "GC-T". For all gravity cores, macroscopic core descriptions were performed. In contrast, sediment and pore water samples were taken for selected cores and distinct sediment intervals only due to their disturbance during extraction of hydrate pieces. In total 15 gravity cores were taken during cruise MSM 15/2 (Table 15), of which 9 were equipped with temperature sensors. The gravity corer was slacked with a rope velocity of 1.0 m s^{-1} and heaved with 2.0 m s^{-1}. Sediment penetration of the core cutting barrel was done with 0.3 to 0.5 m s^{-1}.

10.2 Pore Water and Sediment Sampling

Pore waters were extracted from DAPC sediment cores and selected gravity cores using the Rhizon technique (Seeberg-Elverfeldt et al. 2005; Dickens et al. 2007). Usually pore water samples were taken along the core in 10 cm-intervals. The volume of pore water collected was transferred with medical syringes headspace-free into 10 mL-glass bottles and sealed with screw caps equipped with PTFE inlays. The glass bottles are stored in the darkness at 4°C until analysis in the home lab. Pore water samples will be measured for concentrations of Cl^-, SO_4^{2-}, Ba^{2+}, as well as for $\delta^{18}O$-H_2O, δ^2H-H_20, and $\delta^{13}C$-DIC. In total 101 pore water samples were retrieved during MSM 15/2 (Table 16).

Table 16: List of pore water and sediment samples retrieved for analysis of bulk parameters.

GeoB-No.	GC/DAPC-No.	Location	No. of pore water samples	No. of sediment samples
14308	DAPC-1	Helgoland MV	24	14
14340	GC-6	Helgoland MV	2	2
14341	GC-T-7	Helgoland MV	7	6
14319	DAPC-2	Odessa MV	22	24
14333	DAPC-4	Tbilisi MV	11	11
14360	DAPC-7	New Flare Site	10	13
14325	DAPC-3	Kerch Flare	10	11
14354	DAPC-6	Kerch Flare	12	13
14345	DAPC-5	Colkheti Seep	7	7
		Sum	**105**	**101**

Sediment samples were taken from DAPC cores and selected gravity cores with 10 ml-plastic syringes with the tips cut off. In most cases sediment samples were collected in 10 cm-intervals. The syringes were sealed with plastic caps and stored in the darkness at 4 °C until

analysis in the home lab. Sediment samples will be investigated for sediment porosity, grain size densities, C/N ratios and TOC contents. In total 105 sediment samples were collected during MSM 15/2 (Table 16).

10.3. Sediment Sampling for Mineralogical Analyses

For mineralogical analysis, which will be performed to study the formation and evolution processes at the sampling sites, sediment samples including clay clasts and carbonates were collected. The samples were recovered from the Dvurechenskii MV, the Helgoland MV, the Kerch flare area, and the Colkheti seep (Table 17). Sediments and clay clasts were taken from the cores, cleaned and stored dryly for transport. The sediments are investigated onshore by various mineralogical and geological methods.

Table 17: List of sediment samples collected for mineralogical analysis.

Station No. Location	Burial depth (cmbsf)	Number of Pieces	Approx. size (cm)	Facies	Color Munsell	Color	Comments
GeoB 14310 Dvurechenskii MV	200	1	3 x 2	Clay	10Y 5/1 Gley 1	greenish gray	
	219	1	1 x 1	Clay	5Y 5/2	olive gray	
GeoB 14311 Dvurechenskii MV	10	1	1.5 x 1	Clay	5Y 5/1	gray	
	52	1	1.8 x 1	Clay	5Y 5/1	gray	
	82	1	3 x 1	Clay	5Y 6/1	gray	
	155	1	1.5 x 1	Clay	5GY 6/1 Gley 1	greenish gray	
	162	1	3 x 2	Clay	10Y 6/1 Gley 1	greenish gray	
	231	1	1.5 x 1	Clay	10YR 5/2	grayish brown	
	357	3	1 x 1	Clay	10Y 6/1 Gley 1	greenish gray	broken into small pieces
			1 x 1	Clay			
			1 x 1	Clay			
			1 x 1	Clay			
	374	2	1.6 x 1	Clay	10Y 6/1 Gley 1	greenish gray	
			1.6 x 1	Clay	10Y 6/1 Gley 1	greenish gray	
	440	1		Clay	10Y 5/1 Gley 1	greenish gray	broken into small pieces
	447	1	2.5 x 1.4	Clay	10Y 6/1 Gley 1	greenish gray	
		1			10YR 4/1	dark gray	
GeoB 14336 Dvurechenskii MV	?	1	4 x 5	Clay	5Y 7/2	light gray	
		6	2 x 1.5	Clay	10Y 5/1 Gley 1	greenish gray	
			1.5 x 1	Clay	10Y 5/1 Gley 1	greenish gray	
			1 x 0.5	Clay	5Y 5/1	gray	
			1 x 0.5	Clay	5Y 5/1	gray	
			1 x 0.5	Clay	10Y 5/1 Gley 1	greenish gray	
			1 x 0.5	Clay	10Y 5/1 Gley 1	greenish gray	

Table 17 continued.

Station No. Location	Burial depth (cmbsf)	Number of Pieces	Approx. size (cm)	Facies	Color Munsell	Color	Comments
GeoB 14340	~10	10	6 x 2.5	Carbonate	5Y 8/1	white	
Helgoland MV			2 x 1.5	Carbonate	5Y 8/1	white	
			2 x 1	Carbonate	5Y 8/1	white	
			2 x 1	Carbonate	5Y 8/1	white	
			2 x 1.4	Carbonate	5Y 8/1	white	
			1 x 1	Carbonate	5Y 8/1	white	
			1 x 0.5	Carbonate	5Y 8/1	white	
			1 x 0.5	Carbonate	5Y 8/1	white	
			1 x 0.5	Carbonate	5Y 8/1	white	
			0.5 x 0.5	Carbonate	5Y 8/1	white	
	40	1	6 x 6	Carbonate	5Y 8/1	white	
GeoB 14351	110	1	5.5 x 1.8	Wood	5Y 2,5/1	black	
Kerch Flare	182	2	1.2 x 1	Carbonate	5Y 8/1	white	
			1 x 1	Carbonate	5Y 8/1	white	broken into small pieces
GeoB 14345	0-10	12	4 x 1	Carbonate	5Y 8/1	white	
Colkheti Seep			3 x 2	Carbonate	5Y 8/1	white	
			2.5 x 1	Carbonate	5Y 8/1	white	
			2 x 1.5	Carbonate	5Y 8/1	white	
			2 x 1	Carbonate	5Y 8/1	white	
			2 x 0.5	Carbonate	5Y 8/1	white	
			1.5 x 1.5	Carbonate	5Y 8/1	white	
			1.5 x 1.2	Carbonate	5Y 8/1	white	
			1.5 x 0.7	Carbonate	5Y 8/1	white	
			1 x 1	Carbonate	5Y 8/1	white	
			1 x 0.7	Carbonate	5Y 8/1	white	
			0.7 x 0.7	Carbonate	5Y 8/1	white	
	25	1	4 x 2.5	Carbonate	5Y 6/2	white	

10.4 Core Descriptions

10.4.1 General Description of Upper Quaternary Sediment Sections

The laminated sediments of the Black Sea were discovered more than 100 year ago. However, only after the Atlantis II cruise in 1969 the general features of the Black Sea sedimentology became widely known (Ross et al., 1970; Degens and Ross, 1972; Ross and Degens, 1974). The essential stratigraphy of Pleistocene to Holocene Black Sea sediments is presented in Fig. 80.

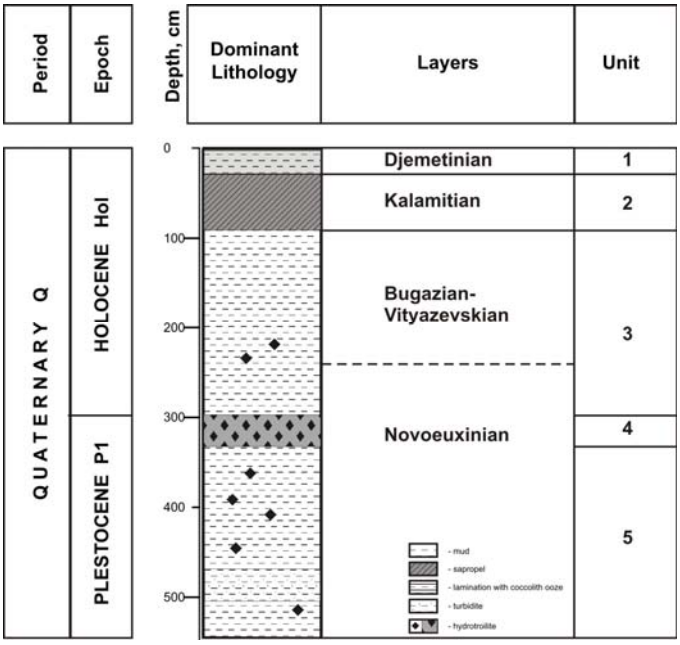

Fig. 80: Stratigraphy of the Black Sea.

Five main lithological units are distinguishable:

Unit 1

The top of Unit 1 is usually very water-saturated. Some cores show thin horizons of pale-grey structureless mud at the very top. Below this mud, a fine-laminated (typically less than 1 mm) sequence of alternating white coccolith-rich laminae, sapropelic mud and pale-grey mud is present. The formation of these laminae depends on seasonal variations in the generation and the transport of particulate matter in the Black Sea basin. The light coccolith laminae are almost entirely comprised of the nannoplanctonic coccolithophorid *Emiliania huxleyi*, whereas terrigenous material largely forms the darker laminae. Very fine-grained turbidites (up to 20 cm thick) occur in this unit. Although these turbidites do not seem to be laterally extensive, they highlight the importance of lateral transport processes in the basin. The lower boundary of Unit 1 is very sharp.

Unit 2

The Unit 1–2 boundary is often abrupt. Unit 2 is characterized by sapropels and sapropelic mud, interbedded with very soft, pale-greenish grey mud. The uppermost part of the upper sapropel contains a few very fine coccolith ooze laminae, and sometimes the sapropels contain fish and plant remnants. The sapropel contains more than 14 wt.-% of organic matter, which has an almost entirely marine origin. $\delta^{13}C$ values indicate increasing proportions of terrestrial organic matter towards the base of the sapropel. Like Unit 1, Unit 2 includes turbidites.

Unit 3

Below the sapropel a series of laminated moderately calcareous clays, with turbidite intercalations characterized by low organic carbon content (about 0.6%) is present. These

laminations, or fine beds, are shown by slight color variations between shades of grey. Unit 3 comprises terrestrial organic matter.

The lacustrine facies of Unit 3 was deposited at a time when the Black Sea has been isolated from the Mediterranean during eustatic sea level lowstand. After this period, climatic changes and reconnection to the Mediterranean some 9000 years before present has led to saline water inflow. This resulted in displacement of nutrient-rich deep waters into the photic zone and a pulse of increased marine productivity represented by the sapropel (Unit 2). Sapropel deposition is believed to have commenced across the Black Sea some 6000 years ago, deposition ended in the shallow waters some 4000 years ago, persisting in the deep waters until 1600 years ago. In the last stage of the Black Sea evolution (Unit 1), full marine conditions are characterised by the invasion of the coccolithophorid species *Emiliania huxleyi*.

Unit 4

Unit 4 comprises black to dark grey mud which is very rich in reduced iron, or hydrotroillite. These can be either massive or show a color banding caused by a variable hydrotroillite concentration.

Unit 5

Unit 5 is characterized by grey finely bedded mud with occasional fine silt laminae and spots of black hydrotroillite. Downcore this unit, the silts become thicker and show sharp, erosive bases and grade downwards into mud. Unit 5 may also contain debris flow deposits.

10.4.2 Site-specific Description of Sediments

15 gravity cores (9 of them equipped with temperature loggers) and 7 DAPC stations were conducted during cruise MSM15/2 (Table 17).

MSU MV

A single gravity core (GeoB 14302) was taken at the centre of MSU (Fig. 20, Table 15). It recovered 19 cm of Unit 1 (coccolite ooze) and 10 cm of the sapropelic section, which was characterized by dark greenish color. Below, a homogeneous, moussy mud breccia, dark greyish-green in color with clacts up to 4 cm in size was found. From 144 to 156 cmbsf the sapropelic material was found as well. This was interpreted as several mud flows occuring concurrently or corer double penetration. Authigenic carbonates were present in Unit 1 and at the 130–144 cmbsf interval.

Dvurechenskii MV

Four gravity cores were taken from the crater region of the Dvurechenskii MV (Fig. 22, Tables 15 and 17). They contained moussy clays with disseminated gas hydrates and sometimes mm-sized clasts. The sediments were highly gas and water saturated and showed the typical porous structure (Fig. 81). Gas hydrates were observed througout GC-T-2 (GeoB 14310) and GC-T-3 (GeoB 14311).

Fig. 81: Soupy sediment recovered from the Dvurechenskii MV.

Helgoland MV

Four gravity cores and a single DAPC core were taken from this structure (Fig. 22, Tables 15 and 17). Very similar to those of the Dvurechenskii MV, the sediments consisted of mousse-like mud breccia with mm-sized clasts and were highly gas and water saturated. Probably small gas hydrate crystals occurred were widespread in the core, but upon recovery no intact hydrates were discernable.

In contrast, core GC-6 (GeoB 14340) showed the typical Black Sea sequence. Unit 1 was observed on top (0–2 cmbsf), whereas Unit 2 was presented by the sapropel (2–13 cmbsf), and the lowermost sequence finished with light grey clay (probably mousse-like mud breccia), which was highly gas and water saturated. Some authigenic carbonate plates and more consolidated mud clasts were also found in this core.

Odessa MV

Two cores GC-3 (GeoB 14318) and DAPC-2 (GeoB 14319) were recovered from the Odessa MV (Fig. 23, Table 15). In both cores the three uppermost Black Sea Units were well preserved. For core GC-3 (GeoB 14318), Unit 1 was found from 0 to 128 cmbsf, followed by Unit 2 (128 – 256 cmbsf), and Unit 3 below. Coccolite ooze appeared within the uppermost 20 cm (e.g. GeoB 14319, DAPC-2), followed by the sapropel (up to 1 m in thickness) and by Unit 3, which was represented by greenish clay with hydrotroillite patches and layers. Within Unit 2 authigenic carbonate crusts were found. Gas hydrates were distributed in core GC-3 as white aggregates and thin plates.

Tbilisi MV

A single core, DAPC-4 (GeoB 14333) was taken from the top of the Tbilisi MV (Fig. 27, Table 15). The core length was 180 cm.

New Flare Site

Three gravity cores and a single DAPC core were taken at the New Flare Site (Fig. 28, Table 15). Core GC-5 (GeoB 14332) comprised grey clay overlapping the sapropel. Gas hydrates were observed within the 430–490 cmbsf interval (Unit 2). They formed small aggregates and thin plates.

Core GC-T-9 (GeoB 14359) revealed light grey homogenous clay (probably Unit 3), was highly gas and water saturated, and emitted a strong H_2S smell. Hydrates formed thin plates and aggregates which were found throughout the 31-145 cmbsf interval.

DAPC-7 (GeoB 14360) repeated the previous station. The sedimentary sequence consisted of very stiff grey clay (Unit 3) which lacked water saturated layers, and thus, evidence for hydrate presence. At the core bottom, a black interval enriched in hydrotroillite was observed (probably Unit 4?). From 177 to 188 cmbsf greenish homogenius stiff clay was recovered (probably Unit 5?) (Fig. 82).

Fig. 82: Boundary between the hydrotroillite black layer (probably Unit 4?) and the greenish grey stiff clay (probably Unit 5?) in core DAPC-7 (GeoB 14360).

Kerch Flare

Two gravity cores and two DAPC cores were collected from the Kerch flare (Fig. 30, Tables 15 and 17). Moussy clay sediments containing disseminated gas hydrates were recovered by GC-T-4 (GeoB 14324). GC-T-8 (GeoB 14351) collected the three uppermost Units: 0–45 cmbsf of coccolite ooze, 45–100 cmbsf sapropel, and 100–240 cmbsf light grey clay. All sedimentary sequences were gas saturated and characterized by strong smell of H_2S. However, no gas hydrates have been observed. A piece of wood was found at 110 cmbsf. Thin carbonate plates were present at around 182 cmbsf.

DAPC-6 (GeoB 14354) collected Unit 1 comprising of coccolite ooze (0-26 cm), Unit 2 of thin lamination of sapropel and clay (26-68 cm), Unit 3 of light grey clay (68-180 cm), and Unit 4 (probably) of black hydroillite layer (180-252 cm) close to the core bottom. Sediments belonging to Unit 3 were very porous, water saturated and emitted the typical smell of H_2S.

Colkheti Seep

Only one core, DAPC-5 (GeoB 14345), was taken from the Colkheti seep (Fig. 33, Tables 15 and 17). It collected 45 cm of light grey clay, which was oil stained througout the entire core (Fig. 83). Carbonate concretions were found at the top (uppermost 10 cm) and at 25 cmbsf.

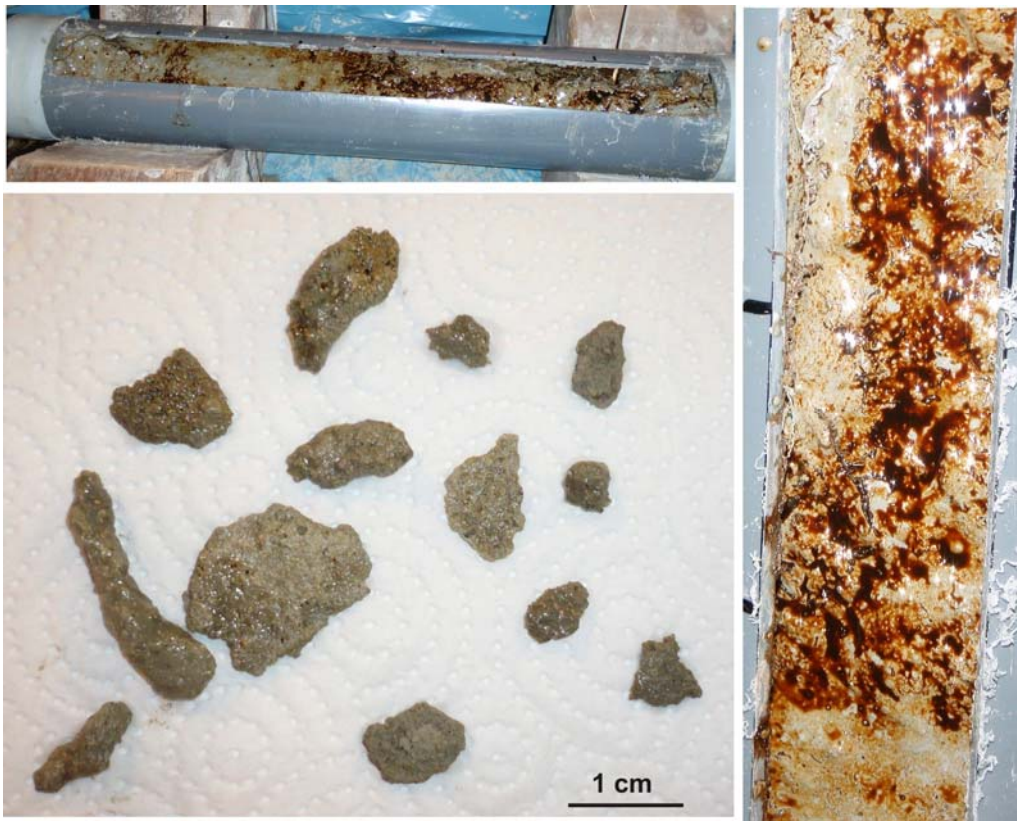

Fig. 83: Core DAPC-5 (GeoB 14345) collected from the Colkheti seep recovered 45 cm of sediment (top left). Close-up of oil saturated clay (right) contained in CAPC-5 and compilation of carbonate concretions and plates extracted from this core (bottom left).

11. Gas Analysis

(T. Pape, T. Malakhova, V. Blinova, K. Dehning)

Submarine gas hydrates are a major global reservoir of the potent greenhouse gas methane. In order to evaluate the methane storage capacity of submarine hydrates and their role for the global carbon cycling, exact knowledge on true gas hydrate and hydrocarbon concentrations in the sediments is required. However, current assessments of global amounts of hydrate-bound carbon vary by one order of magnitude. This is mainly owing to the technical effort required to conduct direct measurements, since gas hydrates decompose when brought outside their stability field, which is defined by high pressure and/or low temperature.

Nonetheless, in recent years numerous technical improvements were achieved for pressure-maintaining tools used to sample submarine sediments and to recover them under *in situ* hydrostatic pressure. These include the Dynamic Autoclave Piston Corer (DAPC; Abegg et al. 2008) which is housed at the MARUM and has been deployed during this cruise.

Previous investigations at several hydrocarbon seepage sites in the Black Sea (cruises M52/1, TTR-15, POS 317/4, M72/3) clearly demonstrated that the molecular composition of gas ascending from deeply buried reservoirs and venting into bottom waters is site-specific (Blinova et al. 2003; Pape et al. 2010a). Moreover, the initial gas composition can be modified by abiotic and biotic processes such as gas hydrate precipitation and dissociation as well as hydrocarbon biodegradation including the anaerobic oxidation of methane (e.g. Blinova et al. 2003; Pape et al. 2010a). The molecular composition of the feeding gas is a major factor controlling the crystallographic hydrate structure formed, and as a consequence, the site-specific hydrate stability.

The major objectives of the onboard gas analytical works during Cruise MSM15/2 were to determine true amounts of volatiles in gas- and hydrate-rich deposits of hydrocarbon seepages in the Northern and Southeastern Black Sea. In addition, molecular compositions of light hydrocarbons and carbon dioxide in vent gas, hydrate-bound gas, and in interstitial waters were analysed to evaluate the gas source type(s) and to calculate *in situ* hydrate amounts and hydrate stabilities. Primary sites of gas investigations during MSM15/2 were four mud volcano (MV) structures in the Sorokin Trough, a cold seep area close to the Kerch Strait and the Colkheti seep offshore Georgia.

11.1 Methods

11.1.1. Autoclave Sampling of Hydrate-bearing Sediments and Vent Gas

For the quantification of *in situ* gas abundances in sediments, autoclave technology, which maintains *in situ* hydrostatic pressure and, thus, prevents degassing of the sampled material, was applied (Heeschen et al. 2007; Abegg et al. 2008; Pape et al. 2010a; Pape et al. 2010b). Two autoclave tools were deployed to sample gas hydrate-containing sediments and gas bubbles venting from the seafloor:

- The Dynamic Autoclave Piston Corer (DAPC) was used to recover, preserve and analyze sediment cores under *in situ* hydrostatic pressure. The DAPC is gear-operated.
- Gas Bubble Samplers (GBS) were operated by the ROV manipulators and used for pressure

sampling and quantification of gas bubble streams close to the seafloor (see chapter 8).

Information on the DAPC core specifics (e.g. length, diameter) are given in chapter 10. Typically a gravity corer station was run to check for the *in situ* presence of gas hydrates (either based on the sediment texture or by direct prove), prior to the DAPC deployment. Details on the GBS handling procedure are given elsewhere (Pape et al. 2010a).

Immediately upon recovery, the respective autoclave tool (either DAPC or GBS) was connected to a so-called gas manifold, this being an assembly of gas-tight valves and connectors for quantification of the gas preserved inside the pressure chamber, pressure recording, and gas subsampling (Pape et al. 2010a; 2010b). Gas release from the pressure chamber was performed incrementally by operating a release port. The overall gas volume was quantified by use of a 'gas catcher' at atmospheric pressure and temperature (Heeschen et al. 2007). At selected pressure levels prevailing in the pressure chamber, two gas subsamples each were taken directly out of the stream of released gas with a gastight syringe. The gas was introduced into 20 mL glass serum vials pre-filled with saturated NaCl solution and sealed with butyl stoppers for (1) onboard gas chromatographic analysis and (2) for longterm storage and onshore carbon and hydrogen isotopic analysis of light hydrocarbons and carbon dioxide. For the DAPC, degassing of the pressure core was considered to be complete when atmospheric pressure was reached and gas release from the pressure chamber ceased. The depressurized core was removed from the pressure chamber and prepared for sediment and pore-water sampling and visual core description (see chapters 10 'Sediment Coring' and 10.4 'Core Descriptions').

11.1.2 Sample Preparation of Hydrate-bound Gas

Volatiles incorporated in gas hydrates were prepared from intact hydrate pieces recovered with the gravity corer (chapter 10, Pape et al. 2010a). The hydrate pieces were cleaned in ice-cooled freshwater, transferred to gas-tight syringes and dissociated under controlled conditions. The gas liberated during hydrate decomposition was transferred into glass serum vials pre-filled with saturated NaCl solution as described above.

11.1.3 Analytical Methods

The gas samples were analyzed onboard for their molecular compositions with a two-channel 6890N (Agilent Technologies) gas chromatograph (GC; Bohrmann et al. 2007; Pape et al. 2010a). Light hydrocarbons (C_1 to C_6) were separated, detected, and quantified with a capillary column connected to a Flame Ionisation Detector, while permanent gases (O_2, N_2, CO_2) as well as C_1 and C_2 hydrocarbons were determined using a stainless steel column packed with mole sieve and coupled to a Thermal Conductivity Detector. Calibrations and performance checks of the analytical system were conducted regularly using commercial pure gas standards and gas mixtures. The coefficient of variation determined for the analytical procedure was lower than 2%.

For onshore analysis of stable isotope ratios ($^2H/^1H$, $^{13}C/^{12}C$) of light hydrocarbons using the GC-Isotope-Ratio-Mass-Spectrometry system newly installed at the MARUM, gas samples were stored in glass vials and sealed with NaCl-saturated water.

11.2 Preliminary Results

11.2.1 Hydrate Quantifications

Seven stations with the Dynamic Autoclave Piston Corer for quantification of gas and gas hydrates were performed at locations well located below the upper boundary of the gas hydrate stability zone (710 m; Pape et al. 2010a) in the Sorokin Trough close to the Kerch Strait and offshore Georgia. Except for DAPC-5 (45 cm), relatively high recoveries (> 170 cm core length, see chapter 10.4 'Core descriptions') were obtained for all cores.

Table 18: Overview of stations performed with the Dynamic Autoclave Piston Corer (DAPC) including accumulated gas volumes and calculated gas-sediment ratios.

GeoB No.	Station no.	Area	Recovery pressure [bar]	Core length [cm]	Core volume [mL]	Gas volume released [mL]	Gas volume / volume wet sediment [mL / mL]
Sorokin Trough							
14308	DAPC-1	Helgoland MV	152.0	265	14.159	35.770	2.53
14319	DAPC-2	Odessa MV	12.3	220	11.754	n.d.	n.c.
14333	DAPC-4	Tbilisi MV	25.0	180	9.617	n.d.	n.c.
14360	DAPC-7	New Flare Site	0.0	188	10.045	n.d.	n.c.
Kerch Flare							
14325	DAPC-3	Kerch Flare	104.3	173	9.243	47.500	5.14
14354	DAPC-6	Kerch Flare	21.2	252	13.464	37.070	2.75
Offshore Georgia							
14345	DAPC-5	Colkheti seep	97.6	45	2.404	129.260	53.76

n.d. = not determined
n.c. = not calculated

For three pressurized cores (DAPC-1, -3, -5), the DAPC pressure inside the DAPC pressure chamber exceeded by far the dissociation pressure for pure methane hydrate in the Black Sea (~71 – 73 bar; Naudts et al. 2006; Pape et al. 2010a), thus, hydrates have been stable during the recovery procedure. Furthermore, for DAPC-3 and DAPC-5 taken at the Kerch flare and the Colkheti seep, respectively, the internal pressure was close to the *in situ* hydrostatic pressure. Interestingly, the volumetric gas-bulk sediment ratio of about 54 L L^{-1} determined for the pressure core taken at the Colkheti seep was the highest of all cores recovered with the DAPC so far (see Bohrmann et al. 2007; Pape et al. 2010b). This confirms the presence of gas hydrates in vast amounts in this core and suggests that seafloor penetration of the DAPC was retarded by shallow hydrates at this station.

However, for some pressure cores, the pressure inside the DAPC pressure chamber was either lower than anticipated from the hydrostatic pressure or even lost during recovery (Table 18). In particular for the cores taken at the Odessa MV (DAPC-2, GeoB14319) and the Kerch flare (DAPC-6, GeoB14354) this was most probably due to some technical issues with the DAPC ball valve related to the potential lack of hydrates in substantial densities in sediments accessible with the tool (as observed for gravity cores GeoB14318 (GC-3; Odessa MV, see chapter 10.4 'Core descriptions') and GeoB14324 (GC-T-4, Kerch flare).

11.2.2 Molecular Composition of Gas Samples

During Cruise MSM 15/2 a total of 140 gas samples was collected from the respective gas reservoirs (sedimentary gas, vent gas, hydrate-bound gas) in the working areas (Table 19).

Table 19: List of samples considered for gas chemical measurements during MSM 15/2.

GeoB No.	Tool	Type of gas sample	Area	Lat. [°N]	Long. [°E]	Water Depth [m]	No. of (sub-) samples
SorokinTtrough							
14339-1	GBS	vent	Helgoland MV	44°17.308	35°00.056	2.066	5
14339-3	GBS	vent	Helgoland MV	44°17.300	35°00.050	2.066	6
14356-1	GBS	vent	Helgoland MV	44°17.312	35°00.066	2.067	5
14308	DAPC-1	sedimentary	Helgoland MV	44°17.280	35°00.040	2.086	13
14318	GC-3	hydrate-bound	Odessa MV	44°23.003	35°09.275	1.813	3
14331	GC-4	hydrate-bound	Tbilisi MV	44°25.302	35°16.080	1.698	1
14332	GC-5	hydrate-bound	Tbilisi MV	44°25.328	35°15.869	1.717	7
14333	DAPC-4	sedimentary	Tbilisi MV	44°25.310	35°16.075	1.679	4
14361-2	GBS	vent	New Flare Site	44°24.863	35°20.683	1.714	5
14361-8	GBS	vent	New Flare Site	44°24.846	35°20.656	1.715	5
14359	GC-T-9	hydrate-bound	New Flare Site	44°24.867	35°20.679	1.748	1
KerchFflare							
14321-1	GBS	vent	Kerch Flare	44°37.240	35°42.283	908	4
14323-2	GBS	vent	Kerch Flare	44°37.218	35°42.288	883	4
14323-3	GBS	vent	Kerch Flare	44°37.220	35°42.288	883	5
14323-4	GBS	vent	Kerch Flare	44°37.220	35°42.288	883	4
14324	GC-T-4	hydrate-bound	Kerch Flare	44°37.215	35°42.286	880	6
14325	DAPC-3	sedimentary	Kerch Flare	44°37.218	35°42.284	880	14
14354	DAPC-6	sedimentary	Kerch Flare	44°37.222	35°42.275	895	17
Colkheti Seep							
14345	DAPC-5	sedimentary	Colkheti Seep	41°58.058	41°06.189	1.129	33
Batumi Seep Area							
14344-2	GBS	vent	Batumi Seep	41°57.533	41°17.272	835	5
		Total					**140**

DAPC: Dynamic Autoclave Piston Corer; GBS: Gas Bubble Sampler (ROV-based); GC: Gravity Corer; GC-T: Gravity Corer equipped with temperature probes

For all gas samples, methane strongly dominated the hydrocarbon fraction and was followed by ethane and propane. In addition, carbon dioxide concentrations surpassed ethane concentrations for all samples, except for sedimentary gas from the Tbilisi MV, for hydrate-bound gas from the New Flare Site, and for vent gas from the Batumi seep area.

Fig. 84 illustrates the molecular hydrocarbon distributions expressed as C_1/C_{2+} values in individual gas types from the different sampling sites. Except for sedimentary gas from the Colkheti seep, all gas samples plot within the empirical field indicating the prevalence of microbial hydrocarbons (C_1/C_{2+} > 1,000; Bernard et al. 1976; Whiticar 1999).

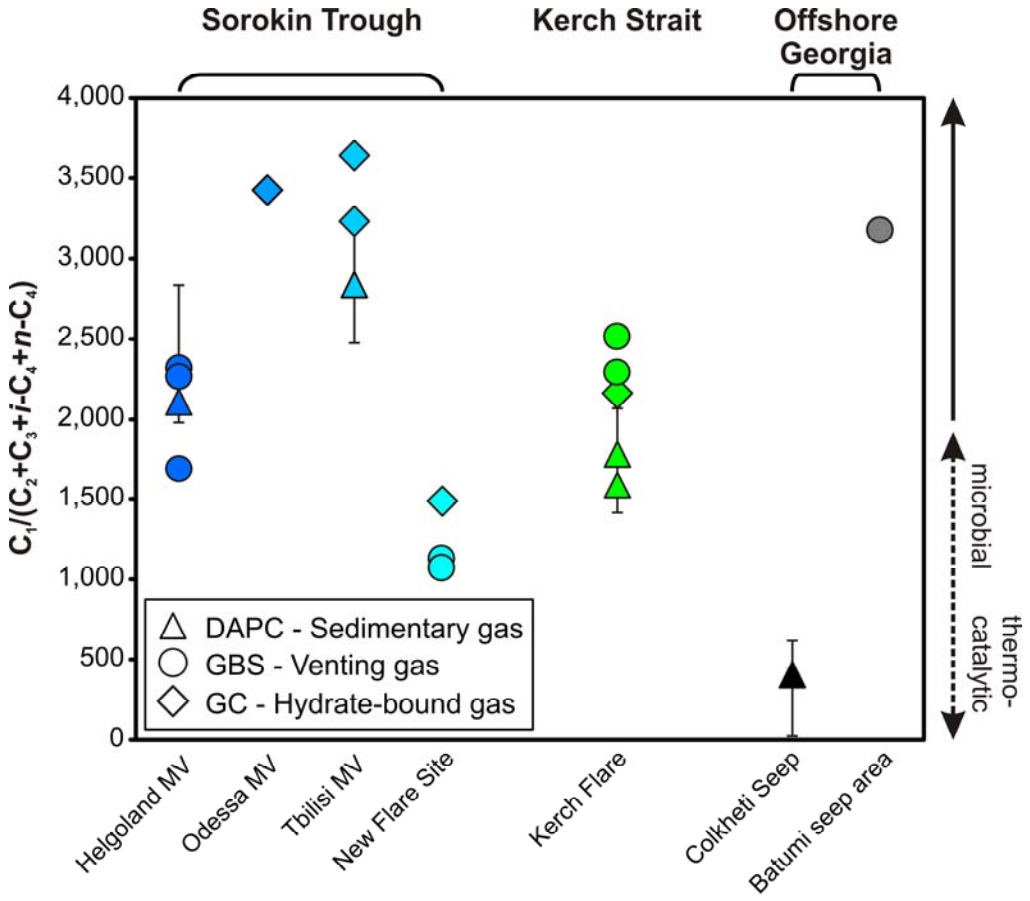

Fig. 84: Hydrocarbon compositions expressed as C_1/C_{2+} ratios of different gas types sampled at the different working areas during Cruise MSM 15/2. Error bars denote the limits of deviation during the DAPC degassing procedure.

During Cruise MSM15/2 molecular compositions of gases associated to four individual hydrocarbon-releasing geological structures in the Sorokin Trough were investigated: The Helgoland MV, the Odessa MV, the Tbilisi MV, and the so-called New Flare Site (for location see chapter '4: Subbottom profiling and plume imaging').

Helgoland MV

For the Helgoland MV a predominance of microbial light hydrocarbons in vent gas was inferred from C_1/C_{2+} values ≥ 1,689 (Bernard et al. 1976; Whiticar 1999; Fig. 84). Methane contributed ≥99.784 mol-% (Σ (C_1–C_4, CO_2)) to the compounds analysed and was followed by carbon dioxide (> 0.104%), ethane (> 0.035%) and propane (> 0.004%).

Gradients in the molecular composition of vent gas were observed with respect to the individual sampling sites, which were situated on a southwest-northeast trending line (Fig. 85).

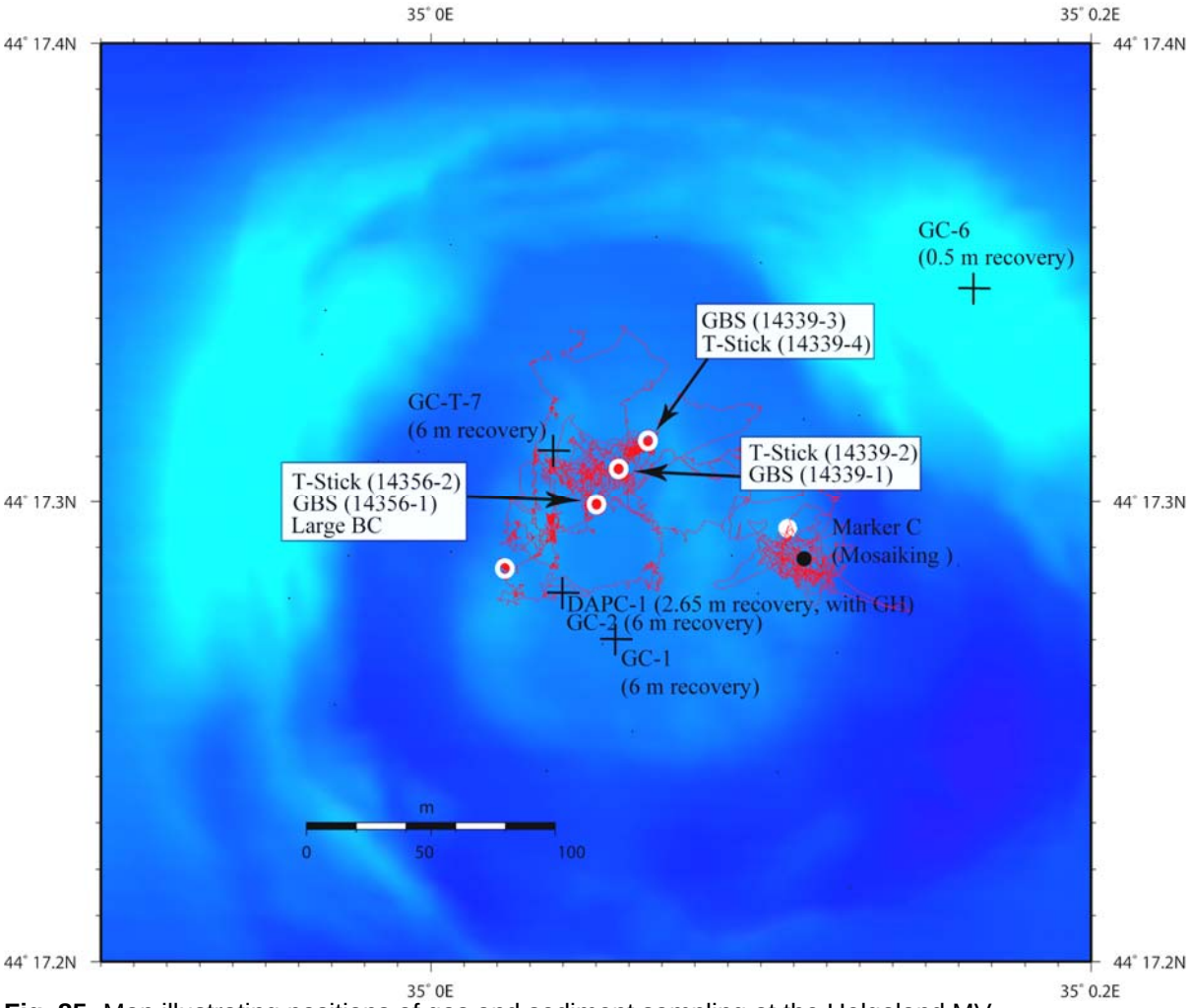

Fig. 85: Map illustrating positions of gas and sediment sampling at the Helgoland MV.

For vent gas collected at a site characterized by fresh mud and relatively intense gas emission (station GeoB 14339-3), enrichments in C_{2+} hydrocarbons compared to the two other GBS stations (GeoB 14339-1; 14356-1) were found. Analysis of gas subsamples from the DAPC station southwest of the GBS stations revealed depletions in methane, propane, as well as *iso*- and *n*-butane but enrichments in carbon dioxide relative to all vent gas samples.

Remarkably, the compositions of the respective gas types sampled at the Helgoland MV during Cruise MSM15/2 resembled those of sedimentary gas from the Dvurechenskii MV (Blinova et al. 2003; Feseker et al. 2009) and of vent gas from the Vodyanitskii MV (Sahling et al. 2009). Both structures are located close to the Helgoland MV and were investigated previously during Cruises M52/1 (2002) and M72/3 (2007).

Odessa MV and Tbilisi MV

The hydrate piece recovered from the Odessa MV showed a strong prevalence of microbial hydrocarbons (C_1/C_{2+} = 3,426, Fig. 84). Hydrate-bound gas from two hydrate pieces recovered from the Tbilisi MV as well as gas released during depressurization of a pressure core was characterized by microbial hydrocarbons with C_1/C_{2+} ratios exceeding 2,839. In comparison to the composition of hydrocarbons extracted from two hydrate pieces from the Odessa MV and from a gravity core recovered from the Tbilisi MV during an earlier study (Stadnitskaia et al. 2008), the gases collected from the two MVs during this cruise were

slightly enriched in methane and depleted in all $C_2 – C_4$ hydrocarbons.

Remarkably, considerable amounts of carbon dioxide (0.749%) were found in hydrate-bound gas from the Odessa MV, while that compound was below detection limit in samples from the Tbilisi MV.

New Flare Site

Vent gas collected from two stations at the New Flare Site (for sampling location see Fig. 29 in chapter 4) was enriched in wet gas components (C_1/C_{2+} = 1,072 - 1,129) compared to vent gas from the Helgoland MV (Fig. 84) while carbon dioxide was below detection limit. The relatively high abundance of wet gas components may indicate that thermocatalytic decay of organic matter has a higher impact on the gas composition at the New Flare Site compared to the other MVs in the Sorokin Trough investigated during Cruise MSM15/2.

A gas hydrate piece (GeoB 14359) collected less than ten meters northwest of the northernmost venting site investigated (GeoB 14361-2) was slightly enriched in methane, but significantly depleted in C_{3+} components (propane, *iso*- and *n*-butane) and carbon dioxide relative to the vent gas.

Kerch Flare

Vent gas collected at four stations at the Kerch flare (see Fig. 30 in chapter 4 and Fig. 40 in chapter 6) showed a dominance of microbial hydrocarbons ($C_1/C_{2+} \geq$ 2,289). Methane was the predominating constituent (> 99.259 mol-%), followed by carbon dioxide (0.532–0.703%), ethane (0.028–0.032%), propane (0.005%), *iso*-butane (0.004%), and *n*-butane (0.002%). Remarkably, for all vent gas samples analysed during Cruise MSM15/2, vent gas from the Kerch flare was characterized by highest carbon dioxide abundances.

Gas from hydrates as well as sedimentary gas retrieved during degassing of two pressure cores showed enrichments in methane and ethane, but depletions in C_{3+} components and carbon dioxide in comparison to vent gas. Based on the enrichments of methane and ethane in the hydrate phase it might be assumed that sI hydrate is the predominant hydrate structure at the Kerch flare.

Colkheti Seep

Sedimentary gas from the Colkheti seep was sampled at a single DAPC-station. On average the gas contained 99.062 mol-% methane, 0.536% carbon dioxide, ethane (0.141%), propane (0.118%) and *iso*-butane (0.139%). The resulting C_1/C_{2+} ratio of 408 was the lowest observed for all gas types collected during the cruise. In comparison to vent gas recovered from the Colkheti seep in 2007 (M72/3), the sedimentary gas sampled during this cruise was slightly enriched in methane and ethane, but depleted in propane, most probably due to molecular fractionation associated to hydrate formation (Pape et al. 2010a).

Batumi Seep Area

The vent gas sample retrieved from flare cluster 3 at the Batumi seep area (see Bohrmann et al. 2007) contained methane as the predominant constituent of the light hydrocarbon fraction (99.968 mol-%), followed by ethane (0.023%), propane (0.005%), and *iso*-butane (0.002%), resulting in a C_1/C_{2+} ratio of 3,176. The vent gas resembled in its hydrocarbon composition

that of vent gases collected from the Batumi seep area in 2007 (M73/2). Nevertheless, slight depletions in methane (0.008%) and enrichments in ethane, propane, and in the butanes became obvious during this cruise. Interestingly, the virtual absence of carbon dioxide in gas emitted at Flare 3 was already observed in 2007. This is in contrast to findings for most other vent gases collected at the Batumi seep area in 2007.

12. Marine Dolphins (Cetaceans) as Indicators for Sea Ecosystems

(G. Komakhidze)

The semi-enclosed nature and unusual chemical composition of the Black Sea makes it one of the world's unique water bodies. It has a surface area of some 420 000 km^2 and a volume of 550 000 km^3. Of the latter, some 87-90% is contaminated by hydrogen sulphide (H_2S), meaning that it contains no life other than some micro-organisms and meiobenthic nematodes that can withstand such conditions. Only the oxygenated surface layer down to a maximum depth of 150 m supports productivity, and representatives of most taxa and virtually all its flora and fauna are found in this layer, from protozoans to mammals (Sorokin, 1982).

Man's main impact on the biodiversity and productivity of the ichthyofauna of the Black Sea is through pollution, of which two types can be highlighted. The first is domestic faecal and industrial waste pollution. The second form is oil pollution.

The Black sea are arounded for six countries: Ukraine, Russia, Georgia, Turkey, Romania, Bulgaria. The Black Sea coast of Georgia is comparatively short, just 315 km. However, with some 150 rivers of various size draining the country's interior (and in certain cases that of neighbouring countries) and emptying into the sea.

Marine mammals can serve as a good indicator of ecosystem health, since 1932 the Black Sea Monitoring Center (before: Georgian Marine Ecology and Fisheries Research Institute) has concentrated effort on such studies and since 1933 the Georgian Institute has organized Black Sea expeditions to carry out a thorough investigation of the Black Sea dolphins. In addition to biological issues, the investigations also covered the problems connected with the Black Sea dolphin's fishery.

In 1974 the Georgian department of the All Union Scientific Fishery and Oceanographic Institute (now the Black Sea Monitoring Center) initiated the building of a dolphinarium in bitumen. Sea water was supplied from a depth of 12 m from the cleanest coastal area without any treatment. The mild subtropical climate, together with suitable mean annual air and sea water temperatures, created favorable conditions for the long-term maintenance and breeding of the Black Sea dolphins in captivity. This is the reason Batumi was chosen for the construction of the dolphinarium which was built for both scientific and entertainment purposes.

From the very beginning the largest Black Sea aperies were kept in the dolphinarium. i.e. Tursiops truncatus Montague. As a result of the special selection of the dolphin specimens there were several births in captivity.

Scientific research was carried out in the dolphinarium in ardor to improve biotechnological maintenance of the species in captivity. Breathing and fin-footed studies were also conducted, as were continuous bacteriological research on the environment, disease etiology, and both prophylactic and post identification cures for viruses.

As a fisheries resource, dolphins yielded a mean annual catch in the Black Sea of some 200,000 animals, including a Turkish catch of 60,000–80,000. The total population of Black Sea dolphins was then estimated to be 800,000 animals, which meant that the annual harvest did not exceed 25% of the total (Gudimovich, 1951). However, by the early 1960s, the number of dolphins in the Black Sea had decreased significantly for several reasons, notably as a result of overfishing.

Table 20: List of the names of three cetaceans (dolphins) In the Black Sea.

English common name	Scientific name	Common names in Range State languages
Black Sea [common] bottlenose dolphin	(*Tursiops truncatus ponticus* (Barabasch, 1940)	BULGARIAN afala, puchtun GEORGIAN afalina (afalina) ROMANIAN afalin, delfinul cu bot de sticla, delfinul cu bot gros RUSSIAN черноморская афалина, бутылконосый дельфин (chernomorskaya afalina, butylkonosyi del'fin*) TURKISH afalina UKRAINIAN чорноморська афаліна (chornomors'ka afalina)
Black Sea [short-beaked] common dolphin	*Delphinus delphis ponticus* Barabash-Nikiforov, 1935	BULGARIAN obiknoven delfin, karakash GEORGIAN tetrgverda delphini (TeTrgverda delfini) ROMANIAN delfin comun RUSSIAN черноморская белобочка, дельфин-белобочка, обыкновенный дельфин (chernomorskaya belobochka, del'fin-belobochka, obyknovennyi del'fin*) TURKISH tirtak UKRAINIAN чорноморська білобочка, дельфін-білобочка, звичайний дельфін (chornomors'ka bilobochka, del'fin-bilobochka, zvychainyi del'fin)
Black Sea harbour porpoise	*Phocoena phocoena relicta* (Abel, 1905)	BULGARIAN morska svinya, mutkur GEORGIAN azovka, zgvis gori (zRvis Rori) GREEK φώκαινα (fokaina) ROMANIAN marsuin, focena, porc de mare RUSSIAN черноморская обыкновенная морская свинья, азовка (chernomorskaya obyknovennaya morskaya svinya, azovka*) TURKISH mutur UKRAINIAN чорноморська звичайна морська свиня, азовка, пихтун (chornomors'ka zvychaina mors'ka svynya, azovka, pykhtun)

Reduction in dolphin populations in the Black Sea necessitated the taking of urgent steps. In 1966 the Soviet Union, Bulgaria and Romania, and later by Turkey took a decision to halt fishing for the Black Sea dolphin. Following the decision, the population along most of the Black Sea and Azov Sea coasts became more well-disposed to the dolphins (A.E. Shevalev, 1974). This moratorium had a positive influence on the dolphin population, in terms of total numbers of animals and also the number and size of schools, as revealed by a joint expedition of Russian, Georgian and Ukrainian scientists in 1984 and 1985 (Komakhidze and Mazmanidi, 1998).

An aircraft survey in 1985 suggested a slight increase in the dolphin population however, the data was not sufficient to guarantee that the decline was not continuing. It is quite possible that, given the dolphin's ability to adapt rapidly to a new habitat, the population is increasing in that part of the Black Sea. But a complete study of the Black Sea is necessary in order to resolve the question.

Aircraft and ship survey data show that Delphinus delphis, which has pelagic feeding habits, inhabits practically the whole Black Sea range. The benthic species *Tursiorps truncatus* is distributed near the coast, but could sometimes be found in the open sea. According to the data obtained the most numerous species is *Delphinus delphis*, followed by *Tursiops truncatus* and then *Phocena phoconea*.

Direct fishing, however, is not the only activity that impacts dolphin populations negatively; (over)exploitation of their fish prey also has a negative impact either through

removing the prey or in incidentally causing mortality of the dolphins in the nets. With this in mind and with financial support from the European Union, Black Sea coastal countries carried out a three-year study of dolphin mortality in 1997, 1998 and 1999. In Georgia, the study took in a 90 km stretch of coast between the mouths of the Rivers Chorokhi and Rioni. To assist in observations, the project team established a network of volunteers among people who either lived or worked at the coast. During the three years of the study, 29 dolphins were taken as bycatch in other fishing activities, 70% of them harbour porpoises (*Phocoena phocoena*) and the balance common dolphins (*Delphinus delphis*). Most of the bycatch was in the fixed nets set for turbot, but a few were drowned during purse-seining for anchovy. Harbour porpoises dominated the bycatch for two reasons, the sheer size of the population and the fact that they only inhabit the coastal fringe. The third species of dolphin common in the area, bottlenose (*Tursiops truncatus*), was not taken as bycatch during the study, but it is known from stranding data that they do occasionally fall foul of fishing gear. Most of the bycatch (direct and stranding) of dolphins is made in spring, when the fixed net fishery for (spawning) turbot is at its peak.

The average number of individuals by Georgian scientists, fishers and volunteers still provide information on dolphin school size 4/5, riding to a maximum of 100. Interpretation of such subjective data is not unanimous, but the consensus is that number of dolphins has not declined, but seems to be recovering.

At present the lack of data makes it impossible to perform a thorough analysis. There is an urgent need for an update of studies on Black Sea mammals populations and biodiversity. To open the Batumi dolphinarium is a matter of vital importance. It may later become a center for the rehabilitation and reproduction of both Black sea dolphins and other sea mammals. In order to breed a healthy dolphin stock the dolphinarium should be furnished with the necessary equipment for their safe maintenance. The dolphinarium could also serve as a powerful tool for the promotion of ecological education and public awareness of the need for environmental protection

Black Sea [common] bottlenose dolphin

Black Sea [short-beaked] common dolphin

Black Sea harbour porpoise

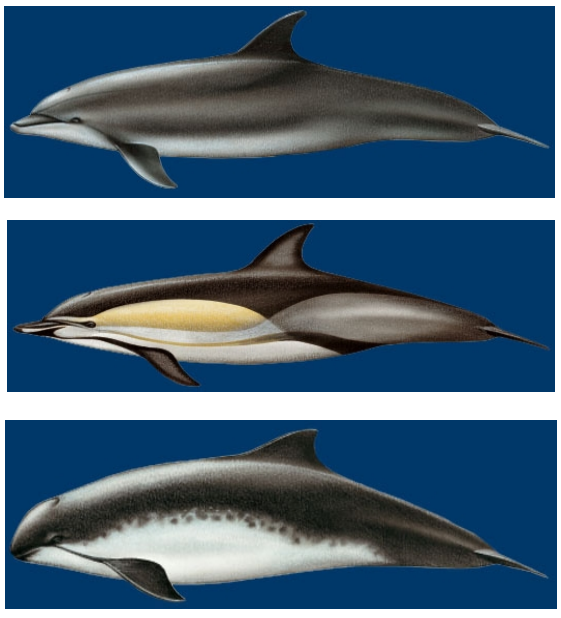

Drawings by Maurizio Würtz © Artescienza

Fig. 86: Three kinds of cetaceans in the Black Sea.

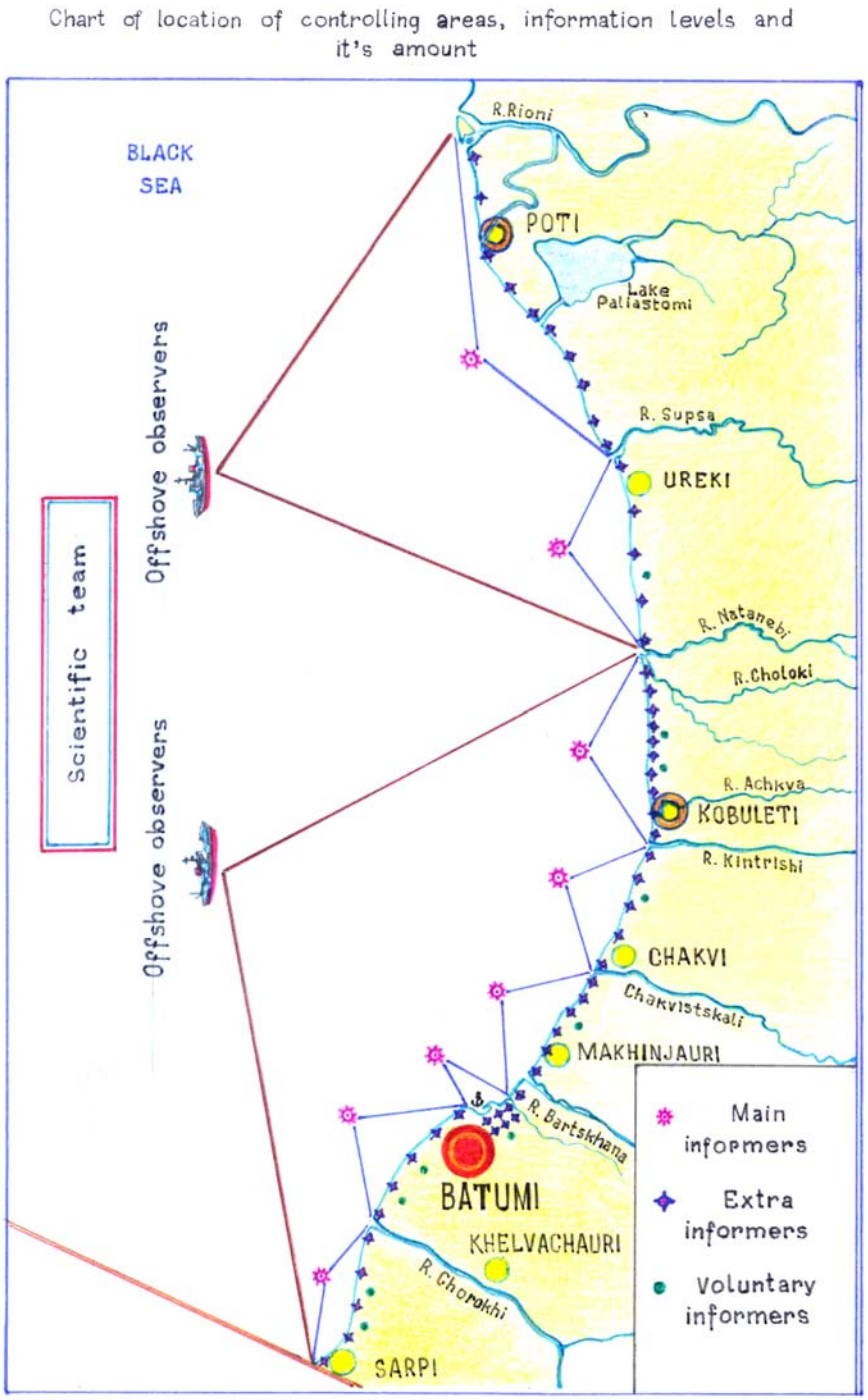

Fig. 87: Chart of location of controlling areas, information levels and its amount.

13. References

Abegg F, Hohnberg HJ, Pape T, Bohrmann G and Freitag J (2008) Development and application of pressure-core-sampling systems for the investigation of gas- and gas-hydrate-bearing sediments. *Deep-Sea Research I: Oceanographic Research Papers* 55(11): 1590-1599.

Akhmetzhanov AM, Ivanov MK, Kenyon NH, Mazzini A and Cruise participants (2007) Deepwater cold seeps, sedimentary environments and ecosystems of the Black and Tyrrhenian Seas and Gulf of Cadiz, *IOC Technical Series* No. 72. UNESCO, 99 pp.

Artemov YG, Egorov VN, Polikarpov GG, Gulin SB (2007) Methane emission to the hydro- and atmosphere by gas bubble streams in the Dnieper Paleo-delta, the Black Sea. *Marine Ecol J* 6: 5–26.

Bernard B B, Brooks JM and Sackett WM (1976) Natural gas seepage in the Gulf of Mexico. *Earth and Planetary Science Letters* 31(1): 48-54.

Blinova V, Ivanov M and Bohrmann G (2003) Hydrocarbon gases in deposits from mud volcanoes in the Sorokin Trough, north-eastern Black Sea. *Geo-Marine Letters* 23 (3-4): 250-257.

Bohrmann G, Ivanov M, Foucher JP, Spiess V, Bialas J, Greinert J, Weinrebe W, Abegg F, Aloisi G, Artemov Y, Blinova V, Drews M, Heidersdorf F, Krabbenhöft A, Klaucke I, Krastel S, Leder T, Polikarpov I, Saburova M, Schmale O, Seifert R, Volkonskaya A, Zillmer M (2003) Mud volcanoes and gas hydrates in the Black Sea: new data from Dvurechenskii and Odessa mud volcanoes. *Geo-Marine Letters* 23: 239-249.

Bohrmann G, Pape T and cruise participants (2007) Report and preliminary results of R/V Meteor cruise M72/3, Istanbul - Trabzon - Istanbul, 17 March - 23 April, 2007. Marine gas hydrates of the Eastern Black Sea. In *Berichte, Fachbereich Geowissenschaften, Universität Bremen*, No. 261, (ed. G. Bohrmann and T. Pape), pp. 176.

Bohrmann G, Schenck S (2002) RV METEOR Cruise Report M52/1, Marine gas hydrates of the Black Sea (MARGASCH), Istanbul-Sevastopol-Istanbul (January 2 - February 1, 2002), *GEOMAR Report* 108: 192 pages.

Bouriak SV, Akhmetjanov AM (1998) Origin of gas hydrate accumulations on the continental slope of the Crimea from geophysical studies. In: JP Henriet and J Mienert (eds.), Gas hydrates: Relevance to world margin stability and climate change. *Geological Society, London., special publications* 137: 215-222.

Çifçi G, Dondurur D, Ergün M (2003) Deep and shallow structures of large pockmarks in the Turkish shelf, Eastern Black Sea. *Geo-Marine Letters* 23: 311-322.

Dickens GR, Koelling M, Smith DC, Schnieders L and IODP Expedition 302 scientists (2007) Rhizon sampling of pore waters on scientific drilling expeditions: An example from the IODP exped. 302, Arctic Coring Expedition (ACEX). *Scientific Drilling* 4.

Feseker T, Dählmann A, Fouche, JP and Harmegnies F, (2009a) In-situ sediment temperature measurements and geochemical porewater data suggest highly dynamic fluid flow at Isis mud volcano, eastern Mediterranean Sea. *Marine Geology* 261: 128-137.

Feseker T, Foucher JP and Harmegnies F (2008) Fluid flow or mud eruptions? Sediment temperature distributions on Håkon Mosby mud volcano, SW Barents Sea slope. *Marine Geology* 247: 194-207.

Feseker T, Pape T, Wallmann K, Klapp SA, Schmidt-Schierhorn F and Bohrmann G (2009) The thermal structure of the Dvurechenskii mud volcano and its implications for gas hydrate stability and eruption dynamics. *Marine and Petroleum Geology* 26(9): 1812-1823.

Garcia-Pineda O, MacDonald I, Zimmer B (2008) Synthetic Aperture Radar Image Processing using the Supervised Textural-Neural Network Classification Algorithm. In: *Geoscience and Remote Sensing Symposium, IGARSS 2008* IEEE International 4: 1265-1268.

Ginzburg AI, Kostianoy AG, Sheremet NA (2004) Seasonal and interannual variability of the Black Sea surface temperature as revealed from satellite data (1982-2000), *Journal of Marine Systems* 52 (1-4): 33-50.

Greinert J, Artemov Y, Egorov V, De Batist M and McGinnis D (2006) 1300-m-high rising bubbles from mud volcanoes at 2028m in the Black Sea: Hydroacoustic characteristics and temporal variability. *Earth and Planetary Science Letters* 244: 1-15.

Gudimovich PK (1951) The Black Sea fishes and fishery. *Overview of the Georg. Dept.of Az.Cher. Niro*, p.18.

Heeschen KU, Hohnberg HJ, Haeckel M, Abegg F, Drews M and Bohrmann G (2007) In situ hydrocarbon concentrations from pressurized cores in surface sediments, Northern Gulf of Mexico. *Marine Chemistry* 107(4): 498-515.

Ivanov MK, Limonov AM, Woodside JM (1998) Extensive deep fluid flux through the sea fllor on the Crimean continental margin (Black Sea). In: JP Henriet and J Mienert (eds.), Gas hydrates: Relevance to world margin stability and climate change. *Geological Society, London., special publications* 137: 195-214.

Judd AG (2003) The global importance and context of methane escape from the seabed. *Geo-Marine Letters* 23: 147-154.

Klaucke I, Sahling H, Bürk D, Weinrebe W and Bohrmann G (2005) Mapping deep-water gas emissions with sidescan sonar. *EOS, Transactions* 86: 341-352.

Komakhidze A, Mazmanidi N (1998) Black Sea Biological Diversity, *Georgia. Black Sea Environmental Series*, Vol. 8. United Nations Publications, New York, p.33-36.

Kvenvolden KA (1998) A primer on the geological occurrence of gas hydrate. In: JP Henriet and J Mienert (eds.), Gas hydrates: Relevance to world margin stability and climate change. *Geological Society, London, special publications* 137: 9-30.

MacDonald IR, Guinasso NL Jr, Ackleson SG, Amos JF, Duckworth R, Sassen R, Brooks JM (1993) Natural Oil Slicks in the Gulf of Mexico Visible From Space. *J Geophys Res* 98.

Michaelis W, Seifert R, Nauhaus K, Treude T, Thiel V, Blumenberg M, Knittel K, Gieseke A, Peterknecht K, Pape T, Boetius A, Amann R, Jørgensen BB, Widdel F, Peckmann J, Pimenov NV, Gulin MB (2002) Microbial reefs in the Black Sea fueled by anaerobic oxidation of methane. *Science* 297:1013–1015.

Naudts L, Greinert J, Artemov Y, Staelens P, Poort J, Van Rensbergen P and De Batist M (2006) Geological and morphological setting of 2778 methane seeps in the Dnepr paleo-delta, northwestern Black Sea. *Marine Geology* 227(3-4): 177-199.

Nikishin AM, Korotaev MV, Ershov AV, Brunet MF (2003) The Black Sea basin: tectonic history and Neogene-Quaternary rapid subsidence modelling. *Sedimentary Geology* 156: 149-168.

Pape T, Bahr A, Rethemeyer J, Kessler JD, Sahling H, Hinrichs KU, Klapp SA, Reeburgh WS and Bohrmann G (2010) Molecular and isotopic partitioning of low-molecular weight hydrocarbons during migration and gas hydrate precipitation in deposits of a high-flux seepage site. *Chemical Geology* 269: 350-363.

Pape T, Kasten S, Zabel M, Bahr A, Abegg F, Hohnberg HJ and Bohrmann G (2010b) Gas hydrates in shallow deposits of the Amsterdam mud volcano, Anaximander Mountains, Northeastern Mediterranean Sea. *Geo-Marine Letters* 30(3-4): 187-206.

Reilinger RE, McClusky SC, Oral MB, King RW, Toksoz MN, Barka AA, Kinik I, Lenk O, Sanli I (1997) Global positioning system measurements of present-day crustal movements in the Arabia – Africa – Eurasia plate collision zone. *Journal of Geophysical Research* 102: 9983- 9999.

Robinson AG, Rudat JH, Banks CJ, Wiles RLF (1996) Petroleum geology of the Black Sea. *Marine and Petroleum Geology* 13:195-223.

Robinson AG (1997) Regional and Petroleum geology on the Black Sea and surrounding region. *American Association of Petroleum Geologists*. 385 pp.

Sahling H, Bohrmann G, Artemov YG, Bahr A, Brüning M, Klapp SA, Klaucke I, Kozlova E, Nikolovska A, Pape T, Reitz A and Wallmann K (2009) Vodyanitskii Mud Volcano, Sorokin Trough, Black Sea: Geological characterization and quantification of gas bubble streams. *Marine and Petroleum Geology* 26(9): 1799-1811.

Sahling H and Cruise participants (2004) Report and preliminary results of R/V Poseidon cruise P317/4, Istanbul – Istanbul, 16 October–4 November 2004. *Berichte aus dem Fachbereich Geowissenschaften der Universit¨at Bremen,* No. 235, Bremen, 92 pp

Seeberg-Elverfeldt J, Schlüter M, Feseker T and Kölling M (2005) Rhizon sampling of porewaters near the sediment-water interface of aquatic systems. *Limnology and Oceanography: Methods* 3: 361-371.

Shevalev AE (1974) The dolphin is looking for a friend. *Publ. "Sabchota Adjara" Batumi,* p. 58.

Simonov AI, Altman EN (Eds.) (1991) Hydrometeorology and Hydrochemistry of the USSR seas. Project ''Seas of the USSR''.vol. IV. *The Black Sea, 1, Hydrometeorological conditions. Gidrometeoizdat, St.-Petersburg.* 429 pp., (in Russian).

Sorokin YI (1982) Phytoplankton – VKN *The Black Sea, Moskow,* Nauka, p.43-80

Stadnitskaia A, Ivanov MK, Poludetkina EN, Kreulen R and van Weering TCE (2008) Sources of hydrocarbon gases in mud volcanoes from the Sorokin Trough, NE Black Sea, based on molecular and carbon isotopic compositions. *Marine and Petroleum Geology* 25(10): 1040-1057.

Topouzelis K (2008) Oil Spill Detection by SAR Images: Dark Formation Detection, Feature Extraction and Classification Algorithms. *Sensors* 8: 6642-6659.

Tugolesov DA, Gorshkov AS, Meysner LB, Soloviov VV, Khakhalev EM, Akilova YV, Akentieva GP, Gabidulina TI, Kolomeytseva SA, Kochneva TY, Pereturina IG, Plashihina IN (1985) *Tectonics of the Mesozoic Sediments of the Black Sea Basin, Nedra, Moscow*. 215 pp., (in Russian).

Wagner-Friedrichs M. (2007) Cold vents in the Black Sea: Acoustic characterization of mud volcanoes and gas seepages offshore Crimea and Georgia correlated to diapiric structures and gas/gas hydrates occurrences. *Ph.D. thesis, University of Bremen*.

Wahl T, Skoelv A, Andersen JHS (1994) Practical use of ERS-1 SAR images in pollution monitoring. In: *Geoscience and Remote Sensing Symposium, IGARSS '94* Surface and Atmospheric Remote Sensing: Technologies, Data Analysis and Interpretation, International, 4: 1954-1956.

Whiticar M J (1999) Carbon and hydrogen isotope systematics of bacterial formation and oxidation of methane. *Chemical Geology* 161: 291-314.

Woodside JM, Ivanov MK, Limonov AF (1997) Neotectonics and fluid flow through seafloor sediments in the Eastern Mediterranean and Black Seas, Part II: Black Sea, *Intergovernmental Oceanographic Commission technical series, UNESCO*, 48.

Yefremova AG, Zhizhchenko BP (1974) Occurrence of crystal hydrates of gases in the sediments of modern marine basins. *Doklady Akademii Nauk SSSR Earth Science Section* 214: 219-220.

Appendix 1: Station List

					Time (UTC)			Begin / on seafloor			End / off seafloor			
Date	St. No.	Instrument	GeoB St.-No.	Location/ Instrument	Begin	on seafloor	off seafloor	End	Latitude N	Longitude E	Water Depth/m	Latitude N	Longitude E	Water Depth/m	Recovery Remarks
10.05.	544	SVP-1	14300	close to Ukrainian border	23:42	00:16	00:16	00:39	43°17.729	32°41.892	2107	43°17.759	32°41.951	2107	1850 m maximum depth in the water
11.05.	545	PE-1	14301	MSU + Yuzhmorgeologia MV	02:58			09:07	43°31.973	33°04.784	2160	43°32.002	33°06.486	2107	Maps of both MV, no flares
11.05.	546	GC-T-1	14302	CenterMSUMV	09:30	10:18	10:30	11:16	43°32.003	33°06.830	2100	43°32.003	33°06.830	2100	~200 cm core recovery, double penetration of sedi.?
11.05.	547	AUV	14303		12:57			13:33	43°37.020	33°20.740	0	43°37.040	33°20.730	0	AUV trim-test on surface
11.05.	548	PE-2	14304	Mayshev, Kornev, Gonsharov	13:52			18:27	43°37.140	33°20.900	2110	43°41.989	33°39.531	2126	No flares
12.05.	549	PE-3	14305	Transit to DMV	21:38			04:10	44°00.360	34°19.080	2138	44°17.109	34°59.592	2083	Flares at Dvurechenskiy & Nameless Seep Site
12.05.	550	AUV-29	14306	DVM	06:02	07:56	12:34	13:44	44°17.010	34°59.679		44°17.090	34°59.500		Dive 29, failed due to navigation problem with pitch
12.05.	551	SVP-2	14307	DMV	10:27			10:40	44°16.961	35°00.006		44°16.961	35°00.006		SVP to 400m
12.05.	552	DAPC-1	14308	Helgoland MV	14:04	14:58	14:59	16:01	44°17.280	35°00.040	2086	44°17.280	35°00.040	2086	Gas hydrates, 31.8 kN, 265 cm core recovery
12.05.	553-1	GC-1	14309-1	Helgoland MV	16:48	17:25		17:56	44°17.270	35°00.056	2088	44°17.270	35°00.056	2088	600 cm (full) recovery, no gas hydrates, 46.5kN
12.05.	553-2	GC-2	14309-2	Helgoland MV	18:25	19:02		19:25	44°17.280	35°00.040	2087	44°17.280	35°00.040	2087	mud, mousy, no gas hydrates, 600 cm core recovery
12.05.	554	GC-T-2	14310	DMV	20:03	20:45		21:11	44°16.990	34°59.110	2059	44°16.990	34°59.110	2059	339 cm recovery, gas hydrates, 52kN
12.05.	555	GC-T-3	14311	DMV	21:38	22:13		22:45	44°16.910	34°58.770	2059	44°16.910	34°58.770	2059	529 cm recovery, some gas hydrates, 49.2kN
12.05.	556	PE-4	14312	DMV	22:53			04:53	44°16.920	34°58.780		44°16.990	34°59.010		1250m high central flare, weaker 1 at the western rim
13.05.	557	PE-5	14313	Helgoland MV	06:06			07:07	44°17.340	34°59.910		44°17.100	34°59.890		spontaneous flare imaging, due to delayed ROV dive
13.05.	558	ROV-263	14314	DMV	09:20	11:10		18:56	44°16.986	34°58.899	2040	44°17.010	34°58.920	2040	T-log string recovery & gas quantification (failed). Posi.
	558	T-Stick	14314-1	DMV	15:44			16:03	44°17.030	34°58.880	2040	44°17.030	34°58.880	2040	at bubble site
13.05.	559	PE-6	14315	DMV, Helgoland, NIOZ	19:32			02:14	44°17.330	35°00.170		44°18.920	35°04.570		all three MV's are active, flares detected
14.05.	560	AUV-30	14316	DMV	03:40			05:36	44°16.985	34°59.746		44°17.120	34°59.090		aborted, grans fault on planes
14.05.	561	PE-7	14317	Odessa MV	07:30			08:47	44°22.811	34°59.198	1820	44°23.150	35°08.410		several gas flares found
14.05.	562	GC-3	14318	Odessa MV	09:09			09:54	44°23.003	35°09.275	1813	44°23.003	35°09.275	1813	gas hydrates, 735 cm recovery, 52kN
14.05.	563	DAPC-2	14319	Odessa MV	10:25	11:04	11:04	11:54	44°23.021	35°09.279	1812	44°23.021	35°09.279	1812	pressure drop to 10bar despite 200 cm core recovery
14.05.	564	PE-8	14320	Kerch Flare	14:21			15:38	44°37.180	35°41.900	896	44°37.260	35°42.340		Flare survey, several flares found
14.05.	565	ROV-264	14321	Kerch Flare	16:41	17:31		03:15	44°37.198	35°42.241	908	44°37.179	35°42.399	908	Protocol in preparation
	565	GBS	14321-1	Kerch Flare	20:46				44°37.240	35°42.283	908	44°37.240	35°42.283	908	at bubble stream 2, T-logger, red tape
	565	T-Stick	14321-2	Kerch Flare	21:17				44°37.239	35°42.282	908	44°37.239	35°42.282	908	
	565	Marker A	14321-3	Kerch Flare	21:21				44°37.240	35°42.281	908	44°37.240	35°42.281	908	bubble stream A, PDI B2
15.05.	566	AUV-31	14322	Kerch Flare	04:59			05:47	44°36.783	35°42.739	908	44°36.779	35°42.451		Dive successful, multibeam data recorded
15.05.	567	ROV-265	14323	Kerch Flare	18:14	19:05		06:10	44°37.198	35°42.332	912	44°37.219	35°42.310		Several gas flares found & sampled
	567	Assmo	14323-1	Kerch Flare	20:46			05:11	44°37.240	35°42.280	883	44°37.240	35°42.280	883	deployed close to Marker A from dive 264
	567	GBS (red)	14323-2	Kerch Flare	23:39				44°37.218	35°42.288	883	44°37.218	35°42.288	883	

Appendix 1: Continuation Station List

					Time (UTC)			Begin / on seafloor			End / off seafloor			
Date	St. No.	Instrument	GeoB St.-No.	Location/ Instrument	Begin	on seafloor	off seafloor	End	Latitude N	Longitude E	Water Depth/m	Latitude N	Longitude E	Water Depth/m	Recovery Remarks
	567	GBS (blue)	14323-3	Kerch Flare	23:58			00:12	44°37.220	35°42.288	883	44°37.220	35°42.288	883	
	567	GBS (yellow)	14323-4	Kerch Flare	00:26			00:32	44°37.220	35°42.288	883	44°37.220	35°42.288	883	
	567	T-Stick	14323-5	Kerch Flare	00:41			00:52	44°37.220	35°42.288	883	44°37.220	35°42.288	883	in bubble site/ conduit
	567	T-Stick	14323-6	Kerch Flare	00:54			01:04	44°37.219	35°42.288	883	44°37.219	35°42.288	883	reference dose to bubble stream
	567	Marker "Werder"	14323-7	Kerch Flare	01:21				44°37.219	35°42.288	883	44°37.219	35°42.288	883	
	567	BC	14323-8	Kerch Flare	02:25			02:30	44°37.219	35°42.287	883	44°37.219	35°42.287	883	aborted
	567	BC	14323-9	Kerch Flare	02:31			02:36	44°37.219	35°42.287	883	44°37.219	35°42.287	883	other bubble stream
	567	T-Stick	14323-10	Kerch Flare	02:49			02:59	44°37.216	35°42.285	883	44°37.216	35°42.285	883	close to bubble site
	567	T-Stick	14323-11	Kerch Flare	03:04			03:14	44°37.216	35°42.285	883	44°37.216	35°42.285	883	in bubble hole
16.05.	568	GC-T-4	14324	Kerch Flare	06:29	06:46	06:56	07:11	44°37.215	35°42.286	880	44°37.221	35°42.302	880	Gas hydates, 450 cm recovered, 35kN
16.05.	569	DAPC-3	14325	Kerch Flare	07:43	08:04	08:06	08:38	44°37.218	35°42.284	880	44°37.218	35°42.284	880	102bar, 19kN rope tension, 173 cm recovery
16.05.	570	PE-9	14326	Kerch Flare	08:52			12:15	44°37.297	35°42.128	904	44°36.500	35°40.982	1024	
16.05.	571	PE-10	14327	Istanbul MV	13:46			02:45	44°24.641	35°25.830	1747	44°17.951	36°10.378	1979	
17.05.	572	AUV-32	14328	DMV	05:12			15:08	44°16.911	34°59.295		44°16.573	34°58.607		High quality multibeam data recorded
17.05.	573	SVP-3	14329	DMV	06:09	06:38		06:44	44°16.775	34°59.316		44°16.912	34°59.299		
17.05.	574	ROV-266	14330	New Flare Site	17:53	19:19		04:22	44°24.879	35°20.644	1730	44°24.815	35°20.687		QC flares found, Posi. bad signals, no sampling!
18.05.	575	GC-4	14331	Tbilisi MV	05:13	05:33		05:55	44°25.302	35°16.080	1688	44°25.302	35°16.081	1698	1679m Kabel at 1697m water depth, 48.8kN
18.05.	576	GC-5	14332	Tbilisi MV	06:22	06:55		07:17	44°25.328	35°15.869	1717	44°25.328	35°15.868	1689	52kN, 530 cm recovery, gas hydrates
18.05.	577	DAPC-4	14333	Tbilisi MV	08:11	08:44	08:44	09:28	44°25.310	35°16.075	1679	44°25.310	35°16.075	1679	25 bar, 180 core recovery, 31kN rope tension
18.05.	578	PE-11	14334	Transit Tbilisi MV to DMV	09:58			10:37	44°23.949	35°12.643	1785	44°22.928	35°08.381	1836	
18.05.	579	GC-T-5	14335	DMV	11:42	12:29	13:41	14:04	44°17.040	34°58.880	2057	44°17.040	34°58.881	2057	200 cm core recovery
18.05.	580	GC-T-6	14336	DMV	14:30	15:11	15:18	16:49	44°17.041	34°58.891	2057	44°17.041	34°58.891	2057	100 cm core recovery
18.05.	581	ROV-267	14337	DMV	17:33	19:16		04:39	44°16.946	34°58.857	2068	44°17.056	34°58.800		
	581	Data logger	14337-1	DMV	20:38				44°16.930	34°58.908	2040	44°16.930	34°58.908	2040	Temperature logger/ mooring recovered
19.05.	582	AUV-33	14338	Helgoland MV	05:45			15:55	44°16.889	34°59.141	2066	44°17.289	35°00.859	2066	Mission aborted due to time lack, good data
22.05.	583	ROV-268	14339	Helgoland MV	16:41	18:04		05:01	44°17.277	35°00.069	2066	44°17.283	35°00.060	2066	
	583	GBS blue	14339-1	Helgoland MV	21:40			21:46	44°17.308	35°00.056	2066	44°17.308	35°00.056	2066	in central mud pool
	583	T-Stick	14339-2	Helgoland MV	22:03			22:13	44°17.308	35°00.057	2066	44°17.308	35°00.057	2066	in central mud pool
	583	GBS yellow	14339-3	Helgoland MV	02:27			22:35	44°17.300	35°00.050	2066	44°17.300	35°00.050	2066	over emission site
	583	T-Stick	14339-4	Helgoland MV	02:52			03:00	44°17.300	35°00.050	2066	44°17.300	35°00.050	2066	in central mud pool
23.05.	584	GC-6	14340	Helgoland MV	05:34	06:03		06:28	44°17.347	35°00.164	2101	44°17.347	35°00.164	2101	only ~50cm core recovery

Appendix 1: Continuation Station List

Date	St. No.	Instrument	GeoB St.-No.	Location/ Instrument	Time (UTC)				Begin / on seafloor			End / off seafloor			Recovery Remarks
					Begin	on seafloor	off seafloor	End	Latitude N	Longitude E	Water Depth/m	Latitude N	Longitude E	Water Depth/m	
23.05.	585	GC-T-7	14941	Helgoland MV	07:22	08:07	08:13	09:44	44°17.311	35°00.037	2104	44°17.311	35°00.037	2104	GC penetrated about 50m bsf, full core recovery
23.05.	586	POSI	14942	near Helgoland MV	10:20			13:48	44°18.469	34°59.850	2066	44°18.469	34°59.679	2071	Calibration after pool change
24.05	587	PE-12	14943	Batumi Seep	14:10			15:53	42°06.828	41°01.298	2072	42°04.511	41°17.409	1186	1 flare found, gap in bathymetry filled
24.05	588	ROV-269	14944	Batumi Seep	17:00	17:53		03:11	41°57.428	41°17.420	834	41°57.488	41°17.192	834	Flares found, sampled and ASSMO deployed
	588	ASSMO	14944-1	Batumi Seep	21:11				41°57.532	41°17.268	834	41°57.532	41°17.268	834	
	588	GBS yellow	14944-2	Batumi Seep	21:59				41°57.533	41°17.272	835	41°57.533	41°17.272	835	
	588	GH experiment I	14944-3	Batumi Seep	23:30				41°57.533	41°17.273	835	41°57.533	41°17.273	835	
	588	Marker D	14944-4	Batumi Seep	23:43				41°57.539	41°17.273	835	41°57.539	41°17.273	835	
	588	GH experiment	14944-5	Batumi Seep	23:58				41°57.533	41°17.272	835	41°57.533	41°17.272	835	
	588	BC	14944-6	Batumi Seep	00:14			00:29	41°57.533	41°17.272	835	41°57.533	41°17.272	835	3 l
	588	T-Stick	14944-7	Batumi Seep	00:37			00:48	41°57.533	41°17.273	835	41°57.533	41°17.273	835	in bubble stream, did not penetrate entirely
	588	T-Stick	14944-8	Batumi Seep	00:50			01:03	41°57.533	41°17.272	835	41°57.533	41°17.272	835	reference site
	588	BC II	14944-9	Batumi Seep	01:14				41°57.538	41°17.271	835	41°57.538	41°17.271	835	Sediment sample (pinadkle)
25.05.	589	DAPC-5	14945	Colkheti Seep	04:26	05:00	05:00	05:34	41°58.058	41°06.189	1129	41°58.058	41°06.189	1129	128 bar, 19kN, 45 cm core recovery
25.05.	590	AUV-34	14946	Colkheti Seep	06:35			15:33	41°57.880	41°07.009	1125	41°58.312	41°06.019		Mission aborted due to time lack, good data
25.05.	591	SVP-4	14947	Colkheti Seep	10:53	11:13		11:25	41°57.369	41°06.568	1125	41°57.369	41°06.568	1125	
25.05.	592	ROV-270	14948	Batumi Seep	18:56	19:35		21:08	41°57.580	41°17.229	880	41°57.580	41°17.202	880	
	592	GHE	14948-1	Batumi Seep	19:50				41°57.534	41°17.274	835	41°57.534	41°17.274	835	Recovery
	592	ASSMO	14948-2	Batumi Seep	20:18				41°57.534	41°17.270	835	41°57.534	41°17.270	835	Recovery
26.05.	593	PE-13	14949	Kerch Flares	21:30			03:01	44°33.948	36°04.778	975	44°51.858	36°00.182	665	Few new flares found
27.05.	594	AUV-35	14950	Kerch Flares	05:20			10:06	44°36.886	35°42.378	896	44°36.893	35°42.366	896	Dive successful
27.05.	595	GC-T-8	14951	Kerch Flares	10:40	10:59	11:09	11:26	44°37.219	35°42.295	896	44°37.219	35°42.295	896	~ 240 cm core recovery, no GH, 1 datalogger lost
27.05.	596	TV-S	14952	Kerch Flares	12:13	12:37	12:40	14:39	44°37.216	35°42.282	897	44°37.218	35°42.296	896	bubble stream A, POI B2, no activity at known site
27.05.	597	ROV-271	14953	Kerch Flares	15:22	16:10		02:04	44°37.191	35°42.291	897	44°37.217	35°42.406	896	
	597	Bubblemeter	1453-1	Kerch Flares	17:01				44°37.229	35°42.276	881	44°37.229	35°42.276	881	near POI
	597	T-Stick	1453-2	Kerch Flares	17:51			17:11	44°37.228	35°42.275	882	44°37.228	35°42.275	882	as scale for bubble measurement
	597	T-Stick	1453-3	Kerch Flares	18:51			19:01	44°37.223	35°42.279	883	44°37.223	35°42.279	883	in sediment at site 1, hydrates rising
	597	Net	1453-4	Kerch Flares	20:24				44°37.238	35°42.289	886	44°37.238	35°42.289	886	sediment sample
	597	T-Stick	1453-5	Kerch Flares	21:08				44°37.247	35°42.289	887	44°37.247	35°42.289	887	as scale for bubble measurement
	597	T-Stick	1453-6	Kerch Flares	21:14			21:26	44°37.247	35°42.289	887	44°37.247	35°42.289	887	in bubble hole
	598	DAPC-6	14954	Kerch Flares	02:22	02:52	02:52	03:33	44°37.222	35°42.275	895	44°37.222	35°42.275	895	252 cm core recovery

Appendix 1: Continuation Station List

					Time (UTC)			Begin / on seafloor			End / off seafloor			
Date	St. No.	Instrument	GeoB St.-No.	Location/ Instrument	Begin	on seafloor	off seafloor	End	Latitude N	Longitude E	Water Depth/m	Latitude N	Longitude E	Water Depth/m	Recovery Remarks
28.05.	599	AUV-36	14355	New Flare Site	08:35			17:16	44°24.938	35°19.742	1748	44°24.771	35°20.387		
28.05.	600	ROV-272	14356	Helgoland MV	19:17	20:35		04:48	44°17.298	35°00.048	2068	44°17.279	35°00.098	2068	
	600	GBS yellow	14356-1	Helgoland MV		21:18	21:12		44°17.312	35°00.066	2067	44°17.312	35°00.066	2067	function not perfect
	600	T-Stick	14356-2	Helgoland MV		21:40	21:50		44°17.312	35°00.062	2067	44°17.312	35°00.062	2067	
	600	large BC	14356-3	Helgoland MV		22:27			44°17.311	35°00.059	2067	44°17.311	35°00.059	2067	used for sediment sampling
	600	Marker C	14356-4	Helgoland MV		01:05			44°17.283	35°00.122	2070	44°17.283	35°00.122	2070	
29.05.	601	AUV-37	14357	Odessa MV	06:52			09:48	44°23.449	35°08.882		44°23.389	35°08.782		Mission aborted because of malfunction
29.05.	602	PE-14	14358	Odessa MV & New Flare Site	10:32			13:13	44°23.348	35°08.758	1796	44°24.827	35°20.470	1750	Flares detected at Odessa MV & NFS
	603	GC-T-9	14359	New Flare Site	13:41	14:05	14:15	14:41	44°24.867	35°20.679	1748	44°24.867	35°20.679	1748	~163cm recovery, some GH in upper 40cm
	604	DAPC-7	14360	New Flare Site	14:47	15:32	15:32	16:22	44°24.874	35°20.690	1748	44°24.874	35°20.690	1748	188 cm core recovery
29.05.	605	ROV-273	14361	New Flare Site	17:00	18:15	00:07	01:24	44°24.848	35°20.673	1748	44°24.820	35°20.609	1737	GBS, T-Stick measurements
	605	BIB	14361-1	New Flare Site		19:01	19:11		44°24.863	35°20.683	1714	44°24.863	35°20.683	1714	
	605	GBS yellow	14361-2	New Flare Site		19:28	19:50		44°24.863	35°20.683	1714	44°24.863	35°20.683	1714	T-logger not in gas
	605	T-Stick	14361-3	New Flare Site		20:16	20:26		44°24.862	35°20.683	1714	44°24.862	35°20.683	1714	
	605	Net	14361-4	New Flare Site	20:59				44°24.862	35°20.692	1714	44°24.862	35°20.692	1714	collection of whitish sediment sample
	605	Marker-Volker	14361-5	New Flare Site	21:11				44°24.861	35°20.699	1712	44°24.861	35°20.699	1712	
	605	Marker St Pauli	14361-6	New Flare Site	22:33				44°24.864	35°20.681	1714	44°24.864	35°20.681	1714	
	605	BIB	14361-7	New Flare Site		23:31	23:37		44°24.847	35°20.655	1715	44°24.847	35°20.655	1715	until 23:35 shutter speed 500, then 250
	605	GBS black	14361-8	New Flare Site		23:48	23:52		44°24.846	35°20.656	1715	44°24.846	35°20.656	1715	

AUV: SEAL 5000
ROV: Quest 4000
DAPC: Autoclave piston corer
GC with temperature
GC-T: Logger
GC: Gravity corer
SVP: Velocity profiler
TV-S: TV-sled
CTD: CTD with hydro casts
PE: PARASOUND/EM120

ROV-Payload
T-S: T-Stick (temperature lance)
GBS: Gas bubble sampler
BC: Bubble cacher
BM: Bubble meter
PC: Push core
NT: Net
ASSMO: Autonomous scanning modul
Marker: Marker a, b, c
BIP: Bubble Imaging plate

ROV-Tools
ROV-S: ROV-Forward looking sonar
ROV-SSS: ROV-Sidescan sonar
ZEUSS: HD camera

Appendix 2: List of all Surveys for Hydroacoustic Observations

Survey-number	GeoB-Nr.	Station-nr.	Location	Start Date/ Time	Lat	Long	End Date/ Time	Lat	Long	Objective	Observations	EM120
PE-1	14301	545	MSU/Yuzhmor-geologiya	10/05/2010 02:58	43°31.98	33°4.73	10/05/2010 09:07	43°31.79	33°7.41	Bathymetric map of bothMVs and flare search	no flares observed	on
PE-2	14304	548	Malyshew/Kornew/ Goncharow/Transit to Dvurechenskiy	11/05/2010 13:52	43°37.14	33°20.90	11/05/2010 18:27	43°42.62	33°39.13	Flare search at the MVs and close the holes of the existing bathymetric map	no flares observed	on
PE-3	14305	549	Transit to Dvure-chenskiy/Dvure-chenskiy/Helgoland	11/05/2010 21:38	44°0.36	34°19.09	12/05/2010 04:23	44°16.96	34°58.47	Passing some interesting points on the way to the mud volcano and search for flares over the MVs	At both MVs we found a flare	on
PE-4	14312	556	Dvurechenskiy	12/05/2010 22:53	44°26.92	34°58.78	13/05/2010 04:53	44°16.99	34°59.01	Detailed survey to locate the seep site - preparation for ROV dive	Crossed the flare 17 times, flare up to 1250 m into the water column. Without multibeam a lot better quality	off
PE-5	14313	557	Helgoland	13/05/2010 06:07	44° 17.34	34°59.91	13/05/2010 07:07	44°17.10	34°59.89	Survey to locate the seep site - preparation for possible ROV dive	Crossed the flare 6 times, flare up to 1200 m into the water column	off
PE-6	14315	559	Helgoland/Vodianitskiy/Nioz	13/05/2010 19:32	44°17.33	35°0.17	14/05/2010 02:14	44°18.92	35°5.59	Detailed mapping of NSS and search for flares at the other MVs	All three MVs with gas emissions	off
PE-7	13217	561	Odessa	14/05/2010 07:28	44°22.81	35°8.41	14/05/2010 08:47	44°23.12	35°8.44	Flare search at the MV	At least two flares found, crossed 11 times	off
PE-8	14320	564	Transit to Kerch Flare/Kerch Flare	14/05/2010 14:19	44°37.18	35°41.90	14/05/2010 15:38	44°37.26	35°42.34	Transit with 12,5 kn. Flare search over the known seep sites	Several strong and high flares found and crossed several times for location of the main emissions - preparation for ROV dive	Transit andcrossing over Kerch flare on, rest off
PE-9	14326	570-1	Kerch Flare	16/05/2010 08:52	44°37.28	35°42.13	16/05/2010 09:40	44°37.12	35°42.42	Enlarge the detailed Parasound mapping for flare search	Found a new flare in the northern part of the center	off
PE-9	14326	570-2	Kerch Flare	16/05/2010 09:41	44°37.13	35°42.52	16/05/2010 12:15	44°36.50	35°40.98	EM120 survey (4 long lines) for a bathymetric and a backscatter map of the whole area		on

Appendix 2: Continuation

Survey-number	GeoB-Nr.	Station-nr.	Location	Start Date/ Time	Lat	Long	End Date/ Time	Lat	Long	Objective	Observations	EM120
PE-10	14327	571	Transit over Istanbul/NFS/Tblisi/ Kazokov to Dvurechenskiy	16/05/2010 13:46	44°24.64	35°25.83	17/05/2010 02:45	44°17.95	35°10.38	Search for flares in the area around Istanbul - detailed survey on NFS - short survey at Kazokov	Found a new flare site (NFS) - mapped the flares for ROV dive preperation - another flare over Tblisi - no flare over Kazokov	on for long transits, off for detailed flare mapping
PE-11	14334	578	Transit over Istanbul/Tbilisi/M12 to Dvurechenskiy	18/05/2010 09:58	44°23.95	35°12.64	18/05/2010 10:37	44°22.93	35°8.38	Use the transit to pass known MVs and interesting structures to search for flares	One flare found by crossing M12	on
PE-12		587	Transit to Georgia	23/05/2010 13:31	44°16.96	34°59.07	24/05/2010 16:34	41°56.49	41°17.47	Transit with 12.5 kn, extend the bathymetry we already have and passing a potential flare site where oil slicks have been observed on radar SAT images	Found a new flare where oil slick have been observed by radar SAT images	on
PE-13	14349	593	Transit to Kerch and Kerch Fan survey	25/05/2010 21:06	41°56.49	41°17.47	27/05/2010 03:01	44°41.86	36°0.18	Transit with 12.5 kn, extend the bathymetry we already have and passing a potential flare site where oil slicks have been observed on radar SAT images	At batumi seep before leaving very intense flare in Parasound, which seem to reach the sea surface. On transit no new flares. At the Kerch Fan several flares in shallower water depth and two new ons in water depth below 750m	on
PE-14	14358	602	Odessa and NFS	29/05/2010 10:32	44°23.35	35°8.76	29/05/2010 13:13	44°24.93	35°20.43	Short surveys crossing both Flare sites for better location of the emissions	Crossed three times Odessa in the central part of the flare and four times at NFs over the known flare positions	on during transit between the two structures
PE-15			Transit to leave the working area	30/05/2010 01:00	44°24.82	35°20.61	30/05/2010 12:22	43°4.262	32°32.161			on

Appendix 3: Core Descriptions

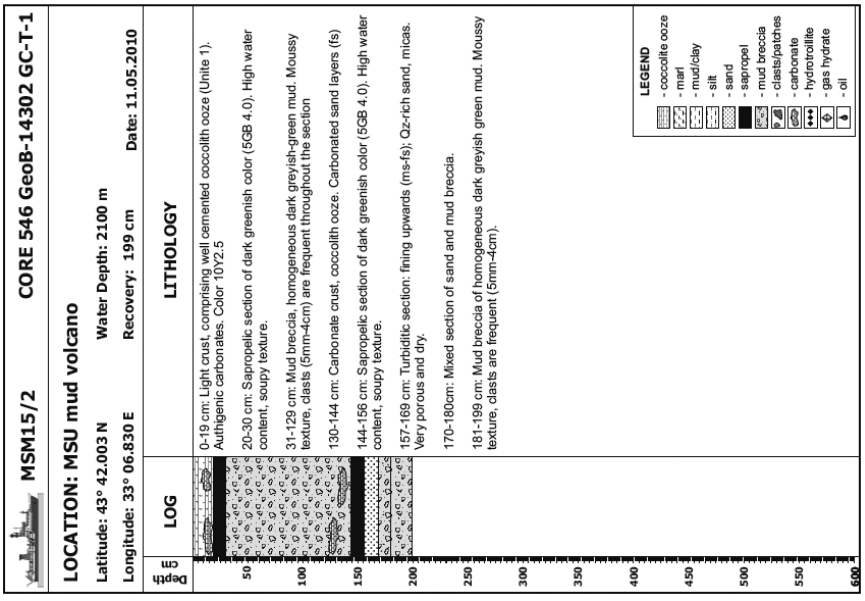

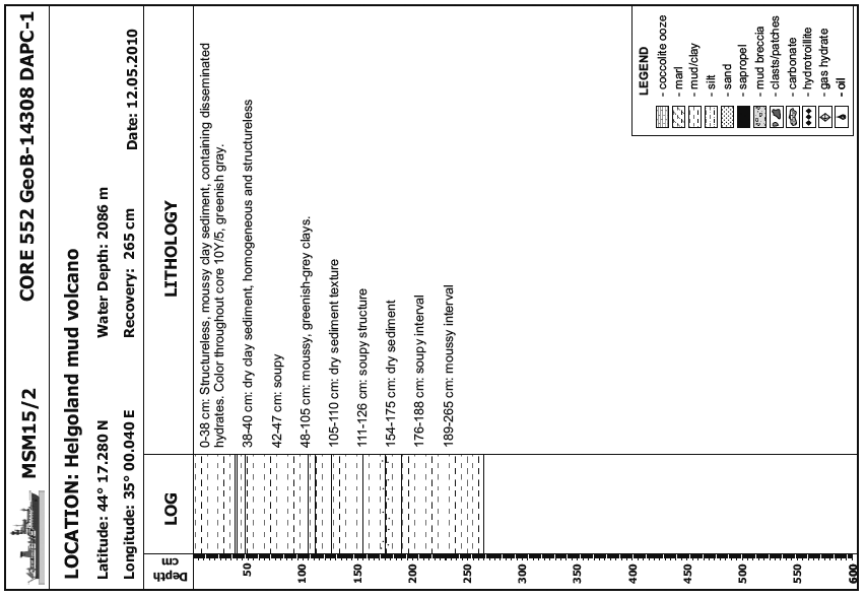

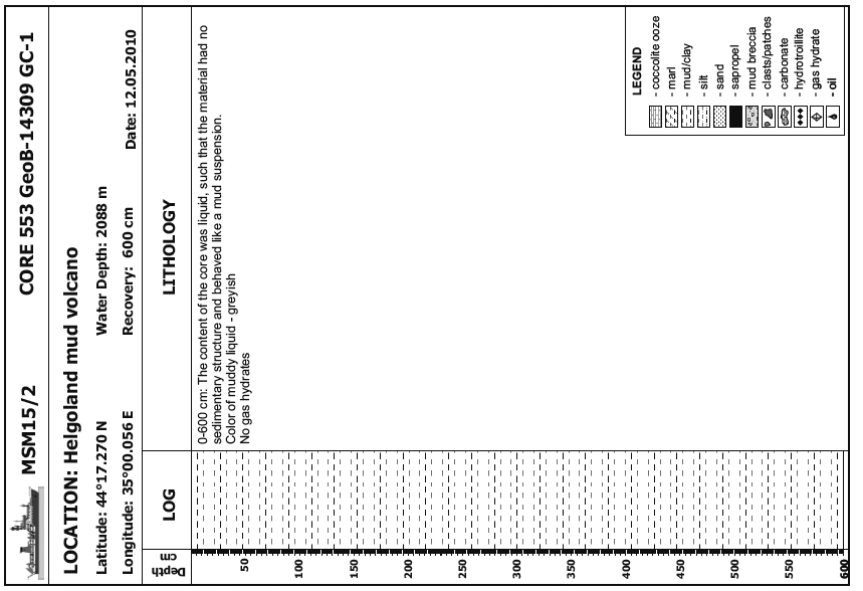

Appendix 3: Continuation

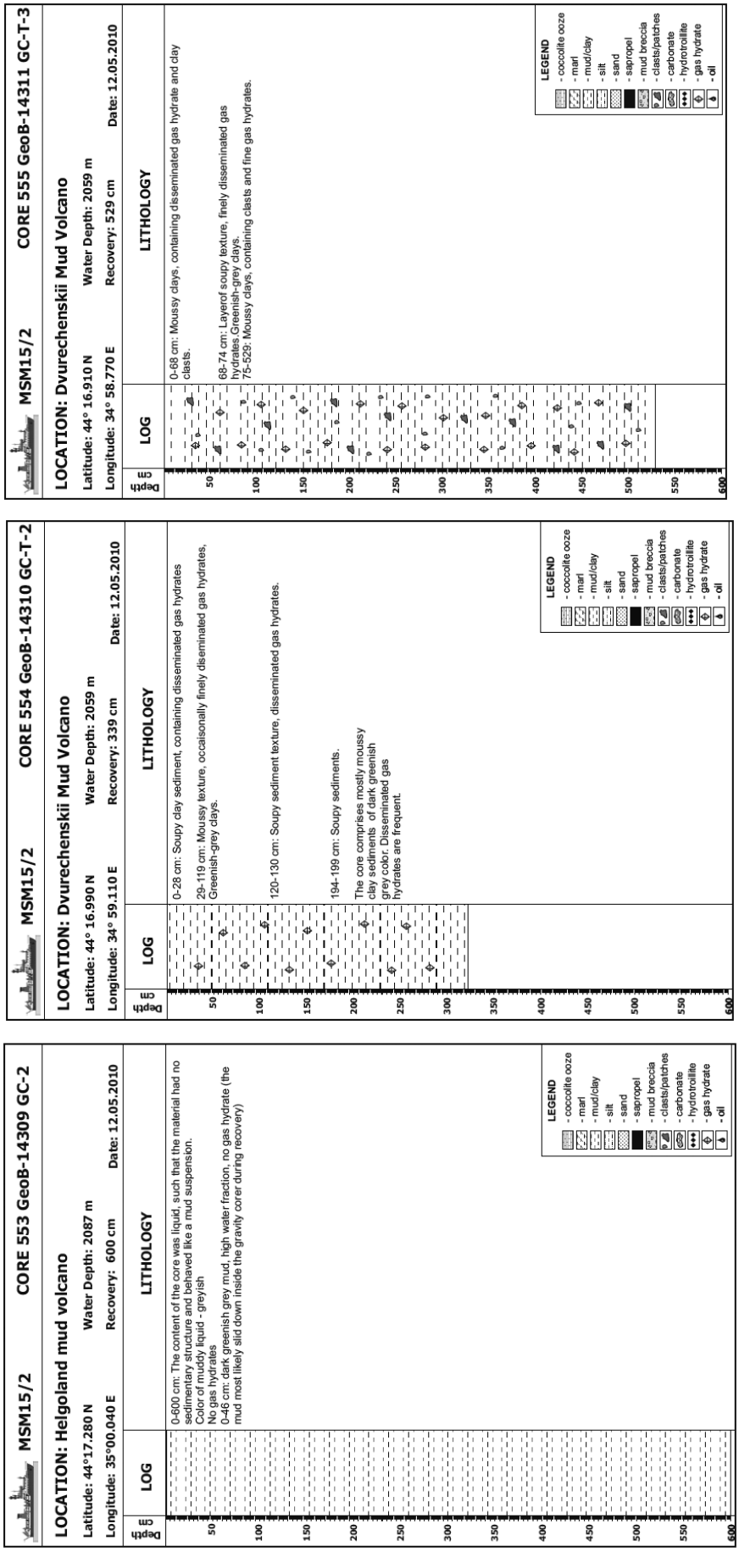

Appendix 3: Continuation

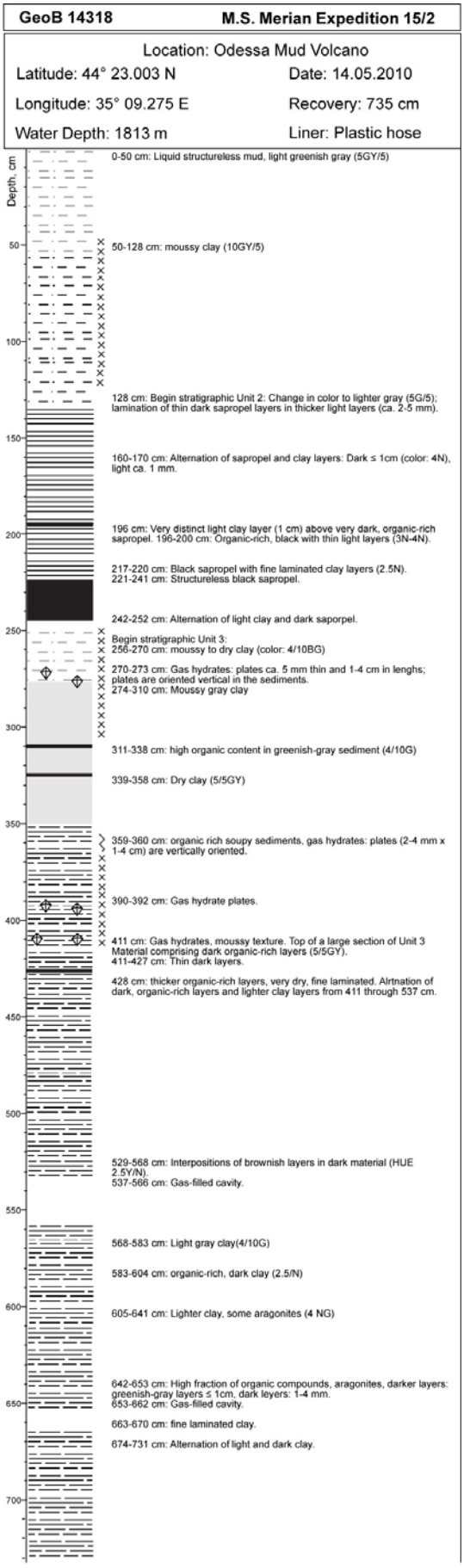

Appendix 3: Continuation

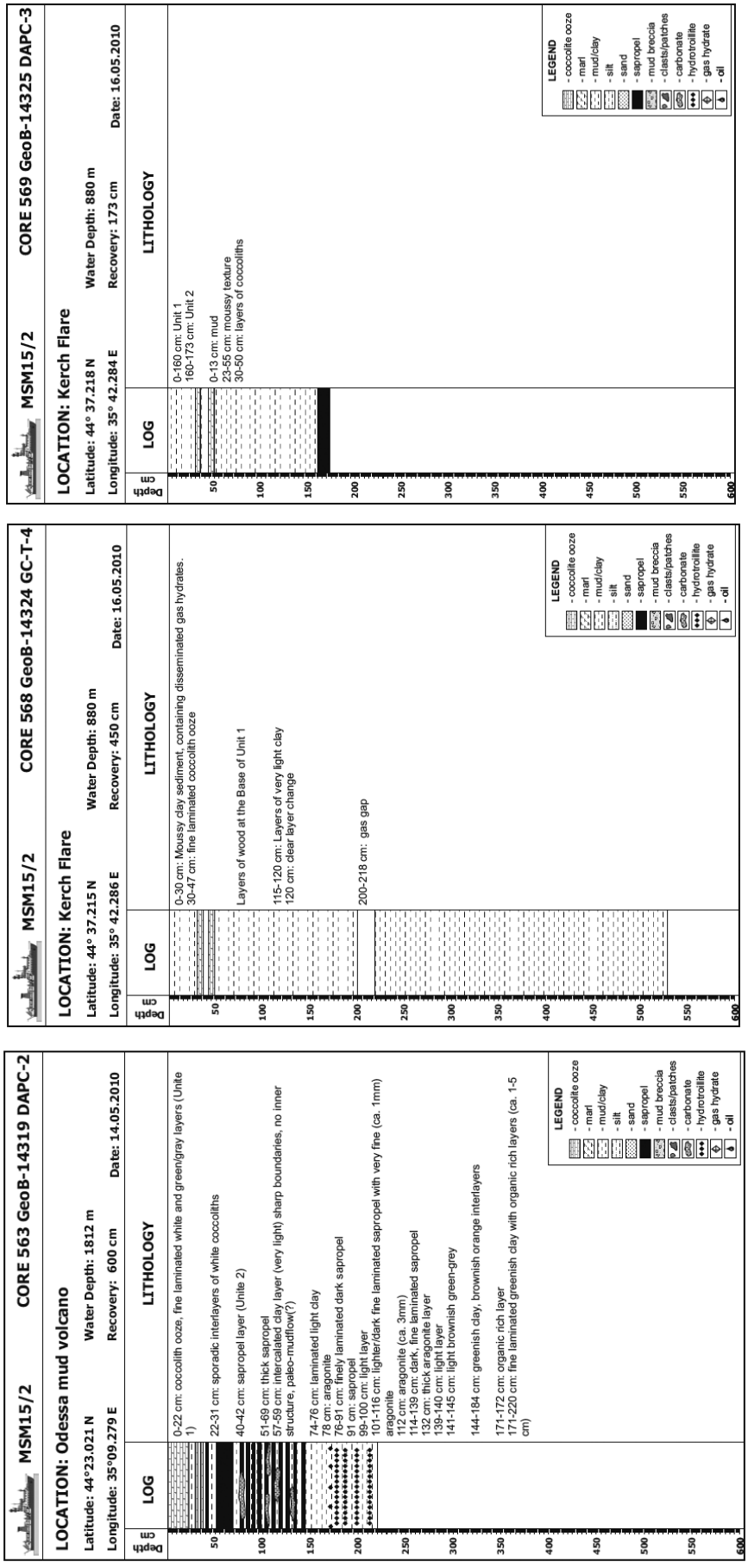

Appendix 3: Continuation

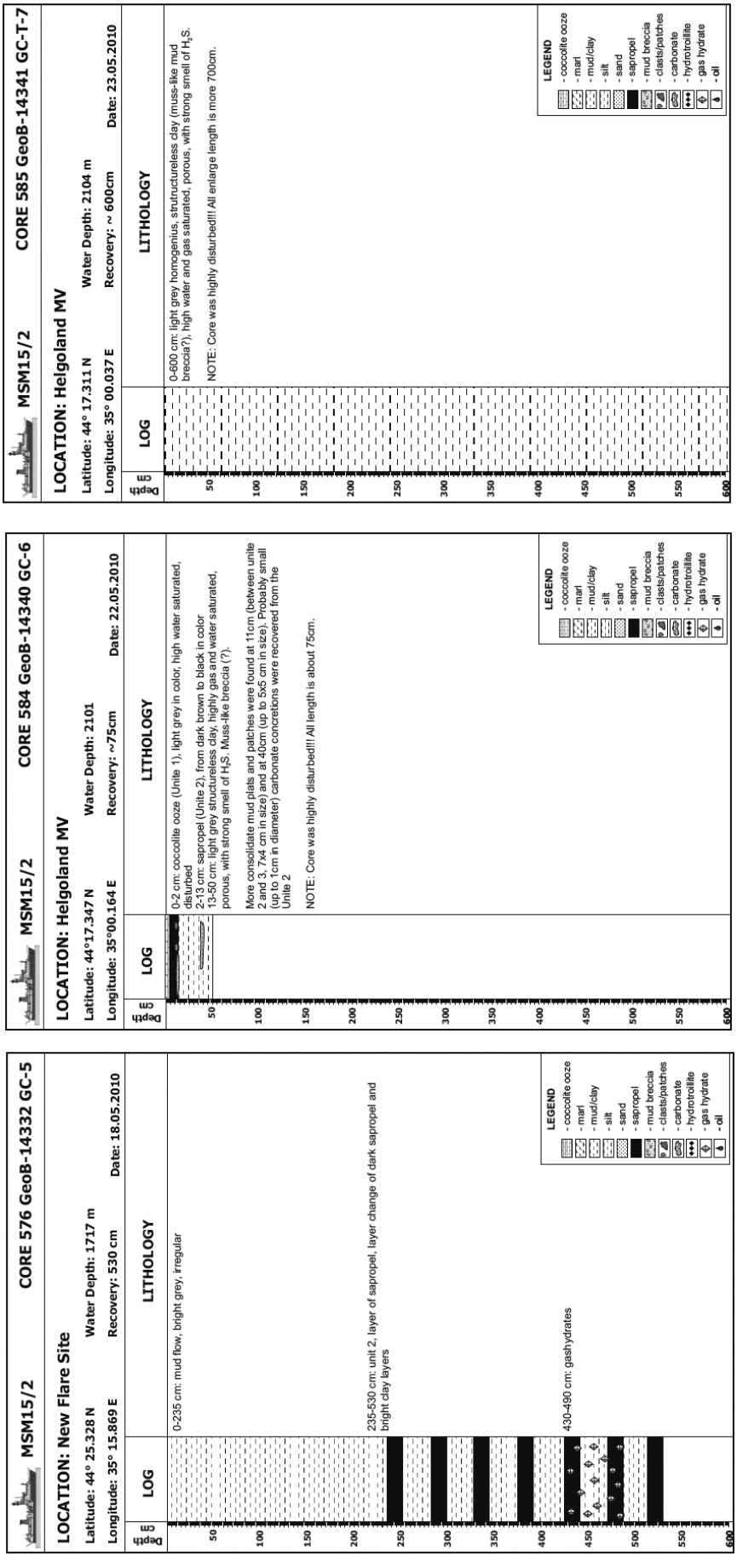

Appendix 3: Continuation

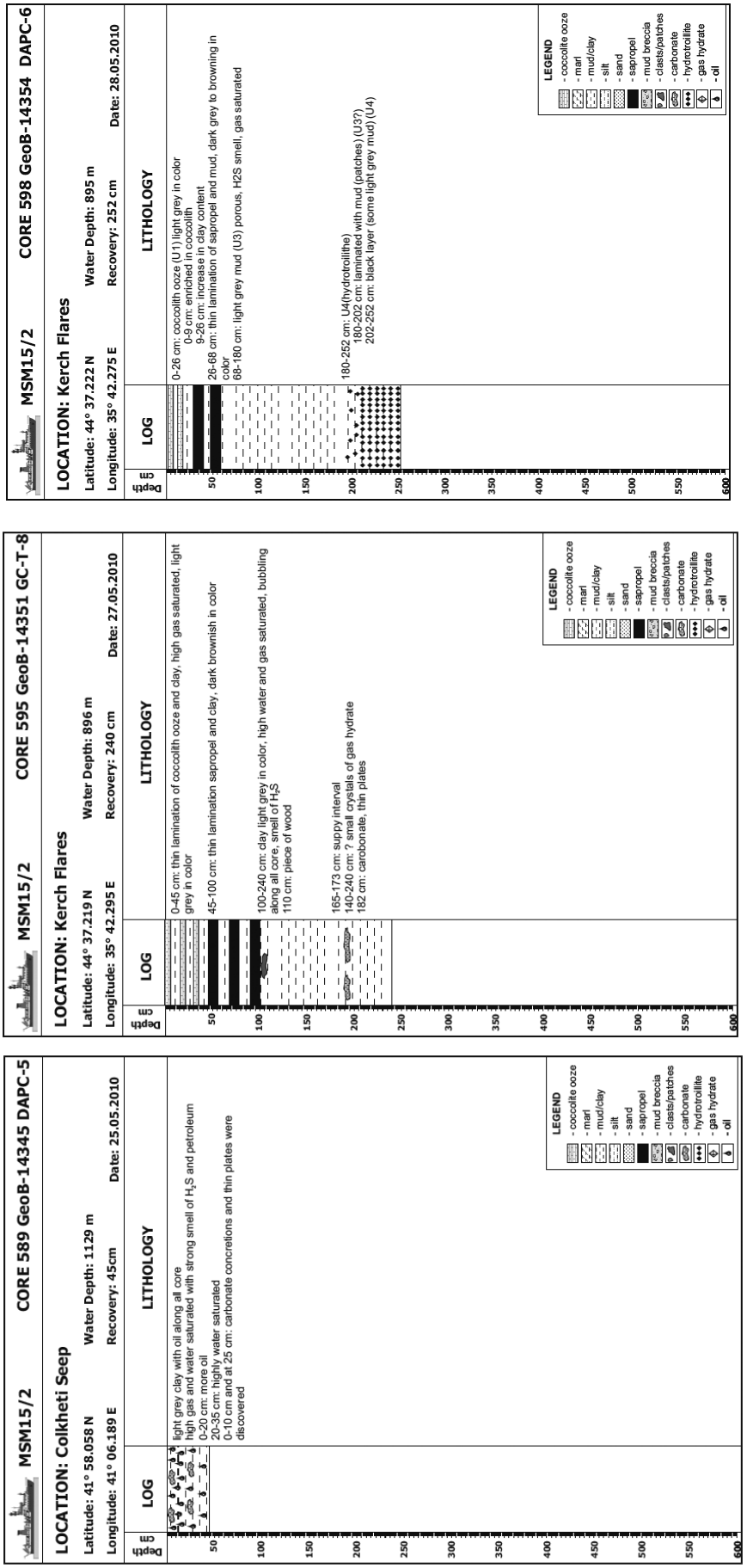

Appendix 3: Continuation

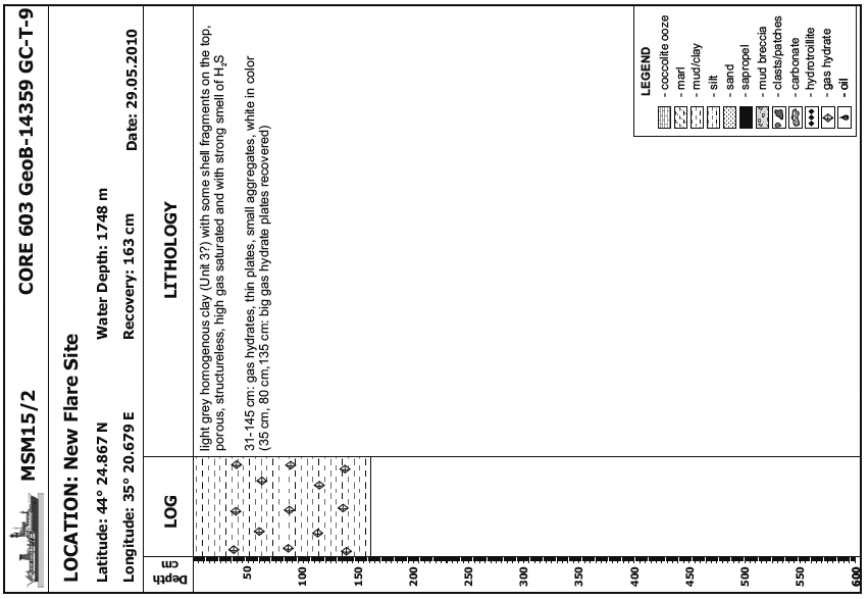

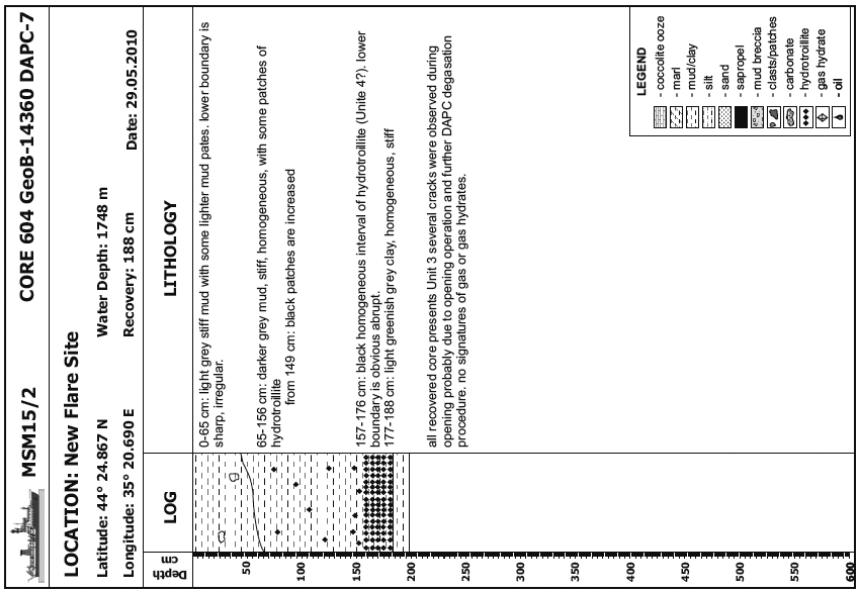

Publications of this series:

No. 1 **Wefer, G., E. Suess and cruise participants**
Bericht über die POLARSTERN-Fahrt ANT IV/2, Rio de Janeiro - Punta Arenas, 6.11. - 1.12.1985.
60 pages, Bremen, 1986.

No. 2 **Hoffmann, G.**
Holozänstratigraphie und Küstenlinienverlagerung an der andalusischen Mittelmeerküste.
173 pages, Bremen, 1988. (out of print)

No. 3 **Wefer, G. and cruise participants**
Bericht über die METEOR-Fahrt M 6/6, Libreville - Las Palmas, 18.2. - 23.3.1988.
97 pages, Bremen, 1988.

No. 4 **Wefer, G., G.F. Lutze, T.J. Müller, O. Pfannkuche, W. Schenke, G. Siedler, W. Zenk**
Kurzbericht über die METEOR-Expedition No. 6, Hamburg - Hamburg, 28.10.1987 - 19.5.1988.
29 pages, Bremen, 1988. (out of print)

No. 5 **Fischer, G.**
Stabile Kohlenstoff-Isotope in partikulärer organischer Substanz aus dem Südpolarmeer (Atlantischer Sektor). 161 pages, Bremen, 1989.

No. 6 **Berger, W.H. and G. Wefer**
Partikelfluß und Kohlenstoffkreislauf im Ozean.
Bericht und Kurzfassungen über den Workshop vom 3.-4. Juli 1989 in Bremen.
57 pages, Bremen, 1989.

No. 7 **Wefer, G. and cruise participants**
Bericht über die METEOR - Fahrt M 9/4, Dakar - Santa Cruz, 19.2. - 16.3.1989.
103 pages, Bremen, 1989.

No. 8 **Kölling, M.**
Modellierung geochemischer Prozesse im Sickerwasser und Grundwasser.
135 pages, Bremen, 1990.

No. 9 **Heinze, P.-M.**
Das Auftriebsgeschehen vor Peru im Spätquartär. 204 pages, Bremen, 1990. (out of print)

No. 10 **Willems, H., G. Wefer, M. Rinski, B. Donner, H.-J. Bellmann, L. Eißmann, A. Müller, B.W. Flemming, H.-C. Höfle, J. Merkt, H. Streif, G. Hertweck, H. Kuntze, J. Schwaar, W. Schäfer, M.-G. Schulz, F. Grube, B. Menke**
Beiträge zur Geologie und Paläontologie Norddeutschlands: Exkursionsführer.
202 pages, Bremen, 1990.

No. 11 **Wefer, G. and cruise participants**
Bericht über die METEOR-Fahrt M 12/1, Kapstadt - Funchal, 13.3.1990 - 14.4.1990.
66 pages, Bremen, 1990.

No. 12 **Dahmke, A., H.D. Schulz, A. Kölling, F. Kracht, A. Lücke**
Schwermetallspuren und geochemische Gleichgewichte zwischen Porenlösung und Sediment im Wesermündungsgebiet. BMFT-Projekt MFU 0562, Abschlußbericht. 121 pages, Bremen, 1991.

No. 13 **Rostek, F.**
Physikalische Strukturen von Tiefseesedimenten des Südatlantiks und ihre Erfassung in Echolotregistrierungen. 209 pages, Bremen, 1991.

No. 14 **Baumann, M.**
Die Ablagerung von Tschernobyl-Radiocäsium in der Norwegischen See und in der Nordsee.
133 pages, Bremen, 1991. (out of print)

No. 15 **Kölling, A.**
Frühdiagenetische Prozesse und Stoff-Flüsse in marinen und ästuarinen Sedimenten.
140 pages, Bremen, 1991.

No. 16 **SFB 261 (ed.)**
1. Kolloquium des Sonderforschungsbereichs 261 der Universität Bremen (14.Juni 1991):
Der Südatlantik im Spätquartär: Rekonstruktion von Stoffhaushalt und Stromsystemen.
Kurzfassungen der Vorträge und Poster. 66 pages, Bremen, 1991.

No. 17 **Pätzold, J. and cruise participants**
Bericht und erste Ergebnisse über die METEOR-Fahrt M 15/2, Rio de Janeiro - Vitoria,
18.1. - 7.2.1991. 46 pages, Bremen, 1993.

No. 18 **Wefer, G. and cruise participants**
Bericht und erste Ergebnisse über die METEOR-Fahrt M 16/1, Pointe Noire - Recife,
27.3. - 25.4.1991. 120 pages, Bremen, 1991.

No. 19 **Schulz, H.D. and cruise participants**
Bericht und erste Ergebnisse über die METEOR-Fahrt M 16/2, Recife - Belem, 28.4. - 20.5.1991.
149 pages, Bremen, 1991.

No. 20 **Berner, H.**
Mechanismen der Sedimentbildung in der Fram-Straße, im Arktischen Ozean und in der Norwegischen See. 167 pages, Bremen, 1991.

No. 21 **Schneider, R.**
Spätquartäre Produktivitätsänderungen im östlichen Angola-Becken: Reaktion auf Variationen im Passat-Monsun-Windsystem und in der Advektion des Benguela-Küstenstroms.
198 pages, Bremen, 1991. (out of print)

No. 22 **Hebbeln, D.**
Spätquartäre Stratigraphie und Paläozeanographie in der Fram-Straße. 174 pages, Bremen, 1991.

No. 23 **Lücke, A.**
Umsetzungsprozesse organischer Substanz während der Frühdiagenese in ästuarinen Sedimenten.
137 pages, Bremen, 1991.

No. 24 **Wefer, G. and cruise participants**
Bericht und erste Ergebnisse der METEOR-Fahrt M 20/1, Bremen - Abidjan, 18.11.- 22.12.1991.
74 pages, Bremen, 1992.

No. 25 **Schulz, H.D. and cruise participants**
Bericht und erste Ergebnisse der METEOR-Fahrt M 20/2, Abidjan - Dakar, 27.12.1991 - 3.2.1992.
173 pages, Bremen, 1992.

No. 26 **Gingele, F.**
Zur klimaabhängigen Bildung biogener und terrigener Sedimente und ihrer Veränderung durch die Frühdiagenese im zentralen und östlichen Südatlantik. 202 pages, Bremen, 1992.

No. 27 **Bickert, T.**
Rekonstruktion der spätquartären Bodenwasserzirkulation im östlichen Südatlantik über stabile Isotope benthischer Foraminiferen. 205 pages, Bremen, 1992. (out of print)

No. 28 **Schmidt, H.**
Der Benguela-Strom im Bereich des Walfisch-Rückens im Spätquartär. 172 pages, Bremen, 1992.

No. 29 **Meinecke, G.**
Spätquartäre Oberflächenwassertemperaturen im östlichen äquatorialen Atlantik.
181 pages, Bremen, 1992.

No. 30 **Bathmann, U., U. Bleil, A. Dahmke, P. Müller, A. Nehrkorn, E.-M. Nöthig, M. Olesch, J. Pätzold, H.D. Schulz, V. Smetacek, V. Spieß, G. Wefer, H. Willems**
Bericht des Graduierten Kollegs. Stoff-Flüsse in marinen Geosystemen.
Berichtszeitraum Oktober 1990 - Dezember 1992. 396 pages, Bremen, 1992.

No. 31 **Damm, E.**
Frühdiagenetische Verteilung von Schwermetallen in Schlicksedimenten der westlichen Ostsee.
115 pages, Bremen, 1992.

No. 32 **Antia, E.E.**
Sedimentology, Morphodynamics and Facies Association of a mesotidal Barrier Island Shoreface (Spiekeroog, Southern North Sea). 370 pages, Bremen, 1993.

No. 33 **Duinker, J. and G. Wefer (ed.)**
Bericht über den 1. JGOFS-Workshop. 1./2. Dezember 1992 in Bremen. 83 pages, Bremen, 1993.

No. 34 **Kasten, S.**
Die Verteilung von Schwermetallen in den Sedimenten eines stadtbremischen Hafenbeckens.
103 pages, Bremen, 1993.

No. 35 **Spieß, V.**
Digitale Sedimentographie. Neue Wege zu einer hochauflösenden Akustostratigraphie.
199 pages, Bremen, 1993.

No. 36 **Schinzel, U.**
Laborversuche zu frühdiagenetischen Reaktionen von Eisen (III) - Oxidhydraten in marinen Sedimenten.189 pages, Bremen, 1993.

No. 37 **Sieger, R.**
CoTAM - ein Modell zur Modellierung des Schwermetalltransports in Grundwasserleitern.
56 pages, Bremen, 1993. (out of print)

No. 38 **Willems, H. (ed.)**
Geoscientific Investigations in the Tethyan Himalayas. 183 pages, Bremen, 1993.

No. 39 **Hamer, K.**
Entwicklung von Laborversuchen als Grundlage für die Modellierung des Transportverhaltens von Arsenat, Blei, Cadmium und Kupfer in wassergesättigten Säulen. 147 pages, Bremen, 1993.

No. 40 **Sieger, R.**
Modellierung des Stofftransports in porösen Medien unter Ankopplung kinetisch gesteuerter Sorptions- und Redoxprozesse sowie thermischer Gleichgewichte. 158 pages, Bremen, 1993.

No. 41 **Thießen, W.**
Magnetische Eigenschaften von Sedimenten des östlichen Südatlantiks und ihre paläozeanographische Relevanz. 170 pages, Bremen, 1993.

No. 42 **Spieß, V. and cruise participants**
Report and preliminary results of METEOR-Cruise M 23/1, Kapstadt - Rio de Janeiro, 4.-25.2.1993. 139 pages, Bremen, 1994.

No. 43 **Bleil, U. and cruise participants**
Report and preliminary results of METEOR-Cruise M 23/2, Rio de Janeiro - Recife, 27.2.-19.3.1993 133 pages, Bremen, 1994.

No. 44 **Wefer, G. and cruise participants**
Report and preliminary results of METEOR-Cruise M 23/3, Recife - Las Palmas, 21.3. - 12.4.1993 71 pages, Bremen, 1994.

No. 45 **Giese, M. and G. Wefer (ed.)**
Bericht über den 2. JGOFS-Workshop. 18../19. November 1993 in Bremen. 93 pages, Bremen, 1994.

No. 46 **Balzer, W. and cruise participants**
Report and preliminary results of METEOR-Cruise M 22/1, Hamburg - Recife, 22.9. - 21.10.1992. 24 pages, Bremen, 1994.

No. 47 **Stax, R.**
Zyklische Sedimentation von organischem Kohlenstoff in der Japan See: Anzeiger für Änderungen von Paläoozeanographie und Paläoklima im Spätkänozoikum. 150 pages, Bremen, 1994.

No. 48 **Skowronek, F.**
Frühdiagenetische Stoff-Flüsse gelöster Schwermetalle an der Oberfläche von Sedimenten des Weser Ästuares. 107 pages, Bremen, 1994.

No. 49 **Dersch-Hansmann, M.**
Zur Klimaentwicklung in Ostasien während der letzten 5 Millionen Jahre: Terrigener Sedimenteintrag in die Japan See (ODP Ausfahrt 128). 149 pages, Bremen, 1994.

No. 50 **Zabel, M.**
Frühdiagenetische Stoff-Flüsse in Oberflächen-Sedimenten des äquatorialen und östlichen Südatlantik. 129 pages, Bremen, 1994.

No. 51 **Bleil, U. and cruise participants**
Report and preliminary results of SONNE-Cruise SO 86, Buenos Aires - Capetown, 22.4. - 31.5.93 116 pages, Bremen, 1994.

No. 52 **Symposium: The South Atlantic: Present and Past Circulation.**
Bremen, Germany, 15 - 19 August 1994. Abstracts. 167 pages, Bremen, 1994.

No. 53 **Kretzmann, U.B.**
57Fe-Mössbauer-Spektroskopie an Sedimenten - Möglichkeiten und Grenzen. 183 pages, Bremen, 1994.

No. 54 **Bachmann, M.**
Die Karbonatrampe von Organyà im oberen Oberapt und unteren Unteralb (NE-Spanien, Prov. Lerida): Fazies, Zyklo- und Sequenzstratigraphie. 147 pages, Bremen, 1994. (out of print)

No. 55 **Kemle-von Mücke, S.**
Oberflächenwasserstruktur und -zirkulation des Südostatlantiks im Spätquartär. 151 pages, Bremen, 1994.

No. 56 **Petermann, H.**
Magnetotaktische Bakterien und ihre Magnetosome in Oberflächensedimenten des Südatlantiks. 134 pages, Bremen, 1994.

No. 57 **Mulitza, S.**
Spätquartäre Variationen der oberflächennahen Hydrographie im westlichen äquatorialen Atlantik. 97 pages, Bremen, 1994.

No. 58 **Segl, M. and cruise participants**
Report and preliminary results of METEOR-Cruise M 29/1, Buenos-Aires - Montevideo, 17.6. - 13.7.1994
94 pages, Bremen, 1994.

No. 59 **Bleil, U. and cruise participants**
Report and preliminary results of METEOR-Cruise M 29/2, Montevideo - Rio de Janiero 15.7. - 8.8.1994. 153 pages, Bremen, 1994.

No. 60 **Henrich, R. and cruise participants**
Report and preliminary results of METEOR-Cruise M 29/3, Rio de Janeiro - Las Palmas 11.8. - 5.9.1994. Bremen, 1994. (out of print)

No. 61 **Sagemann, J.**
Saisonale Variationen von Porenwasserprofilen, Nährstoff-Flüssen und Reaktionen in intertidalen Sedimenten des Weser-Ästuars. 110 pages, Bremen, 1994. (out of print)

No. 62 **Giese, M. and G. Wefer**
Bericht über den 3. JGOFS-Workshop. 5./6. Dezember 1994 in Bremen.
84 pages, Bremen, 1995.

No. 63 **Mann, U.**
Genese kretazischer Schwarzschiefer in Kolumbien: Globale vs. regionale/lokale Prozesse.
153 pages, Bremen, 1995. (out of print)

No. 64 **Willems, H., Wan X., Yin J., Dongdui L., Liu G., S. Dürr, K.-U. Gräfe**
The Mesozoic development of the N-Indian passive margin and of the Xigaze Forearc Basin in southern Tibet, China. – Excursion Guide to IGCP 362 Working-Group Meeting "Integrated Stratigraphy". 113 pages, Bremen, 1995. (out of print)

No. 65 **Hünken, U.**
Liefergebiets - Charakterisierung proterozoischer Goldseifen in Ghana anhand von Fluideinschluß - Untersuchungen. 270 pages, Bremen, 1995.

No. 66 **Nyandwi, N.**
The Nature of the Sediment Distribution Patterns in ther Spiekeroog Backbarrier Area, the East Frisian Islands. 162 pages, Bremen, 1995.

No. 67 **Isenbeck-Schröter, M.**
Transportverhalten von Schwermetallkationen und Oxoanionen in wassergesättigten Sanden. - Laborversuche in Säulen und ihre Modellierung -. 182 pages, Bremen, 1995.

No. 68 **Hebbeln, D. and cruise participants**
Report and preliminary results of SONNE-Cruise SO 102, Valparaiso - Valparaiso, 95.
134 pages, Bremen, 1995.

No. 69 **Willems, H. (Sprecher), U.Bathmann, U. Bleil, T. v. Dobeneck, K. Herterich, B.B. Jorgensen, E.-M. Nöthig, M. Olesch, J. Pätzold, H.D. Schulz, V. Smetacek, V. Speiß. G. Wefer**
Bericht des Graduierten-Kollegs Stoff-Flüsse in marine Geosystemen.
Berichtszeitraum Januar 1993 - Dezember 1995. 45 & 468 pages, Bremen, 1995.

No. 70 **Giese, M. and G. Wefer**
Bericht über den 4. JGOFS-Workshop. 20./21. November 1995 in Bremen. 60 pages, Bremen, 1996. (out of print)

No. 71 **Meggers, H.**
Pliozän-quartäre Karbonatsedimentation und Paläozeanographie des Nordatlantiks und des Europäischen Nordmeeres - Hinweise aus planktischen Foraminiferengemeinschaften.
143 pages, Bremen, 1996. (out of print)

No. 72 **Teske, A.**
Phylogenetische und ökologische Untersuchungen an Bakterien des oxidativen und reduktiven marinen Schwefelkreislaufs mittels ribosomaler RNA. 220 pages, Bremen, 1996. (out of print)

No. 73 **Andersen, N.**
Biogeochemische Charakterisierung von Sinkstoffen und Sedimenten aus ostatlantischen Produktions-Systemen mit Hilfe von Biomarkern. 215 pages, Bremen, 1996.

No. 74 **Treppke, U.**
Saisonalität im Diatomeen- und Silikoflagellatenfluß im östlichen tropischen und subtropischen Atlantik. 200 pages, Bremen, 1996.

No. 75 **Schüring, J.**
Die Verwendung von Steinkohlebergematerialien im Deponiebau im Hinblick auf die Pyritverwitterung und die Eignung als geochemische Barriere. 110 pages, Bremen, 1996.

No. 76 **Pätzold, J. and cruise participants**
Report and preliminary results of VICTOR HENSEN cruise JOPS II, Leg 6, Fortaleza - Recife, 10.3. - 26.3. 1995 and Leg 8, Vítoria - Vítoria, 10.4. - 23.4.1995.
87 pages, Bremen, 1996.

No. 77 **Bleil, U. and cruise participants**
Report and preliminary results of METEOR-Cruise M 34/1, Cape Town - Walvis Bay, 3.-26.1.1996.
129 pages, Bremen, 1996.

No. 78 **Schulz, H.D. and cruise participants**
Report and preliminary results of METEOR-Cruise M 34/2, Walvis Bay - Walvis Bay, 29.1.-18.2.96
133 pages, Bremen, 1996.

No. 79 **Wefer, G. and cruise participants**
Report and preliminary results of METEOR-Cruise M 34/3, Walvis Bay - Recife, 21.2.-17.3.1996.
168 pages, Bremen, 1996.

No. 80 **Fischer, G. and cruise participants**
Report and preliminary results of METEOR-Cruise M 34/4, Recife - Bridgetown, 19.3.-15.4.1996. 105 pages, Bremen, 1996.

No. 81 **Kulbrok, F.**
Biostratigraphie, Fazies und Sequenzstratigraphie einer Karbonatrampe in den Schichten der Oberkreide und des Alttertiärs Nordost-Ägyptens (Eastern Desert, N'Golf von Suez, Sinai). 153 pages, Bremen, 1996.

No. 82 **Kasten, S.**
Early Diagenetic Metal Enrichments in Marine Sediments as Documents of Nonsteady-State Depositional Conditions. Bremen, 1996.

No. 83 **Holmes, M.E.**
Reconstruction of Surface Ocean Nitrate Utilization in the Southeast Atlantic Ocean Based on Stable Nitrogen Isotopes. 113 pages, Bremen, 1996.

No. 84 **Rühlemann, C.**
Akkumulation von Carbonat und organischem Kohlenstoff im tropischen Atlantik: Spätquartäre Produktivitäts-Variationen und ihre Steuerungsmechanismen. 139 pages, Bremen, 1996.

No. 85 **Ratmeyer, V.**
Untersuchungen zum Eintrag und Transport lithogener und organischer partikulärer Substanz im östlichen subtropischen Nordatlantik. 154 pages, Bremen, 1996.

No. 86 **Cepek, M.**
Zeitliche und räumliche Variationen von Coccolithophoriden-Gemeinschaften im subtropischen Ost-Atlantik: Untersuchungen an Plankton, Sinkstoffen und Sedimenten. 156 pages, Bremen, 1996.

No. 87 **Otto, S.**
Die Bedeutung von gelöstem organischen Kohlenstoff (DOC) für den Kohlenstoffffluß im Ozean. 150 pages, Bremen, 1996.

No. 88 **Hensen, C.**
Frühdiagenetische Prozesse und Quantifizierung benthischer Stoff-Flüsse in Oberflächensedimenten des Südatlantiks. 132 pages, Bremen, 1996.

No. 89 **Giese, M. and G. Wefer**
Bericht über den 5. JGOFS-Workshop. 27./28. November 1996 in Bremen. 73 pages, Bremen, 1997.

No. 90 **Wefer, G. and cruise participants**
Report and preliminary results of METEOR-Cruise M 37/1, Lisbon - Las Palmas, 4.-23.12.1996. 79 pages, Bremen, 1997.

No. 91 **Isenbeck-Schröter, M., E. Bedbur, M. Kofod, B. König, T. Schramm & G. Mattheß**
Occurrence of Pesticide Residues in Water - Assessment of the Current Situation in Selected EU Countries. 65 pages, Bremen 1997.

No. 92 **Kühn, M.**
Geochemische Folgereaktionen bei der hydrogeothermalen Energiegewinnung. 129 pages, Bremen 1997.

No. 93 **Determann, S. & K. Herterich**
JGOFS-A6 "Daten und Modelle": Sammlung JGOFS-relevanter Modelle in Deutschland. 26 pages, Bremen, 1997.

No. 94 **Fischer, G. and cruise participants**
Report and preliminary results of METEOR-Cruise M 38/1, Las Palmas - Recife, 25.1.-1.3.1997, with Appendix: Core Descriptions from METEOR Cruise M 37/1. Bremen, 1997.

No. 95 **Bleil, U. and cruise participants**
Report and preliminary results of METEOR-Cruise M 38/2, Recife - Las Palmas, 4.3.-14.4.1997. 126 pages, Bremen, 1997.

No. 96 **Neuer, S. and cruise participants**
Report and preliminary results of VICTOR HENSEN-Cruise 96/1. Bremen, 1997.

No. 97 **Villinger, H. and cruise participants**
Fahrtbericht SO 111, 20.8. - 16.9.1996. 115 pages, Bremen, 1997.

No. 98 **Lüning, S.**
Late Cretaceous - Early Tertiary sequence stratigraphy, paleoecology and geodynamics of Eastern Sinai, Egypt. 218 pages, Bremen, 1997.

No. 99 **Haese, R.R.**
Beschreibung und Quantifizierung frühdiagenetischer Reaktionen des Eisens in Sedimenten des Südatlantiks. 118 pages, Bremen, 1997.

No. 100 **Lührte, R. von**
Verwertung von Bremer Baggergut als Material zur Oberflächenabdichtung von Deponien - Geochemisches Langzeitverhalten und Schwermetall-Mobilität (Cd, Cu, Ni, Pb, Zn). Bremen, 1997.

No. 101 **Ebert, M.**
Der Einfluß des Redoxmilieus auf die Mobilität von Chrom im durchströmten Aquifer. 135 pages, Bremen, 1997.

No. 102 **Krögel, F.**
Einfluß von Viskosität und Dichte des Seewassers auf Transport und Ablagerung von Wattsedimenten (Langeooger Rückseitenwatt, südliche Nordsee). 168 pages, Bremen, 1997.

No. 103 **Kerntopf, B.**
Dinoflagellate Distribution Patterns and Preservation in the Equatorial Atlantic and Offshore North-West Africa. 137 pages, Bremen, 1997.

No. 104 **Breitzke, M.**
Elastische Wellenausbreitung in marinen Sedimenten - Neue Entwicklungen der Ultraschall Sedimentphysik und Sedimentechographie. 298 pages, Bremen, 1997.

No. 105 **Marchant, M.**
Rezente und spätquartäre Sedimentation planktischer Foraminiferen im Peru-Chile Strom. 115 pages, Bremen, 1997.

No. 106 **Habicht, K.S.**
Sulfur isotope fractionation in marine sediments and bacterial cultures. 125 pages, Bremen, 1997.

No. 107 **Hamer, K., R.v. Lührte, G. Becker, T. Felis, S. Keffel, B. Strotmann, C. Waschkowitz, M. Kölling, M. Isenbeck-Schröter, H.D. Schulz**
Endbericht zum Forschungsvorhaben 060 des Landes Bremen: Baggergut der Hafengruppe Bremen-Stadt: Modelluntersuchungen zur Schwermetallmobilität und Möglichkeiten der Verwertung von Hafenschlick aus Bremischen Häfen. 98 pages, Bremen, 1997.

No. 108 **Greeff, O.W.**
Entwicklung und Erprobung eines benthischen Landersystemes zur in situ-Bestimmung von Sulfatreduktionsraten mariner Sedimente. 121 pages, Bremen, 1997.

No. 109 **Pätzold, M. und G. Wefer**
Bericht über den 6. JGOFS-Workshop am 4./5.12.1997 in Bremen. Im Anhang: Publikationen zum deutschen Beitrag zur Joint Global Ocean Flux Study (JGOFS), Stand 1/1998. 122 pages, Bremen, 1998.

No. 110 **Landenberger, H.**
CoTReM, ein Multi-Komponenten Transport- und Reaktions-Modell. 142 pages, Bremen, 1998.

No. 111 **Villinger, H. und Fahrtteilnehmer**
Fahrtbericht SO 124, 4.10. - 16.10.199. 90 pages, Bremen, 1997.

No. 112 **Gietl, R.**
Biostratigraphie und Sedimentationsmuster einer nordostägyptischen Karbonatrampe unter Berücksichtigung der Alveolinen-Faunen. 142 pages, Bremen, 1998.

No. 113 **Ziebis, W.**
The Impact of the Thalassinidean Shrimp Callianassa truncata on the Geochemistry of permeable, coastal Sediments. 158 pages, Bremen 1998.

No. 114 **Schulz, H.D. and cruise participants**
Report and preliminary results of METEOR-Cruise M 41/1, Málaga - Libreville, 13.2.-15.3.1998. Bremen, 1998.

No. 115 **Völker, D.J.**
Untersuchungen an strömungsbeeinflußten Sedimentationsmustern im Südozean. Interpretation sedimentechographischer Daten und numerische Modellierung. 152 pages, Bremen, 1998.

No. 116 **Schlünz, B.**
Riverine Organic Carbon Input into the Ocean in Relation to Late Quaternary Climate Change. 136 pages, Bremen, 1998.

No. 117 **Kuhnert, H.**
Aufzeichnug des Klimas vor Westaustralien in stabilen Isotopen in Korallenskeletten. 109 pages, Bremen, 1998.

No. 118 **Kirst, G.**
Rekonstruktion von Oberflächenwassertemperaturen im östlichen Südatlantik anhand von Alkenonen. 130 pages, Bremen, 1998.

No. 119 **Dürkoop, A.**
Der Brasil-Strom im Spätquartär: Rekonstruktion der oberflächennahen Hydrographie während der letzten 400 000 Jahre. 121 pages, Bremen, 1998.

No. 120 **Lamy, F.**
Spätquartäre Variationen des terrigenen Sedimenteintrags entlang des chilenischen Kontinentalhangs als Abbild von Klimavariabilität im Milanković- und Sub-Milanković-Zeitbereich. 141 pages, Bremen, 1998.

No. 121 **Neuer, S. and cruise participants**
Report and preliminary results of POSEIDON-Cruise Pos 237/2, Vigo – Las Palmas, 18.3.-31.3.1998. 39 pages, Bremen, 1998

No. 122 **Romero, O.E.**
Marine planktonic diatoms from the tropical and equatorial Atlantic: temporal flux patterns and the sediment record. 205 pages, Bremen, 1998.

No. 123 **Spiess, V. und Fahrtteilnehmer**
Report and preliminary results of RV SONNE Cruise 125, Cochin – Chittagong, 17.10.-17.11.1997. 128 pages, Bremen, 1998.

No. 124 **Arz, H.W.**
Dokumentation von kurzfristigen Klimaschwankungen des Spätquartärs in Sedimenten des westlichen äquatorialen Atlantiks. 96 pages, Bremen, 1998.

No. 125 **Wolff, T.**
Mixed layer characteristics in the equatorial Atlantic during the late Quaternary as deduced from planktonic foraminifera. 132 pages, Bremen, 1998.

No. 126 **Dittert, N.**
Late Quaternary Planktic Foraminifera Assemblages in the South Atlantic Ocean: Quantitative Determination and Preservational Aspects. 165 pages, Bremen, 1998.

No. 127 **Höll, C.**
Kalkige und organisch-wandige Dinoflagellaten-Zysten in Spätquartären Sedimenten des tropischen Atlantiks und ihre palökologische Auswertbarkeit. 121 pages, Bremen, 1998.

No. 128 **Hencke, J.**
Redoxreaktionen im Grundwasser: Etablierung und Verlagerung von Reaktionsfronten und ihre Bedeutung für die Spurenelement-Mobilität. 122 pages, Bremen 1998.

No. 129 **Pätzold, J. and cruise participants**
Report and preliminary results of METEOR-Cruise M 41/3, Vítoria, Brasil – Salvador de Bahia, Brasil, 18.4. - 15.5.1998. Bremen, 1999.

No. 130 **Fischer, G. and cruise participants**
Report and preliminary results of METEOR-Cruise M 41/4, Salvador de Bahia, Brasil – Las Palmas, Spain, 18.5. – 13.6.1998. Bremen, 1999.

No. 131 **Schlünz, B. und G. Wefer**
Bericht über den 7. JGOFS-Workshop am 3. und 4.12.1998 in Bremen. Im Anhang: Publikationen zum deutschen Beitrag zur Joint Global Ocean Flux Study (JGOFS), Stand 1/ 1999. 100 pages, Bremen, 1999.

No. 132 **Wefer, G. and cruise participants**
Report and preliminary results of METEOR-Cruise M 42/4, Las Palmas - Las Palmas - Viena do Castelo; 26.09.1998 - 26.10.1998. 104 pages, Bremen, 1999.

No. 133 **Felis, T.**
Climate and ocean variability reconstructed from stable isotope records of modern subtropical corals (Northern Red Sea). 111 pages, Bremen, 1999.

No. 134 **Draschba , S.**
North Atlantic climate variability recorded in reef corals from Bermuda. 108 pages, Bremen, 1999.

No. 135 **Schmieder, F.**
Magnetic Cyclostratigraphy of South Atlantic Sediments. 82 pages, Bremen, 1999.

No. 136 **Rieß, W.**
In situ measurements of respiration and mineralisation processes – Interaction between fauna and geochemical fluxes at active interfaces. 68 pages, Bremen, 1999.

No. 137 **Devey, C.W. and cruise participants**
Report and shipboard results from METEOR-cruise M 41/2, Libreville – Vitoria, 18.3. – 15.4.98. 59 pages, Bremen, 1999.

No. 138 **Wenzhöfer, F.**
Biogeochemical processes at the sediment water interface and quantification of metabolically driven calcite dissolution in deep sea sediments. 103 pages, Bremen, 1999.

No. 139 **Klump, J.**
Biogenic barite as a proxy of paleoproductivity variations in the Southern Peru-Chile Current. 107 pages, Bremen, 1999.

No. 140 **Huber, R.**
Carbonate sedimentation in the northern Northatlantic since the late pliocene. 103 pages, Bremen, 1999.

No. 141 **Schulz, H.**
Nitrate-storing sulfur bacteria in sediments of coastal upwelling. 94 pages, Bremen, 1999.

No. 142 **Mai, S.**
Die Sedimentverteilung im Wattenmeer: ein Simulationsmodell. 114 pages, Bremen, 1999.

No. 143 **Neuer, S. and cruise participants**
Report and preliminary results of Poseidon Cruise 248, Las Palmas - Las Palmas, 15.2.-26.2.1999. 45 pages, Bremen, 1999.

No. 144 **Weber, A.**
Schwefelkreislauf in marinen Sedimenten und Messung von in situ Sulfatreduktionsraten. 122 pages, Bremen, 1999.

No. 145 **Hadeler, A.**
Sorptionsreaktionen im Grundwasser: Unterschiedliche Aspekte bei der Modellierung des Transportverhaltens von Zink. 122 pages, 1999.

No. 146 **Dierßen, H.**
Zum Kreislauf ausgewählter Spurenmetalle im Südatlantik: Vertikaltransport und Wechselwirkung zwischen Partikeln und Lösung. 167 pages, Bremen, 1999.

No. 147 **Zühlsdorff, L.**
High resolution multi-frequency seismic surveys at the Eastern Juan de Fuca Ridge Flank and the Cascadia Margin – Evidence for thermally and tectonically driven fluid upflow in marine sediments. 118 pages, Bremen 1999.

No. 148 **Kinkel, H.**
Living and late Quaternary Coccolithophores in the equatorial Atlantic Ocean: response of distribution and productivity patterns to changing surface water circulation. 183 pages, Bremen, 2000.

No. 149 **Pätzold, J. and cruise participants**
Report and preliminary results of METEOR Cruise M 44/3, Aqaba (Jordan) - Safaga (Egypt) – Dubá (Saudi Arabia) – Suez (Egypt) - Haifa (Israel), 12.3.-26.3.-2.4.-4.4.1999. 135 pages, Bremen, 2000.

No. 150 **Schlünz, B. and G. Wefer**
Bericht über den 8. JGOFS-Workshop am 2. und 3.12.1999 in Bremen. Im Anhang: Publikationen zum deutschen Beitrag zur Joint Global Ocean Flux Study (JGOFS), Stand 1/ 2000. 95 pages, Bremen, 2000.

No. 151 **Schnack, K.**
Biostratigraphie und fazielle Entwicklung in der Oberkreide und im Alttertiär im Bereich der Kharga Schwelle, Westliche Wüste, SW-Ägypten. 142 pages, Bremen, 2000.

No. 152 **Karwath, B.**
Ecological studies on living and fossil calcareous dinoflagellates of the equatorial and tropical Atlantic Ocean. 175 pages, Bremen, 2000.

No. 153 **Moustafa, Y.**
Paleoclimatic reconstructions of the Northern Red Sea during the Holocene inferred from stable isotope records of modern and fossil corals and molluscs. 102 pages, Bremen, 2000.

No. 154 **Villinger, H. and cruise participants**
Report and preliminary results of SONNE-cruise 145-1 Balboa – Talcahuana, 21.12.1999 – 28.01.2000. 147 pages, Bremen, 2000.

No. 155 **Rusch, A.**
Dynamik der Feinfraktion im Oberflächenhorizont permeabler Schelfsedimente. 102 pages, Bremen, 2000.

No. 156 **Moos, C.**
Reconstruction of upwelling intensity and paleo-nutrient gradients in the northwest Arabian Sea derived from stable carbon and oxygen isotopes of planktic foraminifera. 103 pages, Bremen, 2000.

No. 157 **Xu, W.**
Mass physical sediment properties and trends in a Wadden Sea tidal basin. 127 pages, Bremen, 2000.

No. 158 **Meinecke, G. and cruise participants**
Report and preliminary results of METEOR Cruise M 45/1, Malaga (Spain) - Lissabon (Portugal), 19.05. - 08.06.1999. 39 pages, Bremen, 2000.

No. 159 **Vink, A.**
Reconstruction of recent and late Quaternary surface water masses of the western subtropical Atlantic Ocean based on calcareous and organic-walled dinoflagellate cysts. 160 pages, Bremen, 2000.

No. 160 **Willems, H. (Sprecher), U. Bleil, R. Henrich, K. Herterich, B.B. Jørgensen, H.-J. Kuß, M. Olesch, H.D. Schulz,V. Spieß, G. Wefer**
Abschlußbericht des Graduierten-Kollegs Stoff-Flüsse in marine Geosystemen. Zusammenfassung und Berichtszeitraum Januar 1996 - Dezember 2000. 340 pages, Bremen, 2000.

No. 161 **Sprengel, C.**
Untersuchungen zur Sedimentation und Ökologie von Coccolithophoriden im Bereich der Kanarischen Inseln: Saisonale Flussmuster und Karbonatexport. 165 pages, Bremen, 2000.

No. 162 **Donner, B. and G. Wefer**
Bericht über den JGOFS-Workshop am 18.-21.9.2000 in Bremen: Biogeochemical Cycles: German Contributions to the International Joint Global Ocean Flux Study. 87 pages, Bremen, 2000.

No. 163 **Neuer, S. and cruise participants**
Report and preliminary results of Meteor Cruise M 45/5, Bremen – Las Palmas, October 1 – November 3, 1999. 93 pages, Bremen, 2000.

No. 164 **Devey, C. and cruise participants**
Report and preliminary results of Sonne Cruise SO 145/2, Talcahuano (Chile) - Arica (Chile), February 4 – February 29, 2000. 63 pages, Bremen, 2000.

No. 165 **Freudenthal, T.**
Reconstruction of productivity gradients in the Canary Islands region off Morocco by means of sinking particles and sediments. 147 pages, Bremen, 2000.

No. 166 **Adler, M.**
Modeling of one-dimensional transport in porous media with respect to simultaneous geochemical reactions in CoTReM. 147 pages, Bremen, 2000.

No. 167 **Santamarina Cuneo, P.**
Fluxes of suspended particulate matter through a tidal inlet of the East Frisian Wadden Sea (southern North Sea). 91 pages, Bremen, 2000.

No. 168 **Benthien, A.**
Effects of CO2 and nutrient concentration on the stable carbon isotope composition of C37:2 alkenones in sediments of the South Atlantic Ocean. 104 pages, Bremen, 2001.

No. 169 **Lavik, G.**
Nitrogen isotopes of sinking matter and sediments in the South Atlantic. 140 pages, Bremen, 2001.

No. 170 **Budziak, D.**
Late Quaternary monsoonal climate and related variations in paleoproductivity and alkenone-derived sea-surface temperatures in the western Arabian Sea. 114 pages, Bremen, 2001.

No. 171 **Gerhardt, S.**
Late Quaternary water mass variability derived from the pteropod preservation state in sediments of the western South Atlantic Ocean and the Caribbean Sea. 109 pages, Bremen, 2001.

No. 172 **Bleil, U. and cruise participants**
Report and preliminary results of Meteor Cruise M 46/3, Montevideo (Uruguay) – Mar del Plata (Argentina), January 4 – February 7, 2000. Bremen, 2001.

No. 173 **Wefer, G. and cruise participants**
Report and preliminary results of Meteor Cruise M 46/4, Mar del Plata (Argentina) – Salvador da Bahia (Brazil), February 10 – March 13, 2000. With partial results of METEOR cruise M 46/2. 136 pages, Bremen, 2001.

No. 174 **Schulz, H.D. and cruise participants**
Report and preliminary results of Meteor Cruise M 46/2, Recife (Brazil) – Montevideo (Uruguay), December 2 – December 29, 1999. 107 pages, Bremen, 2001.

No. 175 **Schmidt, A.**
Magnetic mineral fluxes in the Quaternary South Atlantic: Implications for the paleoenvironment. 97 pages, Bremen, 2001.

No. 176 **Bruhns, P.**
Crystal chemical characterization of heavy metal incorporation in brick burning processes. 93 pages, Bremen, 2001.

No. 177 **Karius, V.**
Baggergut der Hafengruppe Bremen-Stadt in der Ziegelherstellung. 131 pages, Bremen, 2001.

No. 178 **Adegbie, A. T.**
Reconstruction of paleoenvironmental conditions in Equatorial Atlantic and the Gulf of Guinea Basins for the last 245,000 years. 113 pages, Bremen, 2001.

No. 179 **Spieß, V. and cruise participants**
Report and preliminary results of R/V Sonne Cruise SO 149, Victoria - Victoria, 16.8. - 16.9.2000. 100 pages, Bremen, 2001.

No. 180 **Kim, J.-H.**
Reconstruction of past sea-surface temperatures in the eastern South Atlantic and the eastern South Pacific across Termination I based on the Alkenone Method. 114 pages, Bremen, 2001.

No. 181 **von Lom-Keil, H.**
Sedimentary waves on the Namibian continental margin and in the Argentine Basin – Bottom flow reconstructions based on high resolution echosounder data. 126 pages, Bremen, 2001.

No. 182 **Hebbeln, D. and cruise participants**
PUCK: Report and preliminary results of R/V Sonne Cruise SO 156, Valparaiso (Chile) - Talcahuano (Chile), March 29 - May 14, 2001. 195 pages, Bremen, 2001.

No. 183 **Wendler, J.**
Reconstruction of astronomically-forced cyclic and abrupt paleoecological changes in the Upper Cretaceous Boreal Realm based on calcareous dinoflagellate cysts. 149 pages, Bremen, 2001.

No. 184 **Volbers, A.**
Planktic foraminifera as paleoceanographic indicators: production, preservation, and reconstruction of upwelling intensity. Implications from late Quaternary South Atlantic sediments. 122 pages, Bremen, 2001.

No. 185 **Bleil, U. and cruise participants**
Report and preliminary results of R/V METEOR Cruise M 49/3, Montevideo (Uruguay) - Salvador (Brasil), March 9 - April 1, 2001. 99 pages, Bremen, 2001.

No. 186 **Scheibner, C.**
Architecture of a carbonate platform-to-basin transition on a structural high (Campanian-early Eocene, Eastern Desert, Egypt) – classical and modelling approaches combined. 173 pages, Bremen, 2001.

No. 187 **Schneider, S.**
Quartäre Schwankungen in Strömungsintensität und Produktivität als Abbild der Wassermassen-Variabilität im äquatorialen Atlantik (ODP Sites 959 und 663): Ergebnisse aus Siltkorn-Analysen. 134 pages, Bremen, 2001.

No. 188 **Uliana, E.**
Late Quaternary biogenic opal sedimentation in diatom assemblages in Kongo Fan sediments. 96 pages, Bremen, 2002.

No. 189 **Esper, O.**
Reconstruction of Recent and Late Quaternary oceanographic conditions in the eastern South Atlantic Ocean based on calcareous- and organic-walled dinoflagellate cysts. 130 pages, Bremen, 2001.

No. 190 **Wendler, I.**
Production and preservation of calcareous dinoflagellate cysts in the modern Arabian Sea. 117 pages, Bremen, 2002.

No. 191 **Bauer, J.**
Late Cenomanian – Santonian carbonate platform evolution of Sinai (Egypt): stratigraphy, facies, and sequence architecture. 178 pages, Bremen, 2002.

No. 192 **Hildebrand-Habel, T.**
Die Entwicklung kalkiger Dinoflagellaten im Südatlantik seit der höheren Oberkreide. 152 pages, Bremen, 2002.

No. 193 **Hecht, H.**
Sauerstoff-Optopoden zur Quantifizierung von Pyritverwitterungsprozessen im Labor- und Langzeit-in-situ-Einsatz. Entwicklung - Anwendung – Modellierung. 130 pages, Bremen, 2002.

No. 194 **Fischer, G. and cruise participants**
Report and Preliminary Results of RV METEOR-Cruise M49/4, Salvador da Bahia – Halifax, 4.4.-5.5.2001. 84 pages, Bremen, 2002.

No. 195 **Gröger, M.**
Deep-water circulation in the western equatorial Atlantic: inferences from carbonate preservation studies and silt grain-size analysis. 95 pages, Bremen, 2002.

No. 196 **Meinecke,G. and cruise participants**
Report of RV POSEIDON Cruise POS 271, Las Palmas - Las Palmas, 19.3.-29.3.2001. 19 pages, Bremen, 2002.

No. 197 **Meggers, H. and cruise participants**
Report of RV POSEIDON Cruise POS 272, Las Palmas - Las Palmas, 1.4.-14.4.2001. 19 pages, Bremen, 2002.

No. 198 **Gräfe, K.-U.**
Stratigraphische Korrelation und Steuerungsfaktoren Sedimentärer Zyklen in ausgewählten Borealen und Tethyalen Becken des Cenoman/Turon (Oberkreide) Europas und Nordwestafrikas. 197 pages, Bremen, 2002.

No. 199 **Jahn, B.**
Mid to Late Pleistocene Variations of Marine Productivity in and Terrigenous Input to the Southeast Atlantic. 97 pages, Bremen, 2002.

No. 200 **Al-Rousan, S.**
Ocean and climate history recorded in stable isotopes of coral and foraminifers from the northern Gulf of Aqaba. 116 pages, Bremen, 2002.

No. 201 **Azouzi, B.**
Regionalisierung hydraulischer und hydrogeochemischer Daten mit geostatistischen Methoden. 108 pages, Bremen, 2002.

No. 202 **Spieß, V. and cruise participants**
Report and preliminary results of METEOR Cruise M 47/3, Libreville (Gabun) - Walvis Bay (Namibia), 01.06 - 03.07.2000. 70 pages, Bremen 2002.

No. 203 **Spieß, V. and cruise participants**
Report and preliminary results of METEOR Cruise M 49/2, Montevideo (Uruguay) - Montevideo, 13.02 - 07.03.2001. 84 pages, Bremen 2002.

No. 204 **Mollenhauer, G.**
Organic carbon accumulation in the South Atlantic Ocean: Sedimentary processes and glacial/interglacial Budgets. 139 pages, Bremen 2002.

No. 205 **Spieß, V. and cruise participants**
Report and preliminary results of METEOR Cruise M49/1, Cape Town (South Africa) - Montevideo (Uruguay), 04.01.2001 - 10.02.2001. 57 pages, Bremen, 2003.

No. 206 **Meier, K.J.S.**
Calcareous dinoflagellates from the Mediterranean Sea: taxonomy, ecology and palaeoenvironmental application. 126 pages, Bremen, 2003.

No. 207 **Rakic, S.**
Untersuchungen zur Polymorphie und Kristallchemie von Silikaten der Zusammensetzung Me2Si2O5 (Me:Na, K). 139 pages, Bremen, 2003.

No. 208 **Pfeifer, K.**
Auswirkungen frühdiagenetischer Prozesse auf Calcit- und Barytgehalte in marinen Oberflächen-sedimenten. 110 pages, Bremen, 2003.

No. 209 **Heuer, V.**
Spurenelemente in Sedimenten des Südatlantik. Primärer Eintrag und frühdiagenetische Überprägung. 136 pages, Bremen, 2003.

No. 210 **Streng, M.**
Phylogenetic Aspects and Taxonomy of Calcareous Dinoflagellates. 157 pages, Bremen 2003.

No. 211 **Boeckel, B.**
Present and past coccolith assemblages in the South Atlantic: implications for species ecology, carbonate contribution and palaeoceanographic applicability. 157 pages, Bremen, 2003.

No. 212 **Precht, E.**
Advective interfacial exchange in permeable sediments driven by surface gravity waves and its ecological consequences. 131 pages, Bremen, 2003.

No. 213 **Frenz, M.**
Grain-size composition of Quaternary South Atlantic sediments and its paleoceanographic significance. 123 pages, Bremen, 2003.

No. 214 **Meggers, H. and cruise participants**
Report and preliminary results of METEOR Cruise M 53/1, Limassol - Las Palmas – Mindelo, 30.03.2002 - 03.05.2002. 81 pages, Bremen, 2003.

No. 215 **Schulz, H.D. and cruise participants**
Report and preliminary results of METEOR Cruise M 58/1, Dakar – Las Palmas, 15.04..2003 – 12.05.2003. Bremen, 2003.

No. 216 **Schneider, R. and cruise participants**
Report and preliminary results of METEOR Cruise M 57/1, Cape Town – Walvis Bay, 20.01. – 08.02.2003. 123 pages, Bremen, 2003.

No. 217 **Kallmeyer, J.**
Sulfate reduction in the deep Biosphere. 157 pages, Bremen, 2003.

No. 218 **Røy, H.**
Dynamic Structure and Function of the Diffusive Boundary Layer at the Seafloor. 149 pages, Bremen, 2003.

No. 219 **Pätzold, J., C. Hübscher and cruise participants**
Report and preliminary results of METEOR Cruise M 52/2&3, Istanbul – Limassol – Limassol, 04.02. – 27.03.2002. Bremen, 2003.

No. 220 **Zabel, M. and cruise participants**
Report and preliminary results of METEOR Cruise M 57/2, Walvis Bay – Walvis Bay, 11.02. – 12.03.2003. 136 pages, Bremen 2003.

No. 221 **Salem, M.**
Geophysical investigations of submarine prolongations of alluvial fans on the western side of the Gulf of Aqaba-Red Sea. 100 pages, Bremen, 2003.

No. 222 **Tilch, E.**
Oszillation von Wattflächen und deren fossiles Erhaltungspotential (Spiekerooger Rückseitenwatt, südliche Nordsee). 137 pages, Bremen, 2003.

No. 223 **Frisch, U. and F. Kockel**
Der Bremen-Knoten im Strukturnetz Nordwest-Deutschlands. Stratigraphie, Paläogeographie, Strukturgeologie. 379 pages, Bremen, 2004.

No. 224 **Kolonic, S.**
Mechanisms and biogeochemical implications of Cenomanian/Turonian black shale formation in North Africa: An integrated geochemical, millennial-scale study from the Tarfaya-LaAyoune Basin in SW Morocco. 174 pages, Bremen, 2004. Report online available only.

No. 225 **Panteleit, B.**
Geochemische Prozesse in der Salz- Süßwasser Übergangszone. 106 pages, Bremen, 2004.

No. 226 **Seiter, K.**
Regionalisierung und Quantifizierung benthischer Mineralisationsprozesse. 135 pages, Bremen, 2004.

No. 227 **Bleil, U. and cruise participants**
Report and preliminary results of METEOR Cruise M 58/2, Las Palmas – Las Palmas (Canary Islands, Spain), 15.05. – 08.06.2003. 123 pages, Bremen, 2004.

No. 228 **Kopf, A. and cruise participants**
Report and preliminary results of SONNE Cruise SO175, Miami - Bremerhaven, 12.11 - 30.12.2003. 218 pages, Bremen, 2004.

No. 229 **Fabian, M.**
Near Surface Tilt and Pore Pressure Changes Induced by Pumping in Multi-Layered Poroelastic Half-Spaces. 121 pages, Bremen, 2004.

No. 230 **Segl, M. , and cruise participants**
Report and preliminary results of POSEIDON cruise 304 Galway – Lisbon, 5. – 22. Oct. 2004.
27 pages, Bremen 2004

No. 231 **Meinecke, G. and cruise participants**
Report and preliminary results of POSEIDON Cruise 296, Las Palmas – Las Palmas, 04.04 – 14.04.2003. 42 pages, Bremen 2005.

No. 232 **Meinecke, G. and cruise participants**
Report and preliminary results of POSEIDON Cruise 310, Las Palmas – Las Palmas, 12.04 – 26.04.2004. 49 pages, Bremen 2005.

No. 233 **Meinecke, G. and cruise participants**
Report and preliminary results of METEOR Cruise 58/3, Las Palmas - Ponta Delgada, 11.06 - 24.06.2003. 50 pages, Bremen 2005.

No. 234 **Feseker, T.**
Numerical Studies on Groundwater Flow in Coastal Aquifers. 219 pages. Bremen 2004.

No. 235 **Sahling, H. and cruise participants**
Report and preliminary results of R/V POSEIDON Cruise P317/4, Istanbul-Istanbul ,
16 October - 4 November
2004. 92 pages, Bremen 2004.

No. 236 **Meinecke, G. und Fahrtteilnehmer**
Report and preliminary results of POSEIDON Cruise 305, Las Palmas (Spain) - Lisbon (Portugal), October 28th – November 6th, 2004. 43 pages, Bremen 2005.

No. 237 **Ruhland, G. and cruise participants**
Report and preliminary results of POSEIDON Cruise 319, Las Palmas (Spain) - Las Palmas (Spain), December 6th – December 17th, 2004. 50 pages, Bremen 2005.

No. 238 **Chang, T.S.**
Dynamics of fine-grained sediments and stratigraphic evolution of a back-barrier tidal basin of the German Wadden Sea (southern North Sea). 102 pages, Bremen 2005.

No. 239 **Lager, T.**
Predicting the source strength of recycling materials within the scope of a seepage water prognosis by means of standardized laboratory methods. 141 pages, Bremen 2005.

No. 240 **Meinecke, G.**
DOLAN - Operationelle Datenübertragung im Ozean und Laterales Akustisches Netzwerk in der Tiefsee. Abschlußbericht. 42 pages, Bremen 2005.

No. 241 **Guasti, E.**
Early Paleogene environmental turnover in the southern Tethys as recorded by foraminiferal and organic-walled dinoflagellate cysts assemblages. 203 pages, Bremen 2005.

No. 242 **Riedinger, N.**
Preservation and diagenetic overprint of geochemical and geophysical signals in ocean margin sediments related to depositional dynamics. 91 pages, Bremen 2005.

No. 243 **Ruhland, G. and cruise participants**
Report and preliminary results of POSEIDON cruise 320, Las Palmas (Spain) - Las Palmas (Spain), March 08th - March 18th, 2005. 57 pages, Bremen 2005.

No. 244 **Inthorn, M.**
Lateral particle transport in nepheloid layers – a key factor for organic matter distribution and quality in the Benguela high-productivity area. 127 pages, Bremen, 2006.

No. 245 **Aspetsberger, F.**
Benthic carbon turnover in continental slope and deep sea sediments: importance of organic matter quality at different time scales. 136 pages, Bremen, 2006.

No. 246 **Hebbeln, D. and cruise participants**
Report and preliminary results of RV SONNE Cruise SO-184, PABESIA, Durban (South Africa) – Cilacap (Indonesia) – Darwin (Australia), July 08th - September 13th, 2005. 142 pages, Bremen 2006.

No. 247 **Ratmeyer, V. and cruise participants**
Report and preliminary results of RV METEOR Cruise M61/3. Development of Carbonate Mounds on the Celtic Continental Margin, Northeast Atlantic. Cork (Ireland) – Ponta Delgada (Portugal), 04.06. – 21.06.2004. 64 pages, Bremen 2006.

No. 248 **Wien, K.**
Element Stratigraphy and Age Models for Pelagites and Gravity Mass Flow Deposits based on Shipboard XRF Analysis. 100 pages, Bremen 2006.

No. 249 **Krastel, S. and cruise participants**
Report and preliminary results of RV METEOR Cruise M65/2, Dakar - Las Palmas, 04.07. – 26.07.2005. 185 pages, Bremen 2006.

No. 250 **Heil, G.M.N.**
Abrupt Climate Shifts in the Western Tropical to Subtropical Atlantic Region during the Last Glacial. 121 pages, Bremen 2006.

No. 251 **Ruhland, G. and cruise participants**
Report and preliminary results of POSEIDON Cruise 330, Las Palmas – Las Palmas, November 21th – December 03rd, 2005. 48 pages, Bremen 2006.

No. 252 **Mulitza , S. and cruise participants**
Report and preliminary results of METEOR Cruise M65/1, Dakar – Dakar, 11.06.- 1.07.2005. 149 pages, Bremen 2006.

No. 253 **Kopf, A. and cruise participants**
Report and preliminary results of POSEIDON Cruise P336, Heraklion - Heraklion, 28.04. – 17.05.2006. 127 pages, Bremen, 2006.

No. 254 **Wefer, G. and cruise participants**
Report and preliminary results of R/V METEOR Cruise M65/3, Las Palmas - Las Palmas (Spain), July 31st - August 10th, 2005. 24 pages, Bremen 2006.

No. 255 **Hanebuth, T.J.J. and cruise participants**
Report and first results of the POSEIDON Cruise P342 GALIOMAR, Vigo – Lisboa (Portugal), August 19th – September 06th, 2006. Distribution Pattern, Residence Times and Export of Sediments on the Pleistocene/Holocene Galician Shelf (NW Iberian Peninsula). 203 pages, Bremen, 2007.

No. 256 **Ahke, A.**
Composition of molecular organic matter pools, pigments and proteins, in Benguela upwelling and Arctic Sediments. 192 pages, Bremen 2007.

No. 257 **Becker, V.**
Seeper - Ein Modell für die Praxis der Sickerwasserprognose. 170 pages, Bremen 2007.

No. 258 **Ruhland, G. and cruise participants**
Report and preliminary results of Poseidon cruise 333, Las Palmas (Spain) – Las Palmas (Spain), March 1st – March 10th, 2006. 32 pages, Bremen 2007.

No. 259 **Fischer, G., G. Ruhland and cruise participants**
Report and preliminary results of Poseidon cruise 344, leg 1 and leg 2, Las Palmas (Spain) – Las Palmas (Spain),
Oct. 20th –Nov 2nd & Nov. 4th – Nov 13th, 2006. 46 pages, Bremen 2007.

No. 260 **Westphal, H. and cruise participants**
Report and preliminary results of Poseidon cruise 346, MACUMA. Las Palmas (Spain) – Las Palmas (Spain), 28.12.2006 – 15.1.2007. 49 pages, Bremen 2007.

No. 261 **Bohrmann, G., T. Pape, and cruise participants**
Report and preliminary results of R/V METEOR Cruise M72/3, Istanbul – Trabzon – Istanbul, March 17th – April 23rd, 2007. Marine gas hydrates of the Eastern Black Sea. 130 pages, Bremen 2007.

No. 262 **Bohrmann, G., and cruise participants**
Report and preliminary results of R/V METEOR Cruise M70/3, Iraklion – Iraklion, 21 November – 8 December 2006. Cold Seeps of the Anaximander Mountains / Eastern Mediterranean. 75 pages, Bremen 2008.

No. 263 **Bohrmann, G., Spiess, V., and cruise participants**
Report and preliminary results of R/V Meteor Cruise M67/2a and 2b, Balboa -- Tampico -- Bridgetown, 15 March -- 24 April, 2006. Fluid seepage in the Gulf of Mexico. Bremen 2008.

No. 264 **Kopf, A., and cruise participants**
Report and preliminary results of Meteor Cruise M73/1: LIMA-LAMO (Ligurian Margin Landslide Measurements & Observatory), Cadiz, 22.07.2007 – Genoa, 11.08.2007. 170 pages, Bremen 2008.

No. 265 **Hebbeln, D., and cruise participants**
Report and preliminary results of RV Pelagia Cruise 64PE284. Cold-water Corals in the Gulf of Cádiz and on Coral Patch Seamount (NE Atlantic). Portimão - Portimão, 18.02. - 09.03.2008. 90 pages, Bremen 2008.

No. 266 **Bohrmann, G. and cruise participants**
Report and preliminary results of R/V Meteor Cruise M74/3, Fujairah – Male, 30 October - 28 November, 2007. Cold Seeps of the Makran subduction zone (Continental margin of Pakistan). 161 pages, Bremen 2008.

No. 267 **Sachs, O.**
Benthic organic carbon fluxes in the Southern Ocean: Regional differences and links to surface primary production and carbon export. 143 pages, Bremen, 2008.

No. 268 **Zonneveld, K. and cruise participants**
Report and preliminary results of R/V POSEIDON Cruise P339, Piräus - Messina, 16 June - 2 July 2006. CAPPUCCINO - Calabrian and Adriatic palaeoproductivity and climatic variability in the last two millenia. 61 pages, Bremen, 2008.

No. 269 **Ruhland, G. and cruise participants**
Report and preliminary results of R/V POSEIDON Cruise P360, Las Palmas (Spain) - Las Palmas (Spain), Oct. 29th - Nov. 6th, 2007. 27 pages, Bremen, 2008.

No. 270 **Ruhland, G., G. Fischer and cruise participants**
Report and preliminary results of R/V POSEIDON Cruise 365 (Leg 1+2). Leg 1: Las Palmas - Las Palmas, 13.4. - 16.4.2008. Leg 2: Las Palmas - Las Palmas, 18.4. - 29.4.2008. 40 pages, Bremen, 2009.

No. 271 **Kopf, A. and cruise participants**
Report and preliminary results of R/V POSEIDON Cruise P386: NAIL (Nice Airport Landslide), La Seyne sur Mer, 20.06.2009 – La Seyne sur Mer, 06.07.2009. 161 pages, Bremen, 2009.

No. 272 **Freudenthal, T., G. Fischer and cruise participants**
Report and preliminary results of Maria S. Merian Cruise MSM04/4 a & b, Las Palmas (Spain) – Las Palmas (Spain), Feb 27th – Mar 16th & Mar 19th – Apr 1st, 2007. 117 pages, Bremen 2009.

No. 273 **Hebbeln, D., C. Wienberg, L. Beuck, A. Freiwald, P. Wintersteller and cruise participants**
Report and preliminary results of R/V POSEIDON Cruise POS 385 "Cold-Water Corals of the Alboran Sea (western Mediterranean Sea)", Faro - Toulon, May 29 - June 16, 2009. 79 pages, Bremen 2009.

No. 274 **Zonneveld, K. and cruise participants**
Report and preliminary results of R/V Poseidon Cruises P 366-1 and P 366-2, Las Palmas - Las Palmas - Vigo, 03 -19 May 2008 and 22 -30 May 2008. PERGAMOM Proxy Education and Research cruise off Galicai, Morocco and Mauretania. 47 pages, Bremen 2010.

No. 275 **Wienberg, C. and cruise participants**
Report and preliminary results of RV POSEIDON cruise POS400 "CORICON - Cold-water corals along the Irish continental margin", Vigo - Cork, June 29 - July 15 2010. 46 pages, Bremen 2010.

No. 276 **Villinger, H. and cruise participants**
Report and preliminary results of R/V Sonne Cruise SO207, Caldera-Caldera, 21 June -13 July, 2010. SeamountFlux: Efficient cooling in young oceanic crust caused by circulation of seawater through seamounts (Guatemala Basin, East Pacific Ocean). 161 pages, Bremen 2010.

No. 277 **Fischer, G. and cruise participants**
Report and preliminary results of RV POSEIDON Cruise POS 396, Las Palmas - Las Palmas (Spain), 24 February - 8 March 2010. 22 pages, Bremen 2011.

No. 278 **Bohrmann, G. and cruise participants**
Report and preliminary results of RV MARIA S. MERIAN Cruise MSM 15/2, Istanbul (Turkey) – Piraeus (Greece), 10 May - 2 June 2010. Origin and structure of methane, gas hydrates and fluid flows in the Black Sea. 130 pages, Bremen 2011.